# DEPLOYABLE TENSION-STRUT STRUCTURES:
# CONCEPT, STRUCTURAL BEHAVIOUR,
# AND IMPLEMENTATION

VU KHAC KIEN

NATIONAL UNIVERSITY OF SINGAPORE

2007

# DEPLOYABLE TENSION-STRUT STRUCTURES:
# CONCEPT, STRUCTURAL BEHAVIOUR,
# AND IMPLEMENTATION

VU KHAC KIEN

(*B.Eng. National University of Civil Engineering, Vietnam*)

A THESIS SUBMITTED

FOR THE DEGREE OF DOCTOR OF PHILOSOPHY

DEPARTMENT OF CIVIL ENGINEERING

NATIONAL UNIVERSITY OF SINGAPORE

2007

# ACKNOWLEDGEMENT

I would like to express special thanks to Professor Richard Liew J.Y., who guided me how to learn in-depth and effectively, and to Professor Krishnapillai Anadasivam, who guided me how to learn with an open mind set. Without their continuous guidance, I could not have completed my PhD candidature.

I also want to thank Professor Koh Chan Ghee and Professor Quek Ser Tong, who gave judgments on my research contributions and theoretical works.

I would like to thank Mr Sit Beng Chiat, Mr Ang Beng Oon, and Ms Annie Tan for their helps when experiments are set up and tested.

Thank you very much Mum, Dad, and my little brother Thinh. We all have to sacrifice when I am abroad. Love to my wife, Anh, for your patience and continuous encouragement. Your love really boosts me up at the moment I feel most exhausted.

Thank you, my dear friends, Son, Duc, Trung, Dong, Khoa, and Tun Myint Aung for sharing a long and great time with me. Life would be very boring without any of you.

**TABLES OF CONTENT**

**Chapter I: Introduction**

**Chapter 2: Background**

## Chapter 3: Structural Morphology and Form Creation

## Chapter 4: Non-linear Analysis Methods

**Chapter 7: Prototype Investigations and Potential Applications**

**Chapter 8: Conclusions and Recommendations**

# SUMMARY

This thesis is dedicated to developing a new structural concept which is rapidly deployable and structurally effective. During the recent hundred years, various types of spatial structural systems have been developed for different civil engineering and space applications such as stadium cover, exhibition roof, communication boom, etc. Some of these systems are structurally effective and thus have been used widely such as double-layer space trusses. Some other types of spatial structures have been proposed to be effective in construction time such as deployable structures. The structural products developed in this research inherit both advantages of double-layer space trusses and deployable structures in one system, which is named as Deployable Tension-Strut Structure (DTSS).

Structural morphology of DTSSs is related to their mechanical features. The morphology study shows geometric rules which is linked to deployability of the structures and the locking mechanism. These geometric rules (shape grammar) serve as a basis to develop an exhaustive design creation algorithm which is able to automatically find numerous viable forms of DTSS. Although the algorithm is a generative design tool, it is controllable in comparison with stochastic methods such as genetic algorithm. The reason is shape grammar of DTSS is implemented from the beginning of the design creation process.

Structural behaviour of the proposed DTSSs is investigated by advanced non-linear structural analysis. The understanding of structural performance is a basis to deduce the optimum design parameters of DTSS such as the span to depth ratio, and the

number of module in a span length. The newly proposed DTSS is also compared with conventional double-layer space trusses by using a proposed Structural Efficiency Index, which consider both self-weight and stiffness of the structure in the evaluation. The result shows that DTSS is comparative to double layer space truss in terms of structural efficiency.

Rapid deployment concept of DTSS is proved by prototyping and computer modeling. The computer models show the possibility of deployment and the prototypes show that the details of proposed joint system are suitable to accommodate deployability. Experimental investigations show that the designed steel joints are stronger than the structural steel members. The stiffness of joints allows folding of the structure (removal) after full service load is applied. The tests show that service load level causes insignificant deformation in the joints.

# NOMENCLATURE

A = nominal element section area

$A_{1, 2, 3, 4}$ = constant number

C = number of cylindrical surfaces

D = maximum deflection at the middle of the structure

ds = small change of length of the material at the current load step

$ds_o$ = small change of length of the material at the reference load step

du = variation of displacement in u direction

dv = variation of displacement in v direction

dw = variation of displacement in w direction

dx = variation of distance along the length of the structural element

DTSS = Deployable Tension-Strut Structure

E = modulus of elasticity of material

$e_x$ = Engineering strain

$E_x$ = Green strain

f = frequency

F = External nodal force

FEP = finite element procedure

H = number of horizontal planes

$H_w$ = Work of external loading

I = imposed gravity load

$I_z$ = second moment of inertia of a section around the major z axis of the section

$K_b$ = Nominal bending stiffness

$K_u$ = stiffness of structure

$K_t$ = Nominal torsion stiffness

L = total design unfactored loads, including self-weight

m = mass

n = a number

N = a number

$N_{1,2,3}$ = axial force in element 1, 2, 3

$N_{u,v,w}$ = shape functions in u, v, w direction

P = pre-stress force

$P_c$ = horizontal force caused by pre-stressing

$P_E$ = load bearing capacity of the column

PIP = Pyramid-In-Pyramid structure

POP = Pyramid-On-Pyramid structure

PPC = Pyramid-Pantograph-Cable structure

PPP = Pyramid-Pantograph- Pyramid structure

$q_{u,v,w}$ = generalized constant in direction u, v, w

S = span of the structure

SEI = Structural Efficiency Index

SSM = Symmetric structural module

SSS = Simple strut system

SSU = Simple structural system

w =  displacement in w direction

W = self-weight of the structure, excluding the weight of the joints

u = displacement in u direction

$u_{1,\,2,\,3}$ = nodal displacement in direction 1, 2, 3

U = internal strain energy

v = displacement in v direction

V = number of vertical planes

x = coordinate of section along a structural element

$\alpha$ = coefficient of linear thermal expansion

$\beta$ = parameter to reduce the significance of the ratio S/D in comparison with L/W

$\gamma$ = parameter to normalize SEI in a specified loading and boundary condition

$\Delta T$ = equivalent temperature load

$\theta_t$ = total rotation angle of the boom

$\varepsilon_o$ = the pre-tension strain

$\varepsilon_{1, 2, 3, 4}$ = strain in the element (1), (2), (3), (4)

$\sigma$ = stress

$\pi$ = 3.1414

$\pi$ = total potential energy

$\phi^T$ = assumed shape function

$\{d\}$ = node displacement vector

$\{f\}$ = force vector, representing the external effects

$\{\delta d_t\}$ = matrix of variation of nodal displacement at time t

$\{\delta e_t\}$ = matrix of variation of linear Green strain at time step t

$\{\delta n_t\}$ = matrix of variation of nonlinear Green strain at time step t

$\{\delta u_X\}$ matrix of variation of displacement at time t

$\{f_{body}\}$ = matrix of body force, caused by pre-stress force at time t

$\{f_{int}\}$ = matrix of equivalent nodal load (in external loading side of the equilibrium equation)

$\{K_n\}$ = nonlinear part of stiffness matrix at time $t + \Delta t$ (assume)

{u(x)} = vector of displacement

{N(x)} = vector of shape function

{d} = vector of nodal displacement

$\{\sigma_t\}$ = matrix of pre-stressing stress at time step t

[K] = stiffness matrix of structure

# LIST OF FIGURES

# LIST OF TABLES

# CHAPTER 1

# INTRODUCTION

## 1.1    Overview

Steel structural systems for medium or large span shelters have been developed for more than hundred years. The dominant structural solutions until now are planar steel frame, and double-layer spatial grid structures. Recently, there are more and more structures with cable components, especially large span structures or those with high aesthetic value. Planar steel frames are likely to be used for industrial buildings while spatial grid structures are for civil complexes. As the human world is growing, there is an increasing demand for innovation of steel structural systems which are more economical, attractive, and allow quick installation on site with better control of material quality than the developed structural solutions. Multi-discipline researches are required to investigate the innovative structural systems under sufficiently different perspectives including mechanical manufacturing, construction engineering, and architectural aesthetics.

In this thesis, Deployable Tension-Strut Structures (DTSS) is proposed to inherit the advantages of both tension-strut structures and deployable structures.

Two classes of tension-strut structures are recently proposed, tensegrity, (Motro, 2003) and cable-strut structures, (Wang, 2004). These two systems are distinguished by the design motivations. Tensegrity structures are considered light weight structures with high aesthetic value. However, they are not effective in resisting high load level and

thus the applications of these structural systems are still under investigation. In a different direction of design, cable-strut structures are studied to obtain high structural efficiency, which is higher than that of the conventional double-layer grid structures. The construction of these structures however, may require particular skills and training due to the presence of cable systems. The construction of those tension-strut structures can be more expensive than conventional double-layer grid structures due to the high cost of human resource in developed countries. Rapid and simple construction is essential for an economical design.

Fulfilling this requirement of speed in construction, several deployable structures are proposed in the construction industry (Escrig, 1996). Those deployable structures can be folded to facilitate transportation and deployed quickly on-site, allowing relatively low cost construction. The deployment design of these deployable structures relies on the kinematic chain formed by the pantograph systems. However, those systems alone possess relatively low bending stiffness and thus the application of deployable structures is still limited. Existing deployable structures are yet popular products in the construction industry.

DTSS is a conceptual combination of structurally effective tension-strut structure and rapidly built deployable structure. The current study includes the investigation of structural morphology, generative design, structural efficiency, joint designs, on-site deployment and the manufacturability of the proposed structural concept.

## 1.2    Research objectives and scopes

The research is aimed to

a) Propose and develop a state-of-the-art structural concept which is structurally effective and rapidly deployable. It is named Deployable Tension-Strut Structure (DTSS).

b) Derive the geometric rules (recently adopted as "shape grammar") by investigating the relation between structural morphology and deployment of DTSS; and develop an algorithm to exhaustively generate numerous forms of DTSS using the developed shape grammar.

c) Study the structural performance of the proposed DTSSs and assess structural efficiency by comparing them with conventional space trusses.

d) Propose and evaluate joint designs, investigate design issues for applications of DTSS through numerical modelling, prototype building, and experimental testing of different components of DTSS.

The research scopes include concept development and computerised design creation, numerical modelling, prototyping and experimental testing of Deployable Tension-Strut Structures. These are main parts of a technology development research. The concept proposal is based on the background study and the innovation of the author while computerised design creation provides a tool to generate various forms of

structure which fit in the proposed concept. Numerical modelling using advanced non-linear analysis allows cost effective evaluation of the structural behaviour and structural efficiency of the designs. Prototypes are built to implement the paper-based concept into physical form for verification of deployment concept. Experimental tests are used to check manufacturability and robustness of the joint designs.

## 1.3    Organisation of dissertation

Chapter 2 reviews the background of three fields of research which are closely related to the current writing. Firstly, existing spatial systems are summarized and assessed with regards to structural effectiveness and deployability. Secondly, dominant approaches of computer-based design are discussed. This section of the Chapter serves as a platform for developing an algorithm to generate DTSS geometry in Chapter 3. Finally, non-linear analysis methods are summarized. Numerical analysis is the tool for preliminary assessment on structural efficiency of the proposed systems.

In chapter 3, the concept of DTSS is introduced through several structural forms of DTSS. The structural morphology of those DTSS is studied with regards to the deployment and locking mechanism of the systems. Based on this study, an algorithm to generate various geometric forms of potential DTSS is developed. The effectiveness of the algorithm is illustrated by two case studies.

Chapter 4 introduces and explains the numerical tool, which is used to perform non-linear analysis of DTSSs in later Chapters 5 and 6. The non-linear finite element method to be used is implemented in commercial software, which is based on linear

algebra. Apart from that, the author proposes a non-linear finite element approach which is based on commutative algebra. This approach is compared to the conventional approach to enhance the reliability and understanding of the non-linear analysis which is implemented in commercial software.

In Chapter 5, the parametric study of the proposed DTSS is performed using the non-linear analysis method discussed in Chapter 4. The optimum design parameters are deduced from non-linear analysis of DTSS for a range of span (from 24 m to 60 m) with number of modules per span length ranging from 4 to 12. Structural efficiency of DTSS is compared to conventional double-layer spatial grid structures. Natural frequencies and mode shapes of DTSSs are also investigated to provide preliminary assessment on potential failure modes of the structures and support the design issue investigation which is presented in Chapter 7.

Chapter 6 shows new concepts of deployable boom system that can be used either as back bone of space station or as communication boom towers. Static and dynamic properties of the proposed systems are investigated and compared with that of existing systems. Advantages and drawbacks of all systems are discussed and reviewed.

Chapter 7 discusses the technical issues in manufacturing, assembly and deployment of the DTSS. Various small scale and full scale prototypes of structure and joints are built to verify the viability of deployment concept as well as the proposed joint designs. Different joint designs and corresponding manufacturing process are proposed and evaluated. A case study of 17.8 m span vault is designed and the joints and tube ends are load tested for sufficiency of strength. Recommended steel joint details and

construction method is also introduced. Indicative design guidelines for roof system are provided based on the experience the author obtained during the technology development process. The potential applications are summarized by the end of this Chapter.

Chapter 8 presents the key research findings, and the recommendations for future work, as well as claims for intellectual properties which are related to this research. Two patent applications are supported by the results of this study.

# CHAPTER 2

# BACKGROUND

This chapter exhibits significant academic works and practical design issues, which are most relevant to the present research project. The discussions are divided into three major categories, which are spatial system design, computer-based generative (geometric) design, and non-linear structural analysis. Existing spatial systems are reasonable benchmark for the new structural concept to be proposed in this thesis (Chapter 3). The revision of computer-based generative designs helps to create suitable structural configurations which conform to the proposing concept. Non-linear analysis is the tool for analysing and understanding structural behaviour of the proposing structures.

## 2.1 Structural concept of spatial systems

### 2.1.1 Double-layered space structures

Double-layered space structure is one of the conventional spatial structural systems. These structural systems consist of struts, which are normally hollow sections. The first structures are designed by the German engineers in 1894, (Ramaswamy *et al.*, 2002). The more general name for this system is space frame or lattice structures. Space frames can be single-layered, double-layered, or triple-layered but the double-layered space frames are the most commonly used in practice.

The double-layered structural system is widely used due to its three dimensional stiffness and the flexibility in geometric designs. The structural system is made from

similar modules. Each module is stable itself, and they can be connected together to form a stable structural system. Different combinations of structural modules are the sources for creating various configurations of space frame, which is one of the most attractive features of double-layered space structures. The structural efficiency of double-layered space structures have been investigated by Makowski (1981-1985), El-Sheikh (1998), and Bangash (2003).

Apart from stiffness and variety of structural forms, the inventions of mechanical connectors have significantly contributed to the popularity of double-layered space frame today. Several connection types have been proposed and manufactured such as ball joint, octatube, tubal, nodus, triodetic. Some types of nodes are developed to be relatively cheap in manufacturing like octatube or catrus by El-Sheikh (1999). Some others are stronger and more complicated like the ball joint or the nodus system. The assembly of the structural systems normally requires the use of bolts, which can be easily handled by low cost labour force, and facilitate the on-site quality control. Therefore, bolt connected space frames are more economical than structural systems that require on-site welding.

Advancing geometric flexibility, structural stiffness, and economical connections, space frames continue to be of wide interest in both academic and industrial worlds. Generating more structural geometries of space frame becomes one of the main trends in research and development of space structures. Advanced computer techniques have been used such as those using genetic algorithms, (Kawamura *et al.*, 2000). In the proposed algorithms, the generator of structural geometry is based on the fact that triangular systems, formed by 3 rods, are stable structures.

However, space structural systems, that use hollow sections, cannot make use of material ultimately because high-strength cables are not used. The use of high-strength materials can reduce the self-weight of the structure significantly. New concept of tension-strut structures has been investigated and developed to make use of these high-strength materials.

## 2.1.2   Tension-strut structures

Tension-strut structures are developed later than double-layered space structures. In these systems, the structural components are compressive struts and high-tensile elements. The use of high-tensile cables or rods implies potential material weight savings. The arrangement of struts and tensile elements allows the self-stabilized mechanism, which is essential to maintain stability of tension-strut structures without external anchoring. The various arrangements of these structural elements create various load paths and thus feature different types of tension-strut structures. There are currently two major families of tension-strut structures, which are tensegrity and cable-strut structures.

### 2.1.2.1 Tensegrity structures

Tensegrity is a subjective concept, which is aimed at exotic and ultra-light structures. The first tensegrity structures are designed for exhibition purpose by Snelson, a sculptor. In tension-strut system, compressive elements are not connected together; they are isolated by tensile elements. For that characteristic, Fuller, the pioneer in

developing tensegrity, described tensegrity as "the islands of compressions in the ocean of tensions", (Motro, 2003).

The isolation of compressive elements causes the discontinuity of the compression flow in tensegrity when the structure is subjected to external loads. This discontinuity of compression is against nature because most of the natural structures maintain continuous compression flow such as water body, soil, trees, animal skeleton etc. The compression in a compressive element is balanced by the tensions in tensile elements, Fig. 2.1. However, this equilibrium is maintained by applying high pre-tension force on the tensile elements, which is expensive. For these reasons, present tensegrity structures are not structurally efficient and the applications are still limited to exhibition domes and columns, (Schlaich, 2004).
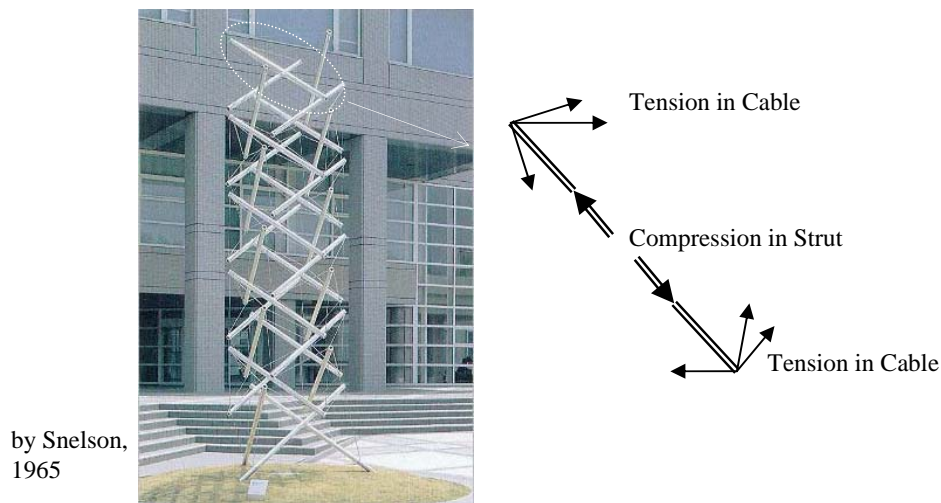


Figure 2.1. Equilibrium of tensegrity structure.

Despite of those limitations, the beauty of tensegrity cannot be rejected with the isolation of compressive elements, which may make the sense that these compressive elements are floating in the air. This special artistic sense inspires many scientists and

researchers such as Adam and Smith (2004), Smaili *et al.* (2004), or Bieniek (2004), seeking for better tensegrity systems.

While structurally efficient tensegrity systems have not been found, another family of tension-strut structures, the cable-strut systems, are developed to obtain better structural performance.

**2.1.2.2 Cable-strut structures**

As mentioned in section 2.1.2.1, the structural inefficiency of tensegrity is due to the isolation of compressive struts. Wang (1998) proposed cable-strut systems to aim for high structural efficiency after a thorough study on tensegrity during his PhD candidature. In cable-strut concept, both cables and struts are contiguous, allowing smooth internal force flow when the structure is subjected to external loads.

Cable-strut structures are structurally efficient. It was proved by extensive analytical works that cable-strut systems can be about 25% lighter than conventional double-layered space structures, (Liew et al., 2003). This weight reduction is due to the use of high-tensile cables at the positions of diagonals and bottom chords of double-layered space structures, (Lee, 2001). The proper combinations of struts and cables also contribute to the structural efficiency of cable-strut systems.

The efficiency of cable-strut structures inspires researchers to find more options for structural geometry of cable-strut systems. Recent works by Wang (2004), introduces various potential geometries of cable-strut structures, associated by possible details of

connections. The introduction of novel geometric forms is by human creation. This means the new forms are derived by human creation, without any computerised technique to generate exhaustive possibilities of cable-strut forms.

The construction of cable-strut structures are more complicated than that of conventional double-layered space structures. The existence of high-tensile cables or rods requires pre-tension process during construction as shown in the experiment and implementation by Liew and Lee (2003), Fig. 2.2. The stabilization of the strut system before pre-tensioning the cable system is another difficulty to the erection procedure. This means the construction cost of cable-strut system may be more expensive than that of double-layered space structures. In developed countries, the human resource is expensive and thus construction cost might be critical for the feasibility of the project with application of cable-strut structures. More effort needs to be put on improving the construction efficiency of this spatial system. This is the inspiration for many innovative designs of spatial structures which are presented in the section 2.1.3.


Figure 2.2. Experiment model (Liew and Lee, 2003).

### 2.1.3   Deployable spatial structures

An efficient method to improve the construction efficiency of spatial structures is to design for deployability. There are various mechanisms for deployability with classification based on the application environments such as earth-based or space environment, the types of structural elements, and/or the structural nature of deployment.

The classification criterion used in this thesis is based on mechanical nature of the deployment as several embryonic forms of deployable structures will be introduced. The following systems cover most of the recent as well as the very old ideas of deployment, applicable for both earth-based and space applications

- Pantograph system
- Telescopic system
- Accordion system
- Retractable system
- Complex system

Each of these deployable systems has its own character in deployment and will be discussed in the following sections.

### 2.1.3.1 Pantograph structural systems

Pantograph structural systems are formed by scissor-like elements or pantograph kinematic chain (Gantes, 2001). Each scissor-like element (SLE) consists of two bars which act like beam-column elements with complex state of stress under external

loadings. These elements are connected together with hinges so that they can rotate relatively. This feature allows the structure to change its geometry by large rotation movements as shown in Fig. 2.3.

Theoretically, the pantograph structures are stress-free during deployment process. If self-weight and friction are ignored, the overall structure behaves like a rigid body motion because there would be no element deformation. Once the angle between a pair of bars is changed, the angles of all the other pairs are changed correspondingly. The whole system of SLEs forms a kinematic chain with one degree of freedom.
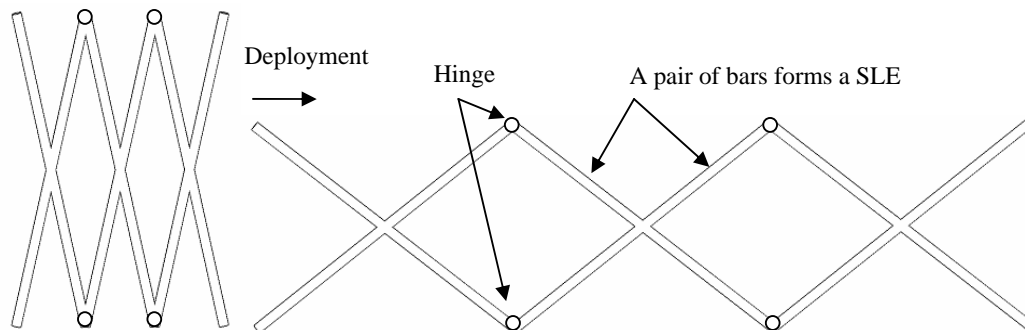


Figure 2.3. Deployment of scissor-like element (SLE).

Such kinematic chain is commonly formed by SLEs in one plane. Each SLE has 4 hinges at their 4 ends. This pantograph system, designed as a column, has been investigated analytically by Raskin and Roorda (1996), Fig. 2.4.

However, the concept proposed by Raskin and Roorda (1996) is restricted to planar column. The structure can be intuitively understood that the bending stiffness is very low because it depends heavily on the bending stiffness of the bars, and much less on the width of the column.
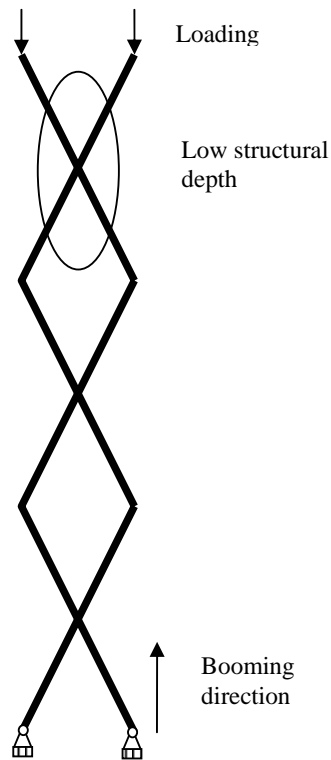
Figure 2.4. Pantograph column (Raskin and Roorda, 1996).
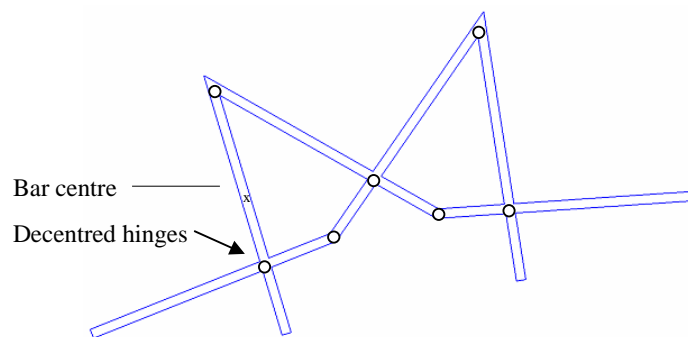


Figure 2.5. Pantograph arch.

One direction of development is the technique of decentring the central hinge, (Sastre, 1996). The central hinge is moved towards one end of the SLE, forming a pantograph arch as shown in Fig. 2.5. Sastre (1996) also expected to develop this concept for dome when arches are expanded to half and united at the top ends. However, the top joint in this proposal of dome must be carefully designed because the eccentricity at joints as

well as the actual dimension of scissor-like elements has not been accounted for in this geometrical design.

Besides, the other novel concepts, *generalized angulated elements* and *multi-angulated rod* (You and Pellegrino, 1996b), open a wide range of new applications for pantograph structures. In these concepts, each bar can have more than one hinge and can be not only straight but also in curved and/or multi-angulated shapes in the plane of SLE. The geometry of pantograph structure can be varied from this combination. On the other hand, the whole system can be bent to form single layer vault and/or dome shape. The 2D structure can be bent to form 3D stable structure. However, neither clearly geometric requirements for compatibility or structural stability conditions have been proposed for the structure. Therefore, whether this class of structure can be used for large scale structure is still an open question. The geometry is quite complicated and it may be used in special structure only, especially for display applications such as radial expansion domes, (Hobberman, 1990-1991).
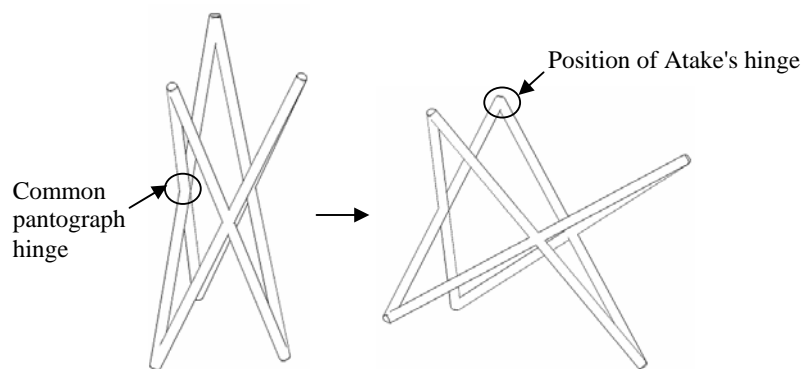


Figure 2.6. Tri-scissor element (Atake, 2000).

Apart from that, the development in geometry of pantograph system does not only rely on the geometry itself but also on the joint solution as in the case of Atake's technique presented in Atake (2000). Atake developed a new type of joint for scissor-like

elements so that they can be combined in the form of triangle, which was called tri-scissor element as shown in Fig. 2.6. Tri-scissor element has one degree of freedom in space as an advantage over the previous generation of pantograph system.

This development provides a new form of pantograph system that can be expanded to many applications with the very special shapes such as chair and/or boat skeleton, (Atake, 2000). The structural module here is not the common planar SLE but a higher form, tri-scissor. However, the weakness of this solution is that the end joints are not stiff in the detailing designs by Atake. In other words, the end joint itself is novel but the weak part of the whole structure. Further development is needed to assure joint stability when this structure is used for large scale applications.

The use of pantograph system with other structures, where the scissors control the movement, is also in development. Several recent proposals by Gomez de Cozar and Garcia Dieguez (2000) are in this trend. The model is a three-dimensional one with two layers of elements, rhombus system and scissor system as shown in Fig. 2.7. The two layers are connected by diagonals and pin joints in the way that makes rhombuses follow scissor movement. The flat rectangular, circular, cylindrical, dome shape has been investigated for compatibility in geometry. Structural stiffness is construed to be controlled by the distance between the layer of SLEs and the layer of rhombuses. This control of stiffness has not been achieved in other design models with pantograph.

It is an advantage that the structure has one degree of freedom and it can be easily deployed by controlling the pantograph movement. However, the practical joints can

be complicated to allow movement of Rhombus-Scissor system in space. That more than one types of joint is needed would increase the cost of the structure.

Rhombus                                    Deployment process
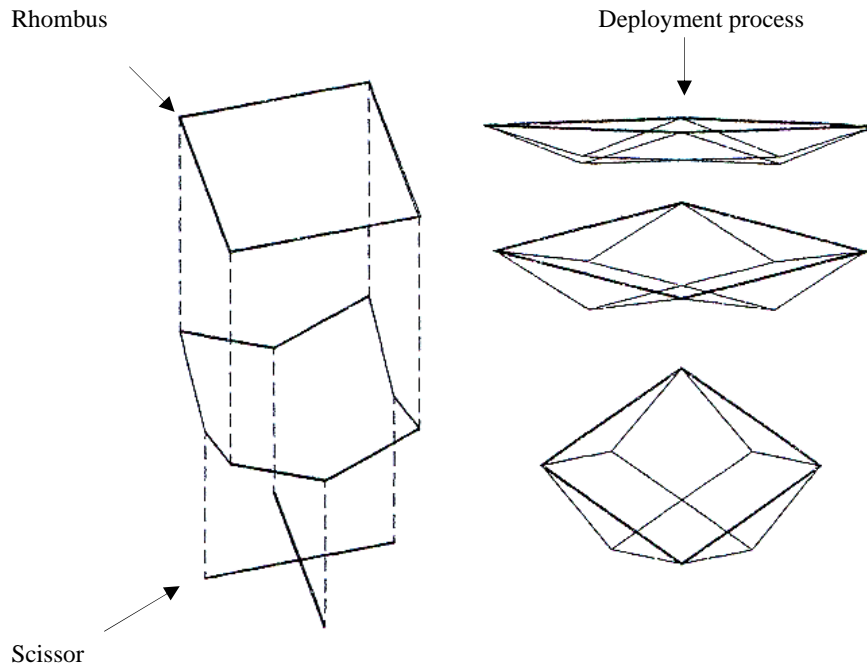


Scissor

Figure 2.7. Rhombus-Scissor system (Gomez and Garcia, 2000).

After all, one of the most significant contributions in this research trend is the swimming pool cover, recently designed and built by Escrig (1996a).



Figure 2.8. Swimming pool cover (Escrig, 1996).

This 30m x 30m roof is formed by a system of scissor-like element, arranged in two perpendicular planes, Fig. 2.8. In each plane of SLE, the elements form an arch shape similar to the mentioned works by Sastre (1996). The bar elements are organized to be out of the plane due to the design of the hinge of SLE. This may cause extra torsion force in the SLE. The diameter of the bars is 120.5 mm, sufficiently large to accommodate the issue. It is a relatively big tube size comparing with other 30 m span roof systems. Because the system of SLEs only is not statically deterministic some special boundary conditions and special elements are added to enhance overall stability. Actually, the conceptual design is not developed very far from the basic concept of SLE but simple enough to be applied in this medium span roof structure. It is obvious that the convenient construction of pantograph structure can be exploited in barrel or dome systems but the low structural efficiency of the pantograph system remains due to low bending stiffness of the system as can be seen from analytical works by Langbecker (2001). Some other pantograph systems can also be found in the review by Escrig (1996b).

### 2.1.3.2 Telescopic systems

The concept of telescope is applied for structures of which parts are made to slide one within another like the tubes of a manual telescope or hydraulic jack. By that way, the structure can be lengthened or shortened in one dimension with little change in other two dimensions of the structure, which are perpendicular to the mechanism axis.

The joint between the two neighbouring elements has the character of prismatic joint. Some good examples can be hydraulic jacks and cables as used in the construction of

Collserola Tower and Valencia Tower, (Martinez-Calzon, 1996) or springs as used in AutoROPS by Gasparetto (2003). It is so convenient to initiate the deployment that the telescopic mechanism is used widely for very different scales from 132 m deployment with 7200 tones lifting, Valencia Tower, to 6 m boom like SSTL-Weitzman deployable boom, Surrey Space Centre (2001).

The major advantage of telescopic mechanism is smoothness and controllability of deployment as specified by Wilmoth (2002). However, the difficulty appears to be wedging problems during deployment and sealing the gaps between different structural blocks as stated by Lallemant (2002).

### 2.1.3.3 Accordion systems

Accordion deployment is featured by the change of structural shape to be less corrugated and the structure occupies larger area. In accordion deployment, one dimension is extended much more than the other two as shown in Fig. 2.9. Each structural block is assumed to act like a rigid plate, which is made from steel trusses and/or complete roof panels.
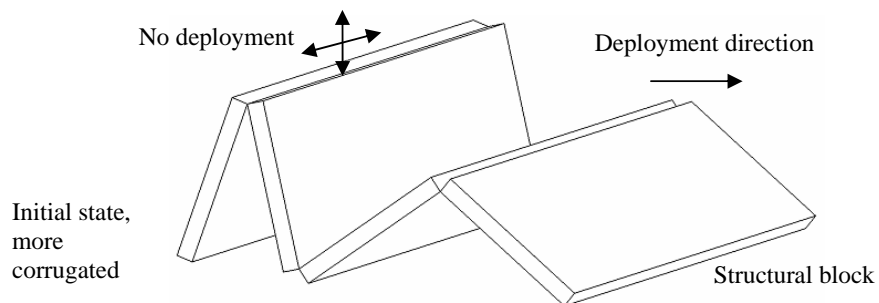
Figure 2.9. Accordion system.

The one-dimensional deployment is the feature of telescopic system while the large rotation of structural units during deployment is the feature of pantograph system. The above features of movement determine the associated mechanism for accordion deployment. Similar to telescopic structure, the deployment of each accordion structural block is independent to others. Therefore if simultaneous deployment is required, additional controlling components should be included such as trolley and cable system in the construction of Venezuelan Pavilion, (Hernandez, 1996). Also similar to pantograph system, the allowance of rotation over the connections of structural units provides several degrees of freedom. To stabilize the structure in deployed shape, special additional stabilising components need to be installed.

One difference of accordion movement from telescopic one is that no structural units are kept in another. Therefore the whole roof structure, including all layers of resistance to water and temperature, can be manufactured for accordion installation, (Hernandez, 1996). The problem of water proof at the joint between two structural units may be overcome by auxiliary pieces of sealing steel cover.

**2.1.3.4 Retractable systems**

Retractable roof is a phenomenon in structural engineering which can be found in many modern stadiums. These roofs are retracted by crane technology and discussed thoroughly in the book by Ishii (2000). The retracted form of the roof allows natural light while the deployed form of the roof protects the ground and stadium seats from snow or heavy rain.

From architectural point, this method provides high flexibility with different modes of use. The degree of openness ranges from 17 % to 100 % in the case of Amsterdam Arena in the Netherlands and Ocean Dome in Japan correspondingly, (Ishii, 2000). Most of the roofs are membrane structures and with the deployability, they provide high level of architectural visualization and utility. However, there is always one part of the roof to be fixed and/or all can move to reveal pre-determined area and occupies a relatively large area. The openness is provided from certain view only e.g. from certain seats in stadiums. The closing and opening process is normally smooth and stable but the maintenance of the system can be more costly than non-retractable systems.

**2.1.3.5 Complex systems**

There are several complex deployment mechanisms which cannot be easily defined based on deployment. The movement can be similar to the mentioned ones but the nature of moving of each structural unit and the source of movement is different from the mentioned systems.

One of these special mechanisms is tensegrity deployment. The deployment is similar to accordion ones but with torsion of structure blocks like mobile tensegrity systems proposed by Motro and Bounderbala (1996). During deployment sequence, each set of cables and struts is rotated while the cables are raised gradually by stressing.

**2.1.4   Summary of current spatial systems**

Various spatial systems have been developed in academic records and in practical designs. This thesis covers a wide range of spatial systems, which are dominant in civil engineering applications. Double-layer grid systems are among the most common spatial structures in practice. Besides, tensegrity is recognised with its special design concept, which is suitable for lightweight systems with high aesthetic value. Recently, cable-strut appears to be an alternative of tensegrity with high structural efficiency which enables the application of cable-strut systems in heavily loaded roof structures. All of the mentioned spatial systems are not yet designed to facilitate transportation and construction. The deployability is needed for a structure to be folded in a compact form, which eases transportation, and to be deployed to cover a large area for utility. Such designs are essential in space applications and are of growing interest in civil engineering industries. However, the current deployable systems are not yet structurally efficient as a trade-off for the construction time savings. Distinguished from the mentioned systems, a novel structural concept, which is deployable and structurally efficient, will be introduced in the chapter 3 of this thesis.

In geometric design, a structural concept can be expanded to different structural configurations. The concept itself is created by human effort but the various associated geometries can be generated by either human or computer-based effort. This geometric design issue will be discussed in the section 2.2.

## 2.2 Computer-based generative designs

Novel structural concepts as those introduced in section 2.1 can be generated using three major approaches.

The first and still now the most effective one is the brainstorming process by designers as many of them can be found in references of section 2.1. The novel concepts are derived based on designers' experience and creativity. However, individual creativity cannot be extensive comparing with computer power.

The second approach is computer-based generative design in which new structures are generated by computer under prescribed constraint such as geometry, loading and capacity and following some rules of geometry. This pure computer-based approach has significant development in recent 20 years while the speed of computer is continuously improved. The advantage of this approach is to make use of computational energy of computers and thus extensive designs can be generated and compared. However, the use of this approach in practical design is still limited because the proposed design language is yet compatible well with computer languages although description of geometry can be well embedded in computer algorithms by some mathematical tools such as formex (Nooshin and Disney, 2000 – 2002). Another reason is that the proposed design process may not be computationally affordable. In other words, the human creativity for design cannot be competed by computer language at this moment.

The third approach is a hybrid approach, which is a combination of the first two approaches. In this approach, the computer-based design engine should be designed to interact with human feedback to learn designers' experience, (Eckert *et al.*, 1999; Sim and Duffy, 2004). Such interactive interface is so complicated that currently no

significant achievement has been recorded. Therefore, the second approach will be of interest in this thesis and its relevant literature will be presented below.

Creation and optimisation are the two major processes in generating designs. The creation of structural designs requires thorough understanding of generated subjects, e.g. trusses, frames, and establishing a suitable shape grammar in computer language, (Brown and Cagan, 1997; Shea and Cagan, 1999). For most design problems, the space of possible designs is immense but the space of impossible designs is much larger. A shape grammar is used to represent the relation between shape and function of the subject, (Stiny, 1980) and thus application of shape grammar in creation can keep creative designs away from impossible families. Optimisation process requires iterative assessments, which is based on certain design criteria, and iterative modification of the design in terms of structural element sizes, shapes, and topology of the whole structures. This process is to assure the feasibility and the competitiveness of the proposed designs. The creative shape of structural design only is not yet a conceptual design.

## 2.2.1   Shape grammars in design generation

For any type of structure, the structure's shape can be featured by certain rules, called shape grammar. Initially, the shape grammar can be used for architectural purposes to represent a certain design style by computer language such as the one for the Queen Anne house (Flemming, 1986). Because the structure's function is related to its shape, a shape grammar may be expanded to represent function's grammars (Mitchell, 1991). Implementation of such concept in computer language can be found in works by

Westerberg et al. (1990). However, the shape grammar cannot replace all physical constraints on the structure except the distinct physical features such as the triangular form of planar trusses (Kawamura *et al.*, 2000), rectangular form of planar frames (Shea, 1997; Shea and Cagan, 1999). Therefore the optimisation process is needed to satisfy both geometric and physical requirements.

### 2.2.2 Optimisation process

Constructions are of very high values and optimisation of designs is essential to assure feasibility if not competitiveness of the solution. Currently, it is a common practice to optimise a design by human engineering resources (El-Sheikh, 1998). The design is optimised by parametric study of shapes and sizes of the structure. However, because such an engineering work is tedious and iterative, it is a wide interest to implement optimisation of designs in computer language. There can be two computer-based methods to optimise designs, which are deterministic and stochastic methods (Bulman *et al.*, 2001).

The deterministic method allows the designer to obtain an optimal design with a prescribed structural concept. In deterministic optimisation, structure's shape and structural components' sizes are changed and the whole structure is analysed iteratively to check the new design with the optimisation criteria (Song and Baldwin, 1999). A specific non-optimised design and pre-defined grids should be provided as input and the optimisation is operated from that design. This method can be ineffective when the design problem is complicated.

In contrast to deterministic method, the stochastic method can provide a near optimal design. There would be no guarantee that the derived design is the optimal one (Bendsoe, 1995). However, the resultant design topology may go beyond human imagination with optimum-orientation. In stochastic method, the evolutionary algorithms are applied such as genetic algorithm (Coelloa and Christiansen, 2000; Miles *et al.*, 2001), simulated annealing (Leite and Topping, 1999; Park and Sung, 2002), or genetic programming (Yang and Soh, 2002). The material flow is located for efficiency of the design without any pre-defined grids. For this reason, stochastic method is a flexible tool for generating optimised design configurations. Due to the computational cost, the stochastic method is used for conceptual design while the final design should be done by engineering convention (Shea and Zhao, 2004).

### 2.2.3   Summaries of computer-based designs

Computer-based generative engines can provide a variety of alternative geometric forms for design. Furthermore, the integration of shape grammar and stochastic optimisation process can provide optimisation-oriented designs with insight into structural performance of the design. However, the available shape grammar is developed for truss and frame only. In this thesis, based on the study on structural morphology, shape grammar for Deployable Tension-Strut Structures (DTSS) is presented as a basis for further development on computer-based design of DTSS in chapter 3.

Once structural concept and its configuration are settled, the next stage of design is evaluating structural performance of the system and sizing the structural component by

structural analysis. In section 2.3, the background literature, which is suitable for analysis of tension-strut structures, is covered.

## 2.3 Non-linear structural analysis

Two dominant methods of structural analysis can be used to investigate the structural behaviour of tension-strut structure; one is analytical method and the other one is finite element method.

### 2.3.1   Analytical method

Analytical method is applied to investigate relatively simple structural behaviour. High accuracy is the major advantage of this method and thus analytical method can be used for verification of other methods (Yau and Yang, 2003). However, the computer-based implementation of this method is limited though matrix forms of this method are available in literature (Hangai and Wu, 1999; Kenneth and Uang, 2005). For complicated structures with non-linear behaviour, finite element method is easier to be implemented in computer language than analytical method.

### 2.3.2   Finite element method

Finite element method (FEM) is applied in analysing complicated structures, which have either large number of structural components, or non-linear behaviour. Most structural systems are complicated, especially non-linear tension-strut structures and thus FEM is preferred to analytical method in practice. However, the accuracy of FE

analysis is subjective to the choice of formulation implemented in the software and the input by users. To obtain relatively good analysis results, the structural features of tension-strut structure should be understood and appropriate FE formulation is used.

**2.3.2.1 Structural features of tension-strut structures**

Tension-strut structure consists of slender elements. Slenderness ratio ranges from 70-110 and 250-400 for struts and cables, respectively. While struts act as beam-column elements, cables are considered tension elements, which have neither compression nor bending stiffness. In the vertical planes, struts are connected by real pin joint to allow deployability. In the perpendicular direction, these struts are moment-connected. The numerical modelling and design detailing should account for such features.

Because common metal such as aluminium or steel is used (Escrig, 1996; Motro, 2005; Wang, 2004), strains of structural elements are expected to be small during load bearing period of the structure for safety. Besides, cable elements used in structure behave non-linearly due to stiffening effect of internal tension force while struts are affected by P-delta effect due to internal compression forces. For these reasons, non-linear small strain large displacement modelling is appropriate (Bathe, 1996).

However, non-linear analysis is computational expensive because the required load level is often divided into many smaller load steps and the analysis is iterative. In contrast, only one load step is required for linear elastic analysis and thus linear analysis might be accepted for preliminary assessment of structural behaviour and

sizing structural components (Pellegrino and Calladine, 1986; Calladine and Pellegrino, 1991; Kawaguchi, 2003).

**2.3.2.2 Non-linear finite element formulation**

The theory behind the analysis must be non-linear with large displacement and small strains to satisfy structural features mentioned above.

There are two non-linear finite element formulations (NFEM) for frame structure analysis, Total Lagrangian formulation and Updated Lagrangian formulation (Bathe, 1996). These formulations allow non-linear analysis with implementation of large displacement features. On elemental level, nonlinear behaviour is accounted for by adding second order strains and updating element axes throughout the deformation process. On global level, the nonlinear effect is represented by updating nodal coordinates after each load step, which is related to the second variation of potential energy below.

The formulation is consistent with variational principles, which is based on variations of potential energy. The first variation of potential energy is used for equilibrium iteration in each load step. This phase can be referred to as predictor. The second variation of potential energy (in incremental form) is the basis for calculation of incremental stiffness. This phase can be referred to as corrector. Finally, checking convergence criteria is needed to terminate these two iterative phases (Yang and Kuo, 1994).

Based on the above theoretical basis, the general procedure is summarised as time history load step with main step solved for incremental stiffness and with the small iteration steps in each main step solved to update the equilibrium status of the structure (SINTEF report, 2003).

The iterative feature of the current non-linear finite element procedure is due to the fact that linear algebra is used to handle non-linear problems. Linear algebra is strong when it is the basis to solve linear problems. However, because linear algebra cannot solve non-linear problems, the structural non-linearity is approximated by many continuous linear problems with fragmented load steps to be compatible with the available computer-based linear algebra tools. In general, the non-linear problems are transformed to suite the available linear mathematical tools. However, the recent development of commutative algebra, which is used to solve polynomial systems, promises that commutative algebra can be used to solve non-linear structural problems. This prospect will be presented in chapter 4 of this thesis.

### 2.3.2.3 Modelling of pre-tensioned structures

Cable/rod has high slenderness as mentioned in section 2.3.2.1. It is expected to be tension-resistible during the load bearing process. Therefore, these tension elements can be slackened when the tension force disappears. To keep tension-strut structure stable, proper level of pre-tensioning needs to be applied and in most cases the pre-tension force is determined from analysis. Therefore appropriate numerical modelling of pre-tensioned tension element is essential to design of tension-strut structures.

Several methods of introducing pre-tension in numerical modelling have been proposed such as force method (Hanaor, 1988; You, 1997) or simplified force method by Kawaguchi (2003), displacement method (Argyris and Sharpf, 1972), theory of extensional and inextensional moded (Pellegrino, 1990). However, in this research FEM is used to model pre-tension effect (Talvik, 2001; Lee, 2001; Liew and Lee, 2003) to facilitate the design of tension-strut structures in combination with other structures such as support frames or trusses, which is based on FEM.

Modelling pre-tensioning force in cables cannot be modelled directly in commercial softwares. Physically, pre-tensioning force is a factor to increase stiffness of cables and is proportional to axial deformation of cable element. It was proposed by Lee (2003) that this internal load can be modelled equivalently by thermal load as shown in equation (2.1).

$$P = -\alpha \Delta TEA \qquad\qquad\qquad (2.1)$$

in which

$\Delta T$ = equivalent temperature load ($^{o}$C) ($\Delta T < 0$)

$P$ = pre-tension force ($P > 0$)

$E$ = modulus of elasticity of material

$A$ = nominal cable section area

$\alpha$ = coefficient of linear thermal expansion ($12 \times 10^{-6} /^{o}$C for steel)

Actually, the pre-tensioning process is done step by step to obtain the required pre-tension force or displacement or deformation. The designed values cannot be obtained directly because of the force re-distribution inside the structure. The same problem

happens in numerical modelling of structure. So analogously, the pre-tension force (temperature) is imposed step by step onto the structure and the nonlinear analysis is required to obtain the correct structural response.

The equation (2.1) can be verified by simulation of a pre-tensioned cable. A steel cable with diameter of 1mm and length of 600 mm is modelled in SAP 2000 (Non-linear version 7.40). At the two ends of the cable, three degrees of freedom of translations are restrained. This means the two ends of the cable cannot be moved. Assume that 150 N pre-tension force need to be applied in the cable.

According to the equation (2.1) $\Delta T = -\dfrac{P}{\alpha EA} = -\dfrac{150}{12\times10^{-6}\times205000\times3.14/4} = -78^0 C$
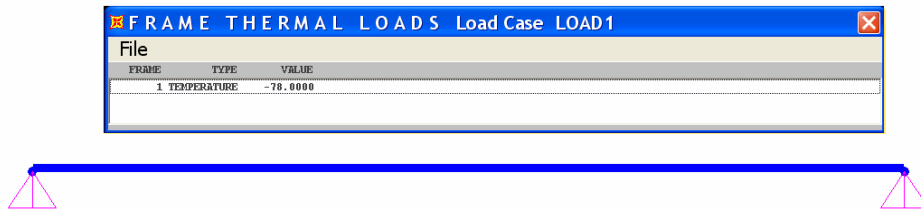


Figure 2.10. Temperature load (-78$^o$C).
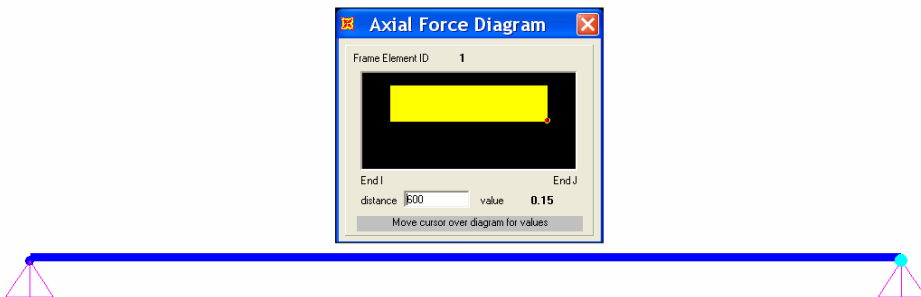


Figure 2.11. Corresponding pre-tension force (0.15 kN).

Apply this temperature force into the modelled cable. The result by this simulation shows that the internal force in the cable is exactly 150 N as shown in Figs. 2.10 and 2.11.

In non-linear formulation mentioned above, the contribution of pre-tension force is accounted for in two sides of the equilibrium equation. One side represents internal forces, and one side represents external forces.

On the side of internal force, the pre-tension force is acknowledged in the non-linear part of work and contributes to the stiffness matrix by affecting non-linear strain as shown in equation (2.2).

$$\int_V \{\delta \overline{n}_t\}^T \{\sigma_t\} dV = \int_V \{\delta u_X\}^T \{\overline{\sigma}_t\} \{u_X\} dV = \{\delta d_i\} \{K_n\} \{d_i\}_{\Delta t} \qquad (2.2)$$

On the other hand, the work by linear strain and pre-tension stress is introduced in terms of equivalent nodal load, equation (2.3).

$$-\int_V \{\delta e_t\}^T \{\sigma_t\} dV = \{\delta d_i\}^T \int_V \{f_{body}\} dV = \{\delta d_i\}^T \{f_{int}\} \qquad (2.3)$$

in which

$\{\delta \overline{n}_t\}$ matrix of variation of nonlinear Green strain at time step t

$\{\sigma_t\}$ matrix of pre-tensioning stress at time step t

$\{\delta u_X\}$ matrix of variation of displacement at time t

$\{\delta d_t\}$ matrix of variation of nodal displacement at time t

$\{K_n\}$ nonlinear part of stiffness matrix at time $t + \Delta t$ (assume)

34

$\{\delta e_t\}$ matrix of variation of linear Green strain at time step t

$\{f_{body}\}$ matrix of body force, caused by pre-tension force at time t

$\{f_{int}\}$ matrix of equivalent nodal load (in external loading side of the equilibrium equation).


## 2.4 Summaries


This Chapter reviews existing spatial structural systems, and discusses the major features of these systems regarding structural efficiency (including material cost and load bearing capacity) and construction efficiency (including speed of construction and corresponding on-site management effort). It is realized that neither of the existing design proposals is considered highly effective in terms of both structural efficiency and construction efficiency. The concept of Deployable Tension-Strut Structures is emerged in this context to fill in this gap. This structural concept is to be introduced and explained in Chapter 3 of this thesis.


Generative design issues are also reviewed regarding shape grammar and optimisation. Generative design allows creating a series of Deployable Tension-Strut Structures (Chapter 3). Structural analysis methods are also reviewed towards analysing pre-tensioned structures. This is an important tool for investigation of the structural behaviour of the proposing structural concept.

# CHAPTER 3

# STRUCTURAL MORPHOLOGY AND FORM CREATION

While space truss systems are believed to possess high structural efficiency, deployable structures are realized to facilitate transportation and on-site construction because of their deployability as explained in chapter 2. This Chapter presents an attempt to combine the advantages of space trusses and deployable structures in only one structural system, Deployable Tension-Strut Structures (DTSS). The concept of DTSS is proposed in this chapter and followed by a study on structural morphology of several proposed DTSS forms to provide insight into their functionality and structural stability condition. Although several basic forms of DTSS are proposed for study in this thesis, it is questionable that they are all the possible forms of DTSS or not. A computer-based approach for exhaustive search for morphological designs of DTSS is proposed to answer this question. It is found out that more DTSS forms can be feasible and thus designers have a wide range of alternative forms for their industrial designs. The study in this Chapter is qualitative while the quantitative study is to be presented in Chapter 5.

## 3.1 Deployable Tension-Strut Structures

The concept of Deployable Tension-Strut Structures (DTSS) is developed to aim for both structural efficiency and construction efficiency, a combination of advantages of conventional space frames and deployable structures which are reviewed in Chapter 2. The proposed system consists of cables and struts, where struts are connected together to form a continuous kinematic chain. Cables act as a locking mechanism. After

manufacturing, DTSS are folded in compact form due to the kinematic chain of struts and the slackened cables to ease transportation. On site, DTSS are deployed and several cables are tensioned to form a rigid, stabilized structural system for load resistance purpose. The arrangement of cables and struts causes structural efficiency while the connections of struts allow deployment. Section 3.2 explains this arrangement and its relations with deployability and structural stability. These relations are used in the exhaustive designs of DTSS which is presented in section 3.3. In the beginning of the research, several DTSS forms are proposed as follows.

a)      Pyramid-On-Pyramid structure (POP), shown in Fig. 3.1a and 3.1b

b)      Pyramid-In-Pyramid structure (PIP), shown in Fig. 3.2a and 3.2b

c)      Pyramid-Pantograph-Cable structure (PPC), shown in Fig. 3.3a and 3.3b

d)      Pyramid-Pantograph-Pyramid structure (PPP), shown in Fig. 3.4a and 3.4b

**3.1.1 Pyramid-On-Pyramid Structure (POP)**

Pyramid-On-Pyramid structure is composed of two pyramids attached to each other at their base as shown in Fig. 3.1a. The "Pyramid" consists of four struts, connected at the center by a pinned joint, to which a detachable strut is attached as shown. This locking cable can be replaced by a telescopic strut which is likely to increase the mechanical complexity of the structure. The units may then be connected together to resist gravity loads with a network of cables attached to the bottom nodes as shown in Fig. 3.1b.  While the top layer of struts resist the compressive forces, the cables are ideally placed at the bottom of the structure to resist the tension and the diagonal members, forming the pyramid resist, shear forces. However, this arrangement is poor

in resisting uplift loads, which may require an additional layer of cables at the top nodes of the structure especially in conditions where the uplift loads may exceed the self weight of the structure.
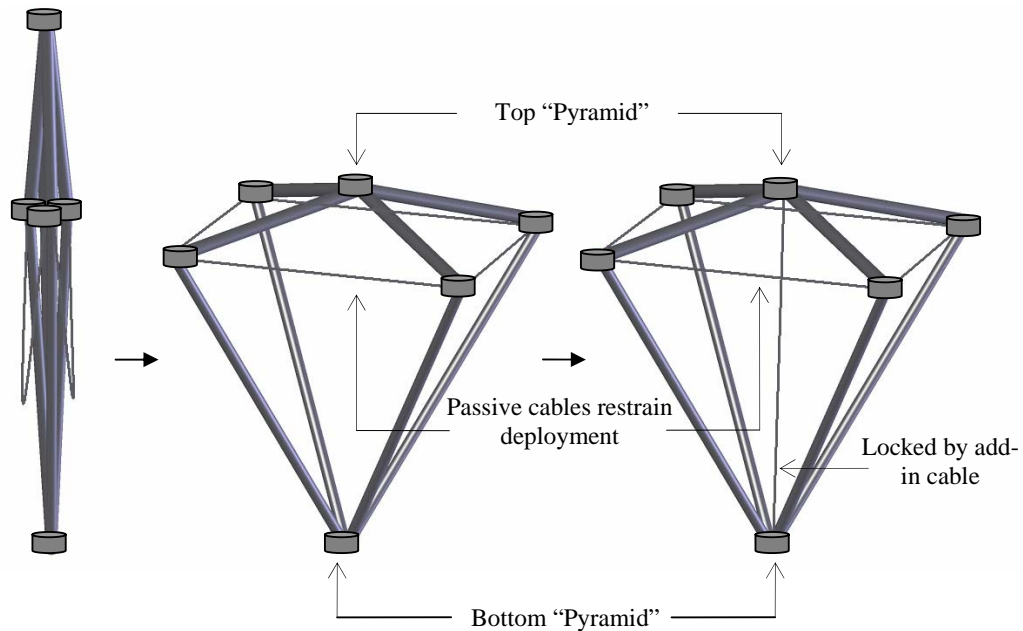


Figure 3.1a. Deployment of Pyramid-On-Pyramid structure.
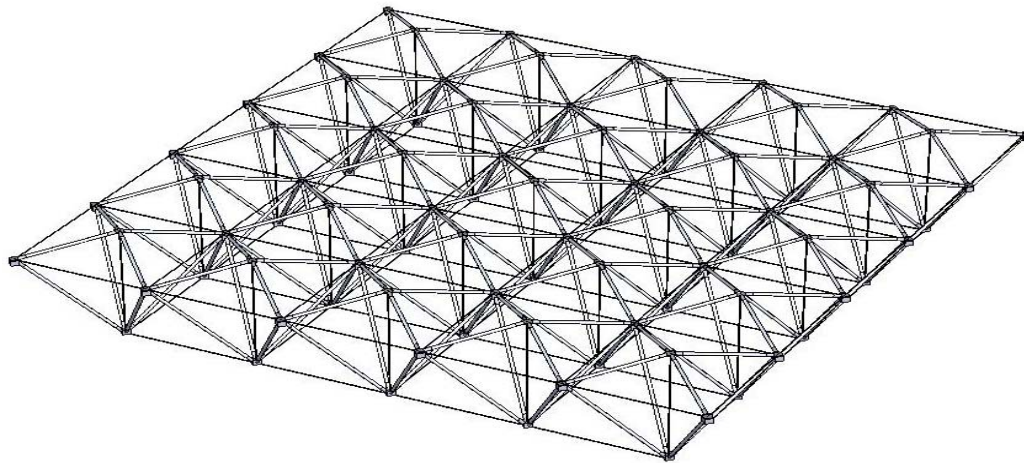


Figure 3.1b. Multiple modules of Pyramid-On-Pyramid structure.

**3.1.2 Pyramid-In-Pyramid Structure (PIP)**

Pyramid-In-Pyramid structure is composed of two pyramids attached at the base but within each other. The "Pyramids" are formed by four pinned connected struts as in the POP structure. The deployment of PIP is achieved by sliding the central joint along the central rod and locking in its final configuration as shown in Fig. 3.2a.
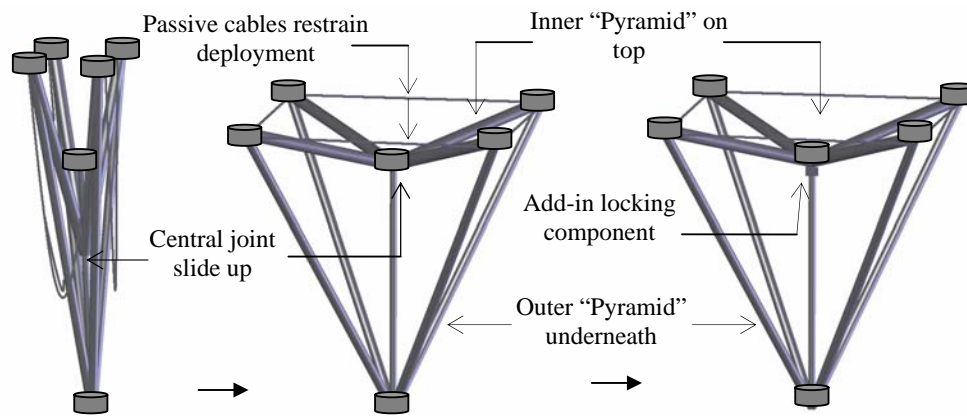


Fig. 3.2a. Deployment of Pyramid-In-Pyramid structure.
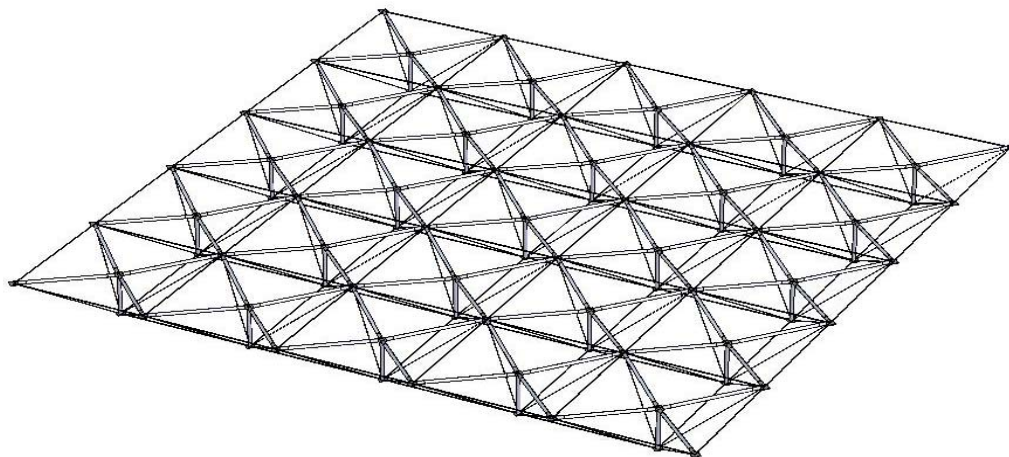


Fig. 3.2b. Multiple modules of Pyramid-In-Pyramid structure.

The key difference between this (PIP) and the POP structure is in the central rod which in the case of POP structure in tension and in the PIP structure is in compression. If the

central rod is made of cable (in POP)  and struts in (PIP) then the variations in their

elastic modules (elasticity of cables being 30% less that structural steal section)  and

the higher cross sectional area of the compressive strut contributes to the higher

stiffness of the PIP module. This advantage is however offset by the higher lengths of

the diagonal elements of the PIP structure compared with POP structure of similar

depth.


### 3.1.3 Pyramid-Pantograph-Cable Structure (PPC)
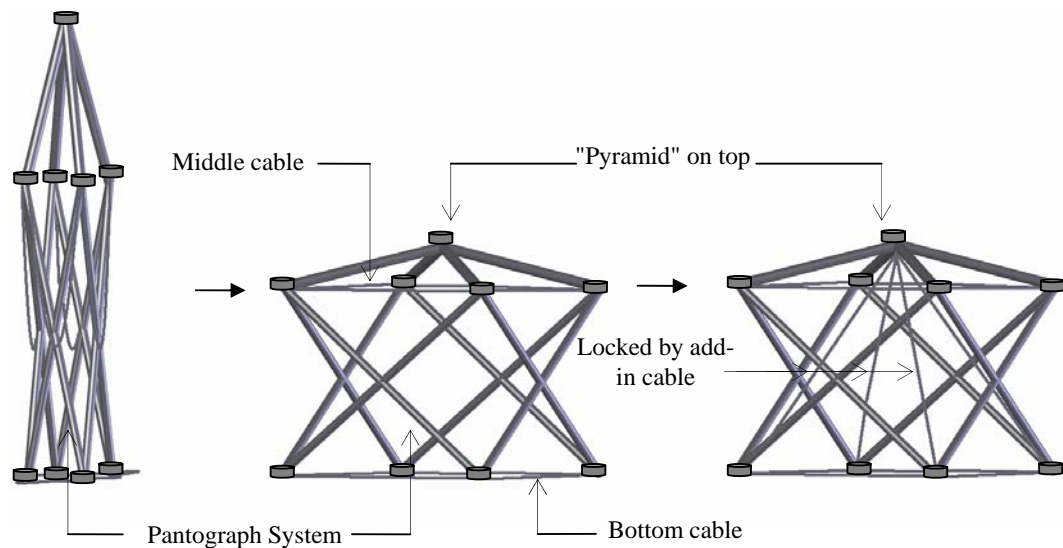


Fig. 3.3a. Deployment of Pyramid-Pantograph-Cable structure.

A new class of structures combing in scissor-like elements (SLE) and pyramidal

elements is proposed. These interlinked SLE forms a kinetic chain which increases the

depth and facilitates deployment of the structure. The Pyramid-Pantograph-Cable is

illustrated in Fig. 3.3a and 3.3b. The structure is stabilized into the deployed state by

attaching the locking cables to the top pivot. Under Gravity loads the compressive

forces are resisted by the top pyramid struts, the tensile forces are resisted by the

network of cables at the bottom of the structure and the shear forces are resisted by the

SLE system.
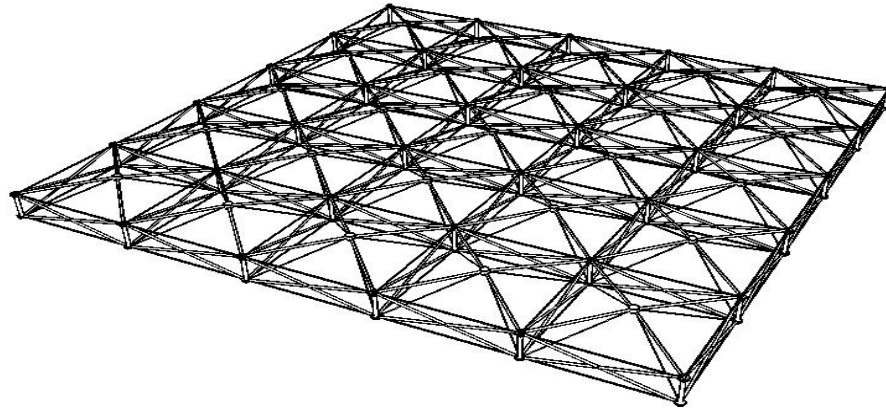


Fig. 3.3b. Multiple modules of Pyramid-Pantograph-Cable structure.

### 3.1.4 Pyramid-Pantograph-Pyramid Structure (PPP)
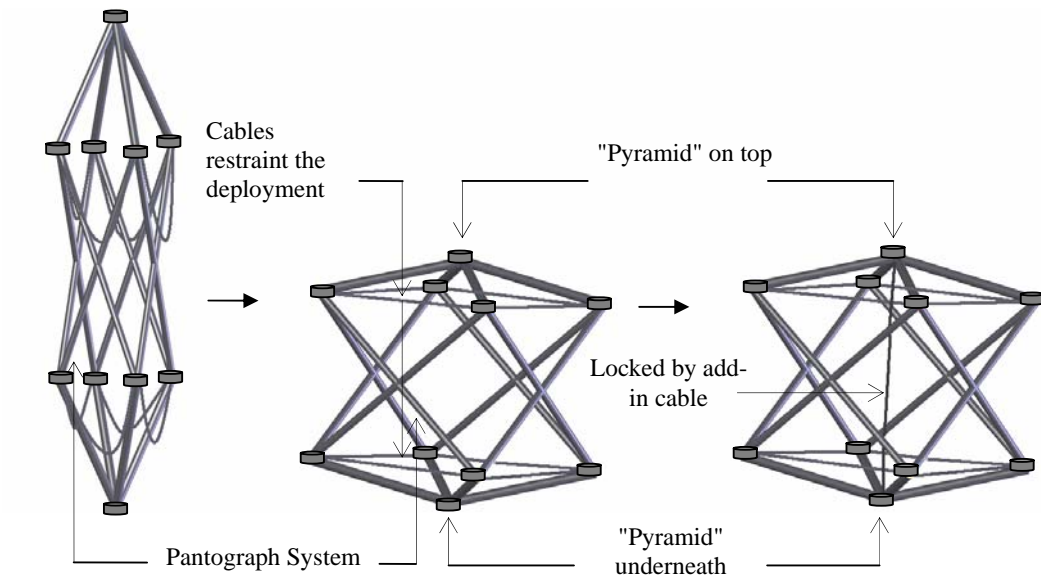


Fig. 3.4a. Deployment of Pyramid-Pantograph-Pyramid structure.

Pyramid-Pantograph-Pyramid structure (PPP) is another SLE-based system. A "Pyramid" is placed under the SLE system as shown in Fig. 3.4a and 3.4b. The

structure is deployed and stabilized by attaching and pre-stressing the central locking cable.

PPP system can resist both gravity and uplift wind loads efficiently. Under gravity loads, the top "Pyramid" resists compression while the bottom "Pyramid" and bottom cables resist tension. The pantograph system resists the shear forces. However, under uplift load the bottom "Pyramid" can resist compression force and the top "Pyramid" and the top cables will resist tension.
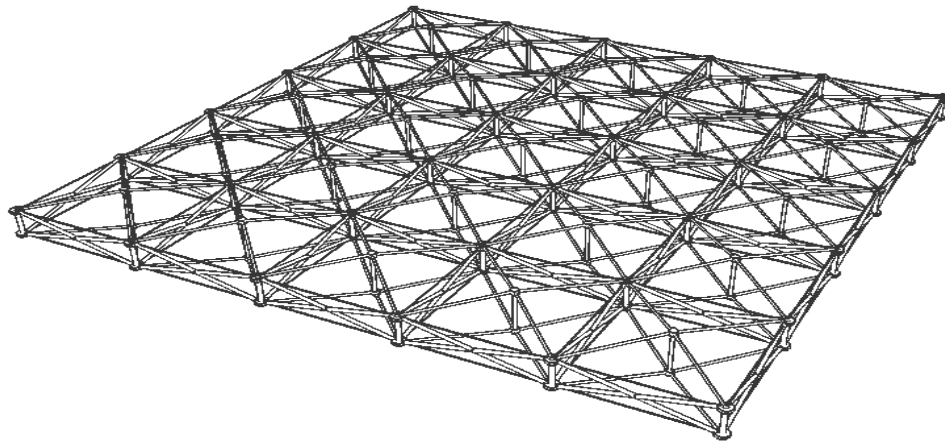
Fig. 3.4b. Multiple modules of Pyramid-Pantograph-Pyramid structure.

## 3.2 Structural morphology study

Two typical Deployable Tension-Strut Structures (DTSS), which are POP and PPP, are chosen for the study of structural morphology. The study is concerned with the change in geometry of DTSS when it is deployed and the method to stabilize the system after deployment. The change in geometry is related to the movement of the strut system of DTSS where one strut is connected to other struts at its two ends. This is different from the tensegrity structure where struts are not allowed to touch each other (Motro, 2003).

Cables are slackened during deployment and thus do not affect the deployment of DTSS.

The central line is the symmetric axis of a structural module, Figs. 3.5-3.6. Each module of DTSS is symmetric so the morphology investigation is performed in one part of the space and the axis of symmetry becomes important. When the structure is folded all joints move in vertical planes towards the central line. For POP structure, joint 1 moves in the vertical plane 1. Joint 4 moves in the vertical plane 2. Joint 2 and 3 move in the central line as shown in Fig. 3.5. For PPP structure, joint 1 and joint 2 move in vertical plane 1. Joint 3 moves in vertical plane 2. Joint 4 and 5 move in vertical plane 3 as shown in Fig. 3.6. This means all the struts moves in vertical planes. In the folded configuration, all struts are on the central line no matter what is the deployed shape. At conceptual level, struts are represented by lines and the physical size is not considered. A strut should be allowed to rotate independently with other struts in the same vertical plane. The conclusion is that no triangular shape is formed by struts in any vertical plane to allow the free rotation between struts.
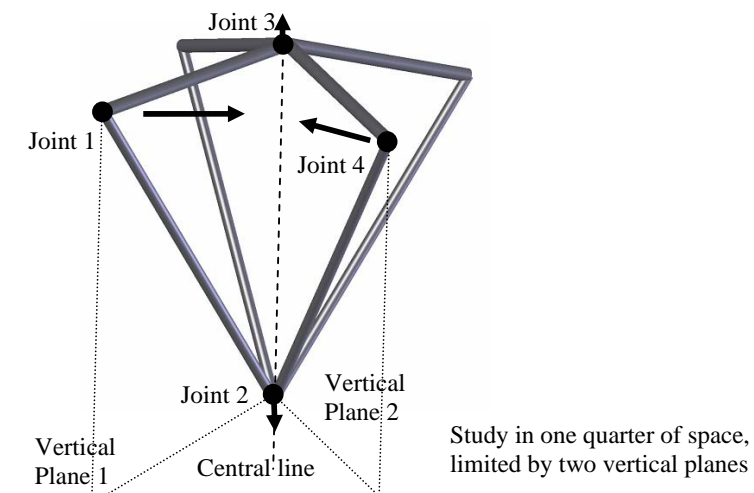


Figure 3.5. Joint movement in folding POP.

In the final folded configuration, the whole module can become a line geometrically. Therefore horizontal planes which go through nodes are separated by equal-length struts. For PPP structure, Fig. 3.7, horizontal plane 1 goes through node J1. Horizontal plane 2 goes through node J2 to J4. Horizontal plane 3 goes through node J6 to J9 and so on. Struts between plane 1 and plane 2 are S1 to S4. All these four struts, S1, S2, S3, and S4, should be of the same length to allow foldability.
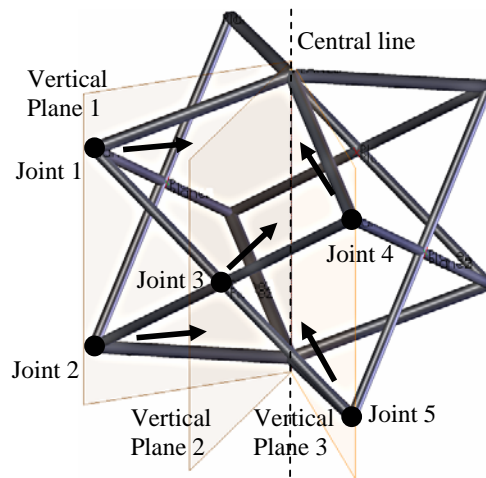


Figure 3.6. Joint movement in folding PPP.
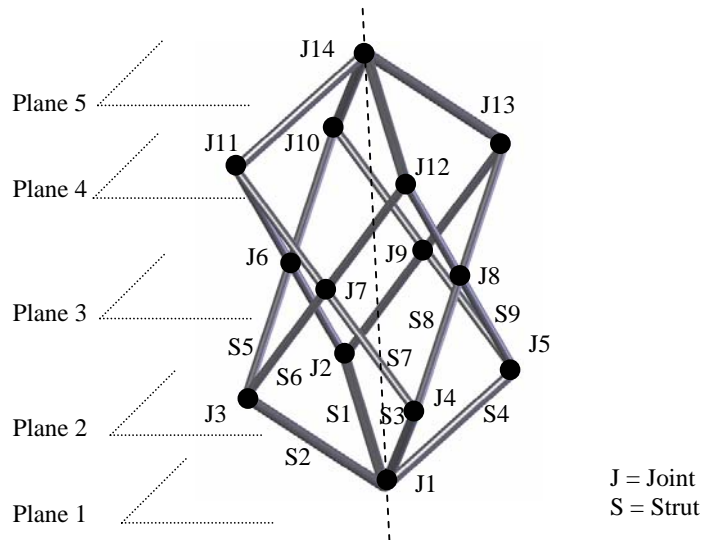


Figure 3.7. PPP structure with corresponding horizontal planes.

No strut exists in the horizontal plane while the structure is being deployed. If a strut is in the horizontal plane, it will reduce the compactness of the structure when the structure is folded. In the final deployed configuration, whether a strut can be on the horizontal plane or not depends on the later stage of analytical parametric study, which is discussed in chapter 5 of this thesis.

To summarize, the geometric rules can be set up due to structural stability and deployment requirement as follows

Nodes are able to move in vertical planes towards the central line

Strut system is continuous

No triangular shape is formed by struts in a vertical plane

Sums of Struts' length between any two different horizontal planes are equal

Struts are not in horizontal planes when DTSS is deployed

These criteria are used to generate more alternatives to the proposed design of DTSS as shown in section 3.3.

## 3.3 Form creation by exhaustive design approach

### 3.3.1   Overview of exhaustive design

For any structural system, once the concept is realized, many geometric structural forms can be created. The creation can either be human or stochastic as mentioned in chapter 2. In this section, exhaustive designs of DTSS are created by a deterministic exhaustive approach where the outcome is under better control than by stochastic method and is more diverse than creation by human.

Structures can be designed to be grid-free or to be repetition of basic structural modules, which are allocated on grids. The first method of designing structure is currently not preferable due to unfeasible cost of manufacturing. Without module or grid, the structural elements will be of various length and specifications. If the second method is used, the rule of symmetry is commonly applied for each structural module. In this research, conceptual design follows two architectural rules of aesthetic, symmetry and repetition. If the repetition rule is applied, the source of creativity is based on the various geometries of structural module. One of these structural modules can be multiplied to be a structural system as shown in Figs. 3.1-3.4. The idea of exhaustive conceptual design is to generate the modules' geometries as alternative to the available forms to assist architects when a new structural system is in demand. The derived geometries need to be in tight relation with the functionality and structural stability conditions as shown in Fig. 3.8.
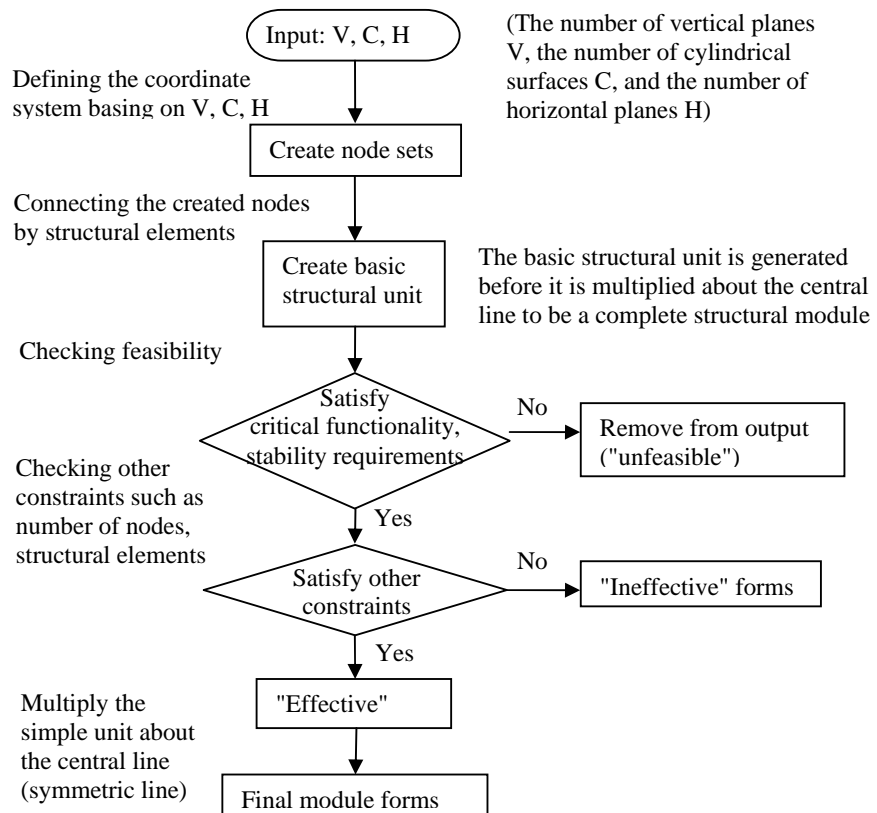


Figure 3.8. Exhaustive conceptual design.

In exhaustive conceptual design, the structure's grid is generated before nodes, and then structural elements are generated to connect nodes and form basic structural units. All the possible geometries are generated due to the exhaustive generative engine and the unfeasible ones are filtered out by filtering engine, which is built with regards to the stability and functionality conditions. Because all possible geometries are generated (for a specific input), the approach is exhaustive. Also, when unfeasible geometries are filtered out, the number of output is minimal. However, the number of output can still be very large. The approach allows the control over excessive number of output by controlling the number of structures' grids as an input.

The generated structural module is based on a system of grids, which are cylindrical surfaces, horizontal planes, and vertical planes. The symmetric axis of a structural module is called the central line and considered as a reduced cylindrical surface. Therefore, all cylindrical surfaces take the central line as their symmetric axis while all vertical lines go through it. Planes and surfaces are numbered in order and if the number of surfaces and planes are given, the grid is unique. Basing on these defined grids, each node of the structure is defined as an intersection of one cylindrical surface, one vertical plane, and one horizontal plane, Fig. 3.9.
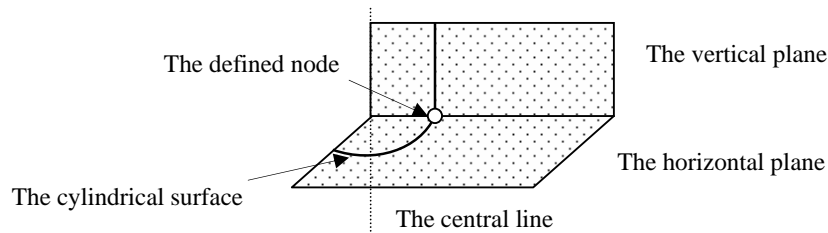


Figure 3.9. Defining one node of DTSS in the space.

When the grid system is given, all the nodes defined by this grid system are numbered in order e.g. from 1 to N. However, generated structures only go through a certain number of nodes e.g. m. The potential set of nodes, where the generated structure goes through, is chosen from the grid system by a selection algorithm, Fig. 3.10.

Input

(Given N ordered items) — N items numbered: 1, 2, …, N

(In output type) — Starting set of m chosen items: 1, 2, …, n-1, n → Set 1

(In output type) — Create to set of m chosen items: 1, 2, …, n-1, n+1 → Set 2

……

(In output type) — Create set of m chosen items: 1, 2, …, n-1, N → Set (N-n)

(In output type) — Create set of m chosen items: 1, 2, …, m, n+1 → Set (N-n+1)

……

(In output type) — Last set of m chosen items: N-n+1, …, N-1, N → Set $\dfrac{N!}{(N-n)!n!}$

End

n is counting index
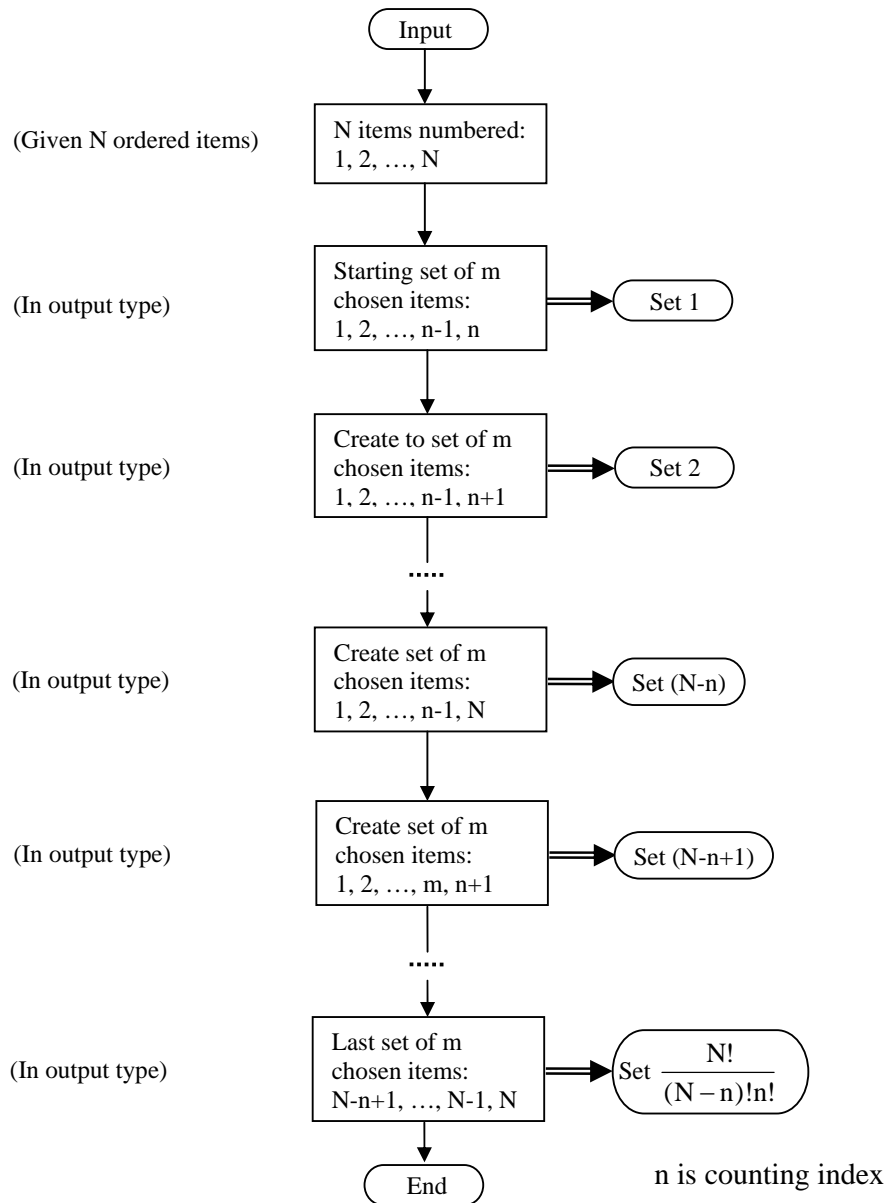
Figure 3.10. Selection algorithm to create all possible sets of node from a set of node.

For each set of nodes, structural elements are generated to be connections of two pre-defined nodes. The definition of structural element through two nodes has been used in

finite-element commercial software such as USFOS, Sintef, Norway. The current algorithm deals with frame system, not membrane, plate, and shell. The generated system of structural elements form a basic structural unit (BSU), which will be later multiplied about the central line to be a complete symmetric structural module (SSM). The use of cylindrical surfaces in the coordinate system of a structural module allows unlimited multiplications to create SSM. In conventional description of space structures, perpendicular coordinate system is used and thus the generated structures will be limited to four multiplications of BSU about the central line. It is noted that the generated BSU needs to go through all planes and surfaces in the pre-defined grids. This is to assure that each set of number of planes and surfaces will be associated with a unique set of generated BSU.

There are many BSU generated with a set of number of planes and surfaces. However, only "useful" forms are kept for output with the assistance of the filtering engine. The filtering criterion to define "useful" form is based on the functionality and structural stability conditions of the SSM.

Graphic outputs are interpreted from matrix of node coordinates and matrix of structural elements. The output format only provides information about the relative position of nodes and structural elements in the space. There is no dimension relation among nodes of the derived BSU. The optimised dimension relation among nodes and the sizes of structural components need to be determined by analytical parametric study.

### 3.3.2 Sample implementation of exhaustive design algorithm

Following the proposed exhaustive algorithm, alternative structural forms of DTSS are generated to adapt to given kinematic and stability requirements in section 3.2.

Because of the rule of repetition and symmetry, generating new DTSS forms is simplified to generating BSU of DTSS which is in the form of being deployed. The final structural module can be three times or more fold of BSU around the central line. It is noted that in the previous sections, the concept of BSU is used. In this section, BSU is replaced by basic strut system (BSS) because the cables, components of BSU are not considered. Only after the BSS is derived, horizontal cables are added to the joints which are not on the central line. These cables are tensioned to stabilize BSU when the add-in components are attached to the suitable nodes, which are most effectively on the central line. Therefore if the BSS is generated all other components of DTSS can be added in a straight-forward manner. The following discussion will focus on generating BSS only.

The basic strut system in the conceptual geometric form is defined basing on a coordinate system of surfaces, including vertical planes, horizontal planes, and parts of cylindrical surfaces, Fig. 3.9.

The proposed algorithm starts when the number of vertical planes, cylindrical surfaces, and horizontal planes are given as input, named as V, C, and H respectively. The generating engine will create all possible sets of nodes for the number of nodes ranging from 3 to H (V(C-1)+1). All the planes and surfaces should be used to define nodes. For each set of nodes, the struts are simply the connections of the created nodes. It is assumed that all struts are pinned-connected in its vertical plane. At the end of this step, a large number of all possible BSS are generated basing on the given V, C, and H.

The filtering engine works when all possible BSS are found with a given coordinate system. The deployability requires that no closed triangular shape is formed by the strut system as mentioned above. Also, the compactness of DTSS requires that no strut is on the horizontal planes. The generated DTSS which does not satisfy these two requirements are removed from the outcome of the algorithm as they are considered "unfeasible". Because of these strict filtering criteria, the number of outcome DTSS is minimal.

The DTSS is considered to be stabilized effectively if the add-in component is on the central line only. This would happen when there are at least two nodes on the central line without any strut between them. If the add-in components are not on the central line, there will be three or more add-in components because the structure is symmetric around the central line. In this case, the stabilizing procedure is more tedious in practice and the details of the joint are more complicated than that for the effectively stabilized DTSS. The generated DTSS, which have more than one add-in component, will still be put in the outcome of the algorithm but with the label "ineffective". The other forms will be labelled "useful". The proposed algorithm can be summarized in a flow chart, shown in Fig. 3.11.

The algorithm can be implemented in a programming language. Two sets of input are used to test the proposed algorithm.
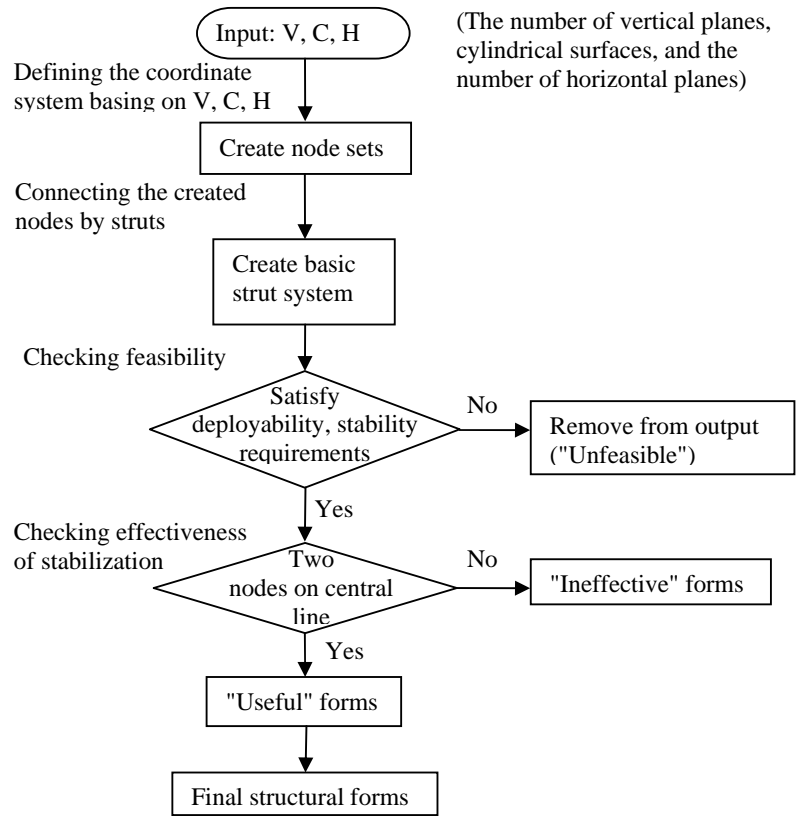
Figure 3.11. Algorithm to generate DTSS.

In this first input, the number of vertical planes V = 1, number of cylindrical surfaces C = 2, and the number of horizontal planes H = 3. The corresponding coordinate system and the all the possible nodes are digitised as shown in Fig. 3.12.
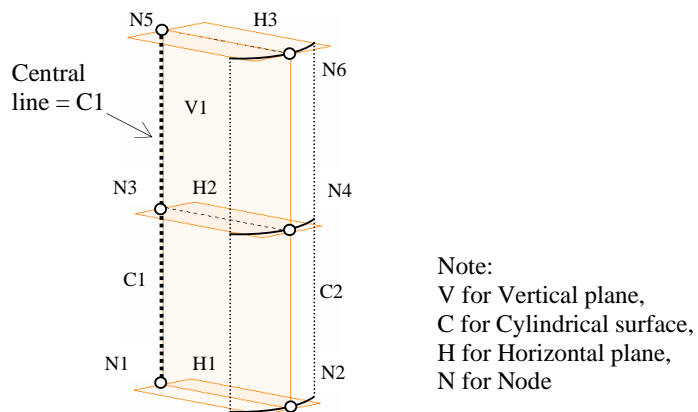


Figure 3.12. Coordinate system (V=1, C=2, H=3).

There are totally 6 possible node positions, numbered as N1 to N6. The number of nodes ranges from 3 to H(V(C-1)+1) = 6. The possible node sets with 3 nodes are shown in Fig. 3.13. Node set 1 and node set 8 are removed in the algorithm because only one cylindrical surface is considered while the requirement is to consider all planes and surfaces, which form the coordinate system. However, the drawings of these node sets are included in Fig. 3.13 to illustrate the exhaustive creation of geometric possibility.
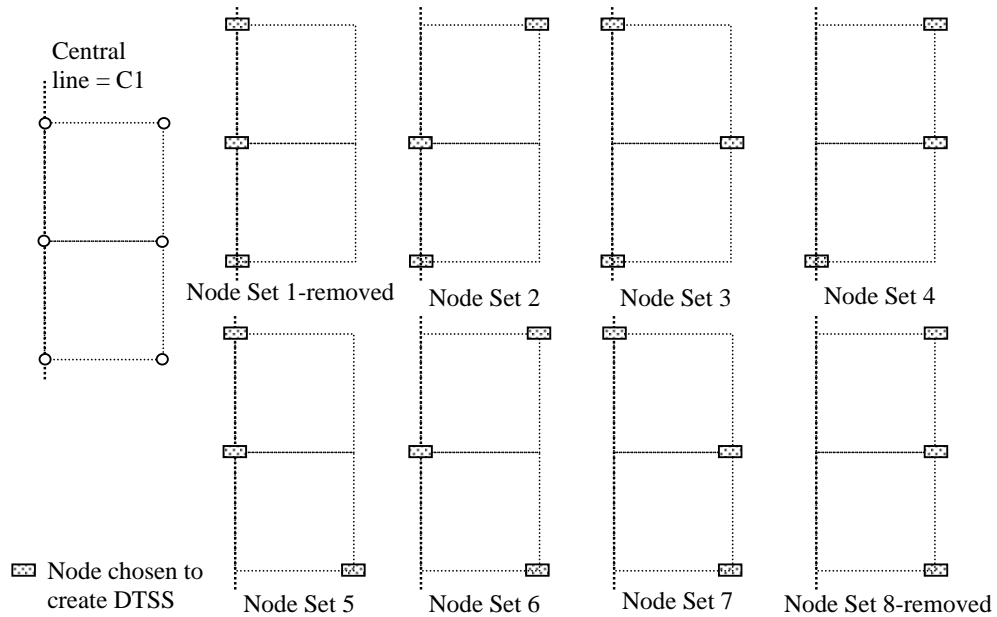


Figure 3.13. Sampling node sets (number of node = 3).

For each node set, different BSS are generated and the geometries are analysed to adapt to functionality and structural stability as summarised in section 3.2. Several samples of BSS, which are generated basing on the mentioned input with 3 nodes, are shown in Fig. 3.14. No BSS with 3 nodes is classified as "unfeasible" because all nodes are distributed in three horizontal planes. However, for BSS with more than 3 nodes, several forms are unfeasible as shown in Fig. 3.15.

| BSS 1 | BSS 2 | BSS 3 | BSS 4 | BSS 5 |
|-------|-------|-------|-------|-------|
| (effective) | (ineffective) | (effective) | (ineffective) | (ineffective) |
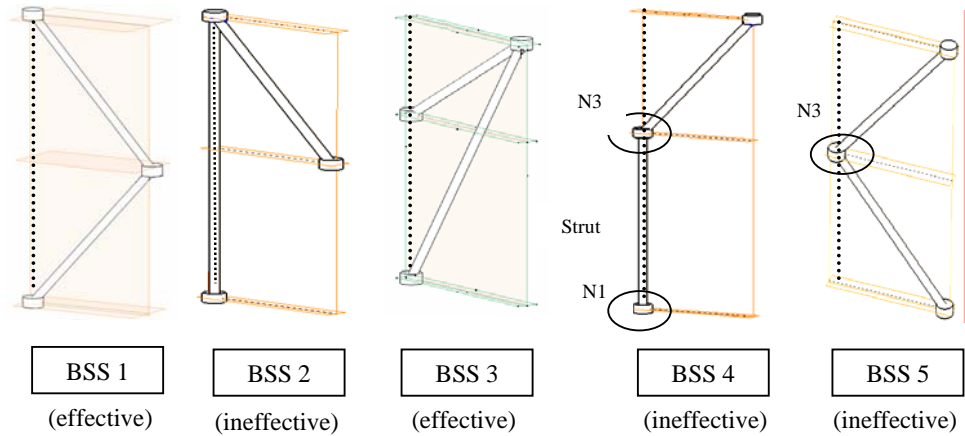
Figure 3.14. Samples of BSS corresponding to 3 nodes.



| BSS 6 | BSS 7 | BSS 8 | BSS 9 |
|-------|-------|-------|-------|
| (4 node BSS) | | (5 node BSS) | |
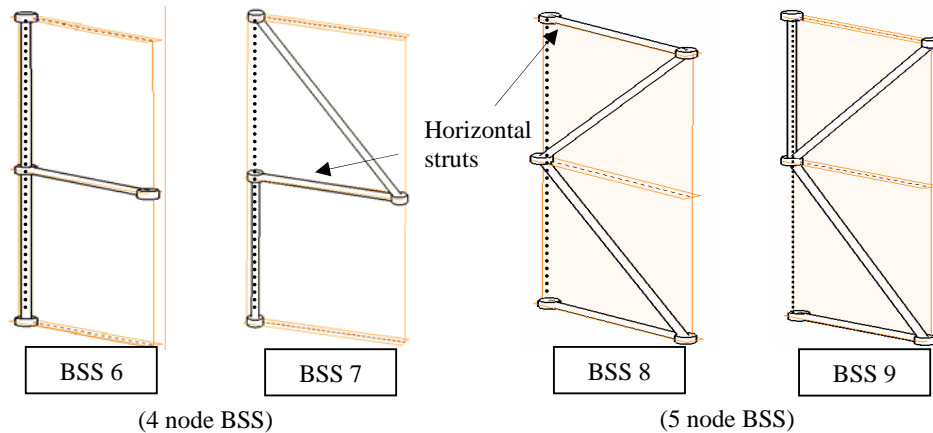
Figure 3.15. Samples of "unfeasible" BSS corresponding to 4 and 5 nodes.

BSS 1 and BSS 2 are based on the node set 3. However, BSS 1 is the "useful" form as it satisfies all requirements for deployability, stability, and stabilizing effectiveness while BSS 2 is an "ineffective" form because there is a strut connecting 2 nodes on the central line of BSS 2. This means that to stabilize the deployed SSM of BSS 1, there is only one locking component while there would be more than one locking component to stabilize SSM of BSS 2. The geometry of BSS 1, its four-fold SSM, and the locking/ stabilizing component are shown in Fig. 3.16. BSS 2 and its four-fold SSM and the four locking components are shown in Fig. 3.17.
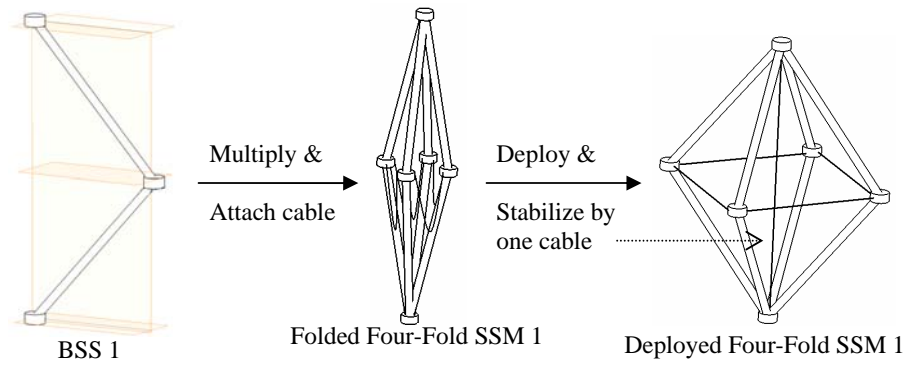
Figure 3.16. "Useful" BSS 1 and its SSM.
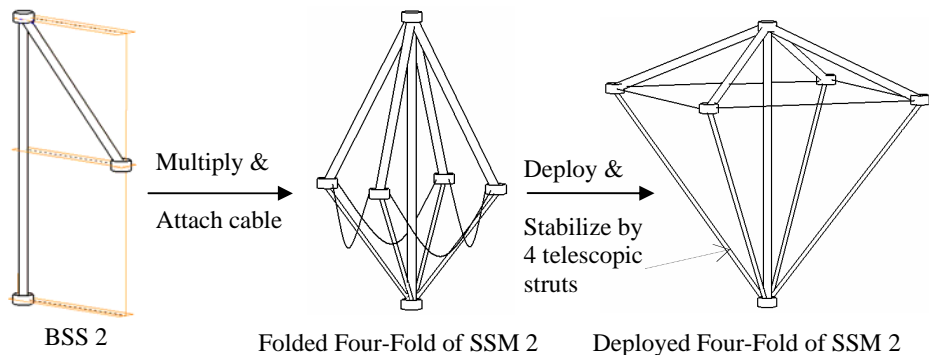


Figure 3.17. "Ineffective" BSS 2 and its SSM.
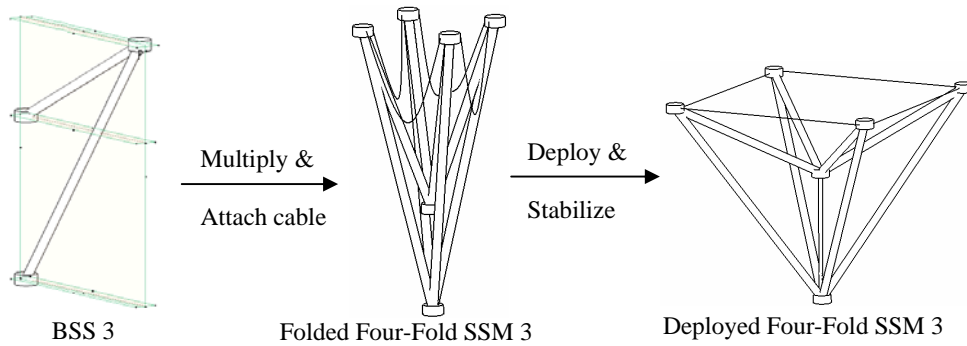


Figure 3.18. "Useful" BSS 3 and its SSM.

BSS 3 and BSS 4 are based on the node set 2. BSS 3 is a "useful" DTSS while BSS 4 is an "ineffective" DTSS. The reason is that SSM of BSS 3 requires only one locking component while four-fold SSM of BSS 4 requires four locking components because of a strut on the central line as shown in Figs. 3.18-3.19.
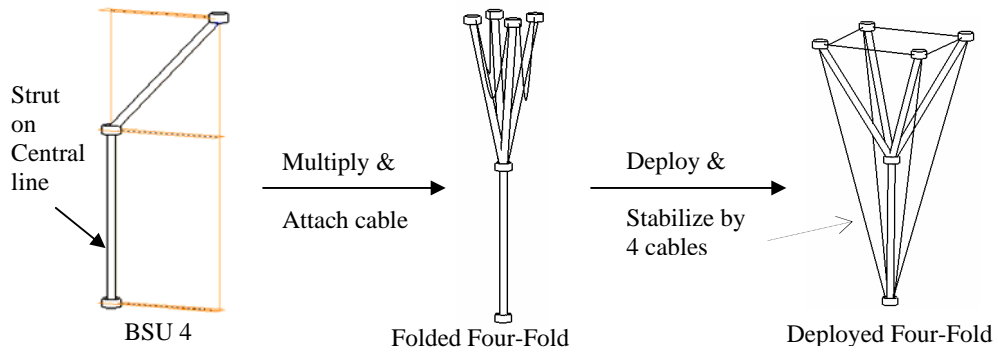
Figure 3.19. "Ineffective" BSS 4 and its SSM.

The SSM 1 and SSM 3 are corresponding to the configurations of POP and PIP structures, proposed in section 3.2. The re-discovery of the previously proposed DTSS means that the using algorithm is consistent with the design concept of previously proposed DTSS.

The BSS 5 is based on node set 6. It is "ineffective" as there is only one node (N3) on the central line. However, this form can still be used and its SSM with 4 stabilizing components are shown in Fig 3.20.
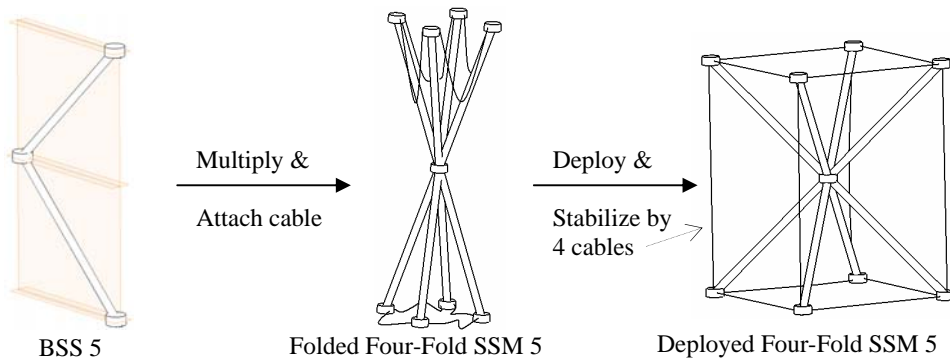


Figure 3.20. "Ineffective" BSS 5 and its SSM.

The BSS 6 to BSS 9 are "unfeasible" because they all contain horizontal struts, Fig. 3.15. They are extracted from the generative engine, before being removed from the exhaustive design output.

Another input is provided for illustration, in which V = 1, C = 2, H = 4. Several forms corresponding to this input are shown in Figs. 3.21 to 3.24. These forms are not proposed before in section 3.2. Also, it can be observed that there is no overlap in resultant designs between different sets of input. Different inputs provide different results.
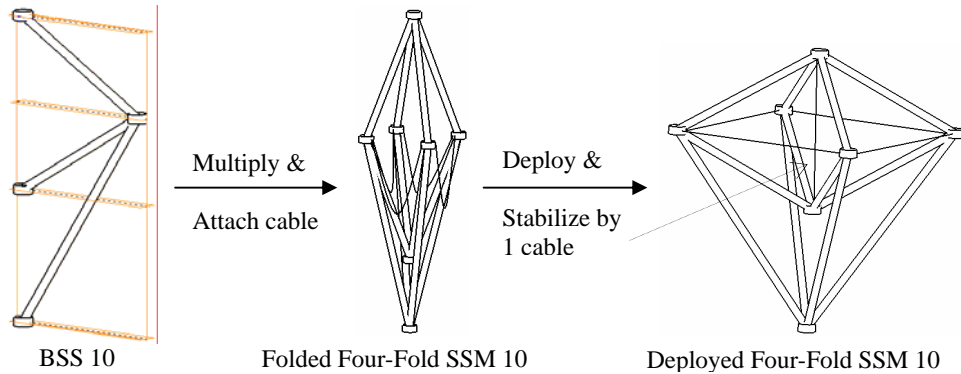


Figure 3.21. "Useful" BSS 10 and its SSM.
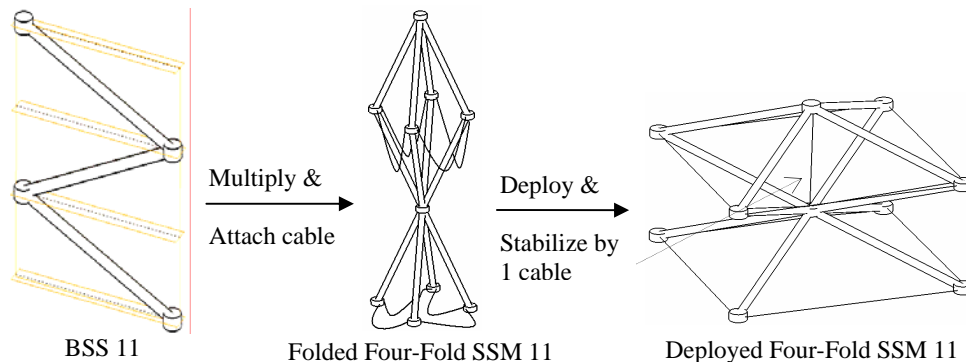


Figure 3.22. "Useful" BSS 11 and its SSM.
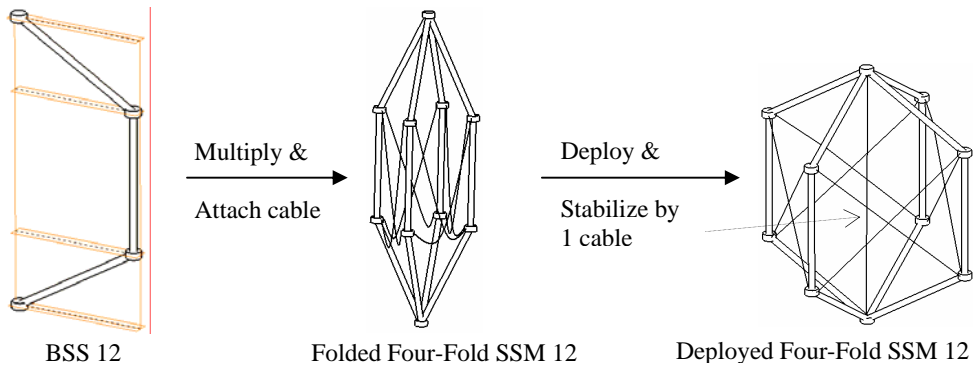


Figure 3.23. "Useful" BSS 12 and its SSM.

BSS 13          Folded Four-Fold SSM 13        Deployed Four-Fold SSM 13
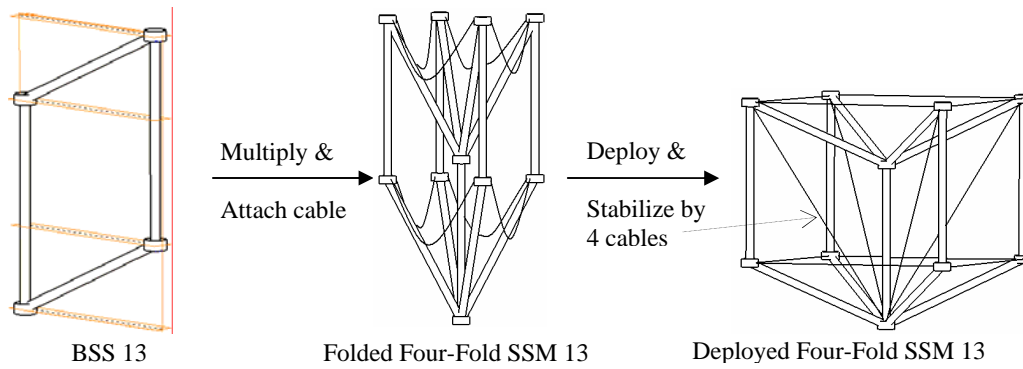
Figure 3.24. "Ineffective" BSS 13 and its SSM.

Many other inputs with different V, C, H can be provided to explore other innovative forms of DTSS. Although the number of inputs is unlimited, for each input the output is well controlled by different geometry requirements to adapt to the kinematic and stability requirements as shown in section 3.3.1. It is noted that the classification of "ineffective" and "useful" is based on the perception of the number of add-in components to stabilize one SSM but not based on the structural efficiency. From each of the created forms of DTSS, analytical parametric studies need to be performed to find out the suitable design parameters such as the number of repetition along a span length and the distance between the grids. This will be presented in Chapter 5.

## 3.4 Discussions

In this Chapter, a new spatial system, DTSS, is introduced and explained. It is well explained in section 3.1, and 3.2 that the proposed DTSS can be deployed and locked and thus the systems are deployable and self-stabilised. Besides, the proposed configurations of deployed DTSS are realized in connection with common load resistance mechanism of beam element. Therefore, it is reasonable to estimate at this moment that the structural efficiency of DTSS is close to that of conventional double

grid structures and cable-strut structures although structural performance of DTSS is discussed in the later chapters.

In Chapter 2, it is generalized that conventional double grid structures and cable-strut systems are the most structurally efficient systems among different spatial systems. Besides, deployable structures are very effective in terms of construction and this leads to high construction savings. The concept of DTSS is raised to combine the advantages of the mentioned systems and its position among other spatial systems can be illustrated in Fig. 3.25.
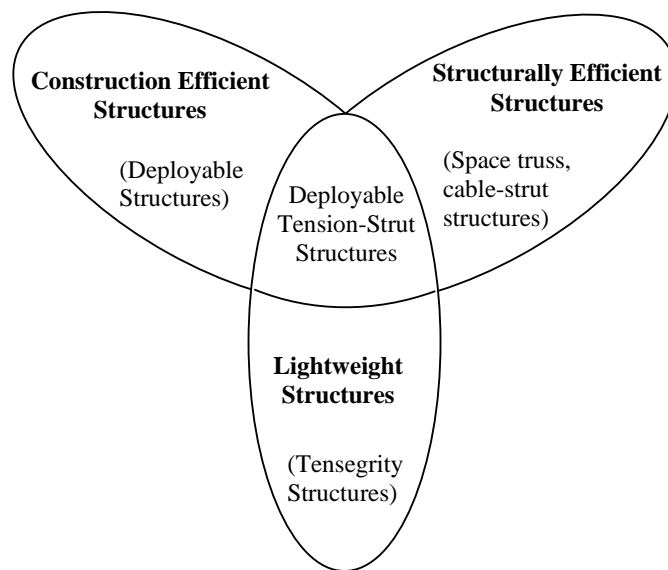


Figure 3.25. Positioning DTSS among spatial structures.

The proposed concept of DTSS is derived with consideration of the strut arrangement in cable-strut systems (Wang, 2004) and a specific deploy & stabilize mechanism (Krishnapilai et al, 2004). It might be worth noting that different "deploy & stabilize" concepts may create different deployable spatial systems. An example is the use of snap-through behaviour in joint system scale or structural system scale (Gantes, 2001)

to deploy & stabilize structures. The contribution of this research is a proposal of a new "deploy & stabilize" mechanism while structural efficiency of the proposed systems is achieved by suitable strut arrangement.
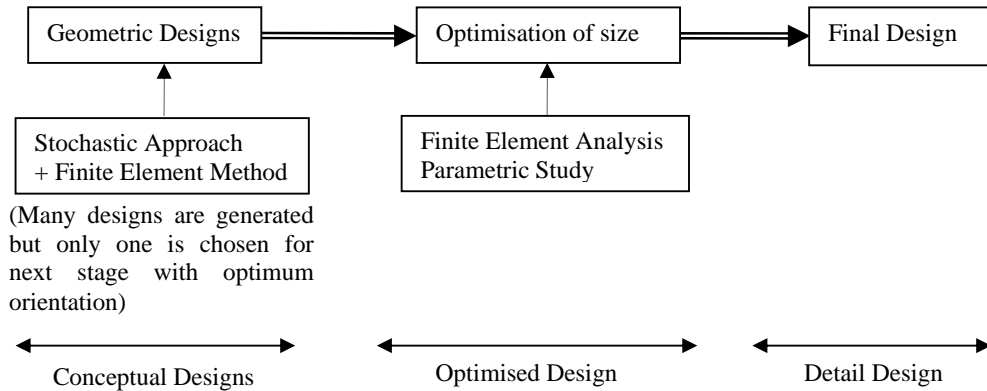


Figure 3.26. Stochastic design procedure.
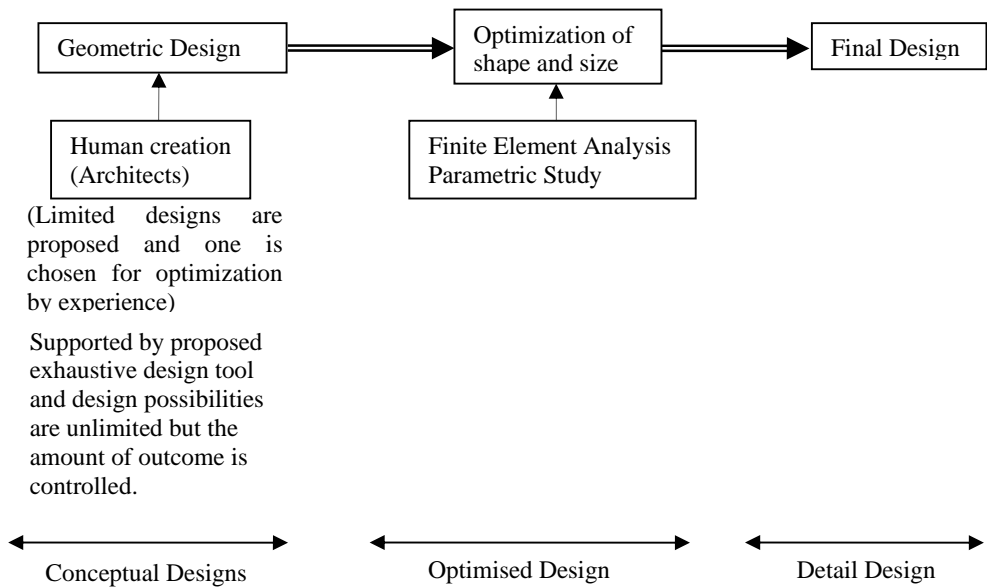


Figure 3.27. Conventional deterministic design procedure.

However, a concept itself can not be enough for practical applications. Beside proposed geometric forms of DTSS systems, a computer-based tool is developed to exhaustively find out all possible geometric forms of DTSS. This tool is called exhaustive conceptual design and the details have been given in the section 3.3.

In fact, there can be other ways to create new geometries of a structural concept as summarized in chapter 2. In the stochastic design procedures, Fig. 3.26, the grid-free approaches such as simulated annealing (Shea, 1997), or genetic algorithm (Kawamura *et al.*, 2000) may create geometric designs which are not cost effective. In The proposed exhaustive conceptual design approach serves as a support to the conceptual design stage of a conventional deterministic design procedure as shown in Fig. 3.27. Although the stochastic approach and the exhaustive approach are different by nature in generating new structural systems, it is a possibility to apply the study result of DTSS structural morphology in the stochastic approaches for further researches. In this research, study result of DTSS structural morphology is limited to provide geometric rules for the exhaustive design and is not applied in stochastic design approaches.

## 3.5 Summaries

This chapter presents a new structural concept, DTSS, and develops a series of corresponding geometric systems of DTSS. The new structural concept combines the advantages of cable-strut structures, and deployable structures to achieve ultimate cost effectiveness in terms of lightweight and construction speed.

Four geometric forms of DTSS are proposed to adapt to the concept, which are POP, PIP, PPC, and PPP. The structural morphology of these structures is studied to depict the major relations among geometry, functionality and structural stability of the proposed DTSS forms.

An exhaustive search for other possible geometries of DTSS is established using the results of the morphology study. This search engine increases the varieties of the proposed family of DTSS. Throughout the two illustrative implementation of the search, geometries of seven other DTBSS are found. The number of output of the search is unlimited due to unlimited number of input. However, unlike stochastic generative design methods, the output can be controlled by the establishment of DTSS shape grammar and suitable coordinate systems. The exhaustive conceptual design might be applied on other spatial systems such as conventional space trusses, cable-strut systems, or tensegrity systems if the shape grammars of these structural systems are available.

# CHAPTER 4

# NON-LINEAR ANALYSIS METHODS

Chapter 4 provides background information on how to investigate structural behaviour of DTSS through numerical modelling which are to be presented in Chapter 5, and 6. The existing advanced non-linear structural analysis method with linear algebra is proposed to be used for this purpose and is reviewed. Non-linear analysis using commutative algebra is proposed to benchmark the above method. The comparison between results of analyses using these two methods will show whether the control of the non-linear analysis through commercial software has been properly done. Because non-linear analysis using commutative algebra requires only one load step to obtain structural response, this study suggests that this analysis method using commutative algebra can be improved further to replace the conventional method using linear algebra in cases where only final response is needed.

## 4.1 Background

It is common sense that a structural product can be used safely and effectively if its behaviour is known or can be accurately estimated. To understand the structural behaviour, there are two dominant approaches, physical modelling and numerical modelling.

Physical modelling is concerning with manufacturing the structure in proper materials and verifying the concept as well as the strength and stiffness of the structure. The size of the physical model can be the same as the real structural product. However, in some cases, physical modelling is limited to prototyping where a small scaled physical

model is built to demonstrate the structural concept and to investigate how to assemble the product in practice. The material may be or may not be the same as that of the real structural product. The discussions on the importance of physical modelling in engineering field can be found in Kawaguchi, 2004. In chapter 7, results and discussions on physical modelling of Deployable Tension-Strut Structures will be presented. This chapter will be mainly contributed to numerical modelling.

Numerical modelling is essential to any research study on structural product. While physical modelling can be very expensive especially when large models are built such as those in the field of offshore engineering (Suzuki, 2004), numerical modelling is much less expensive in terms of both time and cost of building. Therefore, numerical modelling becomes the most popular tool for engineers and researchers to investigate structural properties. In Chapter 5, numerical modelling is also used extensively for parametric study of the proposed structural products, the Deployable Tension-Strut Structures.

Deployable Tension-Strut Structures (DTSS) are composed of beam-column elements (which can resist axial forces and bending) and cable elements (which can resist tension force only) and thus a proper numerical modelling technique to model these elements should be used.

There are many different methods to analyze and model a structure such as finite differential method, finite element method, dynamic relaxation method, finite strip method, etc. Because DTSS are composed of "stick" elements, finite element method is chosen for analysis purpose. The reason is that this method is well developed for

"stick" structural elements and there are various finite element softwares available. However, there are two types of analysis, linear and non-linear and thus a suitable one needs to be chosen for DTSS.

DTSS is a nonlinear system because of the existence of the pre-tensioned cable. That the cable element can resist tension only makes material non-linearity of the system. Once the force in a cable turn to be compression, that force should be converted to zero and thus the system needs to be re-analysed to assure equilibrium. Also, pre-tensioning force creates initial deformation, or in other words geometric change, which causes geometric non-linearity. Therefore, non-linear finite element formulation is chosen to analyze DTSSs.

In the following sections, non-linear finite element approach is explained in view of analyzing DTSSs.

**4.2 Linear algebra-based non-linear finite element method**

**4.2.1 Numerical procedure**

The aim of an analysis is to find out how a DTSS reacts to the external effect such as live load, wind load, or foundation displacement. The reactions needed for engineering design of DTSS is displacement of the structure, stress, and strain in structural elements, vibration modes, natural frequencies, etc. This section will explain how a static analysis of a DTSS is performed while dynamic analysis is discussed in section 4.4.

Among all mentioned structural reactions, displacement of the structure needs to be found because stress and strain of structural elements can be found by kinematic and constitutive conditions when displacement of the analyzing structure is known. The displacement of the structure is represented by displacement of nodes in finite element approach as the displacement of structure between nodes are assumed e.g. by polynomial or trigonometric functions. Node displacements can be found by equilibrium condition (4.1).

$$[K] \{d\} = \{f\} \tag{4.1}$$

where

[K] = stiffness matrix of structure

{d} = node displacement vector

{f} = force vector, representing the external effects

External effects can be estimated by code of practice and considered known in the analysis. Stiffness matrix consists of information about structural stiffness of structural elements and structural geometry. Node displacements are the information needs to be found.

If stiffness matrix is not affected much by the values of node displacements, the solution of the equation (4.1) for node displacement is straight forwards, with linear algebra as mathematical basis.

However, when one or more structural elements of DTSS are not in elastic behaviour or pre-stressing force is large enough, the stiffness matrix is highly dependant on the node displacements. This means the left side of equation (4.1) is non-linearly related to the node displacements and thus linear algebra cannot be used to directly solve the equation. There are two approaches which use either linear algebra or commutative algebra to solve this non-linear problem. The current approach using linear algebra is concerning with the simplification assumptions that allow determining the stiffness matrix before finding the node displacements although they are dependant. The second approach will be discussed in the section 4.3. The followings, within section 4.2, explain the formulation of equation (4.1) so that linear algebra can be used. The idea is that the loadings are divided into smaller load steps. Within each small load step, stiffness matrix is calculated with node displacements of previous load step and thus equation (4.1) can be solved by linear algebra (Chen *et al.*, 1996).

Updated Lagrangian formulation process was chosen. This formulation allows non-linear analysis as well as implementation of large displacement features. On elemental level, nonlinear behaviour is accounted for by adding second order strains and updating element axes throughout the deformation process. On global level, the nonlinear effect is represented by updating nodal coordinates.

The formulation is consistent with variational principles based on equilibrium equation between external forces and internal stresses on two levels of formulation. Firstly, the first variation of potential energy is used for equilibrium iteration in each load step. This phase can be referred to as predictor. Secondly, the second variation of potential energy (in incremental form) is the basis for calculation of incremental stiffness. This

phase can be referred to as corrector. Finally, checking convergence criteria is needed to terminate these two main phases as specified by Yang and Kuo (1994). The details of the formulation is shown as follows

### 4.2.2 Strain-stress measures

Strain measure

$$E_x = \frac{ds^2 - ds_o^2}{2ds_o^2}$$

(4.2)

ds = small change of length of the material at the current load step

$ds_o$ = small change of length of the material at the reference load step

$E_x$ = Green strain. It is chosen for non-linear formulation because of the following reasons (Bathe, 1996)

It is invariant under rigid body rotation of the material.

It is path independent so as to be consistent during large displacement process (Note that the deformation of a structure is independent of the loading sequence, one example is the Betti's law $p_a v_b = p_b v_a$)

It vanishes for rigid body motion.

Stiffness matrix based on Green strain is symmetric (advantage for computation cost).

Stress measure: 2$^{nd}$ Piola - Kirchoff stress was chosen as it is energy conjugate of Green strain.

As small strain behaviours concerned, Green strain is approximate to engineering strain:

$$E_x = e_x + (1/2)\ e_x{}^2 \approx e_x \qquad\qquad (4.3)$$

(Second order strain vanish if small strain is limited to the size of several percentages) Relation between Green strain and displacement is expressed with moderate local deflection as:

$$e_x = \frac{du}{dx} + \frac{1}{2}\left(\frac{dv}{dx}\right)^2 + \frac{1}{2}\left(\frac{dw}{dx}\right)^2 \qquad\qquad (4.4)$$

(Higher order derivative of displacement u(x) is truncated with assumption of small strain).

Similarly, $2^{nd}$ Piola - Kirchoff stress is approximate to Cauchy stress for small strain problems.

**4.2.3 Structural element formulation**

For a common application, a DTSS consists of thousands of structural elements. To achieve simplicity and reduction in computational effort, the formulation of elements by SINTEF, 2003 is used for this research. Each real structural element is represented by a finite element. Each finite element has shape function as the exact solution to $4^{th}$ order differential equation of a beam subjected to end forces. Shape functions N are shown with reference to position of the section, x, as follows.

$$N_u(x) = \phi^T\ q_u \qquad\qquad (4.5)$$

$$N_v(x) = \phi^T q_v \qquad\qquad (4.6)$$

$$N_w(x) = \phi^T q_w \qquad\qquad (4.7)$$

Where as:

$$\phi^T = [\cosh(kx),\ \sinh(kx),\ x/L,\ 1] \qquad\qquad (4.8)$$

with positive end-force P (compression)

$$\phi^T = [\cos(kx),\ \sin(kx),\ x/L,\ 1] \qquad\qquad (4.9)$$

with negative end-force T (tension) where

$$k^2 = \frac{|T|}{EI_z} \qquad\qquad (4.10)$$

while generalized constant $q = [A_1, A_2, A_3, A_4]$ is determined by boundary condition of the element as it is only associated with rigid body motion and has no effect on the element's stiffness (SINTEF, 2003). In matrix form, the displacement along an element can be expressed through shape functions, and displacements of element end nodes.

$$\{u(x)\} = \{N(x)\}\{d\} \qquad\qquad (4.11)$$

Based on the chosen formulation approach, stress and strain measure, and shape functions of finite element, the equilibrium equation can be built consistently by variational principle as follows:

Internal strain energy:

$$U = \frac{1}{2}\int_0^1 EA\left(\frac{du}{dx} + \frac{1}{2}\left(\frac{dv}{dx}\right)^2 + \frac{1}{2}\left(\frac{dw}{dx}\right)^2\right)^2 dx + \frac{1}{2}\int_0^1 EI_z\left(\frac{d^2v}{dx^2}\right)^2 dx + \frac{1}{2}\int_0^1 EI_y\left(\frac{d^2w}{dx^2}\right)^2 dx \qquad (4.12)$$

EA = axial stiffness, $EI_{z,y}$ are bending stiffness of the element section

The first term represents axial strain energy, and the two last terms represent bending strain energy. Torsion will be added directly to the final tangent stiffness matrix.

Work of external loading:

$$H_w = -\left( Fu + \int_0^1 q_x u\,dx + \int_0^1 q_y v\,dx + \int_0^1 q_z w\,dx \right) \qquad (4.13)$$

Total potential energy: $\pi = U + H_w$

The structure is stable when total energy is stationary i.e. minimum. This is determined by conditioning variational forms of energy.

This process is traditional so that only first variation of internal strain, used for iteration to reach equilibrium and incremental form of virtual work, used to obtain tangent stiffness are presented as they are directly relevant.

First variation of internal forces:

$$\delta U = \int_0^1 EA \frac{du}{dx}\frac{d\delta u}{dx}\,dx + \int_0^1 EI_z \left( \frac{d^2v}{dx^2}\frac{d^2\delta v}{dx^2} - \frac{N}{EI_z}\frac{dv}{dx}\frac{d\delta v}{dx} \right)dx +$$

$$\int_0^1 EI_y \left( \frac{d^2w}{dx^2}\frac{d^2\delta w}{dx^2} - \frac{N}{EI_z}\frac{dw}{dx}\frac{d\delta w}{dx} \right)dx - \int_0^1 \left( N + EA\frac{du}{dx} \right)\frac{d\delta u}{dx}\,dx \qquad (4.14)$$

The first term is linear axial strain contribution. The next two terms are bending contribution accounting for P-delta effect by including magnification due to axial strain. The last term is nonlinear axial strain caused by the combination of lateral

deflection v and w. To explain this argument, the expression of element axial force can be referred to as follows:

$$N = -EAe_x = -EA\left(\frac{du}{dx} + \frac{1}{2}\frac{d^2v}{dx^2} + \frac{1}{2}\frac{d^2w}{dx^2}\right) \tag{4.15}$$

Incremental form of virtual work is formed from internal work and work by external loading.

Increment of internal work:

$$\delta U = \delta\left(U + \Delta U - U\right) = \delta\left(U + \Delta U\right) - \delta U = \int_0^l EA\Delta\frac{du}{dx}\frac{d\delta u}{dx}dx +$$

$$+\int_0^l EIz\left(\Delta\frac{d^2v}{dx^2}\frac{d^2\delta v}{dx^2} - \frac{N}{EIz}\Delta\frac{dv}{dx}\frac{d\delta v}{dx}\right)dx + \int_0^l EIy\left(\Delta\frac{d^2w}{dx^2}\frac{d^2\delta w}{dx^2} - \frac{N}{EIy}\Delta\frac{dw}{dx}\frac{d\delta w}{dx}\right)dx +$$

$$+\int_0^l EA\left(\Delta\frac{du}{dx}\frac{dv}{dx}\frac{d\delta v}{dx} + \Delta\frac{dv}{dx}\frac{dv}{dx}\frac{d\delta u}{dx}\right)dx + \int_0^l EA\left(\Delta\frac{du}{dx}\frac{dw}{dx}\frac{d\delta w}{dx} + \Delta\frac{dw}{dx}\frac{dw}{dx}\frac{d\delta u}{dx}\right)dx + \tag{4.16}$$

$$+\int_0^l EA\left(\Delta\frac{dv}{dx}\left(\frac{dv}{dx}\right)^2\frac{d\delta v}{dx}\right)dx + \int_0^l EA\left(\Delta\frac{dw}{dx}\left(\frac{dw}{dx}\right)^2\frac{d\delta w}{dx}\right)dx +$$

$$\int_0^l EA\left(\Delta\frac{dv}{dx}\frac{dv}{dx}\frac{dw}{dx}\frac{d\delta w}{dx} + \Delta\frac{dw}{dx}\frac{dw}{dx}\frac{dv}{dx}\frac{d\delta v}{dx}\right)dx$$

It was stated in SINTEF, 2003 that the above formula has truncated the higher order terms of derivatives of v(x) and w(x).

Increment in work of external loading:

$$\delta\Delta H = -\Delta F\delta u - \int_0^l \Delta q_x\delta u dx - \int_0^l \Delta q_y\delta v dx - \int_0^l \Delta q_z\delta w dx \tag{4.17}$$

Applying shape functions from (4.11) on these variation formulas, tangent stiffness matrix [K] can be obtained and it is ready for solving the system of non-linear equations (4.1).

Using linear algebra to solve non-linear problem requires a lot of computational effort in the sense that the whole procedure is repeated for each small load step. The stiffness matrix is re-calculated when node displacements are updated. Intermediate parameters, which are required to assemble the stiffness matrix, is produced at the end of each load step while only the result of analysis at the final load step is needed for assessment of the strength and stiffness of the structures in most practical engineering designs. There is also risk of accumulative errors that cannot be avoided completely.

In the next section 4.3, another approach to solve this non-linear problem is presented without excessive iteration of calculating stiffness matrix by the use of commutative algebra, a mathematical tool for solving systems of polynomials.

## 4.3 Commutative algebra-based non-linear finite element method

### 4.3.1 Advantages of commutative algebra approach

Current non-linear analysis using linear algebra requires many load steps to obtain the structural responses such as stress or displacements. It is proposed in this thesis that non-linear analysis requires one load step for a sufficiently accurate result and thus the procedure is computationally efficient if commutative algebra is used. In this thesis, the objective of investigating non-linear analysis using commutative algebra is limited to verifying the analysis result, done with a commercial software, and the way author control the analysis through the software.

Linear algebra is a special case of commutative algebra. Linear algebra deals with the system of linear equations or polynomials of first order. Commutative algebra deals with a system of polynomial equations of any finite order. Recent achievements in commutative algebra allow obtaining properties of polynomial system of equations as much as properties of linear system of equations using linear algebra. The solution procedures are computation-oriented as described by Cox *et al.* (1997). The approximation of different nonlinear functions by polynomials can be achieved by different techniques such as the use of Taylor series (Mathematica manual). From these arguments, it can be expected that if the Finite Element Procedure (FEP) can be formed so that in the equilibrium equations, only polynomials exist and thus the nonlinear polynomial system can be solved by commutative algebra.

In this section, the FEP using commutative algebra is explained towards the analysis of deployable tension-strut structures. A comparison study is done by comparing the analysis result between the conventional FEP and the proposed one.

**4.3.2   Numerical procedure**

The FEP to solve a nonlinear problem using commutative algebra is presented as follows

(1). Discretize the structure into finite structural elements

(2). Formulate the governing algebraic equations for each structural element by

>   (2.1). Assume shape functions to represent the displacements through the node displacements. Polynomials such as Legrandre polynomials are used for shape functions.

>   (2.2). Calculate strain (Green strain or engineering strain for this small strain problem). The relation between the strain and displacement described by polynomials above is derivation and thus the strain will be in polynomial form.

>   (2.3). Calculate stress based on the stress-strain relation. For linear relation, the relation is polynomial of first order. For nonlinear relation, the stress-strain curve described by or approximated by polynomials is recommended to be used.

>   (2.4). Apply virtual work principle to derive the governing equation which is a system of polynomial equations.

(3). Assemble the governing equations using translation and rotation matrix. The rotation matrix is in trigonometric functions and approximated by polynomials.

(4). Apply the boundary conditions to obtain the final governing equations in form of a system of polynomials, solved by Buchberger's algorithm. The result will be interpreted to obtain stress and strain of the structural elements.

The difference between the proposed FEP and the conventional procedure is in the steps (2.1), (2.3), (3), and (4).

In the step (2.1), the conventional procedure allows different types of shape functions while the proposed one allows only polynomial functions.

In the step (2.3), polynomial relation between stress and strain, exactly or approximately, is required in the proposed procedure. There can be many descriptions of material in the plastic range as shown by Charkrabatty (2000). Although those descriptions may not be in polynomial form they can be approximated by polynomials.

In the step (3), the trigonometric functions in the rotation matrix are approximated by polynomials in the proposed procedure. Taylor series can be used for this purpose. For conventional FEP, those trigonometric functions are calculated to be a specific value by assuming that the geometry of the structure is remained to be the same as in the previous load step.

In the step (4), the most important step in the FEP, the governing polynomial equations are solved by Buchberger's algorithm described by Bose *et al.* (2003). In the conventional FEP, these governing equations are solved by linear algebra with iterations. To apply linear algebra in solving nonlinear equations, it is assumed that the geometric and mechanical properties of the structure are maintained to be the same as in the previous load step using an Updated Lagrangian Formulation. The iteration of assembling stiffness matrix and solving governing equations is required to improve the accuracy of the analysis. If commutative algebra is used, no such assumptions are required.

### 4.3.3 Comparison Study

The comparison study is based on the Pyramid-On-Pyramid structure, which has been described in chapter 3. The symmetric Pyramid-On-Pyramid module with boundary condition is shown in Fig. 4.1 (a). The problem is to find the limit length of central rod with which the snap-through problem appears.
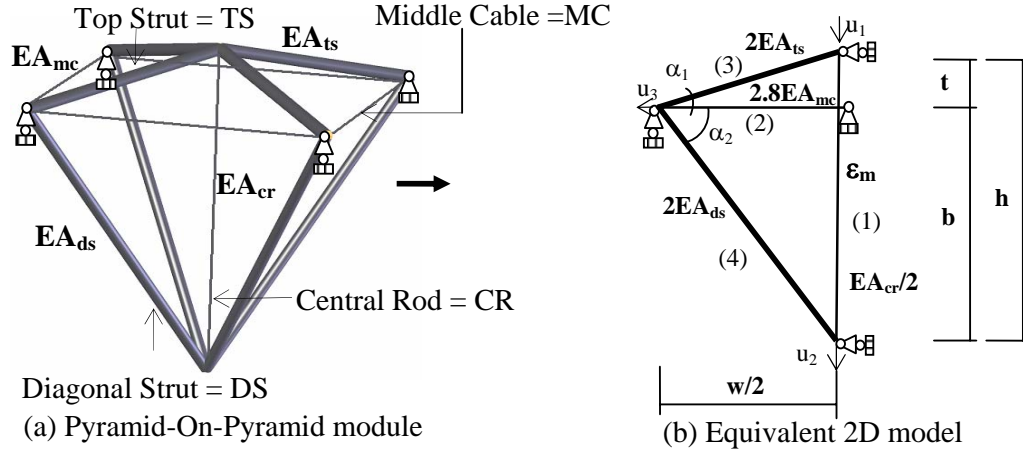
Figure 4.1. The Pyramid-On-Pyramid structure.

The Top Struts, TS, and the Diagonal Struts, DS are made of steel circular hollow section 38.1mm x 2.8mm with the modulus of elasticity of $E_s = 210$ kN/mm$^2$. Central Rod, CR, Middle Cable, MC, are made of cable with diameter of 8 mm and the modulus of elasticity, $E_c$, of 145 kN/mm$^2$.

Therefore $\dfrac{EA_{ts}}{EA_{cr}} = 8.93$, $\dfrac{EA_{ds}}{EA_{cr}} = 8.93$, $\dfrac{EA_{mc}}{EA_{cr}} = 1$.

If the length of the CR is equal to the height h then the structure is stress free. If the manufactured length of CR is shorter than h then the structure is in a self-stress equilibrium state and the tension force in the CR exists. At the limit length, when the length is shortened the tension force in the CR is reduced. The aim of the analysis is to find out the relation between the manufactured length of CR and the tension force in the CR and to detect the mentioned limit length. The analysis is based on the large displacement and small strain assumptions. The cables are modelled by tension elements and the struts are modelled by beam-column elements. The structure is analyzed in elastic range.

For the conventional FEP, the analysis is iterated to improve the accuracy as mentioned in section 4.2 while for the proposed FEP with commutative algebra, no iteration is required and the FEP is explained below.

The strain within a cable or strut is assumed uniform as far as no external load is applied on the element and the strut is proportion not to reach its buckling capacity. The strain is calculated as shown in equations (4.18) to (4.21).

$$\varepsilon_1 = \frac{u_2 - u_1}{h} - \varepsilon_o \tag{4.18}$$

$$\varepsilon_2 = \frac{u_3}{w/2} = \frac{2u_3}{w} \tag{4.19}$$

$$(\varepsilon_3 + 1)^2 = \frac{(t - u_1)^2 + \left(\frac{w}{2} + u_3\right)^2}{t^2 + \left(\frac{w}{2}\right)^2} \Rightarrow \varepsilon_3 = \frac{1}{2}\left[\frac{(t - u_1)^2 + \left(\frac{w}{2} + u_3\right)^2}{t^2 + \left(\frac{w}{2}\right)^2} - 1\right] \tag{4.20}$$

$$(\varepsilon_4 + 1)^2 = \frac{(b + u_2)^2 + \left(\frac{w}{2} + u_3\right)^2}{b^2 + \left(\frac{w}{2}\right)^2} \Rightarrow \varepsilon_4 = \frac{1}{2}\left[\frac{(b + u_2)^2 + \left(\frac{w}{2} + u_3\right)^2}{b^2 + \left(\frac{w}{2}\right)^2} - 1\right] \tag{4.21}$$

w = 2.12 m, h = 1.15 m, t = 0.085 m, b = 1.065 m as shown in Fig. 4.1 (b). $\varepsilon_1$, $\varepsilon_2$, $\varepsilon_3$, $\varepsilon_4$ are strain in the element (1), (2), (3), (4), respectively. $u_1$, $u_2$, $u_3$ are node displacement shown in Fig. 4.1. $\varepsilon_o$ is the pre-tension strain, applied on the element 1.

The constitutive condition is based on the Hook's law as far as the material is within the elastic range.

$$\sigma = E \times \varepsilon \rightarrow N_i = \varepsilon_i \times EA_i \text{ or } \varepsilon_i = N_i / EA_i \tag{4.22}$$

The equilibrium at three nodes in the direction of $u_1$, $u_2$, $u_3$ is presented in the following three equations

$$N_3 \sin\alpha_1 + N_1 = 0 \tag{4.23}$$

$$N_4 \sin\alpha_2 + N_1 = 0 \tag{4.24}$$

$$N_3 \cos\alpha_1 + N_4 \cos\alpha_2 + N_2 = 0 \tag{4.25}$$

The angle $\alpha_i$ are calculated based on the final (deflected) configuration of the structure.

Combining the equations (4.18) to (4.25), the governing equations are in the form of a system of polynomials

$$\frac{2EA_{ts}}{EA_{cr}}\left[\frac{(t-u_1)^2+\left(\dfrac{w}{2}+u_3\right)^2}{t^2+\left(\dfrac{w}{2}\right)^2}-1\right]\frac{t-u_1}{\sqrt{(t-u_1)^2+\left(\dfrac{w}{2}+u_3\right)^2}}+\left(\frac{u_2-u_1}{h}-\varepsilon_0\right)=0$$

$$\tag{4.26}$$

$$\frac{2EA_{ds}}{EA_{cr}}\left[\frac{(b+u_2)^2+\left(\dfrac{w}{2}+u_3\right)^2}{b^2+\left(\dfrac{w}{2}\right)^2}-1\right]\frac{b+u_2}{\sqrt{(b+u_2)^2+\left(\dfrac{w}{2}+u_3\right)^2}}+\left(\frac{u_2-u_1}{h}-\varepsilon_0\right)=0$$

$$\tag{4.27}$$

$$\frac{2EA_{ts}}{EA_{cr}}\left[\frac{(t-u_1)^2+\left(\frac{w}{2}+u_3\right)^2}{t^2+\left(\frac{w}{2}\right)^2}-1\right]\frac{\frac{w}{2}+u_3}{\sqrt{(t-u_1)^2+\left(\frac{w}{2}+u_3\right)^2}}+$$

$$+\frac{2EA_{ds}}{EA_{cr}}\left[\frac{(b+u_2)^2+\left(\frac{w}{2}+u_3\right)^2}{b^2+\left(\frac{w}{2}\right)^2}-1\right]\frac{\frac{w}{2}+u_3}{\sqrt{(b+u_2)^2+\left(\frac{w}{2}+u_3\right)^2}}+\frac{2.8EA_{mc}}{EA_{cr}}\frac{4u_3}{w}=0$$

$$(4.28)$$

In equations (4.26) to (4.28), there are two types of non-polynomial functions in the form

$$f(x)=\frac{1}{x^2+a^2}$$

$$(4.29)$$

$$f(x,y)=\frac{1}{\sqrt{(x+a)^2+(y+b)^2}}$$

$$(4.30)$$

These functions can be approximated by polynomials using Taylor series

$$f(x)=\frac{1}{x^2+a^2}\approx\frac{1}{a^2}-\frac{1}{a^4}x^2+...$$

$$(4.31)$$

$$f(x,y)=\frac{1}{\sqrt{(x+a)^2+(y+b)^2}}\approx\frac{1}{2\sqrt{a^2+b^2}}+\frac{1}{1!}16\left(a^2+b^2\right)^{-3/2}\left[a(x-a)+b(y-b)\right]+...$$

$$(4.32)$$

Substitute (4.31), and (4.32) into (4.26) to (4.28), a system of polynomials can be achieved. This polynomial system is solved by deriving the Groebner basis using Buchberger's algorithm (Cox *et al.*, 1997). This Groebner basis with respect to

lexicographic order is used in elimination process, similar to Gauss elimination technique in linear algebra. Finally, only a polynomial in one variable is obtained and solved numerically using current techniques such as Newton-Raphson. The other variables are found by back substitution and thus the polynomial system is solved without reassembling the whole non-linear systems.
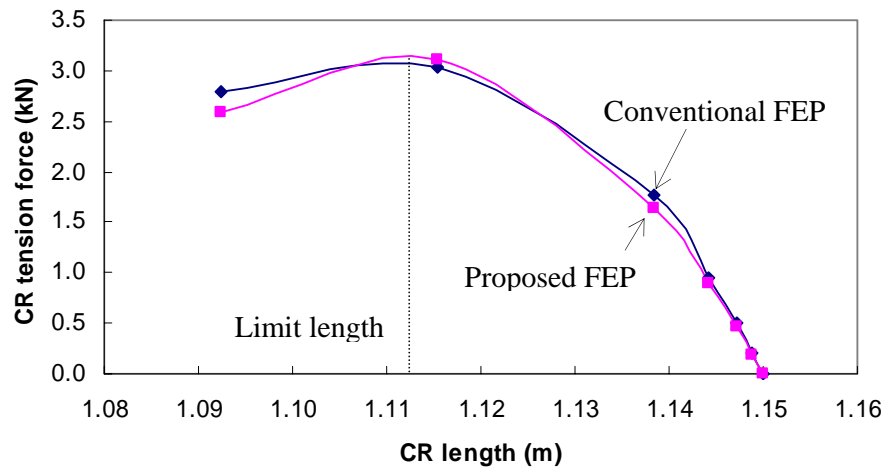
Figure 4.2. CR length and tension force relation.

Results of the two analyses are shown in Fig. 4.2. The difference between the two FEP is less than 7.5 %. The limit length is approximate 1.11 m for both FEPs. This means the two FEPs provide consistent results.

**4.4 Free vibration analysis of pre-stressed tension-strut structures**

In engineering design, important information about a structure includes structural dynamic properties, which are vibration modes and natural frequencies. The order of mode shapes provides hint about the potential failure mode of the structure. Natural frequencies will help to determine whether a structure is suitable for a region with high

earthquake or strong wind. This information can be obtained from free vibration analysis. The theory for free vibration analysis of structure has been developed for long and can be found in text books such as by Mukhopadhyay, 2000.

However, the free vibration analysis of pre-tensioned structures requires a formulation which can account for the pre-tension force and geometric non-linearity. The following illustration will explain the contribution of pre-tension force and geometric non-linearity to the free vibration analysis of a pre-tensioned cable structure, shown in Fig. 4.3.
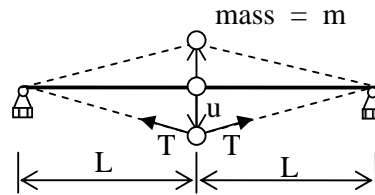


Figure 4.3. Deformed configuration of a pre-tensioned cable.

If the strain $\varepsilon_o$ is applied on the cable before vibration, the stiffness of the cable depends very much on pre-tension force and the geometric non-linearity as shown in equation 4.33.

$$K_u = \left[ 2EA \left( \frac{1}{2} \frac{u^2}{L^2} + \varepsilon_o \right) \frac{1}{\sqrt{L^2 + u^2}} \right] \qquad (4.33)$$

The equilibrium condition during vibration can be established as

$$m\ddot{u} + K_u u = 0 \qquad (4.34)$$

Replace (4.33) into (4.34)

$$m\ddot{u} + \left[ 2EA \left( \frac{1}{2} \frac{u^2}{L^2} + \varepsilon_o \right) \frac{1}{\sqrt{L^2 + u^2}} \right] u = 0 \qquad (4.35)$$

For linear one-degree-of-freedom problem, the equation 4.34 can be solved easily because the structural stiffness $K_u$ is not dependant on displacement u of the structure.

For the current problem, when the pre-tension and geometric non-linearity is involved the problem is more complicated as shown in equation 4.35 and cannot be solved in a straight forward manner.

When the pre-tension force is given, $K_u$ will just depend on the level of deflection u during vibration. This means the stiffness of the structure depends on not only the static structural properties but also the level of displacement of the structure during vibration. $K_u$ is adaptive in the sense that when the displacement is higher, the stiffness $K_u$ is higher to resist against displacement.

As the proposed DTSSs consist of pre-tensioned cable elements, this study concludes that the free vibration frequency is an important structural property. Conventional free vibration analysis for linear system can be used when the pre-tension force has been accounted for when geometric non-linearity is ignored. When geometric non-linearity is not considered the stiffness of the cables is lower and thus the frequencies obtained are lower than the actual values. This analysis approach offers lower bound natural frequencies.

This section is limited to investigation of the structural properties without considering the external dynamic loadings which can be found in Stoker, 1950 and Dinca and Theodosin, 1973.

## 4.5 Summaries

The objectives of this thesis are not about numerical modelling. However, understanding the issues in modelling of the newly proposed DTSS will help the designers to have better control of the numerical technique and sufficiently reliable analysis results can be expected.

This chapter has summarized the basis which is necessary when static and dynamic behaviour of DTSS is investigated by numerical modelling. Non-linear finite element method is chosen for the static analysis, in which Green strain is the strain measure. However, with a step of updating pre-tension force and structural geometry under pre-tension force, linear finite element formulation can be used to predict lower bound natural frequencies and mode shapes of DTSSs.

Another half of this chapter is contributed to introducing the proposed finite element procedure, based on commutative algebra. Conventional finite element approach is based on linear algebra and it requires many load steps and iterations of stiffness matrix assembly for a non-linear analysis. It can be more computationally effective if finite element procedure is formed based on commutative algebra because less load steps are required in this approach. The example shows that the proposed approach provides as good result as that of conventional approach while only one load step is needed.

# CHAPTER 5

# STRUCTURAL BEHAVIOUR AND STRUCTURAL EFFICIENCY

# EVALUATION

The concept and morphology of Deployable Tension-Strut Structures has been explored in Chapter 3. Methodology of analyzing these structural systems has also been covered in Chapter 4. In this Chapter, the structural behaviour are investigated and explained through advanced non-linear analysis. Free vibration analysis of Deployable Tension-Strut Structures is performed to provide deeper understanding about structural stiffness and its relation to pre-stressing level of Deployable Tension-Strut Structures. The robustness of the structures is investigated by assessing structural response when critical components are removed. Finally, conventional double-layer space trusses with equivalent span length and shape are also analysed and their structural efficiency is compared to that of Deployable Tension-Strut Structures. The comparative study will provide quantitative assessment on structural efficiency of the proposed Deployable Tension-Strut Structures.

## 5.1 Introduction

This Chapter presents quantitative assessment on structural behaviour and efficiency of the four proposed Deployable Tension-Strut Structures (DTSS), which are Pyramid-On-Pyramid (POP), Pyramid-In-Pyramid (PIP), Pyramid-Pantograph-Cable (PPC), and Pyramid-Pantograph-Pyramid (PPP). In Chapter 3, only qualitative assessment has been made at very conceptual level. Quantitative assessment through structural analysis is essential to accurately evaluate effectiveness of the proposed systems as

well as giving some preliminary guidelines on how to design these structural systems effectively.

The first objective of this Chapter is to provide optimum design parameters, which are Span/Depth ratio and Structural Span/Module Width ratio through parametric study. The study is limited to flat structures with medium spans (24 m to 60 m). The assessment of optimum structural configuration is based on the maximum value of the proposed Structural Efficiency Index, which is explained in section 5.2.

The second objective is to study natural frequency and vibration mode shapes of DTSSs to gain better understanding about the structural behaviour of DTSS, including the pre-stressing effects. Section 5.5.1 explains why pre-tensioning level needs to be considered in the design; and section 5.5.2 investigates the effects of pre-tensioning on structural behaviour of DTSSs.

Finally, structural efficiency of DTSSs is evaluated by comparing with that of equivalent conventional double-layer space frames. This quantitative assessment will verify the proposed concept of DTSSs, which is "structurally effective" besides the major advantage of deployability.

## 5.2 Structural efficiency index

A comparison of structural efficiency between two different structural systems will be fair, only if they are both optimally designed under the same boundary and loading conditions. It is common to focus on the weight of the optimally designed structures

when structural efficiency is studied. In the present approach, a new structural efficiency index (SEI) is proposed taking into account of the maximum deflection (D), structural self weight (W), span length (S), and loading (L):

$$SEI = \frac{1}{\gamma}\frac{L}{W}\left(\frac{S}{D}\right)^{\frac{1}{\beta}}$$

(5.1)

Where

$\gamma$ = parameter to normalize SEI in a specified loading and boundary condition (assumed to be 141.4)

$\beta$ = parameter to reduce the significance of the ratio S/D in comparison with L/W, ($\beta$ >1, assumed to be 2)

L = total design unfactored loads, including self-weight.

  L = W + I

  I = imposed gravity load (assumed to be 0.75 kN/m$^2$)

  W = self-weight of the structure, excluding the weight of the joints

  S = span of the structure

  D = maximum deflection at the middle of the structure.

The value of $\gamma$ is calculated to be $10 \times 200^{1/2} \approx 141.4$, which means if S/D = 200 and L/W = 10, SEI is normalized to be 1.0. S/D = 200 is the serviceability limit for space frame design and the load to self weight ratio L/W is estimated to be 10. For medium span applications, the self weight W, of the space truss structure is estimated to be about 10 kg/m$^2$ for medium span and the total gravity load, L, of 100 kg/m$^2$ is assumed for heavily loaded roof. This L/W ratio can be modified to accommodate other ranges of loadings and/or other types of structure.

A high SEI index corresponds to a higher structural efficiency. For structures of the same span length and under the same loading condition, the more efficient structure will have either lower self-weight W, or less displacement, D. As mentioned, the proposed SEI is better than the criterion based on self-weight alone in evaluating the structural efficiency. Illustrations are given in Appendix A to show that SEI criterion is less sensitive than self-weight criterion when the member sizes are changed. In other words, SEI is more dependant on the structural configuration rather than the specific designs of the same configuration.

Comparison may be made using self weight criterion alone in cases where deflection of the structures being compared is very insignificant (which is often the case of short span structures with high structural depth). In such cases the design is often controlled by the strength requirements in the Ultimate Limit State rather than deflection and the vibration requirements in the Serviceability Limit State. In such cases, SEI can be evaluated by equation (2) where deflection is ignored

$$SEI = \frac{1}{10} \frac{L}{W} \qquad\qquad (5.2)$$

## 5.3 Parametric studies and optimum design parameters

Parametric study is performed to find out the optimum design parameters, Span/Depth ratio and the Span/Module Width ratio and to compare the structural performance of different DTSSs.

Non-linear analysis is used to analyze the DTSS. The details of modelling and analysis process can be found in Chapter 4 of this thesis and will not be repeated here.

The proposed structures are designed and analyzed by an iterative process where the optimal sections are chosen from Handbook of structural steelwork, 2002 to satisfy the codes limit state criterion (BS 5950. Part 1: Structural use of steel works in building, 2000). One section size is chosen for each type of structural member e.g. diagonals, top struts. The struts are made of circular hollow sections with yield strength of 275 $N/mm^2$ and the high-tensile cables are made of steel with breaking stress of 1089 $N/mm^2$. The Young modulus of the steel is taken to be $210x10^3$ $N/mm^2$ and the Young modulus of the high strength steel cable is $145x10^3$ $N/mm^2$.

The imposed live load of 0.75 $kN/m^2$ is imposed on all structures, which is common for heavily loaded roof. The load is assumed to be distributed at the bottom nodes of the structures. Spans ranging 24 m, 36 m, 48 m and 60m are considered while structures are made of 8x8, 10x10 and 12x12 modules with span to gross height ratio of 8, 10 and 12.  All boundary nodes are restrained against displacements. The serviceability deflection limit is taken as 1/200 the span of the structure as prescribed by BS 5950:2000, Part 1.

As the load-displacement behaviour of the DTSS is non-linear, the pre-stressing force, self-weight load and gravity imposed loads are applied sequentially to closely resemble the actual loading sequence.

It can be construed that if the number of modules is very small for a specific span, the number of structural elements and joints are reduced. This may lead to a reduction in the self-weight of structure but cause an increase in deflection. When the number of module is increased, self-weight of structure is increased while the deflection is

reduced. The optimum number of module can be evaluated at the maximum SEI where both the self-weight of the structure and the deflection are reasonably low. The use of SEI is explained in section 5.2.

If the span/depth ratio is relatively large, the member lengths are very long and thus large section sizes are required to resist buckling. This results in higher self-weight of the structure while deflection is low due to excessively high structural stiffness. For such cases, the ultimate limit state requirements tend to control the design. When the span/depth ratio is reduced, the self-weight is reduced while the deflection is increased significantly. Similar to the above argument, the optimum span/depth ratio is evaluated at the maximum SEI with low self-weight and low deflection (high stiffness).
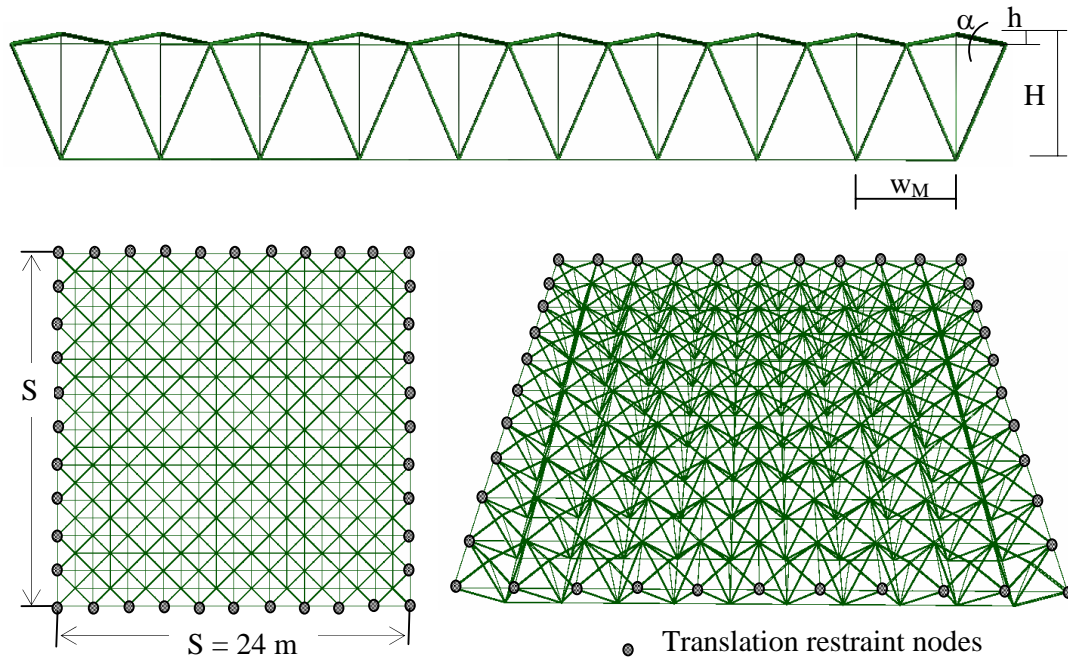


Figure 5.1. Pyramid-On-Pyramid structure 24 m span.

The detailed results of the study including displacements, average self-weight and SEI of the DTSS structures are presented in the tables in Appendix B. The followings are summary points which are deduced from the data in this Appendix B.

Figs. 5.1 to 5.4 show several structural configurations with different spans that have been analysed in the parametric study.
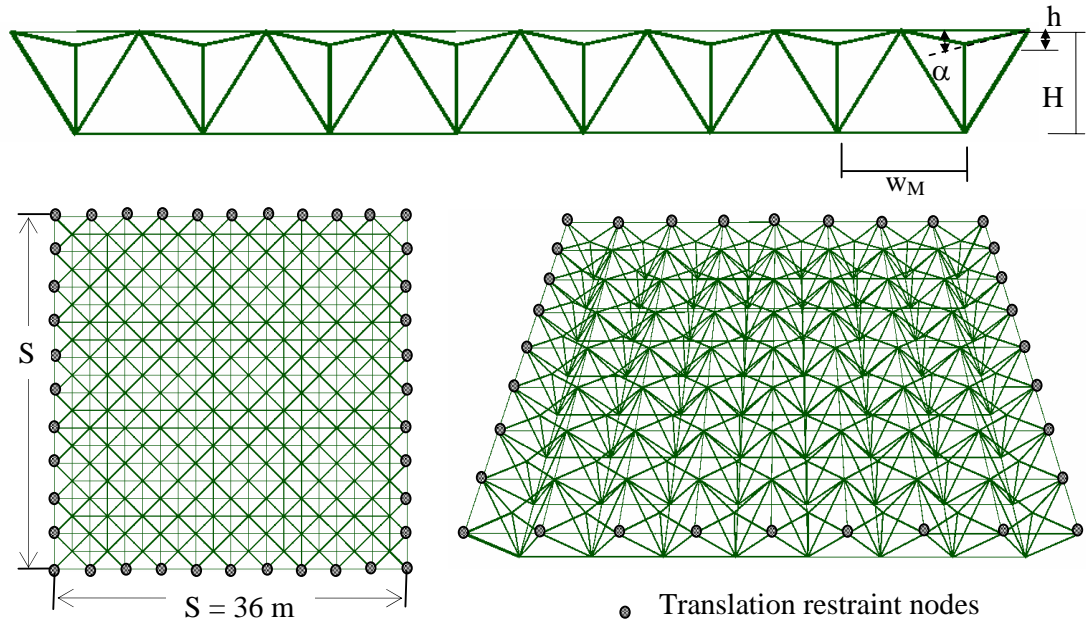


Figure 5.2. Pyramid-In-Pyramid structure 36 m span.
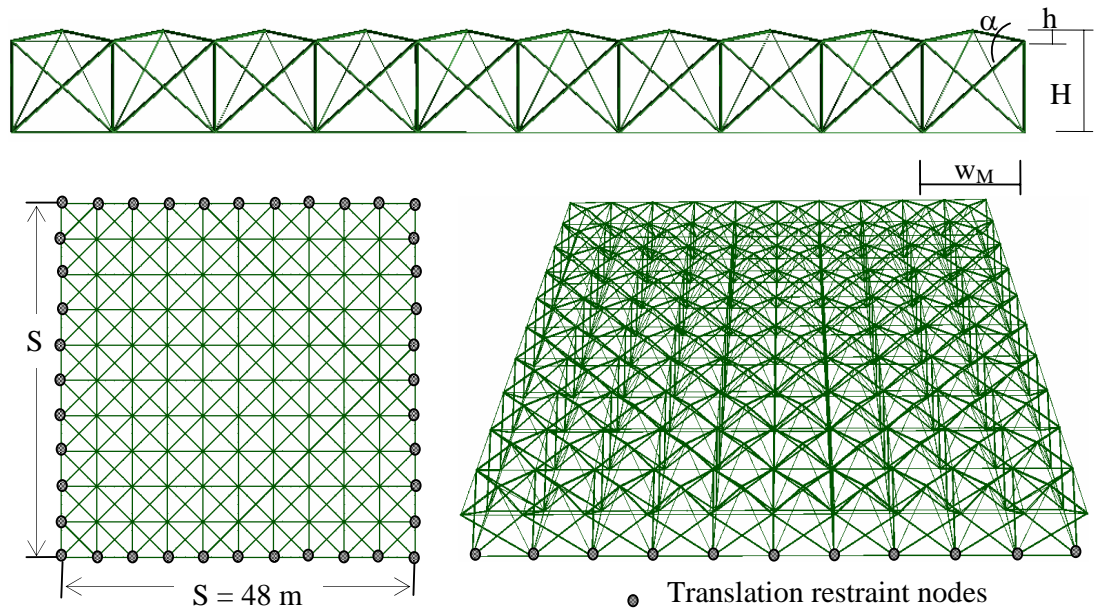


Figure 5.3. Pyramid-Pantograph-Cable structure 48 m span.
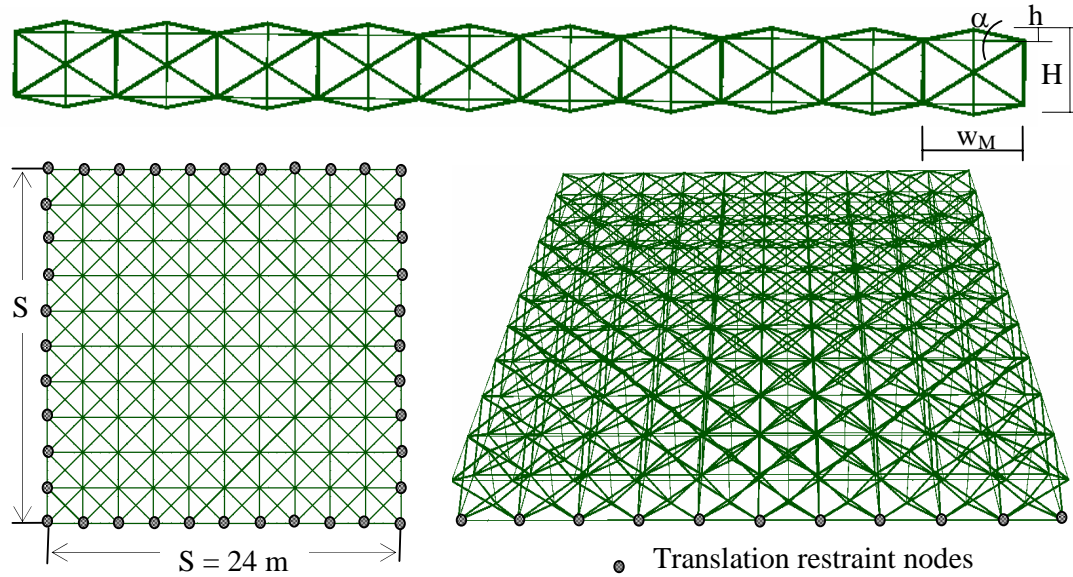
Figure 5.4. Pyramid-Pantograph- Pyramid structure 24 m span.

For purposes of comparison the gross height H is kept the same. The inclination ratio defined as the ratio between the inclination height and half module width ($w_M/2$), as illustrated in Figs. 5.1 – 5.4, is

$$\tan(\alpha) = 2h/w_M$$

This inclination ratio $\tan(\alpha)$ is maintained at 0.15 for all DTSS. Higher $\tan(\alpha)$ leads to lower efficient of the structures while lower $\tan(\alpha)$ may lead to the snap-through buckling of the top chords.

Initial pre-stressing force is applied to all the cable elements to ensure that the tension-strut modules are stable before applying the external loads. The initial strain in the pre-stressed cables is kept at 0.001, which is about 1/8 of breaking strain.

DTSS with span of 24 m is analyzed and the change in self-weight corresponding to the change in number of module is plotted in Fig. 5.5. It is in agreement with the above judgment that when the number of module is increased, the self-weight of the structure

is also increased. The structure with maximum self-weight is corresponding to a solid beam with the same span/depth ratio but infinite number of modules.
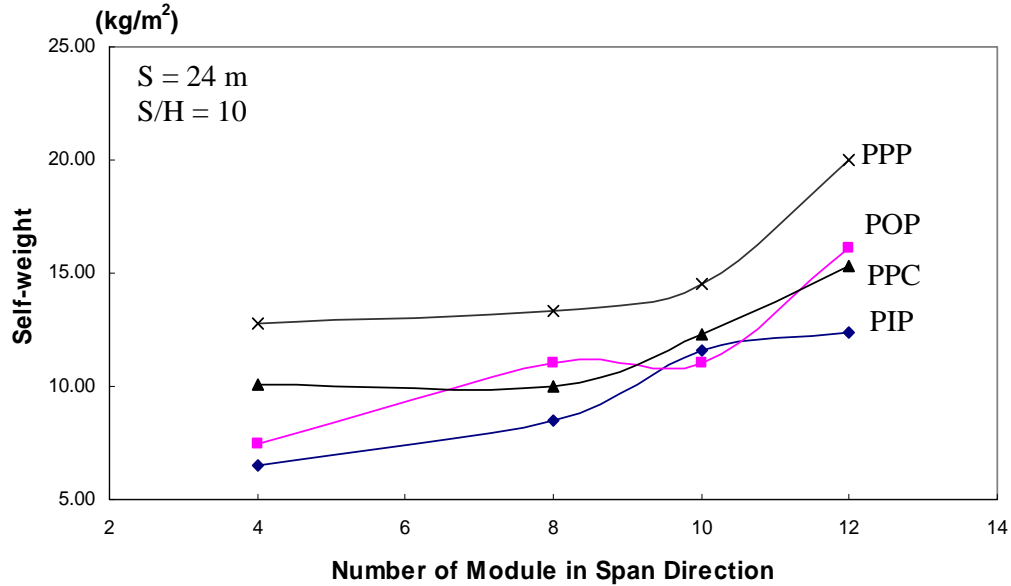


Figure 5.5. Self-weight of DTSS with span of 24 m.

Self-weight of PIP ($6 - 12$ kg/m$^2$) appears to be the lowest among the four DTSS and thus it can be estimated that this is the most structurally effective DTSS in this study. In contrary, self-weight of PPP ($13 - 20$ kg/m$^2$) is the highest. PPP includes a system of bottom strut and bottom cable and thus having higher weight than other system where no bottom strut is required. However, the bottom strut system allows PPP resisting up-lift wind load effectively and weight increase is a trade-off of this advantage.

Referring to the shapes of the slopes in Fig. 5.5, it can be misunderstood that when the number of module is reduced and the structural efficiency is increased. As explained in Section 5.1.1, the structural efficiency cannot be assessed by self-weight only and SEI is used to include structural stiffness in the efficiency assessment.

Figures 5.6 to 5.9 show relations between Structural Efficiency (SEI) and Number of Module (in Span Direction) of POP, PIP, PPC, and PPP with different span length, ranging from 24 m to 60 m.
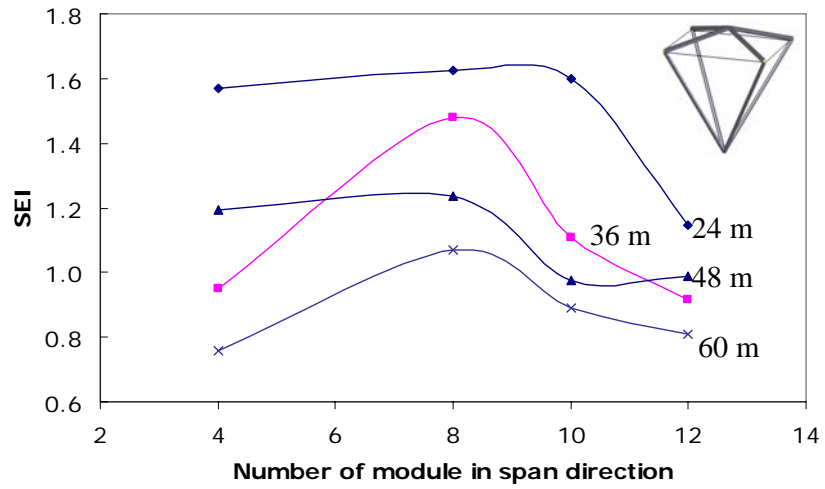


Figure 5.6. SEI of POP with Span/Depth = 10.
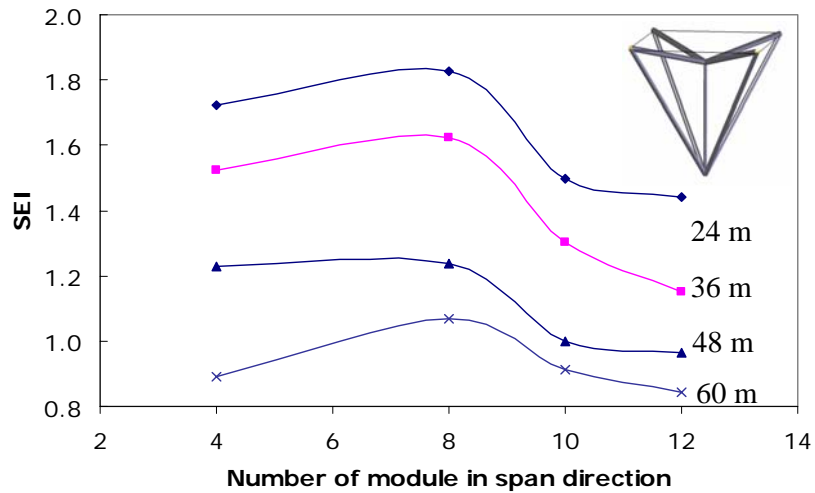


Figure 5.7. SEI of PIP with Span/Depth = 10.
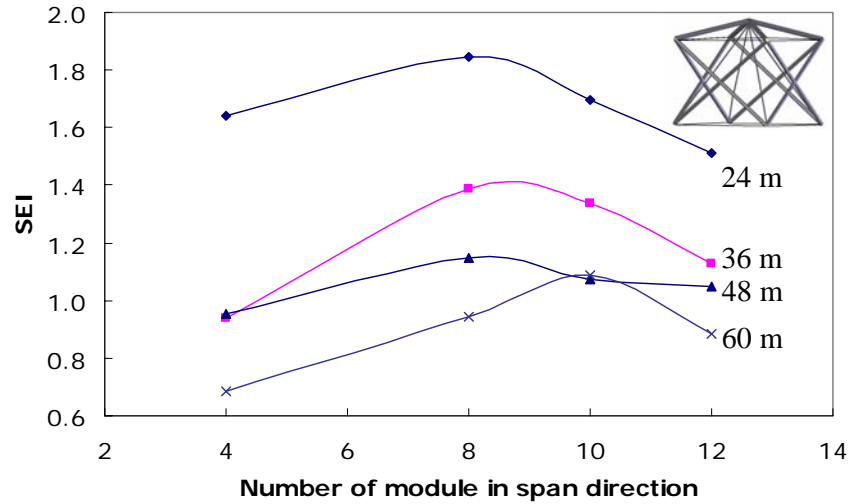
Figure 5.8. SEI of PPC with Span/Depth = 10.
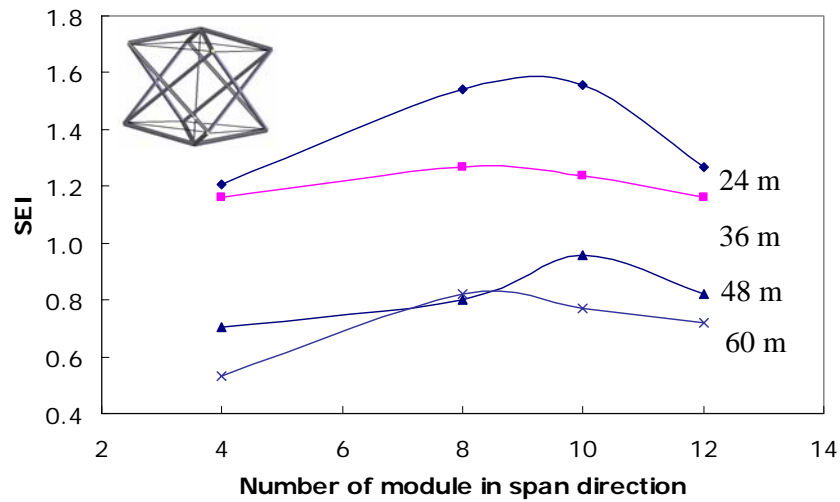


Figure 5.9. SEI of PPP with Span/Depth = 10.

SEI of all the four DTSS is low (less than 1.2) for the large span systems (48 m to 60 m span). For small span systems (24 m to 36 m), SEI is about 40% higher than that of 48-m-to-60-m span systems. The reason lies behind the design strategy and manufacturing possibilities. The design strategy in this chapter requires that each type of structural element is assigned one section size. If only one section size is used, the section size will be large to accommodate the most critical internal forces such as those near to support joints. The use of large size section for all other structural elements

causes wastage of material. Large span systems (48 m to 60 m) often have high variety in internal forces while variety in internal forces in small span systems is lower and thus the waste of material in larger span systems is higher. Therefore, SEI of large span system is lower. This situation of course can be improved when the larger span systems are designed with more section sizes. However, the waste of material cannot be avoided because the internal forces can be changed gradually while struts and cables are manufactured in larger steps of section sizes, which can be found in any manufacturers' section catalogues.

High SEI can be observed with the number of modules of 6x6 to 10x10 for any DTSS with any span length. Higher number of modules will cause higher self-weight while lower number of modules may reduce stiffness of the structure and both cases would lead to reduction in SEI. The above study finds out the optimum number of modules in each span direction. However, the Span/Height (S/H) ratio is another important design parameter and Figs. 5.10 to 5.13 show its relation to SEI. The word "Height" is used in stead of conventional word "Structural Depth" because the structural depth of DTSS is different from its height due to the inclination of top struts.
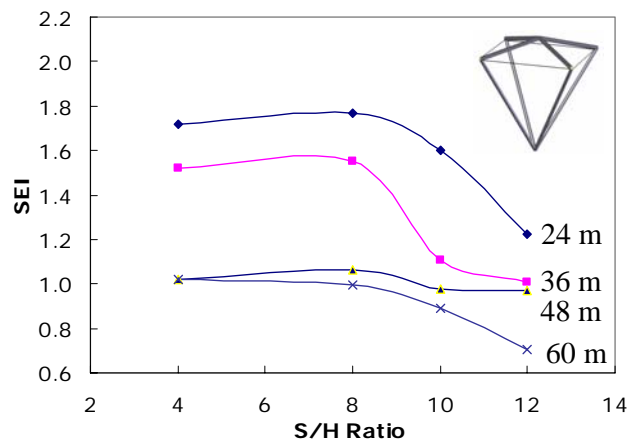


Figure 5.10. SEI of POP with 10x10 Modules.
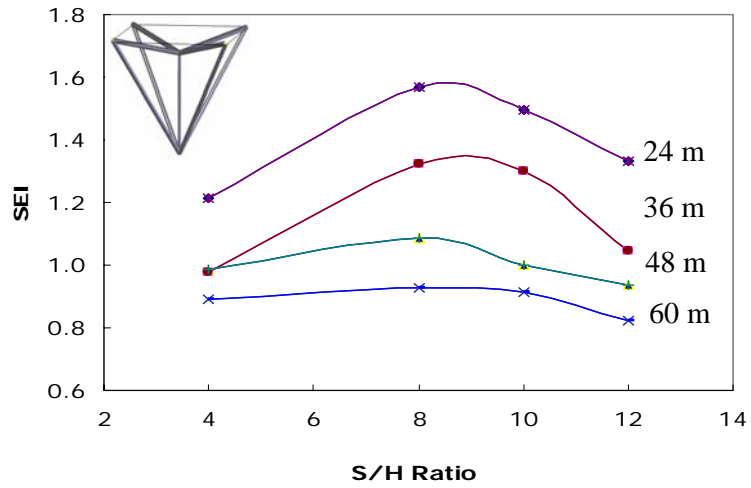
Figure 5.11. SEI of PIP with 10x10 Modules.
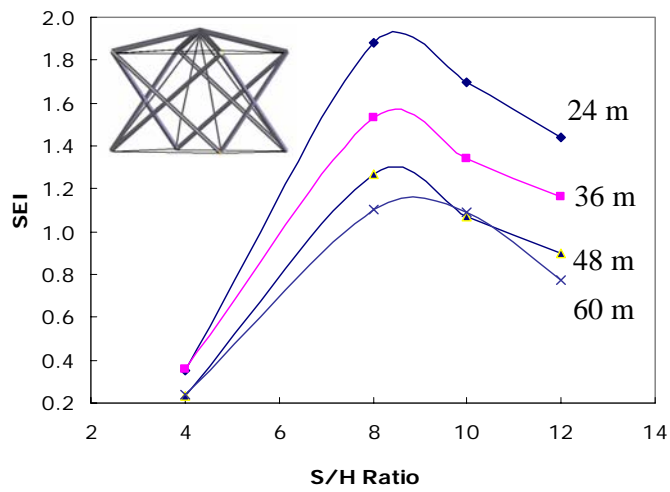


Figure 5.12. SEI of PPC with 10x10 Modules.
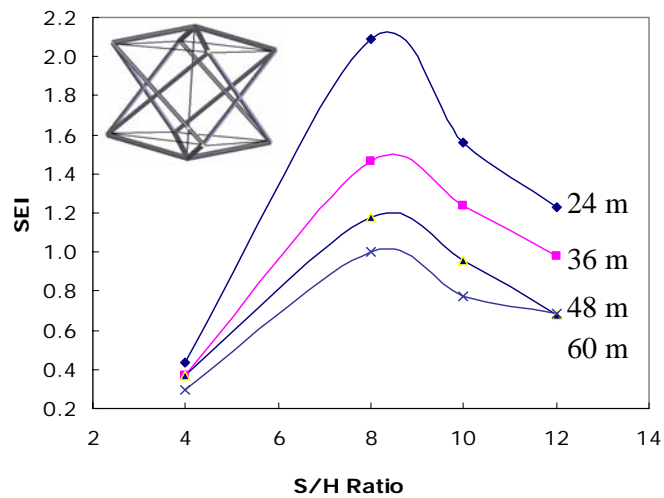


Figure 5.13. SEI of PPP with 10x10 Modules.

97

The highest SEI of 2.1 can be observed in PPP configuration with 24 m span where the Span/Depth ratio is 8 and the number of module is 10x10.

As can be observed from Figs. 5.10 to 5.13, the optimum Span/Height ratio is 8 to 10. The optimum configuration is corresponding to the highest SEI. When the Span/Height ratio is higher than the optimum range, the stiffness of the structure is much lower and the structural behaviour is closer to membrane. When the Span/Height ratio is lower than the optimum range, the diagonals are long and slender, and the self-weight of structures is higher. The structural behaviour in this case is closer to short beams.

Combining the optimum parameters Number of modules (6 to 10), Span/Height (8 to 10), the optimum shape of a structural module can be determined as follows.

Span/Module Width = 6 – 10

Span/Module Height = 8 – 10

→ *Module Height/Module Width = 0.6 – 1.25*

This rule may be used for designing DTSS other than flat systems such as those in vault or dome shape for preliminary design.

The highest average SEI of 1.19 is observed in PIP structure while it is 1.17, 1.09, and 0.98 for POP, PPC and PPP respectively. This finding is in agreement with the comment, corresponding to Fig. 5.7. The self-weight of PIP is least and its average SEI is highest, in comparison with the other three DTSS.

## 5.4 Natural frequencies and mode shapes

To understand the structural behaviour of space frames, most researchers did not consider natural frequencies as an important structural property (El-Sheikh, 1998) or free vibration analysis is only considered as a tool to create structural imperfection in works by Langbecker (2000). However, designers are well aware that natural frequency will affect the design significantly for a light structure in strong wind. To support designers' assessment in their design of DTSS for such vibration-sensitive applications, this section provides an estimation of the range of natural frequencies of different DTSS with different span lengths. The implication of frequency distribution is also discussed.

It is aware that the coupled vibration modes of the structural system and the interaction with the supporting systems such as steel frames or concrete walls may be different from vibration modes of the structural system with rigid boundary nodes. In this study, to avoid complexity of considering the flexibility of boundary nodes, these nodes are assumed fixed in direction. The detailed study to consider flexibility of the supporting system needs to be done with the specific design supporting system for each particular design project. The result of the current study can be used as a reference to double check or for preliminary estimation of dynamic loading and its effect on structural behaviour of DTSS.

The study shows that the vibration modes of POP and PIP are similar to each other. The vertical movement of the central nodes is dominant in the first mode as shown in Fig. 5.14.
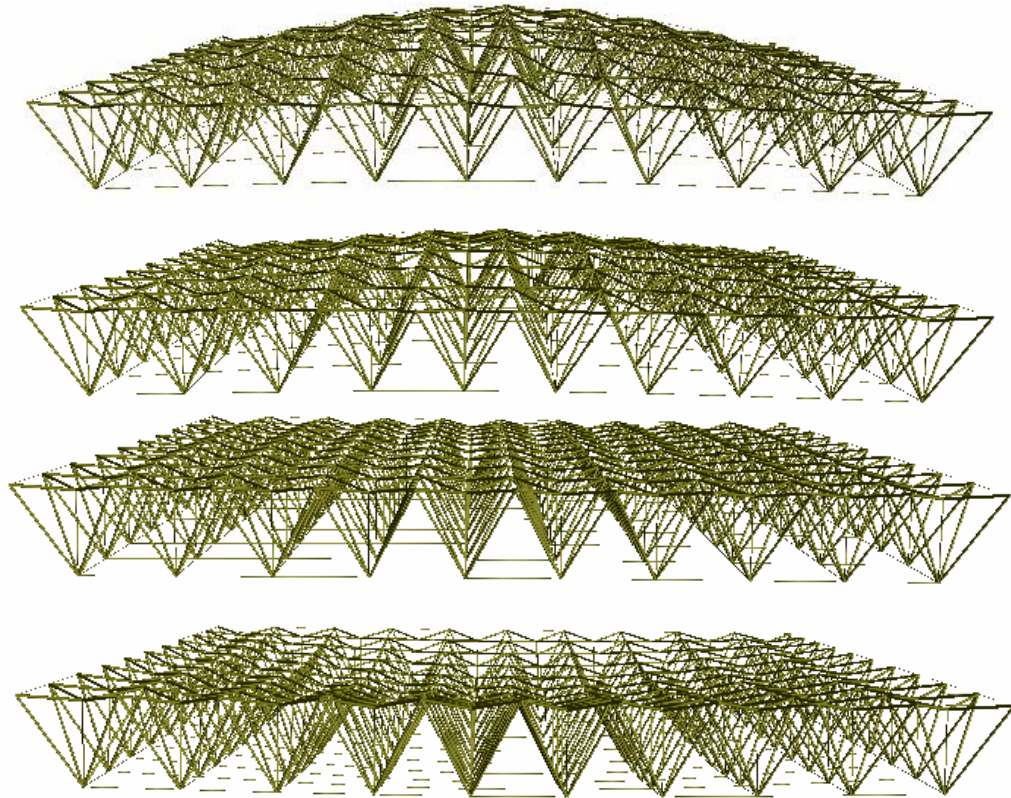
Figure 5.14. PIP vibration mode 1.

The next two modes of vibration are featured by the vertical movement of nodes near the four corners as shown in Fig. 5.15. The symmetric line of the vibration mode shape is the diagonal line.

The first three vibration modes of PIP and POP are similar to those of a plate. Therefore the critical failure might be similar to the failure of the plate which is either the "bending" failure at the centre of the structure or the "shear" failure at the corner of the structure. The absolute values of natural frequencies of PIP are shown in Table C1, Appendix C for reference. In general, the natural frequencies of PIP are not close in comparison with other structures (15%-50% different) which means the wide

separation of modes assures that PIP may vibrate in one specific mode but not in a combination mode under external excitation.
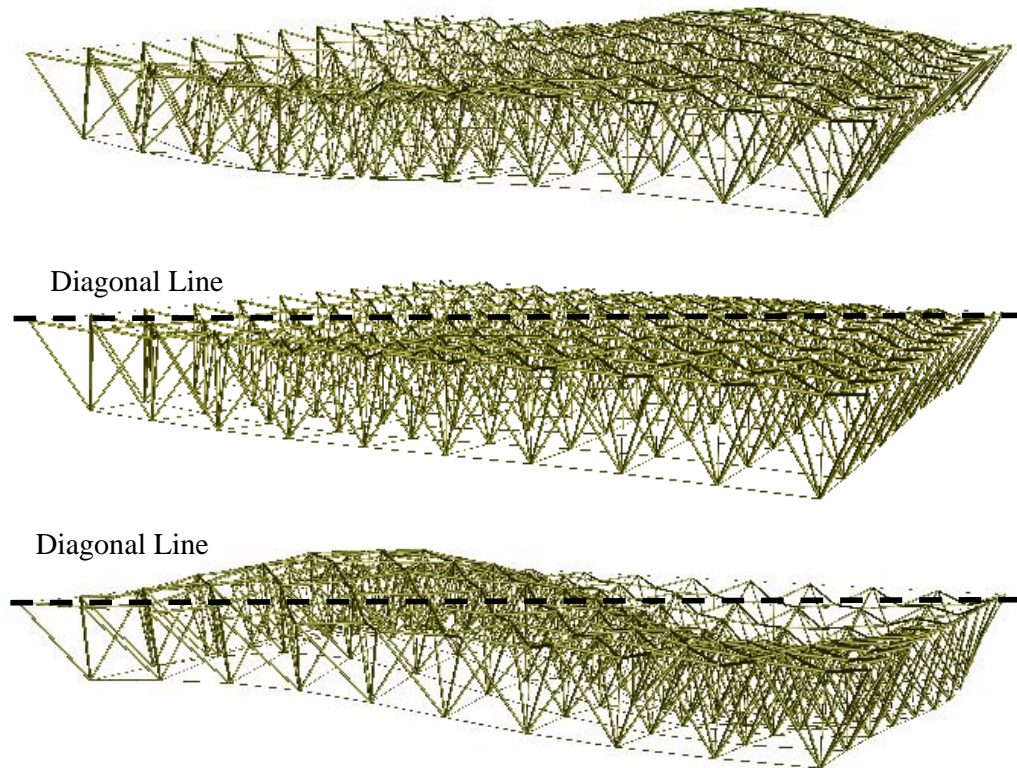


Figure 5.15. PIP vibration Mode 2.

For PPC and PPP structure, the first vibration mode is the same as that of PIP with the dominance of vertical movement of the central nodes as shown in Figs. 5.16-5.17.
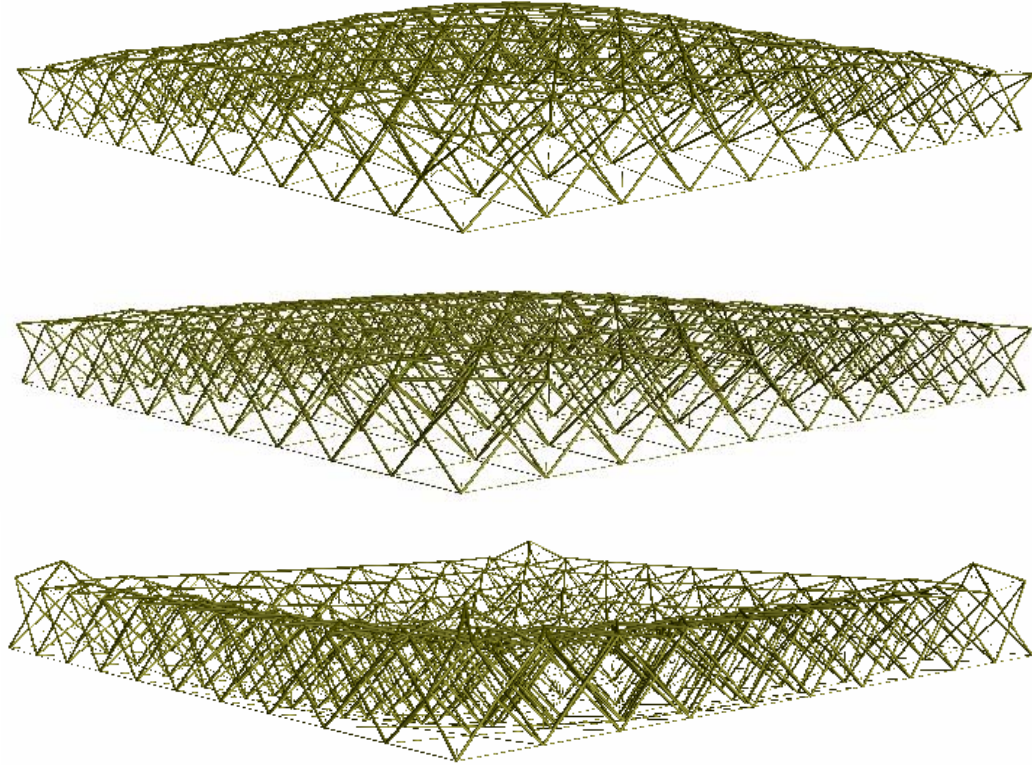
Figure 5.16. PPC 1$^{st}$ Vibration Mode.

However, the next two vibration modes of PPC and PPP are featured by the horizontal movement of the hinge of the scissor-like elements (SLEs) as shown in Figs. 5.18-5.19. The reason is that the SLE bars are slender in the direction perpendicular to the SLE plane. The result of this analysis suggests that rectangular hollow section can be chosen for SLE bar but the longer edge of the section should be in the deformation direction and thus structural stability can be improved.
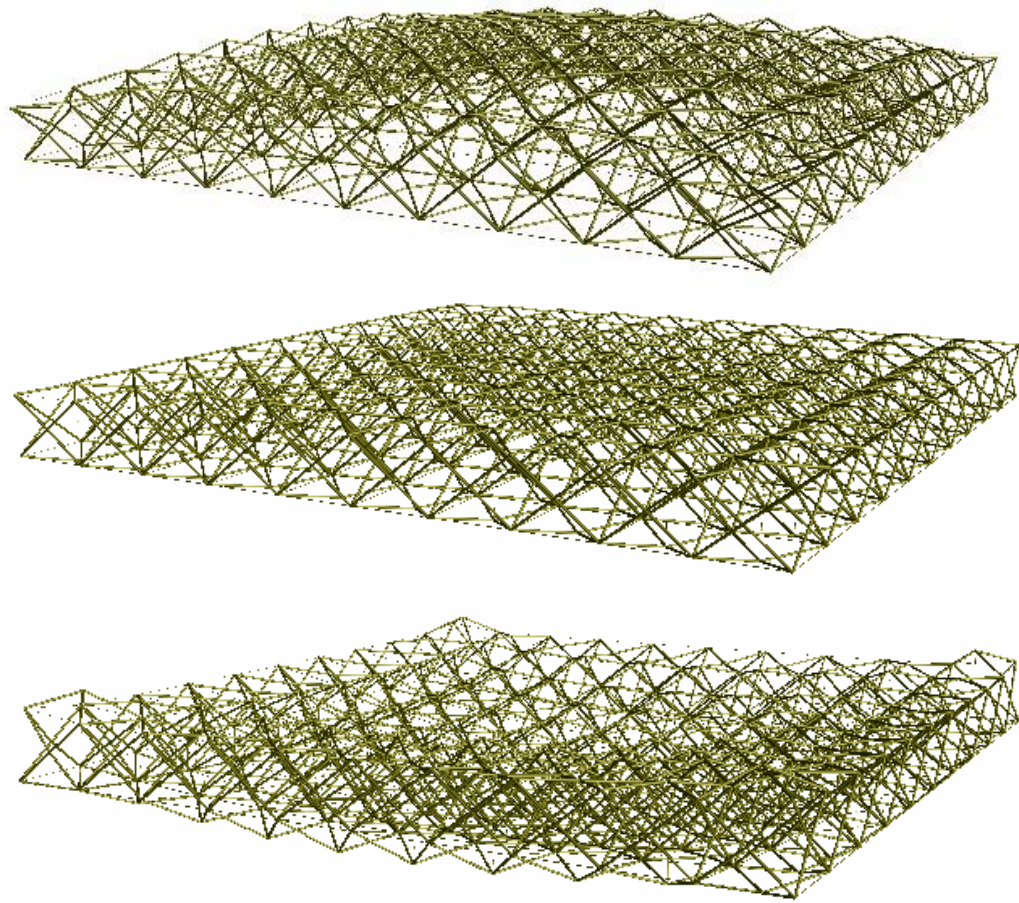
Figure 5.17. PPP 1$^{st}$ Vibration Mode.

For most PPC and PPP structures, the first natural frequency is about 40% - 50% smaller than the second natural frequency. The frequencies are largely separated. This means, similar to PIP, under external load, probably only one vibration mode is excited.
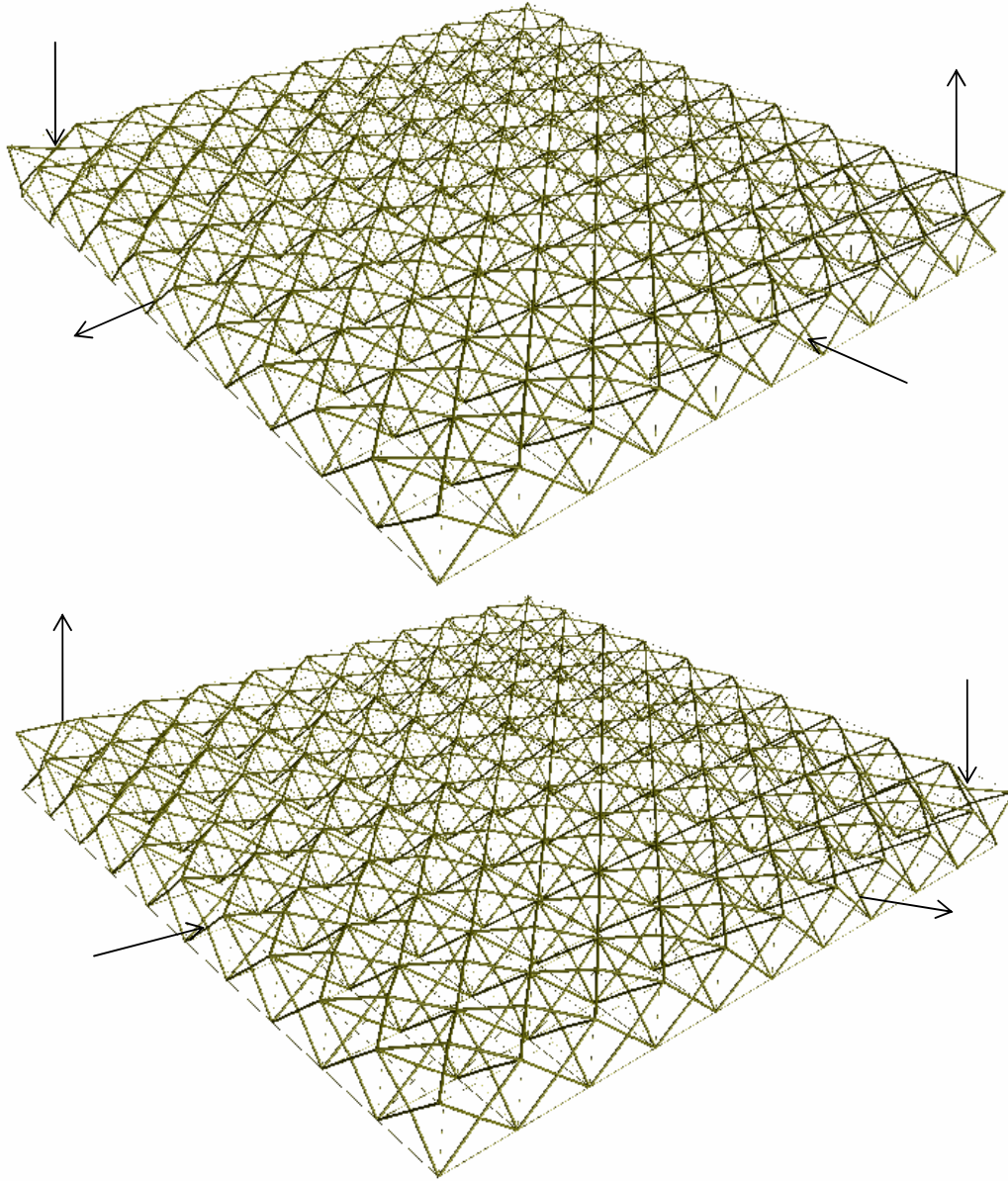
Figure 5.18. PPC 2$^{nd}$ Vibration Mode.

However, for deep structure (with Span/Depth < 10) the SLE bars are so slender that the first three frequencies are very close, which may cause structural instability under external excitation. The first three modes are associated with the vibration of the SLE bars and there is no vertical movement of central nodes which appears in the case of

low-structural-depth DTSS. It is recommended that the size of SLE bars in these cases is increased in comparison with the size of the top and bottom struts.
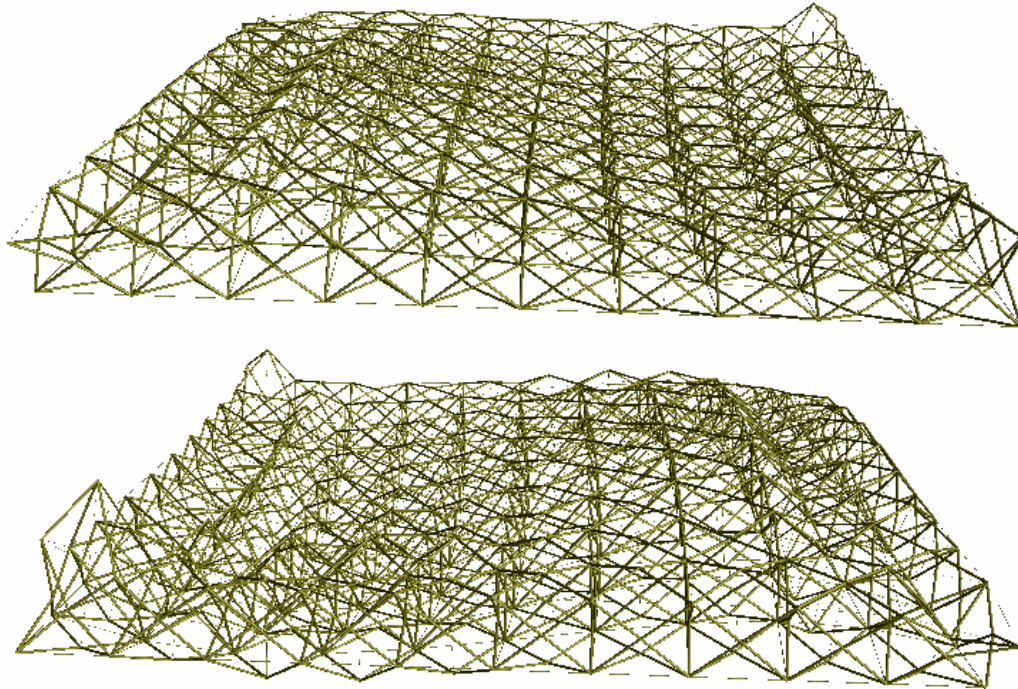


Figure 5.19. PPP 2<sup>nd</sup> Vibration Mode.

As can be observed in the first three modes, the length of the vertical cables at the four corners is sensitive to vibration and they can be in severe tension force. It would be a wise choice for designers to choose a larger size for these cables in comparison with the size of the internal vertical cables.

**5.5 Effects of pre-tensioning on structural behaviour of tension-strut structures**

**5.5.1 Effects of pre-tensioning on existing tension-strut structures**

In general, when a cable is in tension, the stiffness of the cable is increased. The following example illustrates the stiffening effect.
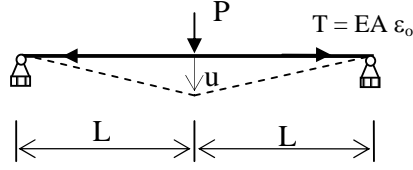
Figure 5.20. Deformed configuration of a cable.

When a cable is subject to a pre-tension force T causing initial strain $\varepsilon_o$ as shown in Fig. 5.20, the stiffness of the cable to resist an applied load P is

$$K_u = \left[ 2EA\left(\frac{1}{2}\frac{u^2}{L^2} + \varepsilon_o\right)\frac{1}{\sqrt{L^2 + u^2}} \right] \tag{5.3}$$

For example if $\dfrac{u}{L} = \dfrac{1}{200}$ (serviceability limit of deflection for steel structures, BS 5950: Part I, 2000), and $\varepsilon_o = 0.0002$ (about 10% of the yield strain of steel) then contribution by membrane action ($\frac{1}{2}\frac{u^2}{L^2} = 0.0000125$) is 6.25% of $\varepsilon_o$. The contribution of the initial strain $\varepsilon_o$ to structural stiffness is much higher than membrane action if structure deflects within serviceability limit. Membrane action is considerable only when $\dfrac{u}{L} = \dfrac{1}{50}$ then $\frac{1}{2}\frac{u^2}{L^2} = 0.0002 = \varepsilon_o$ . Pre-tensioning affects structural stiffness significantly in all cases.

However, in different cable-reinforced structural systems, pre-tensioning may leads to different effects. Pre-tensioned Cable-Stayed Columns (PCSC) in Fig. 5.21 are studied and the effects of pre-tensioning on the structural behaviour of these structures are investigated. The size of the main strut is 48.3x2.3 and the size of the horizontal struts is 25x1. They are made of steel grade 275, in correspondence with BS 5950-2000: Part 1. The size of the cables is 6 mm. The cables have elastic modulus of 145E+9 N/m$^2$ and breaking stress of 1.089E+09 N/m$^2$, i.e. the minimum breaking load (MBL) of the cable is 30 kN. If the column does not have any cable and bracing struts, the load carrying capacity is 4.6 kN with 6.2275 m effective length.
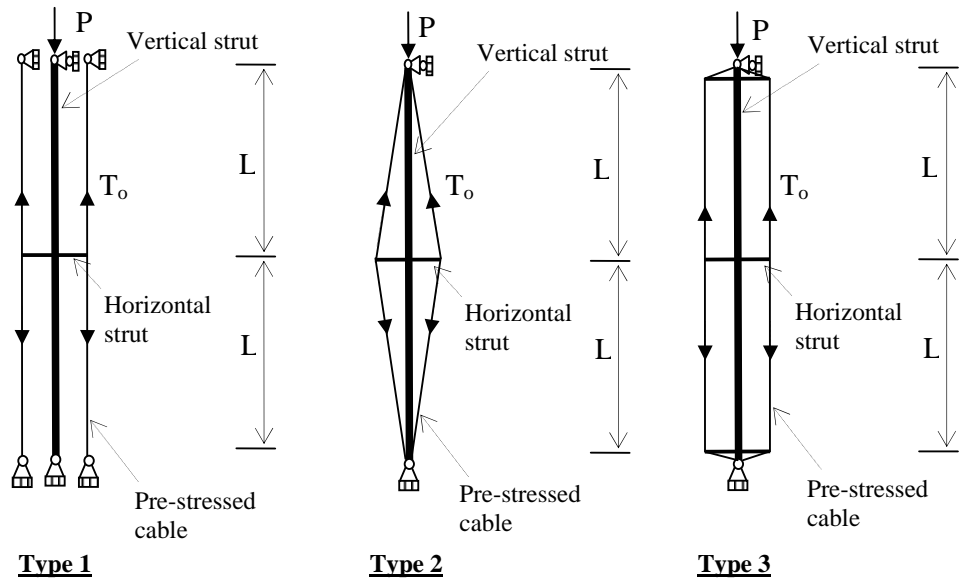
Figure 5.21. Pre-tensioned cable-stayed column.
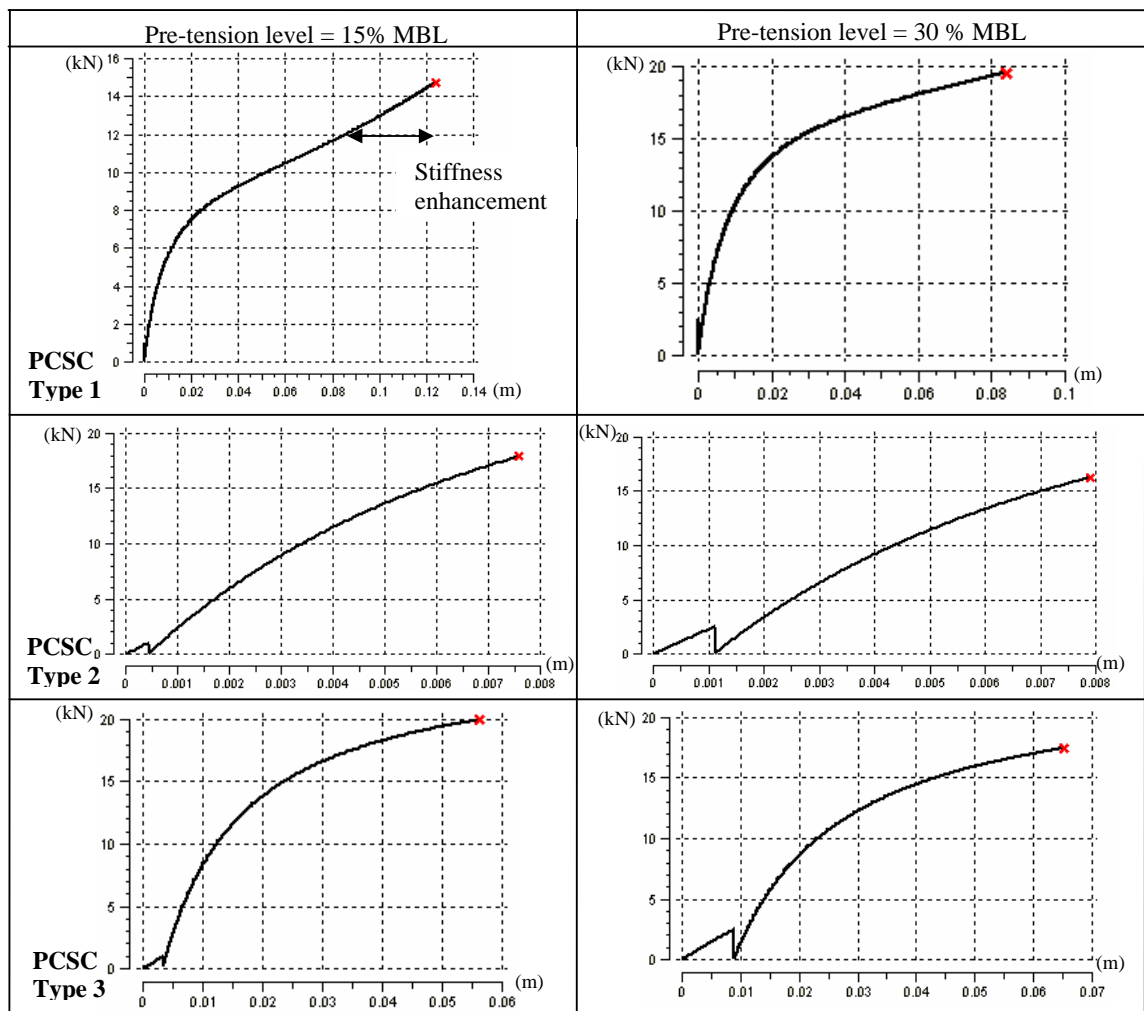


Figure 5.22: Load – horizontal mid-column displacement curve of PCSC

As shown in Fig. 5.22, for PCSC-type-1, load carrying capacity is increased to 15 kN and 20 kN (when pretension is increased to 15% and 30% MBL, respectively) due to stability enhancement by pre-tensioned cables. However, for PCSC-type-2 and PCSC-type-3, when the pre-tensioning level is increased from 15% MBL to 30% MBL, the load bearing capacity is dropped due to high compression force from pre-tensioned cables.

**5.5.2 Effects of pre-tensioning on deployable tension-strut structures**

As explained in the chapter 3, the Deployable Tension-Strut Structures (DTSSs) are stabilized by pre-stressing the add-in structural components. Therefore, it is of interest to evaluate the effect of pre-stressing level on structural behaviour of structures. This section provides clues to how pre-stressing level affects the structural behaviour of DTSSs. Four typical DTSSs with 60 m span are analysed for this investigation. Both static and free vibration analyses are performed to assure a comprehensive understanding of the pre-stressing effects. The results of the analysis are shown in Tables 5.1 – 5.4. The first column of the tables from left presents the pre-strain of the add-in components. The second column of the tables presents the displacement of the mid-span node under pre-stressing effect. The third column presents the displacement of mid-span node under both external loads and pre-tension load. The last column presents the first frequency of the structure after its add-in components are pre-stressed. In these analyses, the structures are maintained unchanged except the pre-stressing force, which is expressed in the Tables by initial pre-strain. The pre-strain of 0.001, 0.002, and 0.003 is applied on the add-in cables and the corresponding load will be

corresponding to 10%, 20%, and 30% of minimum breaking load (MBL) of the cables.

The static loading condition is the same as that in section 5.2.

Table 5.1: Pre-stress effects on 60-m-span PIP

| Pre-strain | After pre-stress Displacement (mm) | Final Displacement (mm) | Frequency (Hz) |
|---|---|---|---|
| 0.001 | 0 | 101 | 4.51 |
| 0.002 | 0 | 101 | 4.50 |
| 0.003 | 0 | 101 | 4.49 |

Table 5.2: Pre-stress effects on 60-m-span POP

| Pre-strain | After pre-stress Displacement (mm) | Final Displacement (mm) | Frequency (Hz) |
|---|---|---|---|
| 0.001 | 0 | 111 | 3.05 |
| 0.002 | 0 | 106 | 3.04 |
| 0.003 | 0 | 96 | 3.03 |

Table 5.3: Pre-stress effects on 60-m-span PPC

| Pre-strain | After pre-stress Displacement(mm) | Final Displacement (mm) | Frequency (Hz) |
|---|---|---|---|
| 0.001 | -12 | 94 | 4.76 |
| 0.002 | -26 | 82 | 4.76 |
| 0.003 | -41 | 67 | 4.76 |

Table 5.4: Pre-stress effects on 60-m-span PPP

| Pre-strain | After pre-stress Displacement(mm) | Final Displacement (mm) | Frequency (Hz) |
|---|---|---|---|
| 0.001 | 7 | 100 | 3.94 |
| 0.002 | 14 | 90 | 3.93 |
| 0.003 | 21 | 84 | 3.92 |

From Tables 5.1 – 5.4, it is obvious that the first natural frequencies of DTSSs are not affected much (less than 1%) while the pre-strain is doubled or tripled. This means the pre-stressing force does not have significant effect on the stiffness of DTSS. However, observing the static analysis results, increase in pre-stressing level would result in a reduction in displacement which is similar to a pre-cambering effect. The bottom

nodes of DTSS are lifted upwards due to the increase in pre-stressing level. This finding is useful in maintenance service of DTSS. Pre-stressing can be used to reduce excessive deflection while it does not affect the overall stiffness of the structure. For example, PPC displacement is reduced up to about 30% when pre-strain is increased from 0.001 to 0.003.

**5.6 Efficiency comparison with conventional space truss systems**

To evaluate the structural efficiency of DTSS, the least structurally effective DTSS, which is PPP, is compared to the conventional double-layer space truss. With the same loading conditions and boundary conditions in parametric study above, PPPs and space frames are compared and the results of this comparison are given in Table B7, Appendix B. Fig. 5.23 shows SEI of PPPs and space frame with a range of span from 36 m to 60 m. It is found that the SEI of PPP structures is on average 9% lower than that of conventional double-layer space frame. Because PPP is the structure with lowest SEI among DTSS, it can be concluded that DTSS is comparable to double-layer space frame in terms of structural efficiency.
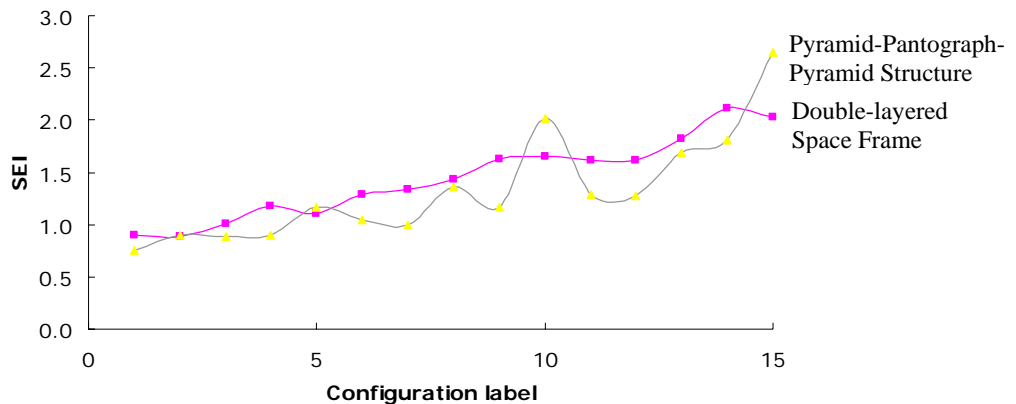


*Note: The configuration corresponding to label in the horizontal axis can be found in Table B8, Appendix B. From left to right: span length 60 m – 36 m*

Figure 5.23. Structural efficiency index of PPP and space frame.

The effect of changing inclination angle $\alpha$ of top and bottom struts on SEI is also studied. SEI increases by 23% on average when tan ($\alpha$) changes from 0.15 to 0.08 based on the results in Table B7, Appendix B.

**5.7 Robustness**

When a new structural form is proposed for applications, there is always a question of how robust the form is or in other words, what happen if certain structural element is added or removed from the form. This section is to answer how much removal or addition of structural element may affect DTSS structural response.

Pyramid-Pantograph-Cable (PPC) structure is chosen for this study. The structure spans 48x48 m, supported at the boundary joints as shown in Fig. 5.24. Span/height ratio is 10 and the number of module is 4x4. The loading condition is the same as mentioned in the parametric study (section 5.3).
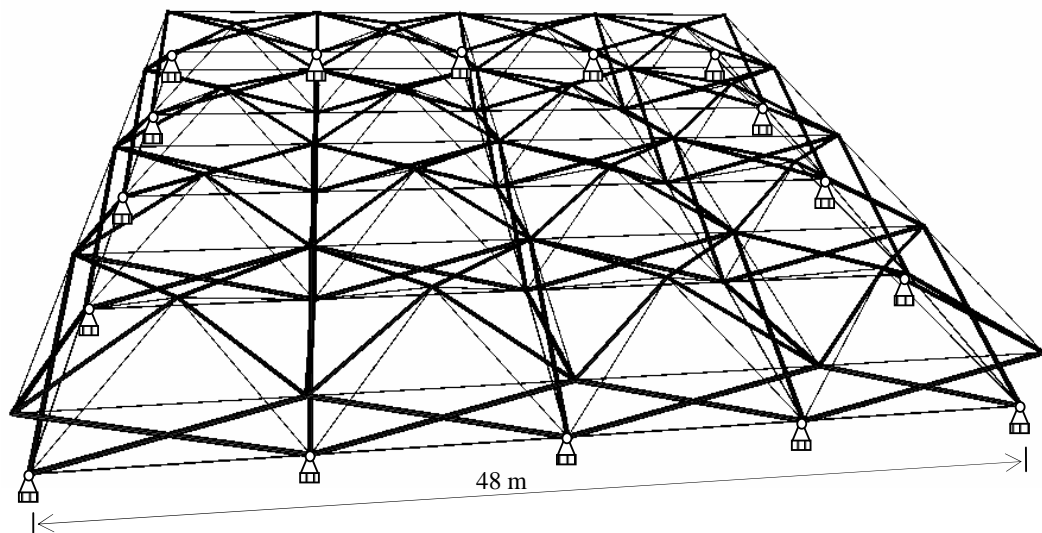


Figure 5.24. Structural form of Pyramid-Pantograph-Cable structure.

The robustness study includes the cases of removing one cable element, one strut element, and adding vertical struts to connect middle joints as shown in Figs. 5.25 – 5.27 respectively. The load-displacement curves of these structures are shown in Fig. 5.28. Initial phase is pre-tensioning of add-in cables (load level reaches 1.0) and causes pre-cambering and then imposed load is applied until the structure fails. The imposed load level of 1.0 equals to the previous study in section 5.2.
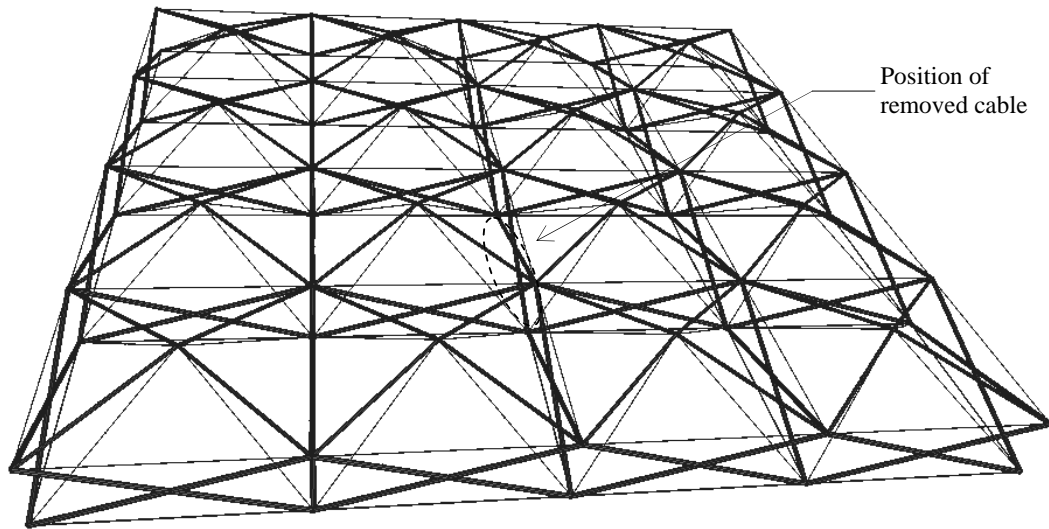


Figure 5.25. Structural form of PPC with removal of one bottom cable.
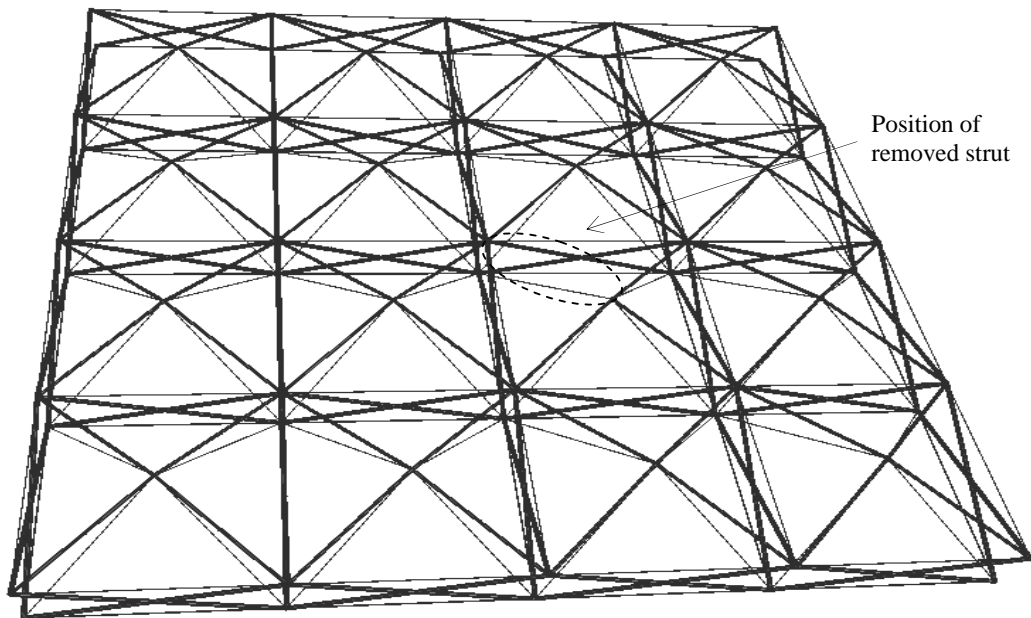


Figure 5.26. Structural form of PPC with removal of one top strut.
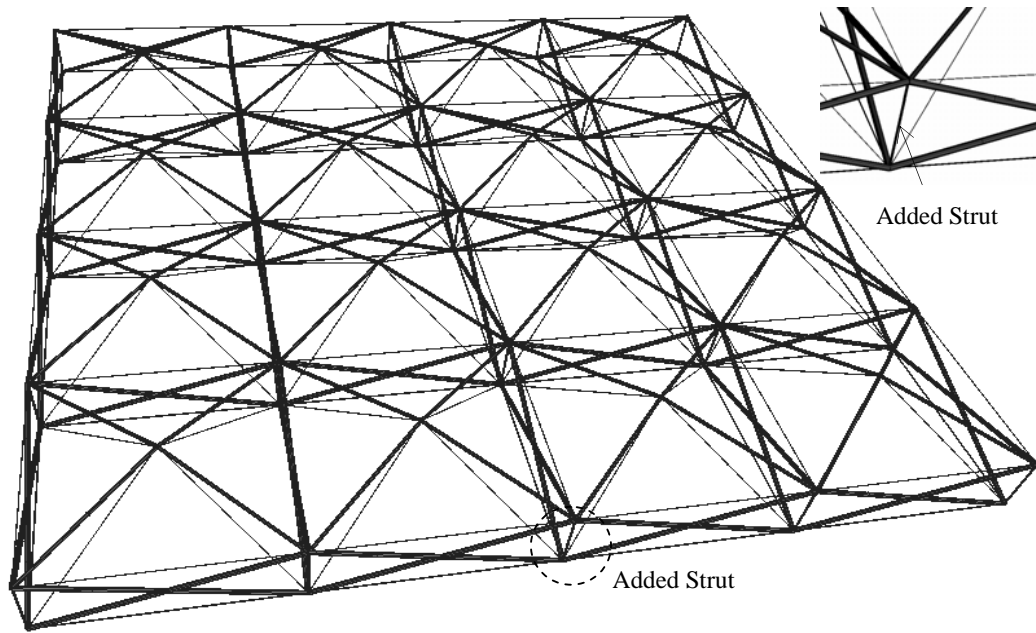
Figure 5.27. Structural form of PPC with addition of vertical struts.
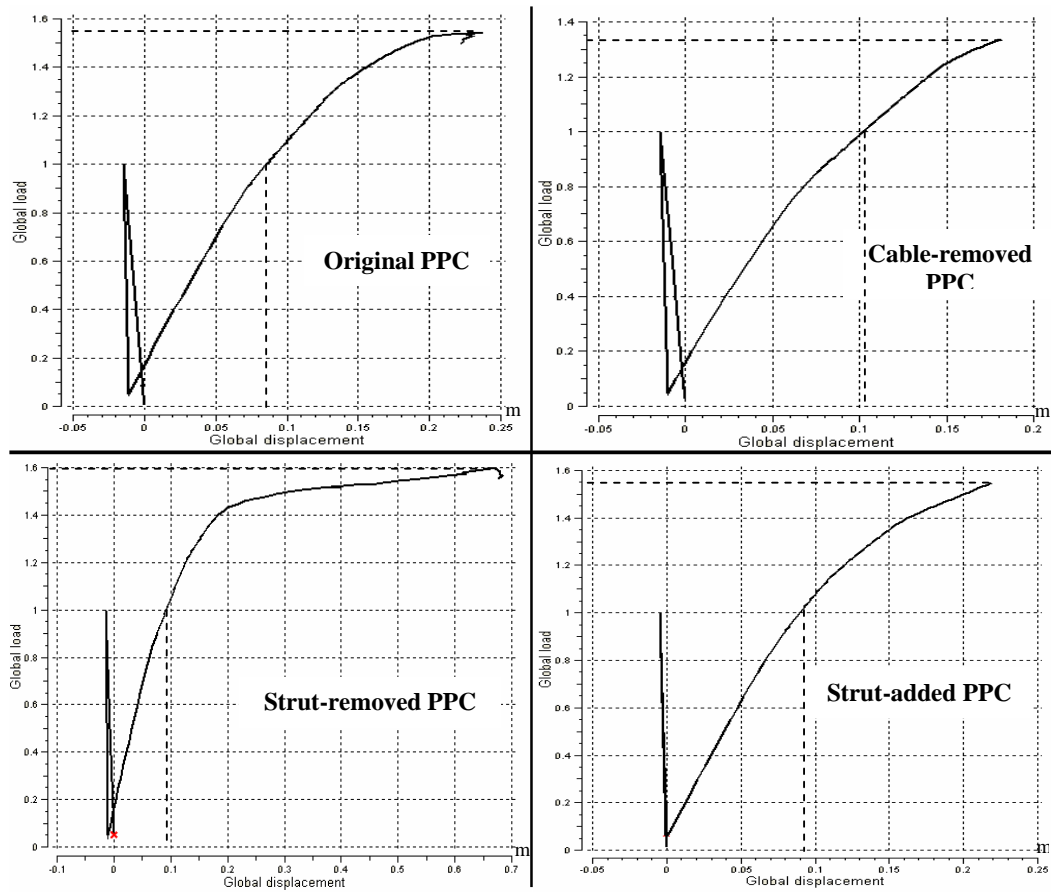


Figure 5.28. Load-displacement curves of different structural forms.

In all the cases of removal or addition of structural elements, it is found that the displacement of the mid-span joint (shown in the curves, Fig. 5.28, as global displacement) is higher than the original configuration (measured at global load level equals to 1.0). The maximum displacement difference is (0.11-0.085)/0.085 = 30% in the case where a bottom cable is removed. It is also the case where the ultimate load bearing capacity of the whole structure is affected the most (reduction of (1.55-1.34)/1.55 = 13.5%). This proves that the structure has high redundancy but the bottom cables are critical to the structural performance of DTSSs.

**5.8 Summaries**

Deployable Tension-Strut Structures (DTSSs) are proved to be comparable with conventional space frame in terms of structural efficiency. SEI of one of the DTSS (Pyramid-Pantograph-Pyramid structure) is found to be only 9% lower than that of space frame for the range of span from 36 m to 60 m. The parametric study on DTSS for the range of span from 24 m to 60 m shows optimum design parameters of DTSS for flat structures. The optimum Span/Module Height ratio is 8 – 10 and the optimum Span/Module Width = 6 – 10.  The optimum Module Height/Module Width ratio is 0.6 – 1.25. In addition, it is found that PIP is the most effective DTSS in this study with SEI of 1.19 while it is 1.17, 1.09, and 0.98 for POP, PPC and PPP, respectively. Pre-tensioning does not affect structural stiffness of DTSS as significantly as in cable-stayed column but it can affect the displacement of the bottom nodes considerably. This feature can be used in maintenance of DTSS where long-term deflection of DTSS needs to be reduced by increasing pre-tension force. DTSSs have high redundancy in terms of strut but sensitive to removal of bottom cables. This hints a caution in designing bottom cable connections to the structure.

# CHAPTER 6

# DEPLOYABLE BOOM STRUCTURES

Chapter 6 is devoted to developing Deployable Tension-Strut Structure as "linear deployment device" or boom structures for space application. The existing boom systems are reviewed and compared with proposed Deployable Tension-Strut Booms. Both static structural behaviour and dynamic structural properties (natural frequency) of these structures are studied using analysis methods which are mentioned in Chapter 4. The study shows the viability of the proposed Deployable Tension-Strut Boom concept and when to choose this system for design of space station with regards to their advantages and disadvantages.

## 6.1  Overview

Space station requires a "back bone" structure to support its operation such as docking shuttle vehicles or mounting communication devices. It is common that these "back bone" structures are made of truss (or articulated mast) due to its lightness, rigidity and clear view for users, as shown in Fig. 6.1. The "back bone" truss systems are transported from the Earth to the operating location by launchers. It is essential that the transportation form of the "back bone" truss should be compact to avoid significant increase in drag force during the flight. In other words, deployability is essential for these trusses. In this section, several common forms of deployable booms are reviewed and two new forms of deployable boom are proposed. It is noted that there are other types of boom such as wire deployer, tubular boom, telescopic boom, and coilable

mast but this thesis will deal with articulated mast only because this type is considered

the most effective in load bearing capacity (Bowden, 1998).
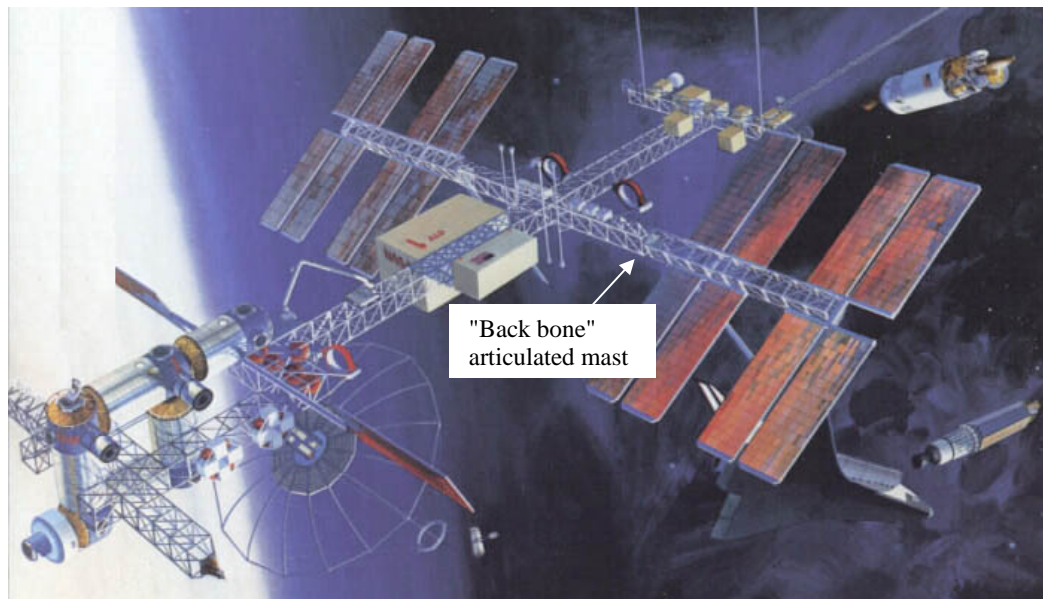


Figure 6.1. Power Tower – Space Station.
(Designed by NASA, 1984)

### 6.1.1 Existing boom structures

Although the demand for deployable boom structures is high with long history of

space structure development, there are currently three distinguished boom systems:

ABLE Engineering boom (ABLE boom for short, ABLE is the name of the company),

tensegrity boom (Tibert, 2002), and cable-stiffened pantographic boom (You and

Pellegrino, 1996b).

ABLE boom is formed by truss system with special articulated joint design (Douglas,

1993) as shown in Fig. 6.2. The articulated mechanical joints control deployment of

the whole truss and thus the structural stiffness of the system relies on the rigidity and

reliability of these mechanical joints. If mechanism in the joint which control

deployment of the boom fails under high stress, the structure will collapse into the

folded form. Therefore, this type of joint is costly to make due to its complication and high requirement of reliability. The overall structural performance of the ABLE boom is similar to the conventional truss system, except the fact that the overall bending stiffness is 25% lower to account for the flexibility of the articulated joints.
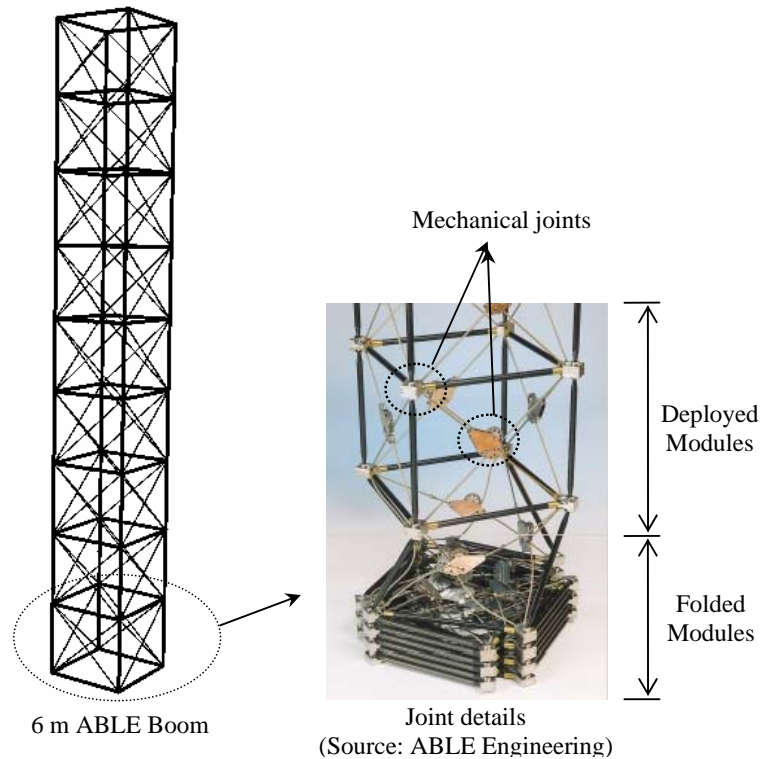


Figure 6.2. ABLE Engineering boom.

Tensegrity boom, shown in Fig. 6.3, is studied by Tibert (2002). Initially, the concept of tensegrity seems to be suitable to be applied in Boom due to the deployability with regards to the discontinuity of strut systems. However, the deployed tensegrity boom is more flexible than ABLE boom. For the comparative case study of 60 m long boom the tensegrity boom is about 100 times more flexible than ABLE boom according to Tibert (2002).
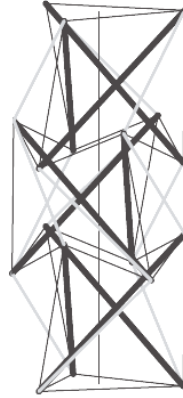
Figure 6.3. Tensegrity boom.
(Source: Tibert, 2002)

Cable-stiffened pantographic boom (CSP boom) consists of a triangular pantograph system, which is reinforced by continuous cable systems as shown in Fig. 6.4. You and Pellegrino (1996) proposed that cables can improve the structural stiffness of 3-D pantograph column while the structure can still be folded and deployed in similar manner to pantograph.
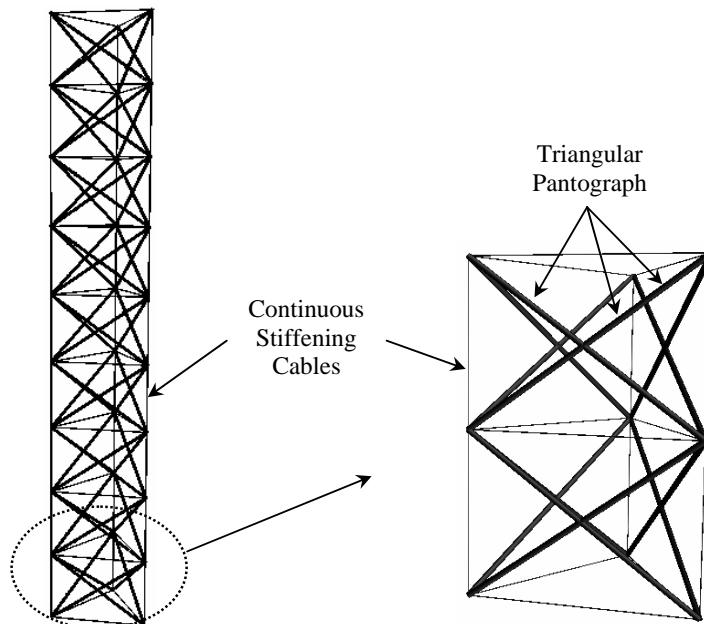


Figure 6.4. Cable-stiffened pantographic boom.

ABLE boom is most structurally efficient among the three articulated boom systems due to the stiffness of the struts, which are located at a distance further from the central axis of the boom. However, the complication and reliability of ABLE articulated joint makes this system considerably more expensive than others. Tensegrity boom is much more flexible than ABLE boom. The structural properties and structural morphology of these systems will be discussed further in the section 6.2 and 6.3.

### 6.1.2    Novel boom structures

In this thesis, three boom systems are proposed for practical usage: Pyramid-On-Pyramid boom, Expanded Pyramid-On-Pyramid boom, and Twisted Triangular boom. The motivation is to develop a deployable boom system which can be as structurally effective as ABLE boom but less complicated in joint design and deployment control.

Pyramid-On-Pyramid boom (POP boom) preserves the major deployment mechanism of POP structures, which is the Pyramid components introduced in chapter 3. These Pyramid components are connected in stacks so that it can form boom and cables are attached to the external nodes to improve the bending stiffness of the boom. The form of POP boom is shown in Fig. 6.5.

Expanded Pyramid-On-Pyramid boom (XPOP boom) is a variation of POP boom with better bending stiffness. The top node of the Pyramid components is expanded to be a stiff two-dimensional component as shown in Fig. 6.6. It is obvious that the struts on the edges of the Pyramid components are far from the central axis of XPOP boom and

almost parallel to this axis. The inclination of these struts determines the efficiency of

transferring compressive force through these structural elements.

Compression
Flow

Inclination
between Pyramid
strut and
stiffened cable

Pyramid
Component

Continuous
Stiffened
Cables
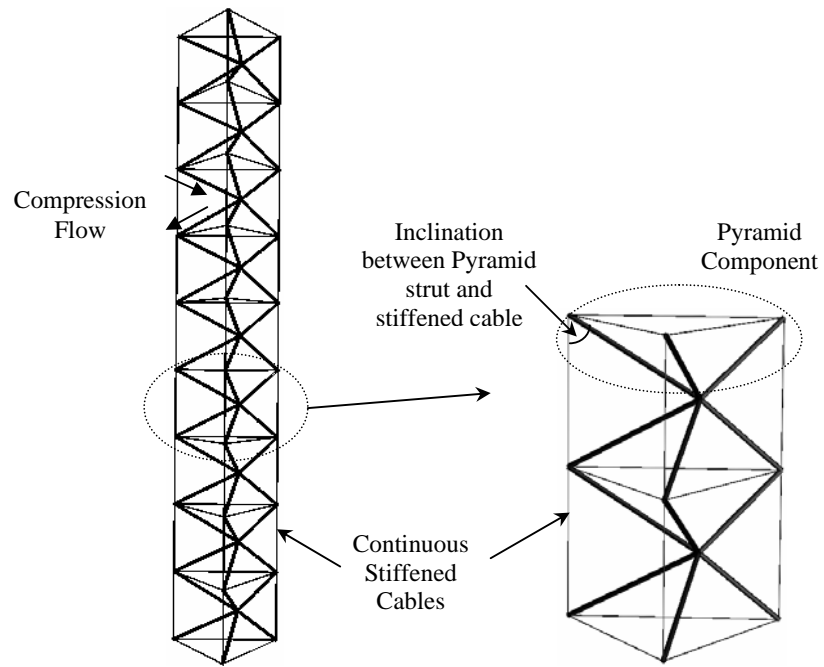
Figure 6.5. Pyramid-On-Pyramid boom.

Compression
Flow

Edge struts
are on the
extreme
fibre of the
boom

Expanded
Pyramid
Component

Rigid
Triangle

Continuous
Stiffened
Cables
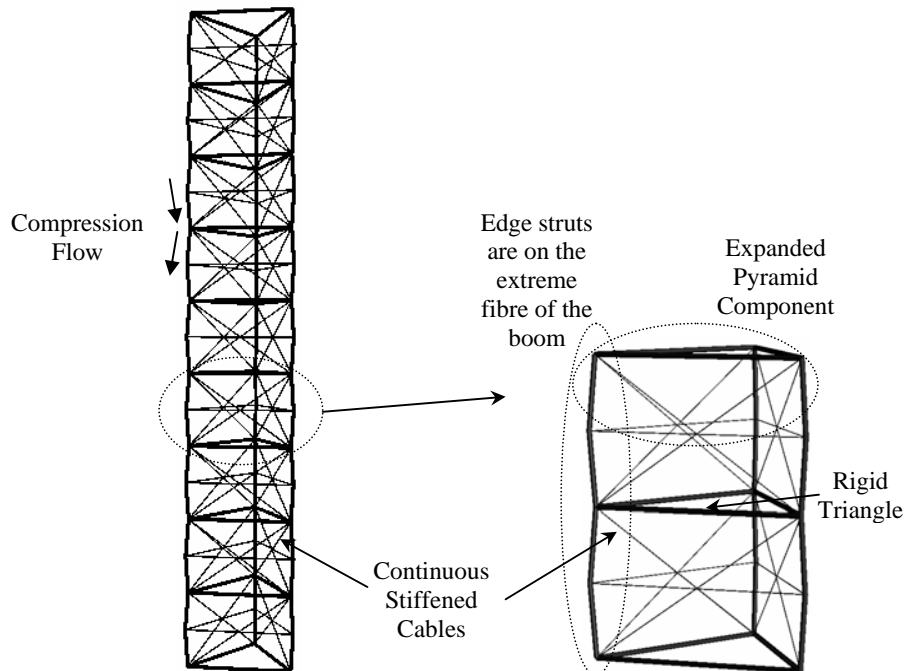
Figure 6.6. Expanded Pyramid-On-Pyramid boom.

Twisted Triangular boom (TWT boom) is designed to follow the concept of deployable stiff plates as each set of three struts forms a rigid triangle. These triangular plates resist compression while the stiffened cables resist tension. The form of TWT boom is shown in Fig. 6.7.
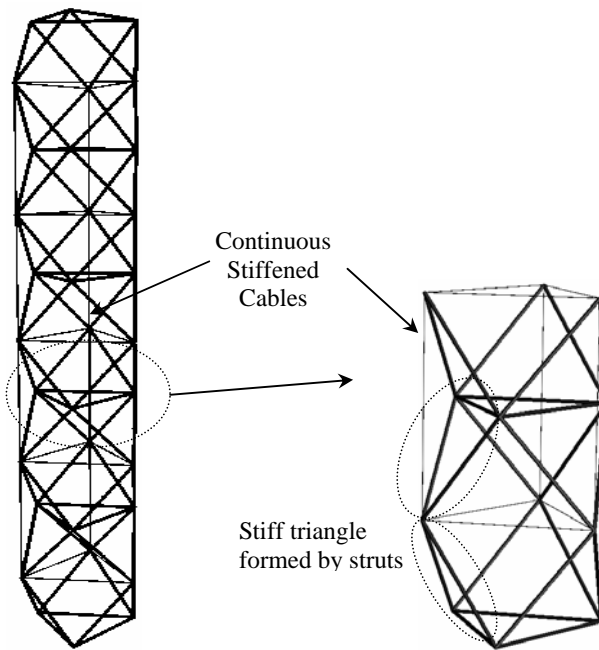


Figure 6.7. Twisted Triangular boom.

## 6.2    Natural frequencies and mode shapes

Spacecraft attitude control and pointing of sensors and antennas are based on control analysis which requires information about mode shapes and modal frequencies. In this section, these dynamic properties of different boom systems, ABLE boom, POP boom, XPOP boom, TWT boom, and CSP boom, are investigated. The frequencies are compared to preliminarily assess the structural effectiveness of booms regarding bending and torsion. The mode shapes are used to assess the critical failure mode of booms.

All the booms are designed with the same geometric proportion as that of the practical ABLE boom. There are totally 9 modules along the boom and the height of each module is 0.6975 m. The total height of the boom is 6.2775 m. The bottom nodes of the boom are located on a circle of 0.56 m diameter. All struts are assigned a circular hollow section of 25 mm diameter and 1 mm thickness. All cables are assigned a section of 5 mm diameter. This section assignment follows the study on tensegrity boom by Tibert (2002) to facilitate comparison. All cables are pre-stressed to the same level before performing the free vibration analysis. The result of this analysis is shown in Table 6.1.

Table 6.1. Free vibration analysis of boom structures.

| ID | Type | Mass (kg) | Bending mode1 | | Bending mode 2 | | Torsion mode 1 | |
|---|---|---|---|---|---|---|---|---|
| | | | Mode no. | f (Hz) | Mode no. | f (Hz) | Mode no. | f (Hz) |
| 1 | ABLE | 6.71 | 1 | 29.78 | 2 | 29.78 | 3 | 35.76 |
| 2 | XPOP | 7.04 | 1 | 24.70 | 2 | 24.90 | 3 | 34.69 |
| 3 | TWT | 9.37 | 1 | 10.84 | 2 | 10.84 | 6 | 146.35 |
| 4 | CSP | 8.59 | 1 | 10.80 | 2 | 10.80 | 6 | 126.58 |
| 5 | POP | 5.05 | 2 | 13.30 | 3 | 13.48 | 1 | 6.82 |

From Table 6.1, it is obvious that ABLE boom and XPOP boom possess the best dynamic property with the first frequency of 29.78 Hz and 24.70 Hz, respectively. All other boom systems have frequencies of less than half of that of ABLE boom. In this analysis, it is assumed that all mechanical joints of ABLE boom are ideal, which means it does not affect the stiffness of the boom. It is also noted that the first mode of vibration of ABLE boom and XPOP boom is bending while first vibration mode of tensegrity boom is axial (Tibert, 2002) and that of POP boom is torsion. This means torsional stiffness of ABLE boom and XPOP boom are relatively better than bending stiffness. The first modes of vibration of different booms are given in Figs. 6.8 to 6.10.
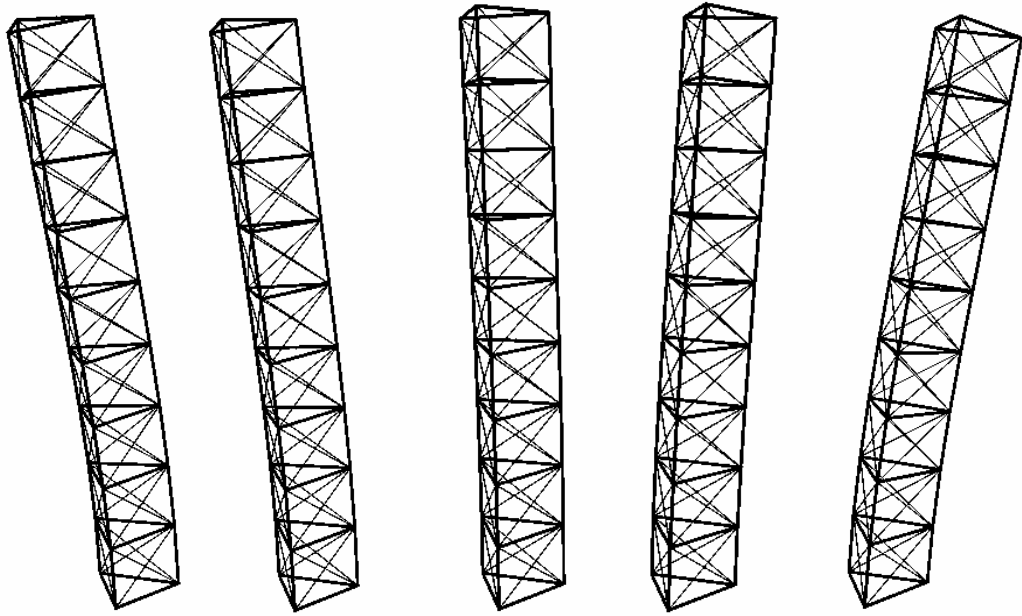
Figure 6.8. First mode of vibration of ABLE boom - Bending.
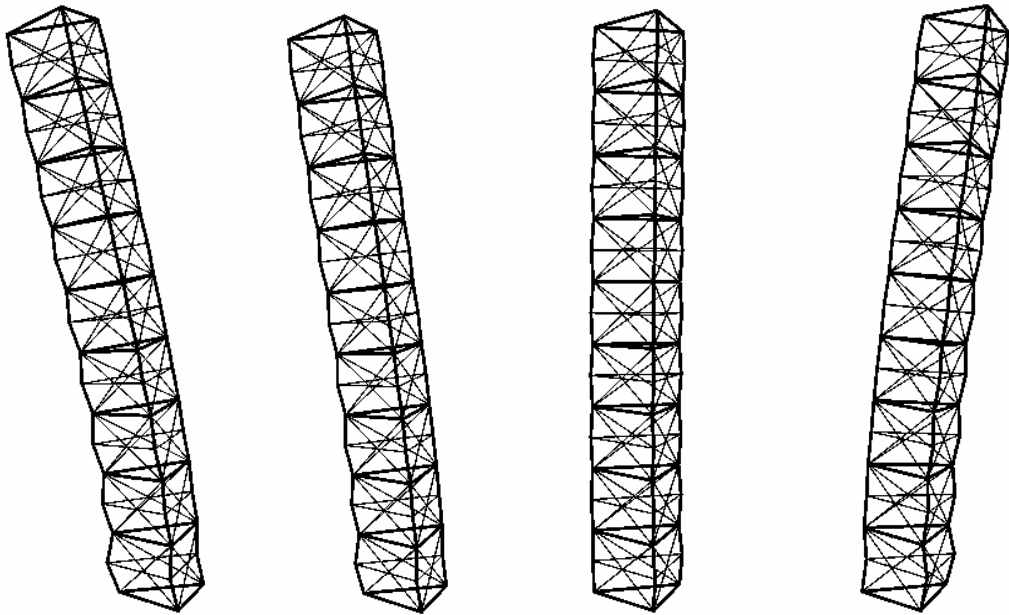


Figure 6.9. First mode of vibration of XPOP boom - Bending.
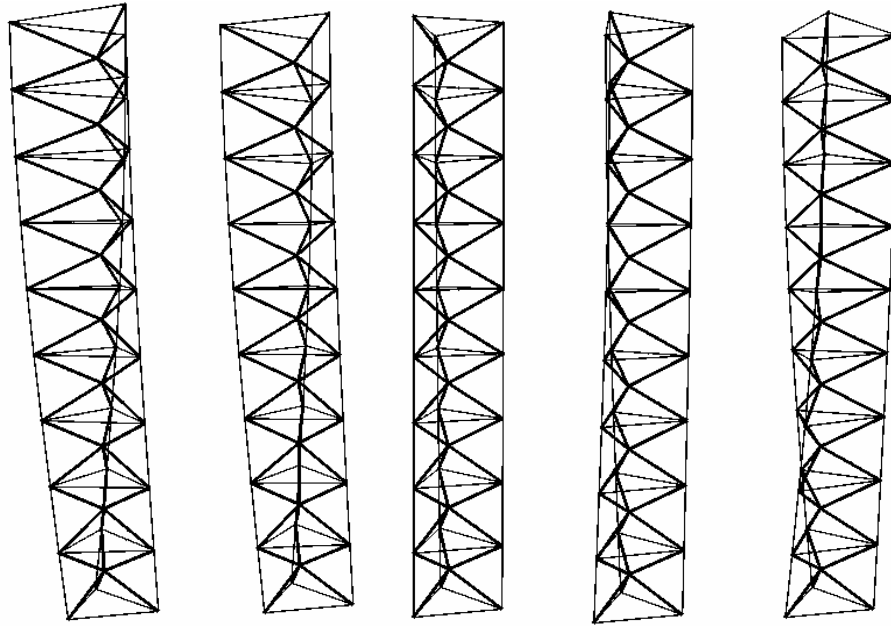
Figure 6.10. First mode of vibration of POP boom - Torsion.

CSP and TWT have lowest bending resistance with first bending frequency of about 10 Hz, about 30 % of that of ABLE boom. However, torsion stiffness of these two systems is better than the other boom systems. The first torsion frequency of CSP and TWT, which are about 130 Hz, are significantly higher than torsion frequency of the other booms, which are less than 40 Hz. In addition, torsion is the third mode of ABLE and XPOP booms but the sixth mode of CSP and TWT boom. The high torsion stiffness of CSP and TWT boom is due to the high number of struts on the surface of the boom and these struts are aligned in diagonal directions.

In general, the behaviour of ABLE boom and XPOP boom is similar with high bending stiffness due to the high density of strut at the edges of the boom. The behaviour of CSP boom and TWT boom is similar to each other with high torsion stiffness due to high density of strut on the surface of the boom. CSP and TWT boom is the best to resist torsion force while ABLE and XPOP boom is more suitable to resist bending moment.

## 6.3 Static structural behaviour

Static load-displacement response can provide detailed information about performance of booms for specific static load cases. Due to the complication in actual boom usage, two standard load cases, which are bending and torsion, are proposed to evaluate static structural performance of different boom systems. The imposed load for each standard load case is shown in Fig. 6.11. Load-displacement curve is recorded to evaluate the structural stiffness of booms, correspondingly.



(a) Bending        (b) Torsion
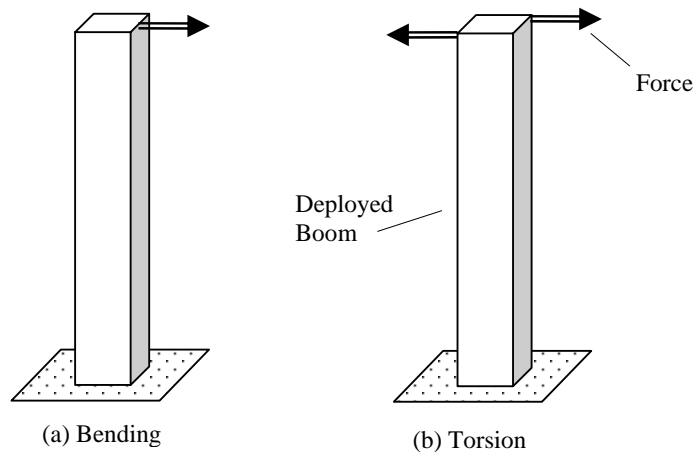
Figure 6.11. Standard load cases.

All booms are 6.2775 m high and the structural elements are the same as those used in free vibration analysis (section 6.2).

The bending stiffness of boom per unit length, $K_b$, will be determined by using tip displacement while it is assumed that the stiffness is uniform along the boom

$$K_b = \frac{P_t l^3}{3 \times D_t} \qquad (6.1)$$

where

$P_t$ = Horizontal imposed load at the top of the boom

$D_t$ = Horizontal maximum tip displacement

l = length of the boom

The torsion stiffness of the boom per unit length, Kt, is determined by using the rotation angle of the top plane, formed by the top nodes of the boom. It is assumed that the torsion stiffness is uniform along the boom.

$$K_t = \frac{M_t}{\theta_t}$$

(6.2)

where

$M_t$ = Imposed torsion moment at the top of the boom

$\theta_t$ = rotation angle of top plane under torsion moment

It is noted that all load-displacement curves are plotted until the boom fails to find out the strength. The stiffness may be changed when load is increased. However, only the initial stiffness is of interest because it is the in-service stiffness of the structure.

### 6.3.1  Pyramid-On-Pyramid boom

Two standard load cases are applied on POP boom as shown in Figs. 6.12, and 6.13. Nodes 28, 29, and 30 are top nodes of the boom.
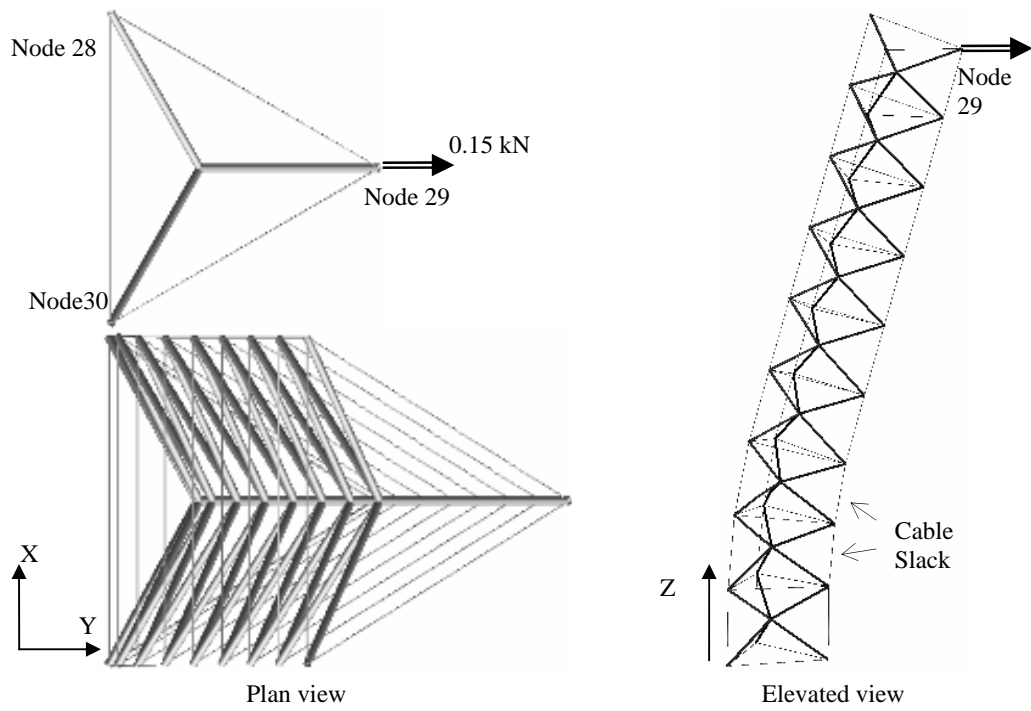
Figure 6.12. Bending – POP boom.
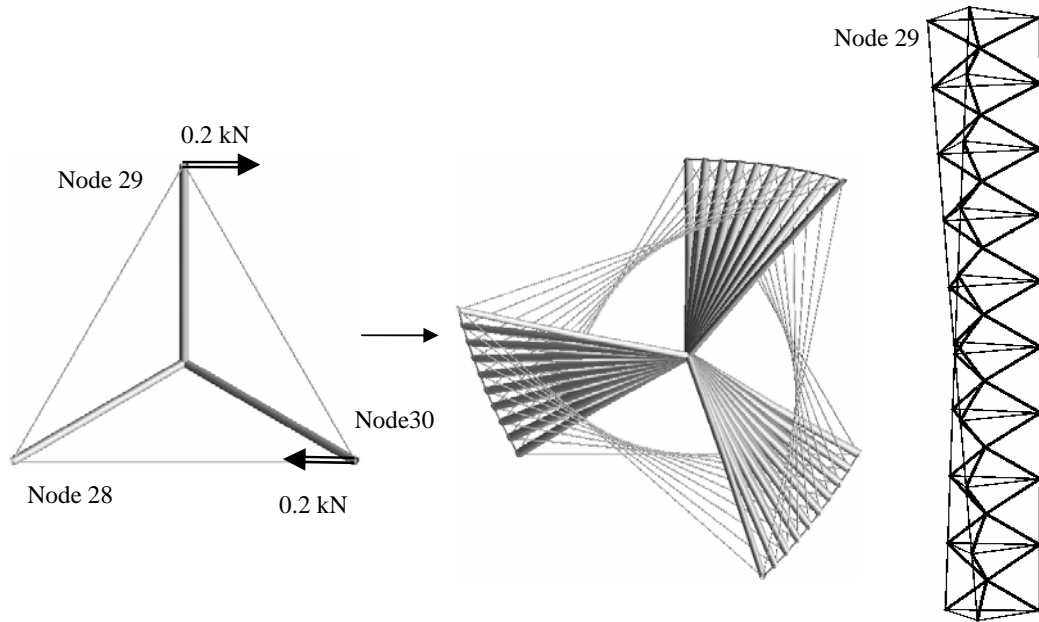


Figure 6.13. Torsion – POP boom.

The resultant displacements of top nodes are shown in Table 6.2 to be used in calculation of the stiffness of the boom. The X, Y, Z directions are shown in Fig. 6.12.

127

Table 6.2. Displacement of top nodes under standard load cases – POP boom

| Load Case | | Bending | Torsion | |
|---|---|---|---|---|
| Node | | 29 | 28 | 30 |
| X        (m) | | 0.0000 | 0.4850 | -0.4850 |
| Y        (m) | | 0.5600 | -0.2800 | -0.2800 |
| Z        (m) | | 6.2775 | 6.2775 | 6.2775 |
| dX       (m) | | 0.0000 | -0.0900 | -0.0560 |
| dY       (m) | | 0.0600 | -0.1150 | 0.1350 |
| dZ       (m) | | -0.0024 | 0.0010 | 0.0010 |
| X'       (m) | | 0.0000 | 0.3950 | -0.5410 |
| Y'       (m) | | 0.6200 | -0.3950 | -0.1450 |
| Z'       (m) | | 6.2751 | 6.2785 | 6.2785 |

X, Y, Z and X', Y', Z' are coordinates of nodes before and after loadings. dX, dY, dZ are changes in coordinates after loadings. Because the stiffness of the boom is changed after 0.15 kN as shown in Fig. 6.14 due to cable slack, the stiffness is calculated by structural response under the load step from 0 kN to 0.15 kN. Applying equation (6.1)

$$K_b = \frac{P_t l^3}{3 \times D_t} = \frac{0.15 \times 6.2275^3}{3 \times 0.06} = 201.26 \ (kNm^2) \tag{6.3}$$
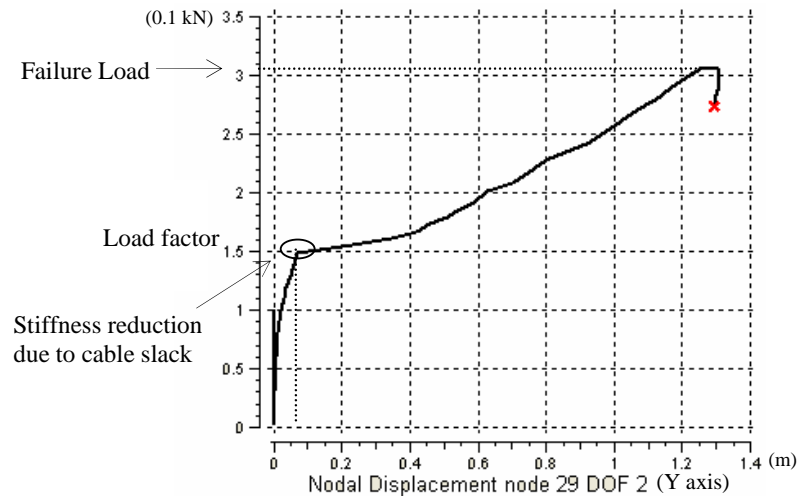


Figure 6.14. Load- top node displacement curve of POP boom under bending load case.

The POP boom fails at 0.31 kN, two times higher than cable slack load limit, 0.15 kN. It can also be observed in Fig. 6.12 that the boom bends more near to the support because of high moment. This bending mode is different from uniform stiffness cantilever beam under tip loading in which the cantilever bends more near to the tip, not the support.

Nominal torsional stiffness of the boom is calculated by applying equation (6.2)

$$K_t = \frac{M_t}{\theta_t} = \frac{0.2 \times 0.84}{\arcsin[(0.115 + 0.135)/(2 \times 0.485)]} = \frac{0.168}{0.0833} = 2.01 \ (kNm) \tag{6.4}$$

### 6.3.2 Cable-Stiffened Pantographic boom

The two standard load cases are also applied on Cable-Stiffened Pantographic boom, (CSP boom). The modes of displacement of the CSP boom under different load cases are shown in Figs. 6.15, and 6.16. The resultant displacements are shown in Table 6.3 and will be used for calculating nominal stiffness.

The displacement mode of CSP boom in bending is similar to that of POP boom with more bending near to the support as can be seen in Fig. 6.15. From Fig. 6.16, it can be observed that the torsion of the CSP is not uniform with relatively higher rotation at the two ends than the middle of the boom.
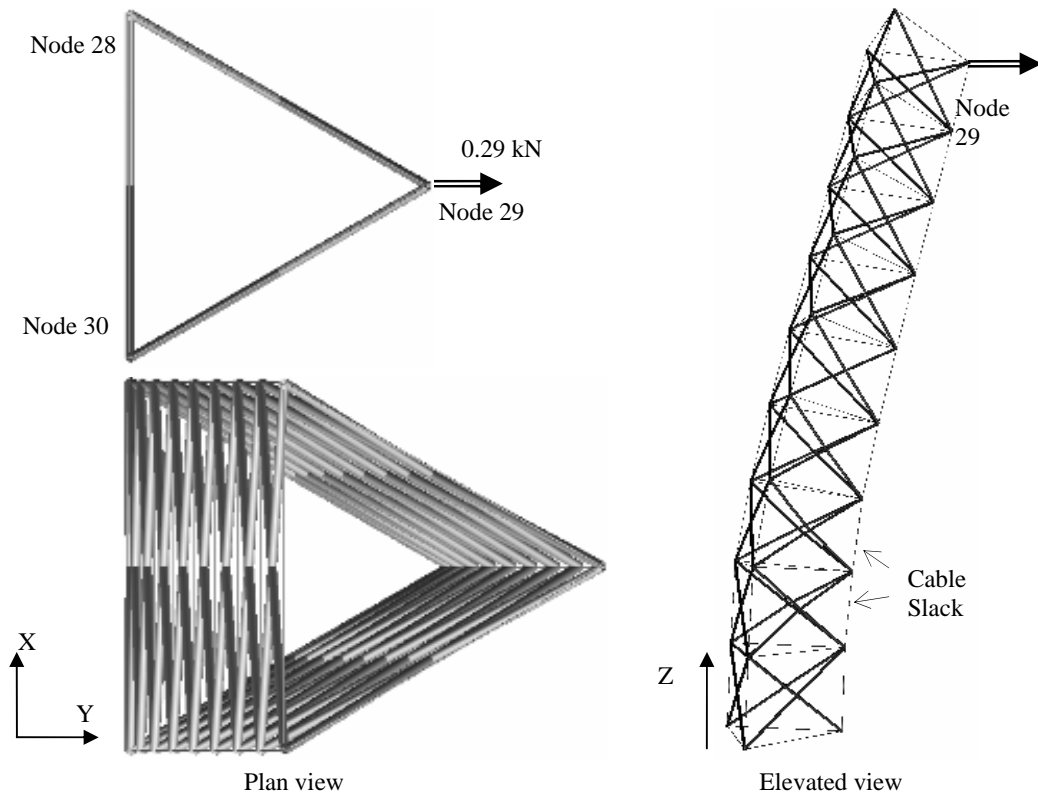
Figure 6.15. CSP boom under bending load case.
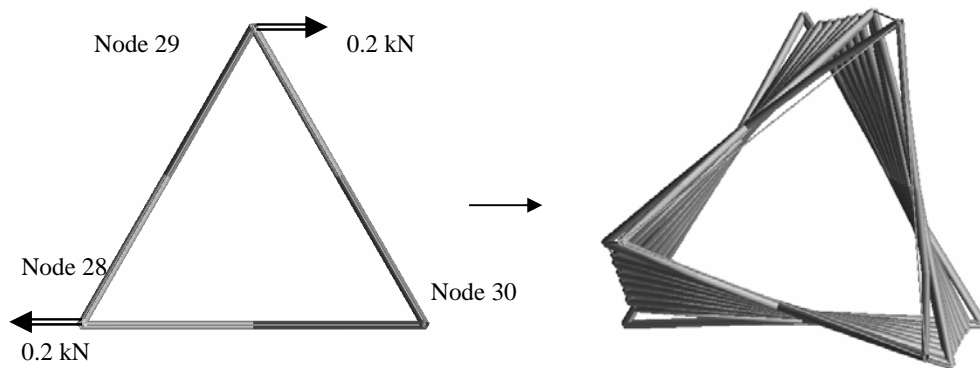

Figure 6.16. Plan view - CSP boom under torsion load case.

Table 6.3. Displacement of top nodes under standard load cases – CSP boom.

| Case | Bending | Torsion | |
|------|---------|---------|---------|
| NODE | 29 | 28 | 30 |
| X | 0.0000 | 0.4850 | -0.4850 |
| Y | 0.5600 | -0.2800 | -0.2800 |
| Z | 6.2775 | 6.2775 | 6.2775 |
| dX | 0.0000 | -0.00038 | 0.00018 |
| dY | 0.0700 | 0.0000 | 0.00031 |
| dZ | -0.0030 | 0.0029 | 0.0029 |
| X' | 0.0000 | 0.48462 | -0.48482 |
| Y' | 0.6300 | -0.2800 | -0.27969 |
| Z' | 6.2745 | 6.2804 | 6.2804 |

130

Nominal bending stiffness of the CSP boom is calculated by the equation (6.1). The cable slack load limit for CSP boom is 0.29 kN as shown in Fig. 6.17.

$$K_b = \frac{P_t l^3}{3 \times D_t} = \frac{0.29 \times 6.2275^3}{3 \times 0.07} = 333.52 \ (kNm^2) \tag{6.5}$$
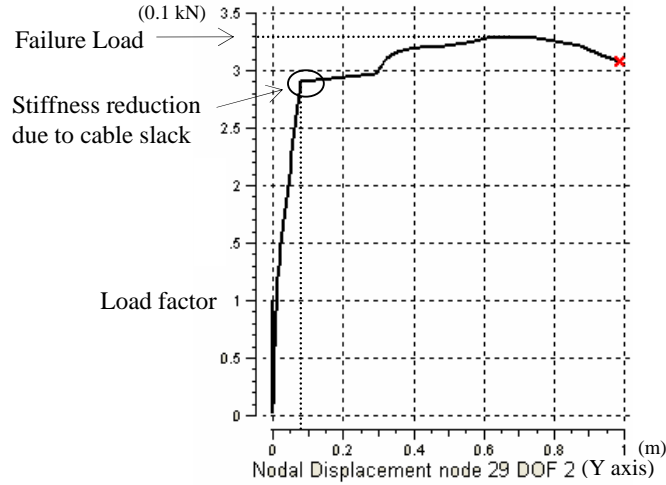


Figure 6.17. Load-displacement curve of CSP boom under bending load case.

Although the cable slack load is much higher than that of POP boom, (0.29 kN comparing with 0.15 kN) the failure load of CSP boom is 0.33 kN, slightly higher than POP boom (0.31 kN)

Torsional stiffness of the structures is evaluated by equation (6.2)

$$K_t = \frac{M_t}{\theta_t} = \frac{0.2 \times 0.84}{\arcsin\left[(0.00031)/(2 \times 0.485 + 0.00038 + 0.00018)\right]} = \frac{0.168}{0.0001} = 1652 \ (kNm) \tag{6.6}$$

### 6.3.3 Twisted Triangular boom

The Twisted Triangular boom (TWT boom) is analysed under two standard loading conditions as mentioned above and the displacement modes under these load cases are shown in Figs. 6.18 - 6.19.
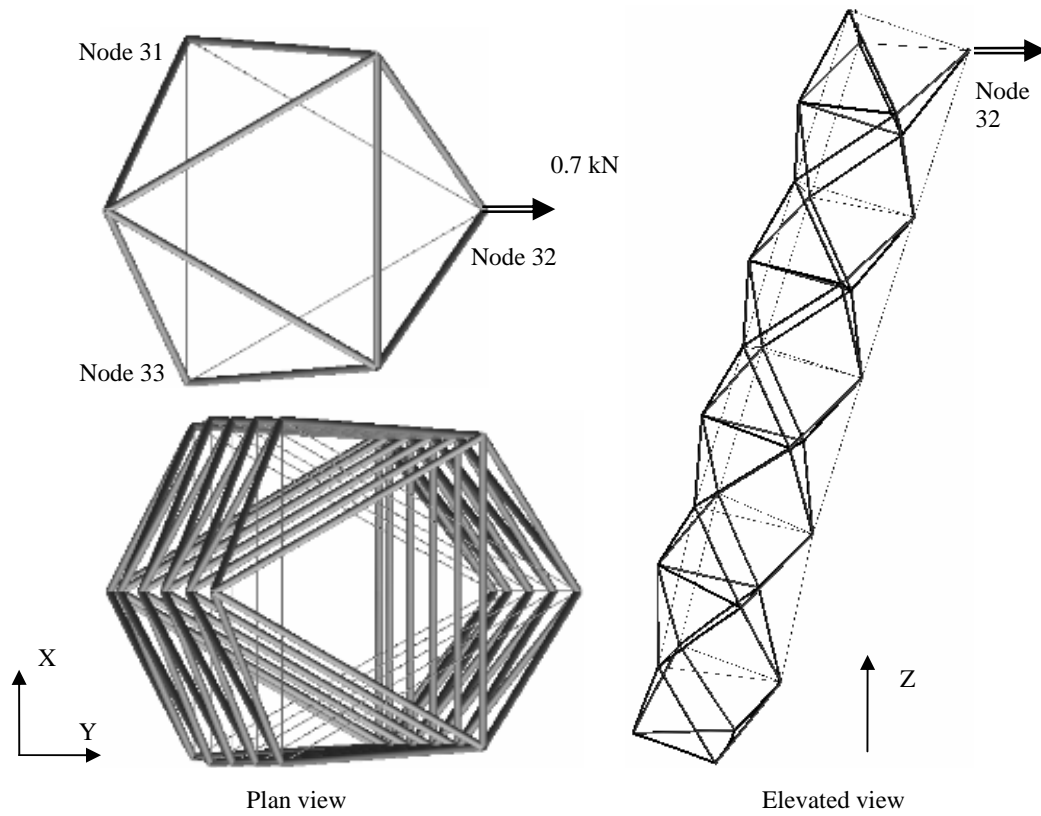
Figure 6.18. TWT boom under bending load case.
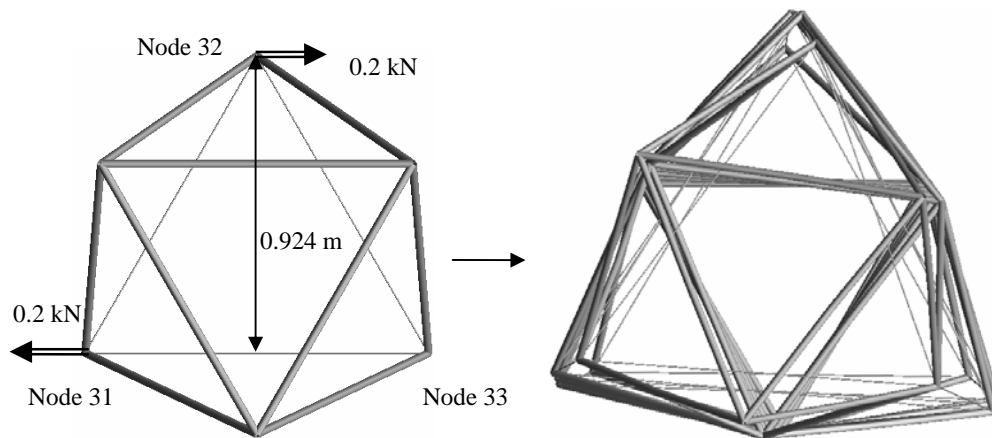


Figure 6.19. Plan view - TWT boom under torsion load case.

Table 6.4 shows the displacements at the top nodes of TWT boom, which are used to evaluate nominal stiffness of the structure.

Table 6.4. Displacement of top nodes under standard load cases – TWT boom.

| Case | Bending | Torsion | |
|---|---|---|---|
| NODE | 32 | 31 | 33 |
| X    (m) | 0.0000 | 0.5335 | -0.5335 |
| Y    (m) | 0.6160 | -0.3080 | -0.3080 |
| Z    (m) | 6.2775 | 6.2775 | 6.2775 |
| dX   (m) | 0.0000 | 0.0000 | -0.00016 |
| dY   (m) | 0.1600 | -0.00011 | 0.0000 |
| dZ   (m) | -0.0045 | -0.0014 | 0.0029 |
| X'   (m) | 0.0000 | 0.5335 | -0.53366 |
| Y'   (m) | 0.7760 | -0.30811 | -0.3080 |
| Z'   (m) | 6.2730 | 6.2761 | 6.2804 |

Under bending load case, the structural stiffness is not significantly changed until the failure load of 0.7 kN as show in Fig. 6.20. Therefore applying the equation (6.1) to calculate bending stiffness of TWT using structural response under 0.7 kN loading

$$K_b = \frac{P_t l^3}{3 \times D_t} = \frac{0.7 \times 6.2275^3}{3 \times 0.16} = 352.2 \ (\text{kNm}^2) \tag{6.7}$$
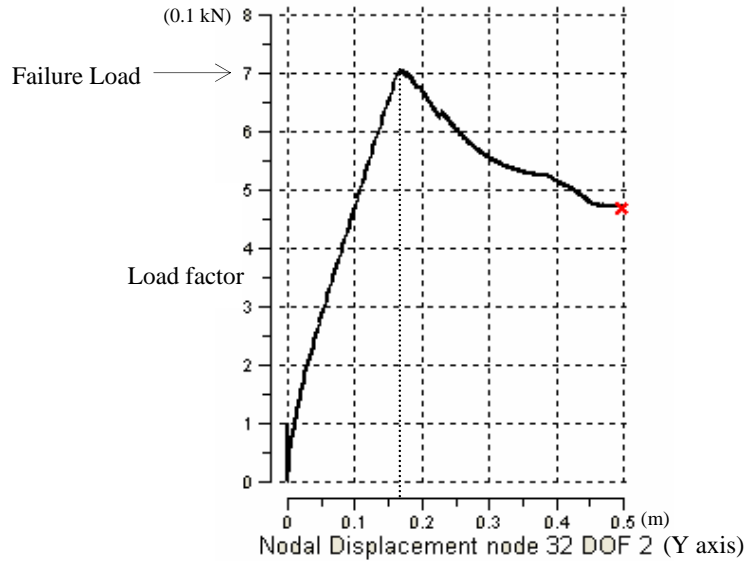


Figure 6.20. Load-displacement curve of TWT boom under bending load case.

The nominal torsion stiffness is calculated as follows

$$K_t = \frac{M_t}{\theta_t} = \frac{0.2 \times 0.924}{\arcsin[(0.00011)/(2 \times 0.5335 - 0.00016)]} = \frac{0.168}{0.320 \times 10^{-2}} = 5118 \ (\text{kNm}) \tag{6.8}$$

133

### 6.3.4 Expanded Pyramid-On-Pyramid boom

Node 30

Node 28

0.2 kN

Node 28

Node 29

X

Z

Y

Plan view                                              Elevated view
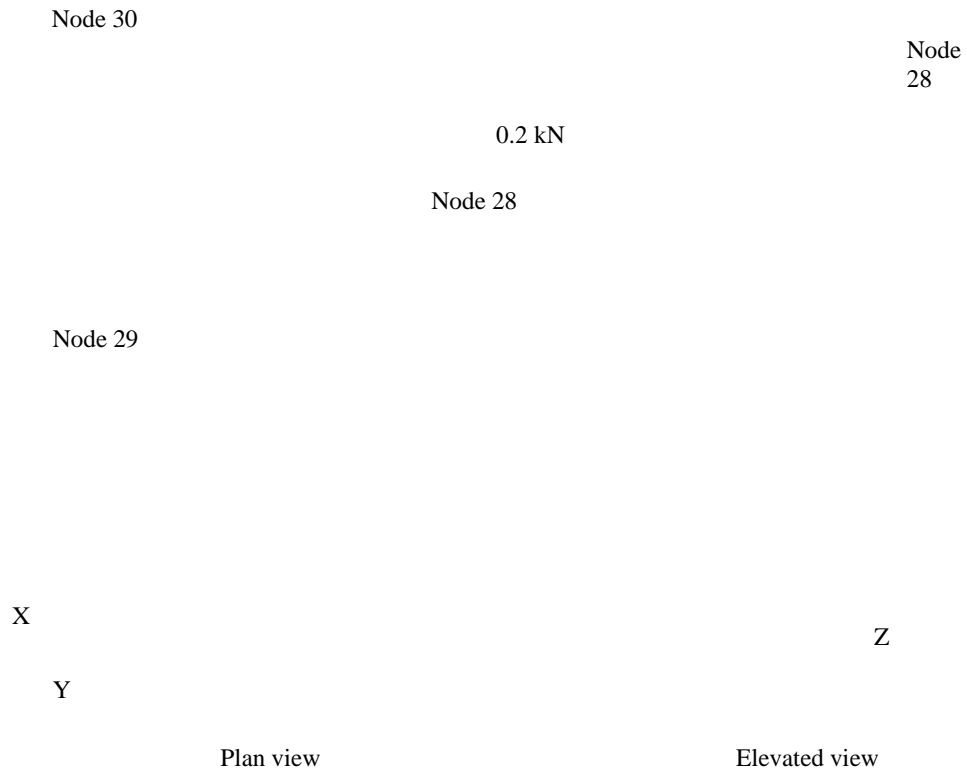
Figure 6.21. XPOP boom under bending load case.

0.2 kN

Node 28

0.2 kN        Node 30              Node 29
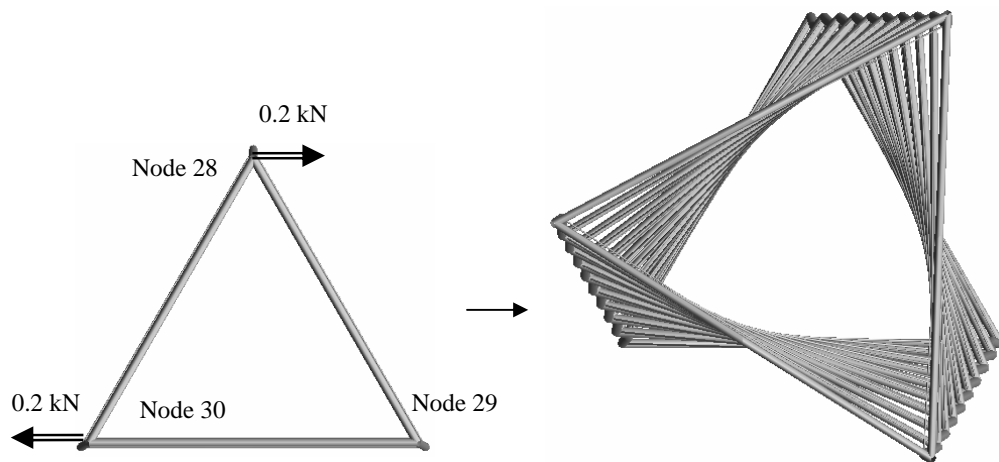
Figure 6.22. Plan view - XPOP boom under torsion load case.

The two standard load cases are applied on Expanded Pyramid-On-Pyramid (XPOP) boom and the corresponding deformations are shown in Figs. 6.21, and 6.22. The corresponding maximum displacements are presented in Table 6.5.

Table 6.5. Displacement of top nodes under standard load cases – XPOP boom.

| Case | Bending | Torsion | |
|---|---|---|---|
| NODE | 28 | 29 | 30 |
| X | 0.0000 | -0.4850 | 0.4850 |
| Y | 0.5600 | -0.2800 | -0.2800 |
| Z | 6.2775 | 6.2775 | 6.2775 |
| dX | 0.0000 | -0.0016 | -0.0017 |
| dY | 0.0340 | 0.0031 | -0.0030 |
| dZ | 0.00025 | 0.0007 | 0.0010 |
| X' | 0.0000 | -0.4866 | 0.4833 |
| Y' | 0.5940 | -0.2769 | -0.2830 |
| Z' | 6.27775 | 6.2782 | 6.2785 |

Under bending load case, the structural stiffness is not significantly changed until the structure is failed by local yielding under load of 1.25 kN as shown in Fig. 6.23. From this curve, it can be concluded that the stiffness of the boom is not much affected by cable slack. The nominal bending stiffness can be evaluated by applying equation (6.1)

$$K_b = \frac{P_t l^3}{3 \times D_t} = \frac{1.25 \times 6.2275^3}{3 \times 0.034} = 2959.72 \ (kNm^2) \tag{6.9}$$

Figure 6.2

# CHAPTER 7

# PROTOTYPE INVESTIGATION AND POTENTIAL

# APPLICATIONS

Prototypes and experiments are essential to develop an understanding on how the proposed Deployable Tension-Strut Structures physically work. While analytical results can be validated by physical experiments and testing, prototypes provides additional information which are essential for manufacturing and production and for verification of the deployment concept, which is proposed in Chapter 3. This Chapter discusses prototypes and experiments on Deployable Tension-Strut Structures and relevant design issues. Potential applications of the systems are also explored.

## 7.1 Introduction

Due to the development of information technology, numerical modelling becomes more economical than physical modelling. Therefore, physical modelling is less to be used as the exploration approach in an engineering study. It is now more popularly used for experimental verification of numerical analysis as a verification approach. This fact is reflected by the number of publications and conferences on numerical modelling in comparison with physical modelling. However, it cannot be ignored that for complicated and novel products, the initial understanding about the structure can be achieved in a reliable way of building physical models as mentioned by Kawaguchi (2004). In the first place, to "touch and feel" the physical models provides an insight into the force flow of the new products. Secondly, the trial of manufacturing will

disclose the difficulty in manufacturing as well as help resolve the assembly methods and relevant issues.

Chapters 5 and 6 of this thesis discuss the design issues of Deployable Tension-Strut Structures. However, those discussions are limited to the matter of forms, shapes and sizes of the proposed systems. In this chapter, the design aspects to allow practical deployment of Deployable Tension-Strut Vault system and manufacturing feasibility are investigated through prototypes building and manufacturing. The study provides in-depth understandings about how to design to cater for deployability. Different methods of deployment are introduced and discussed. Prototypes were built to verify the deployment concept and design issues gained from prototyping are discussed. A design for deployable shelter is proposed. Experimental models were built, deployed, and load tested to verify both the feasibility of deployment methods and structural strength. The success of the experiment proves that the proposed design of Deployable Tension-Strut Structures (DTSSs) is feasible. Several potential applications of DTSSs are then proposed.

## 7.2 Prototype investigation

This section investigates the feasibility of Deployable Tension-Strut Structures through prototype building, investigation of their deployment, and the assembly procedure.

### 7.2.1    Prototype assembly

Deployable Tension-Strut Structures (DTSS) are developed for flexible use. This means the users can transform the system for different uses. The joint design should allow convenient connecting, detaching and reassembling structural elements. As shown in Fig. 7.1, several forms of Pyramid-On-Pyramid system are constructed from the same module units and the number of structural module is kept at 30.
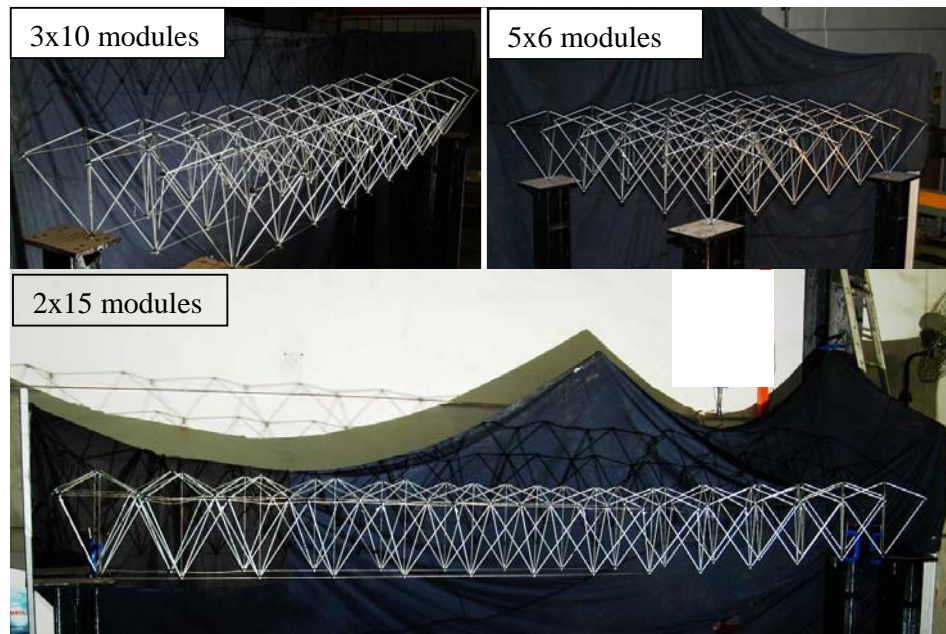


Figure 7.1. 30 modules of Pyramid-On-Pyramid structure in different assemblies.

### 7.2.2    Deployment investigation

### 7.2.2.1 Deployment methods

DTSS can be deployed by parts or deployed as a whole structural system. The decision depends on the size of the whole structure and availability of lifting equipments.

The deployment of DTSS by parts is shown in Fig. 7.2. This method is applied when the whole structure is very heavy and there is no suitable crane to lift the whole structural system.
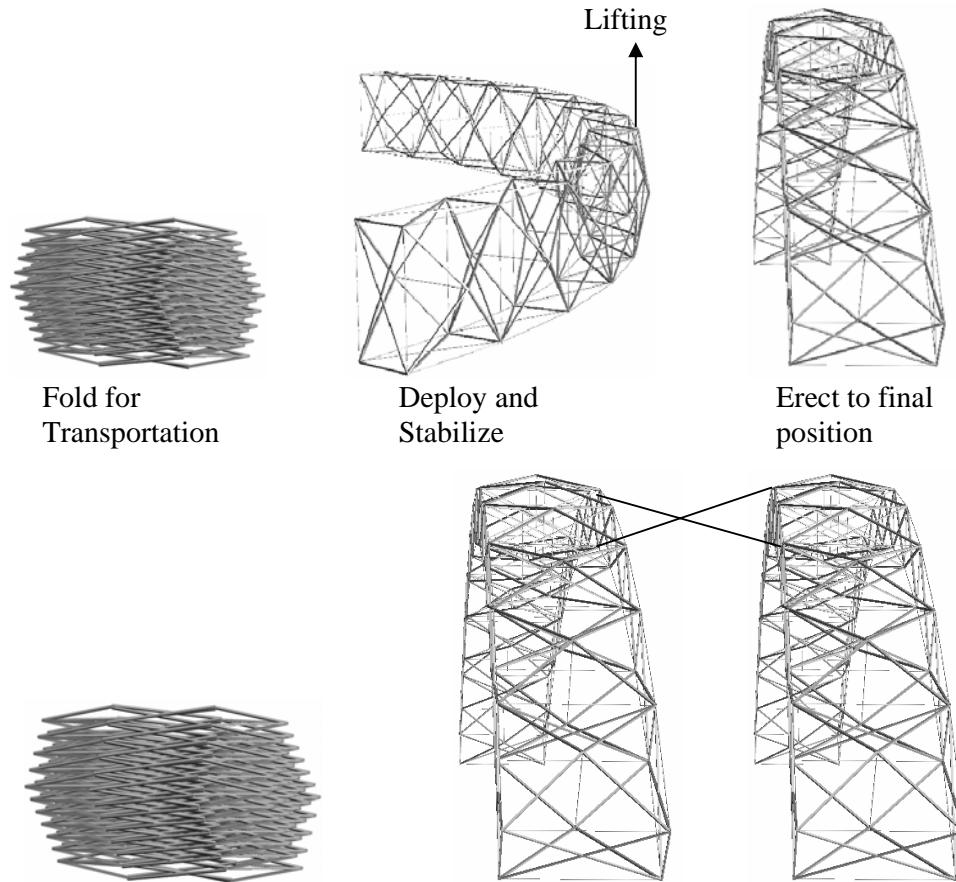


Figure 7.2. Deployment and erection of PPP structure.

The deployment of DTSS as a whole (Fig. 7.3) is applied when proper lifting equipment is available and the strength/ stiffness of the structure is checked under self-weight loads.
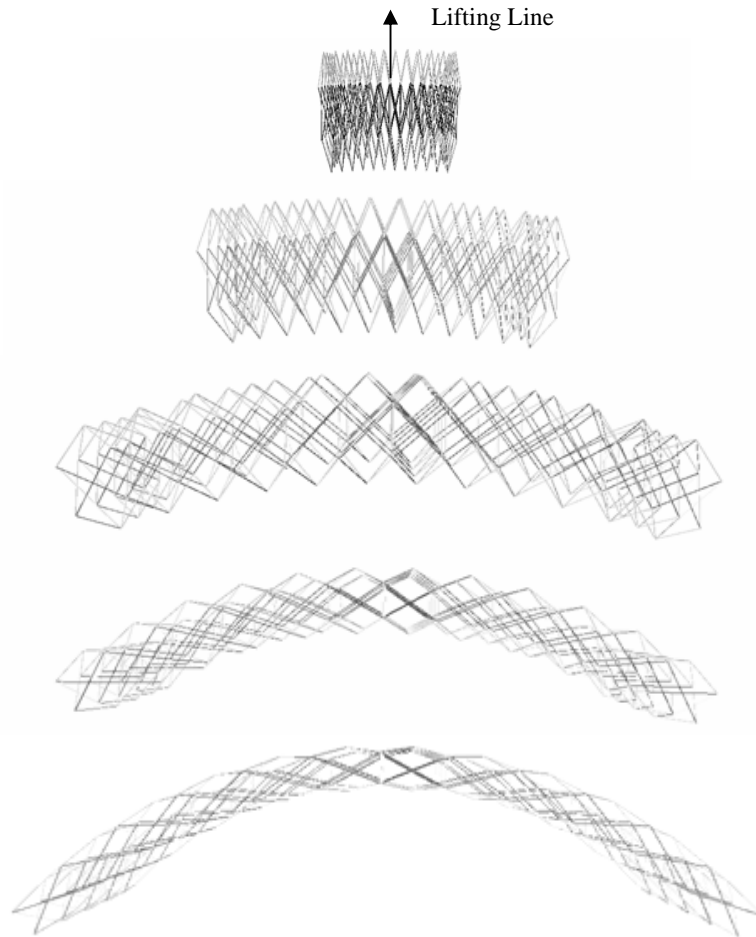
Figure 7.3. Deployment of the whole DTSS.

## 7.2.2.2 Prototype deployment

Prototypes were built to verify the deployment of DTSSs. The first DTSS prototype is built from aluminium to represent Pyramid-On-Pyramid structure and spans 6 m. The deployment of the system is shown in Fig. 7.4 which illustrates the second method of deployment. The systems of DTSS acts as a kinematic chain during deployment as can be seen from Figs. 7.4 to 7.6. It is noted that the self-weight of DTSS tends to speed up the deployment process and thus lifting forces (Fig. 7.6) are needed to control the

speed of the deployment and thus excessive stress due to fast deployment can be controlled. In Fig. 7.6, the first method of deployment is illustrated.



Figure 7.4. Deployment of Pyramid-On-Pyramid Structure.



Figure 7.5. Deployment of Pyramid-Pantograph-Cable Structure.

Figure 7.6. Deployment of Pyramid-Pantograph-Pyramid Structure.
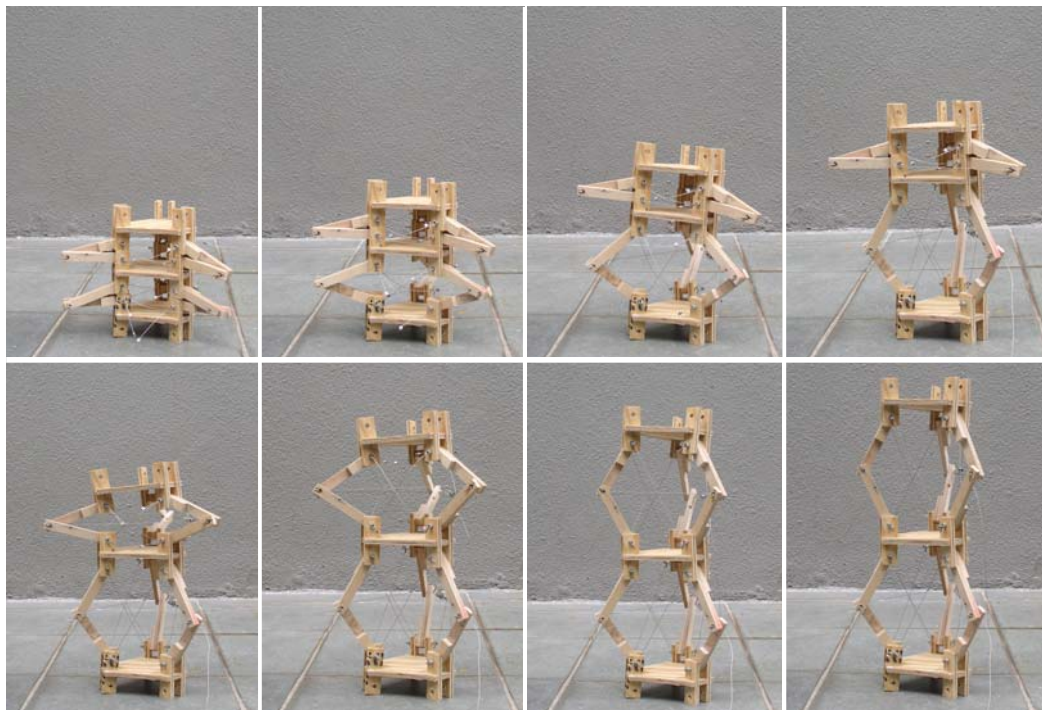

Figure 7.7. Independent deployment of each module of Deployable XPOP Boom.

The deployment of Deployable XPOP Boom system, proposed in Chapter 6, is different from the pantograph-based systems (e.g PPP). The deployment of this structure is featured by the module-by-module deployment as shown in Fig. 7.7. The reason is the strut systems does not form a kinematic chain but rather a set of chain.
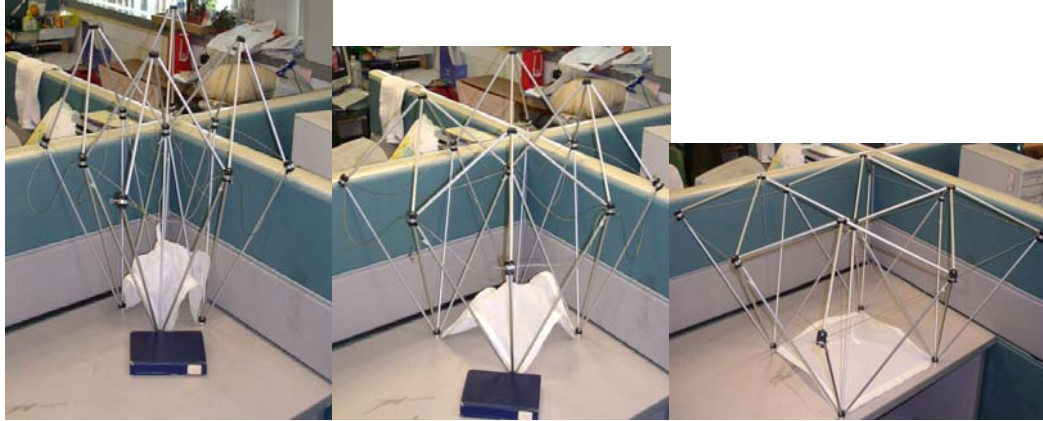
Figure 7.8. Deployment of DTSS with attached membrane.

Finally, DTSS can be integrated with membrane to provide a full covering application. With the deployment of the prototype shown in Fig. 7.8, it can be concluded that the deployment of DTSS with properly attached membrane is feasible and the extra requirement is to avoid scratch of the membrane during the deployment process. In this prototype, the bottom cables are encased in the membrane and at the internal middle joint, a cable is provided to tension the membrane in the final position.

### 7.2.2.3 Deployment safety issues

Full scale prototypes are used to assess the fabrication possibilities as well as investigating potential difficulty when the size and weight of the structure is accounted for during deployment. In Figs. 7.4, 7.7, and 7.8, small scale prototypes are used to verify the concept and cannot be used to assess large scale deployment safety issues as shown in Figs. 7.5 and 7.6. The deployment of full scale prototypes requires safety considerations with regrads to workers and structural strength.

Firstly, workers need to be taught about how the structure will be deployed. None of them are allowed to step inside the structure during deployment because if the structure folds again by accident the worker can be clamped inside the structure.

Secondly, the SLE systems need to have sufficient strength to resist self-weight of the structure during deployment when the structure has not been locked into the final deployed configuration. The structure may need temporary support during deployment to avoid high force due to its self-weight. A possible solution for deployment is shown in Fig. 7.9 with mid-span support.
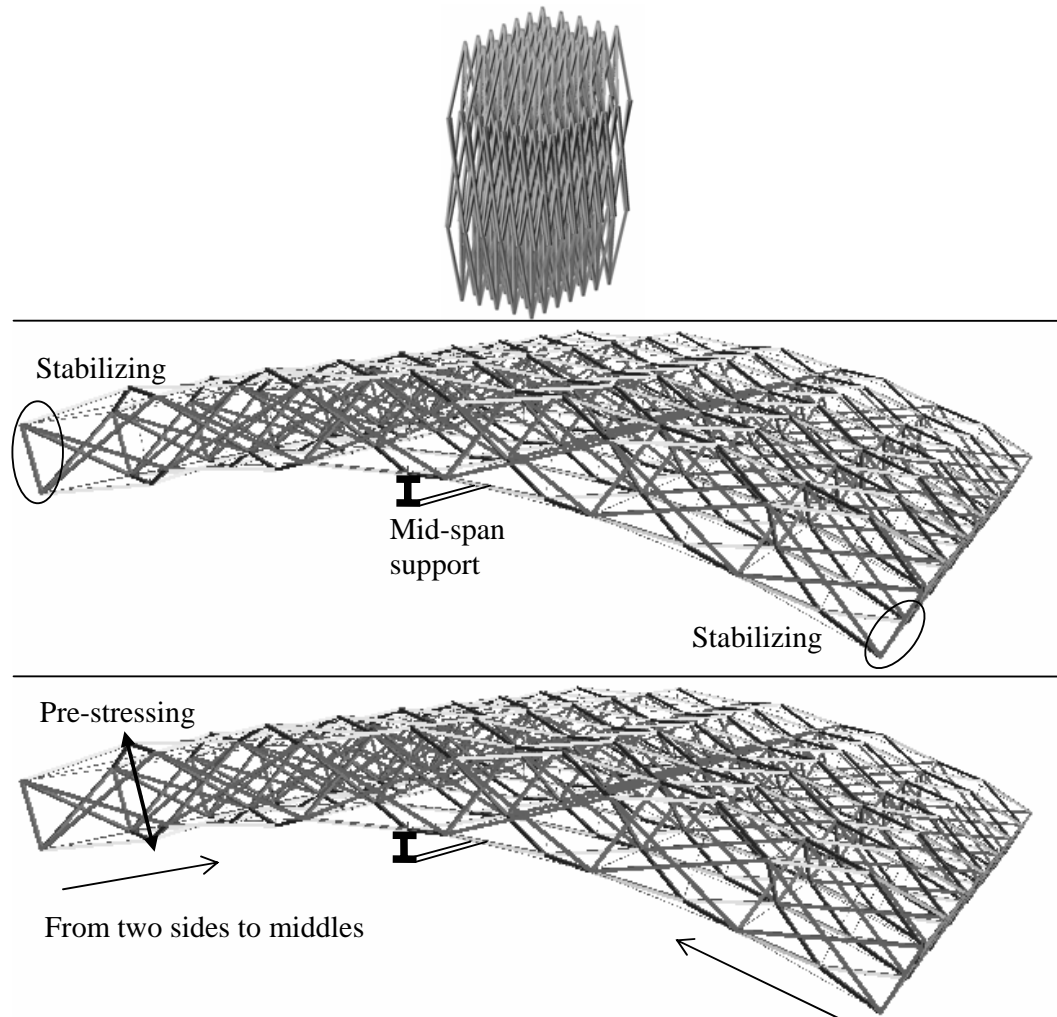


Figure 7.9. Deployment of DTSS with mid-span support.

## 7.3 Design issues

### 7.3.1 Structural design

This section presents a set of preliminary structural design parameters for terrestial flat roof which is formed by DTSS. The followings are parameters that are considered in developing this design guideline

Flat roof structures are considered

Membrane is used as covering material.

Span length L = 24 m to 60 m

Circular hollow sections are used for all struts

Imposed load = 0.75 kN/m$^2$

Maximum deflection of structure < L/200 under unfactored imposed load

Number of modules = 10x10

Span/depth ratio = 10

Simple supports are at all boundary joints (roof is supported at the four edges)

Optimum design parameters of the overall structure are shown in Fig. 7.10 (derived from Chapter 5).
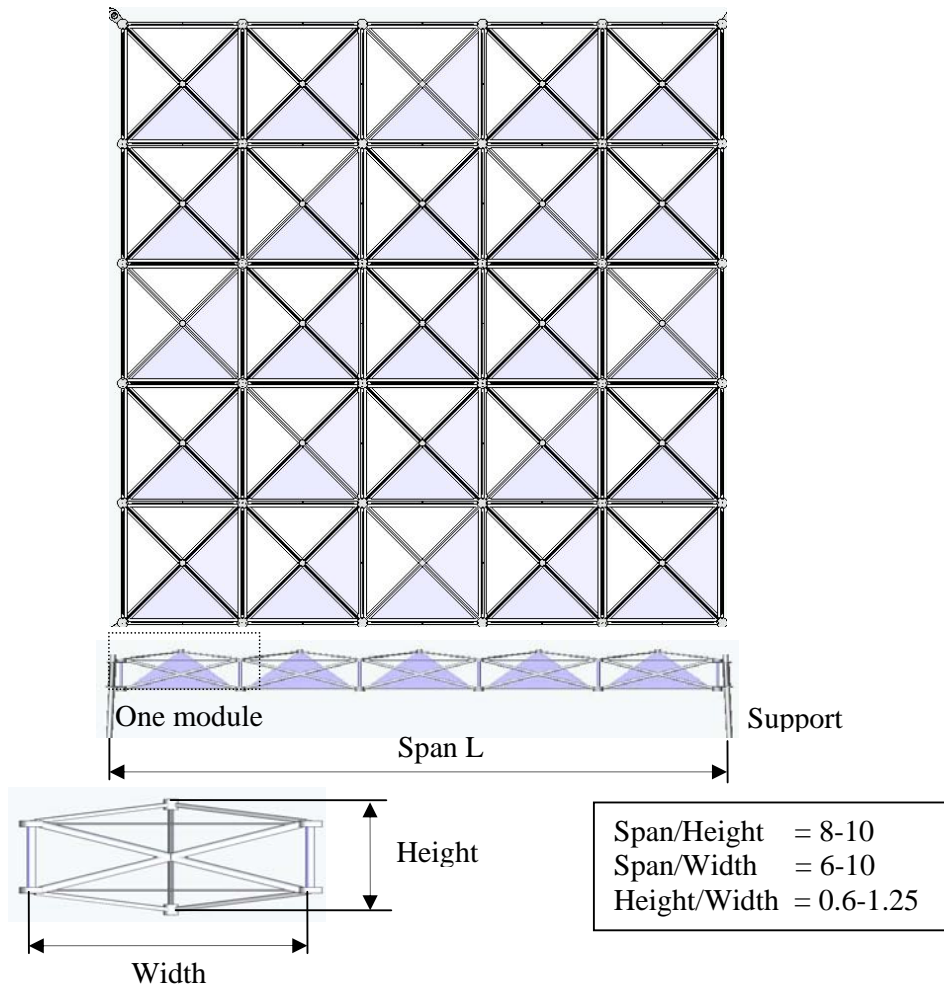
Figure 7.10. Optimum design parameters of DTSS.

Table 7.1 provides the preliminary recommended sections for structural elements of DTSS, which are used in the analyses in Chapter 5. It is noted that there are two types of design table. The first type is design table for products which produce standard products' properties and corresponding load carrying capacity. The second type is design table for solutions which provides recommended design sections for structural elements under a specific boundary condition and loading condition. The design table 7.1 falls into the second category.

**Table 7.1.** Recommended design sections – Two-way square-grid DTSS

| Span (m) | DTSS | Top Strut (mm) | Diagonal Strut (mm) | Bottom Strut (mm) | Bottom Cable (mm) | Middle Cable (mm) | Locking rod/strut (mm) | Weight (kg/m$^2$) | SEI |
|---|---|---|---|---|---|---|---|---|---|
| 24x24 | PIP | 60.3x2.6 (70.3x2.9) | 46x2.3 (88.9x3.2) | NA | 18 | 6 | 22x2.3 | 11.58 | 1.5 |
| | POP | 60.3x2.3 (101.6x2.9) | 48.3x2.3 (101.6x2.9) | NA | 20 | 6 | 6 | 11.02 | 1.6 |
| | PPC | 70x2.3 (114.3x7.1) | 42.4x2.3 (114.3x7.1) | NA | 16 | 6 | 6 | 12.27 | 1.7 |
| | PPP | 68.3x2.3 | 48.3x2.3 | 40x2.3 | 14 | 6 | 6 | 14.5 | 1.6 |
| 36x36 | PIP | 76.1x2.6 (168.3x3.2) | 60.3x2.3 (168.3x3.2) | NA | 24 | 8 | 42x2.3 | 11.35 | 1.3 |
| | POP | 88.9x2.9 (127x3.2) | 88.9x2.9 (127x3.2) | NA | 28 | 8 | 10 | 15.5 | 1.1 |
| | PPC | 88.9x2.6 (114.3x7.1) | 68.3x2.3 (114.3x7.1) | NA | 24 | 8 | 6 | 13.24 | 1.3 |
| | PPP | 70x2.6 | 60.3x2.6 | 60.3x2.3 | 24 | 8 | 8 | 14.32 | 1.2 |
| 48x48 | PIP | 168.3x2.9 (127x4) | 88.9x2.6 (139.7x4) | NA | 36 | 8 | 68.3x2.3 | 16.56 | 1 |
| | POP | 168.3x2.6 (214.3x2.9) | 114.3x2.6 (191.0x2.6) | NA | 36 | 10 | 12 | 16.59 | 1 |
| | PPC | 114.3x2.6 (114.3x7.1) | 127x2.6 (114.3x7.1) | NA | 36 | 10 | 10 | 18.64 | 1.1 |
| | PPP | 127x2.9 | 88.9x2.9 | 101.6x2.9 | 28 | 10 | 12 | 19.41 | 1 |
| 60x60 | PIP | 191x2.9 (214.3x4) | 168.3x2.6 (214.3x4) | NA | 48 | 16 | 88.9x2.3 | 20.65 | 0.9 |
| | POP | 191x2.9 (214.3x2.9) | 168.3x2.6 (191x2.6) | NA | 48 | 16 | 16 | 19.58 | 0.9 |
| | PPC | 191x2.9 (114.3x7.1) | 168.3x2.6 (114.3x7.1) | NA | 48 | 16 | 16 | 23.93 | 1.1 |
| | PPP | 191x2.9 | 191x2.9 | 168.3x2.9 | 48 | 18 | 18 | 30.87 | 0.8 |

Note: The strut sizes in bracket are for the module at the corners where high axial forces require larger Circular Hollow Sections.

**7.3.2 Joint design**

This section provides joint designs of DTSS developed for the manufacturing process of prototypes and large scale models in two common construction materials, aluminium and steel. Joint designs require significant effort after the conceptual design is settled. The joints for DTSSs need to be sufficiently stiff, and strong, and are formed to assure proper deployment of the assembled DTSSs.

Deployability of DTSSs requires that all the struts are connected to joints by pins (or bolts). The sectional area of the pin is designed to be higher than that of struts to assure that the struts fail before the pin. This requirement will increase the size of the joints because the joints should be large enough to accommodate the pin. To simplify manufacturing and avoid confusion in assembly, no more than two sizes of pin are recommended.

Joints are made of two components, which are pins as mentioned above and the flanges, which transfer the force from pins to pins. However, steel and aluminium joint designs are of very different shapes to adapt to different manufacturing process as will be shown in session 7.3.2.2.

## 7.3.2.1 Prototype joint system
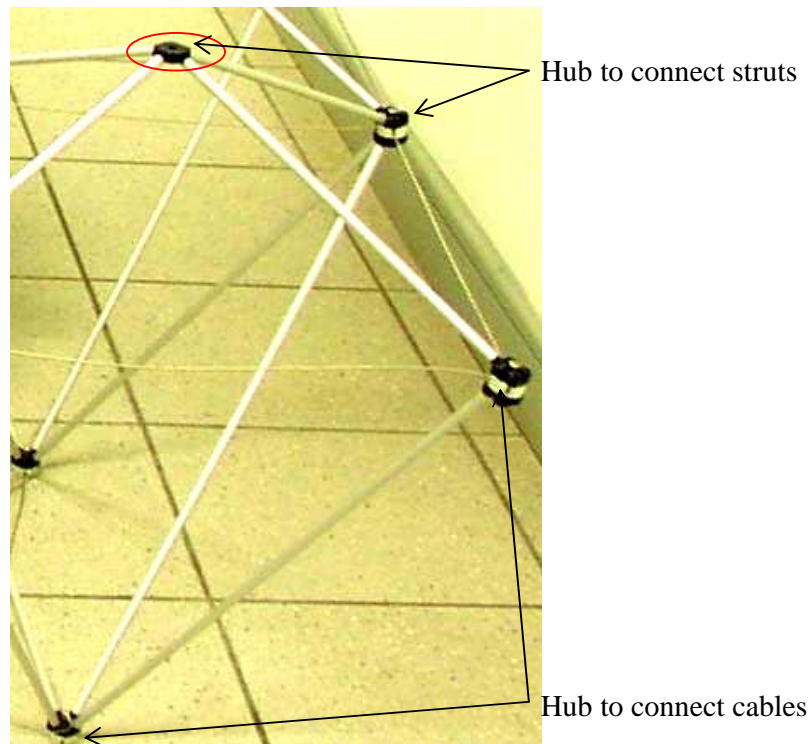


Figure 7.11. Components of joints.

In the joints of fabricated prototype in Fig. 7.4, there are only two main components that limit the complexity of joint. The first component is the hub to connect to the pin at the end of struts and the second component is the hub to allow cable to run through and clamp them as shown in Fig. 7.11. However, the cable does not run-through the middle of the second hub and thus in the pre-tension equilibrium state the joint can be tilted as can be seen in Fig. 7.12.
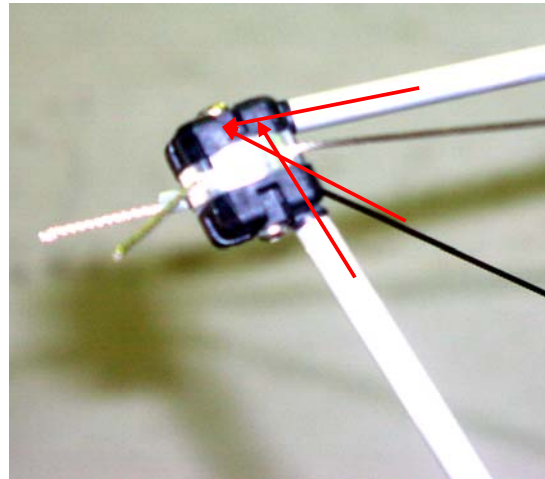


Figure 7.12. Tilted boundary middle joints.



Figure 7.13. Symmetric forces acting on the internal middle joint.

The tilt of joints happens to the boundary middle joints only because the equilibrium of internal middle joints is maintained by symmetric forces as shown in Fig. 7.13. For boundary middle joints, the joint suffers complicated stress status because the forces do not intersect at one point. To resolve this problem, it is recommended that the cable hole in the joints must be carefully positioned to assure that in the deployed configuration of DTSS, all structural components intersect at one point. The word "position" means not only calculation of geometry on the axis of structural elements but also consideration of the size of joints and the manufacturing process (whether such a hole can be placed at the design position). This principle is applied in an experiment model, which is introduced in later section.
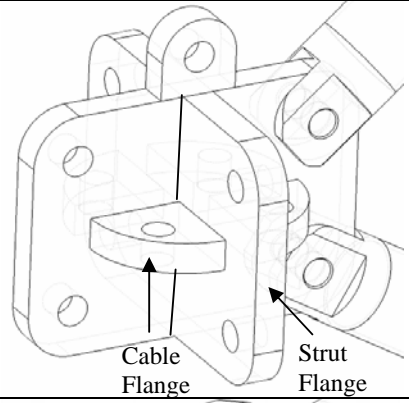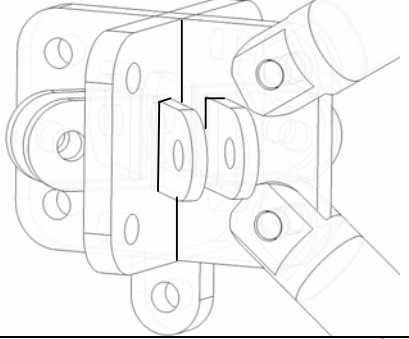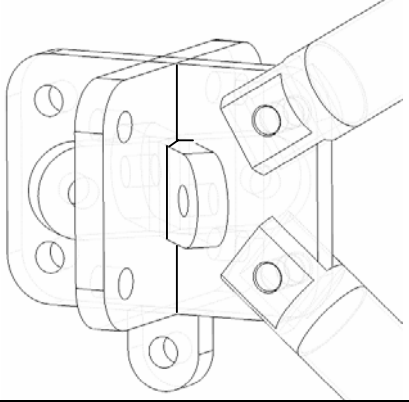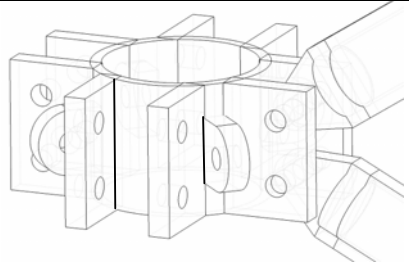
### 7.3.2.2 Proposed joint designs
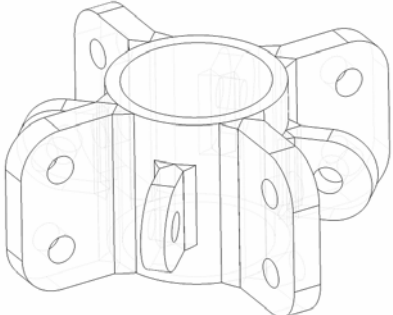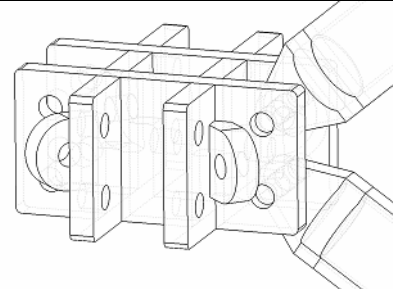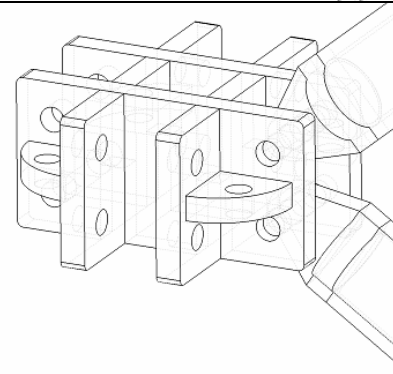
### Steel joint design

The fabrication issues of DTSS are most likely to be related to the joint detail of the structures. Major components of DTSS are struts, cables, pin joints, and cable anchors. Struts, cables, and cable anchors are standardised and only minor customisation is required. The major issue of fabrication is to create reasonably small joints with "real pin" while structural strength and stiffness of the joint is assured. Various joint concepts were considered and preliminarily assessments are shown in Tables 7.2 and 7.3. The criteria for discussion include amount of material, number of components, number of weld lines, level of ease in welding, relative joint size, effectiveness of force transfer path.

**Table 7.2.** Concentric joint designs

| No | Joint Design | Description | Advantage | Disadvantage |
|---|---|---|---|---|
| 1 |  Cable Flange    Strut Flange | - Steel plates are cut and welded<br><br>- Cable Flange is perpendicular to Strut Flange | - Minimum cutting<br><br>- Cable Flange enhance stability of Strut Flange | - Size of joint is generally larger than joint no. 3 due to the Cable Flange position<br><br>- Difficult to attach non-structural element so an extra hole (on top) is required |
| 2 |  | - Steel plates are cut and welded<br><br>- Cable Flange is parallel to Strut Flange | - The vertical Cable Flange allows cable end to drop naturally in vertical plane when the structure is folded | - Difficult to weld |
| 3 |  | - Steel plates are cut and welded<br><br>- Cable Flange is parallel to Strut Flange | - Simpler than no. 2 with less flange components and weld lines | - Difficult to weld<br><br>-Discontinuous cable to be connected |
| 4 |  | - Plates are welded to central pipe | - Central hollow allows easier attachment | - More material is required comparing with first three joint designs<br><br>-Poor force transfer path as the force is transferred through the curved pipe |

| | | | | |
|---|---|---|---|---|
| 5 |  | - Plates are welded to central pipe | - Easier to weld than all of previous designs | - Punching shear may be critical<br><br>-Poor force transfer path as the force is transferred through the curved pipe |
| 6 |  | - Plates are welded to form a central hollow<br><br>- Cable Flange is parallel to Strut Flange | - Good force transfer path as the force can be transferred in a straight Strut Flange | - More weld lines<br><br>- Difficult to weld inside hollow |
| 7 |  | - Plates are welded to form a central hollow<br><br>- Cable Flange is perpendicular to Strut Flange | - Good force transfer<br><br>- Cable Flange enhance stability of Strut Flange | - More material comparing with the first three joint designs |

(Note: the joint drawings are for middle joints so the Strut Flanges are with two holes to allow pin/ bolt through while the Cable Flanges have one hole as shown in Fig. 7.14).
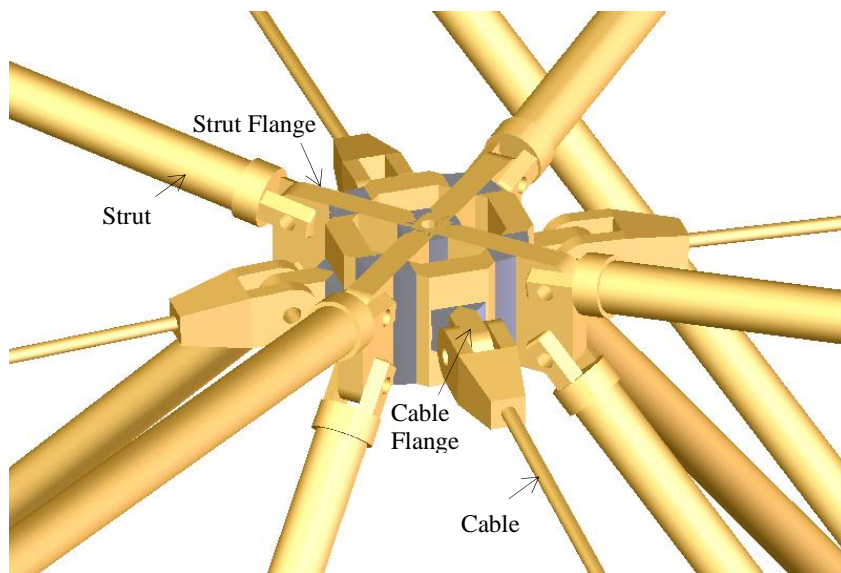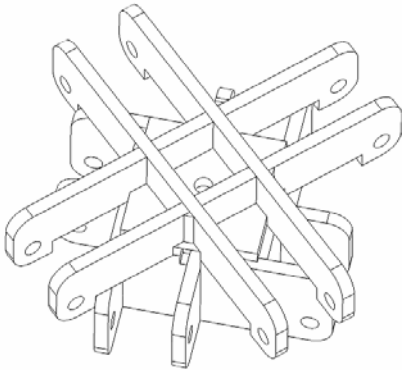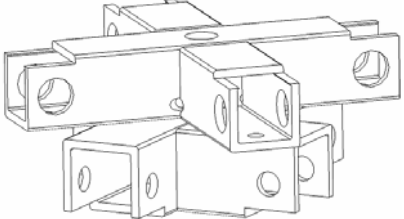


Figure 7.14. A middle joint design.

**Table 7.3.** Eccentric joint designs

| No | Joint Design | Description | Advantage | Disadvantage |
|---|---|---|---|---|
| 1 |  | - Welded plate | - Flexibility in shape and size | - Many weld lines<br>- Many cuts<br>- Difficult to weld the upper part to the lower part |
| 2 |  | - Welded tube | - Less weld lines and fabrication effort than the previous design | - Less flexible in sizes due to limitation in standard size of tubes |

(Note: the eccentric joint designs include eccentric part (lower) to connect SLE bars and concentric part (upper) to connect top chords)

Concentric joints are suitable for non-SLE types of DTSS such are Pyramid-On-Pyramid or Pyramid-In-Pyramid (refer to Chapter 3 for the structural concepts of these structures).

SLE types of DTSS such as Pyramid-Pantograph-Pyramid, or Pyramid-Pantograph-Cable, require eccentric joint due to the eccentric nature of pantograph. Two designs are proposed and preliminarily compared in Table 7.3.

Prototypes show that both of the eccentric joint concepts are workable. Fig. 7.15 shows the overall design of welded plate joint for top and middle position in a module of Pyramid-Pantograph-Pyramid structure and the corresponding wood prototype.
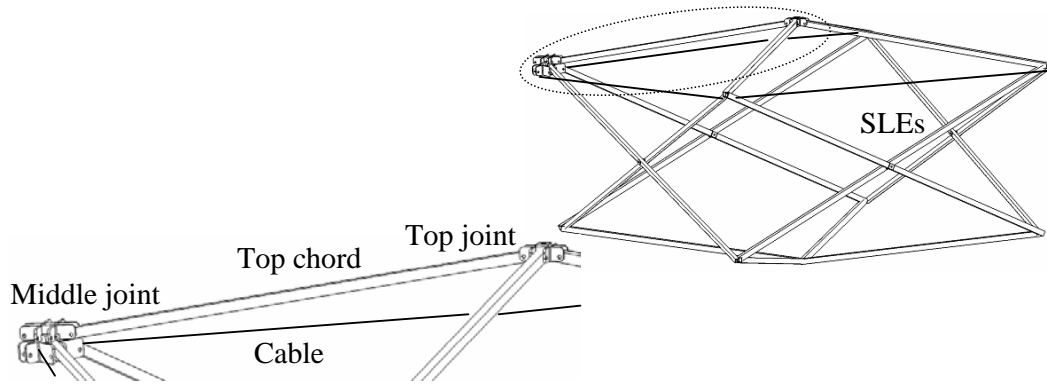
Figure 7.15. Welded plate joint for Pyramid-Pantograph-Pyramid Structure.
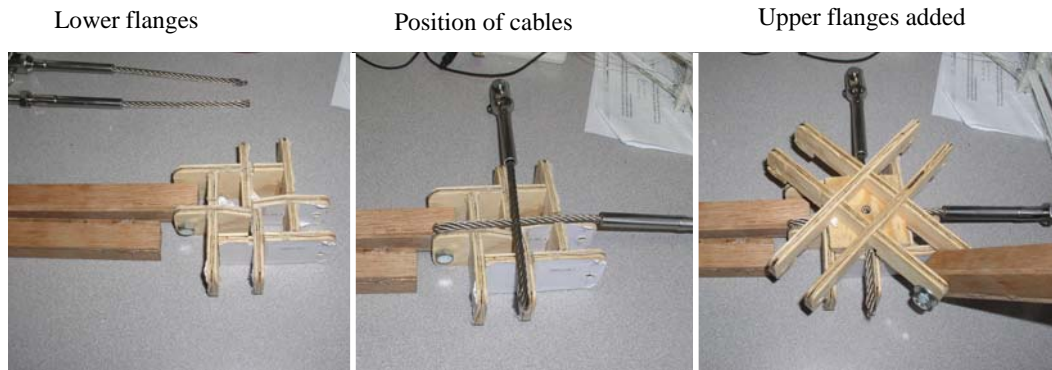


Figure 7.16. Assembly procedure for welded plate joint.

Figure 7.16 shows the assembly procedure of the welded plate joint at 1:1 scale. The assembly shows that it is relatively difficult to weld the top part of the joint to the bottom part of the joint due to limited space between flanges. There are 13 pieces of plates to be cut, drilled and then welded together.

The welded tube joint is believed to be more practical than the welded plate joint due to lower number of components (7 pieces of the same tube size), Fig. 7.17. The sizes of the tube used in joint design are recommended to be the same to avoid confusion in manufacturing process. The assembly of top struts to the structure is shown in Fig. 7.18.
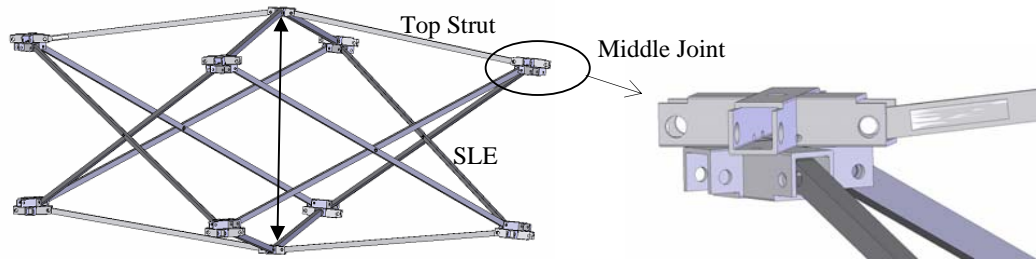
Figure 7.17. Upper middle joint of PPP Structure.
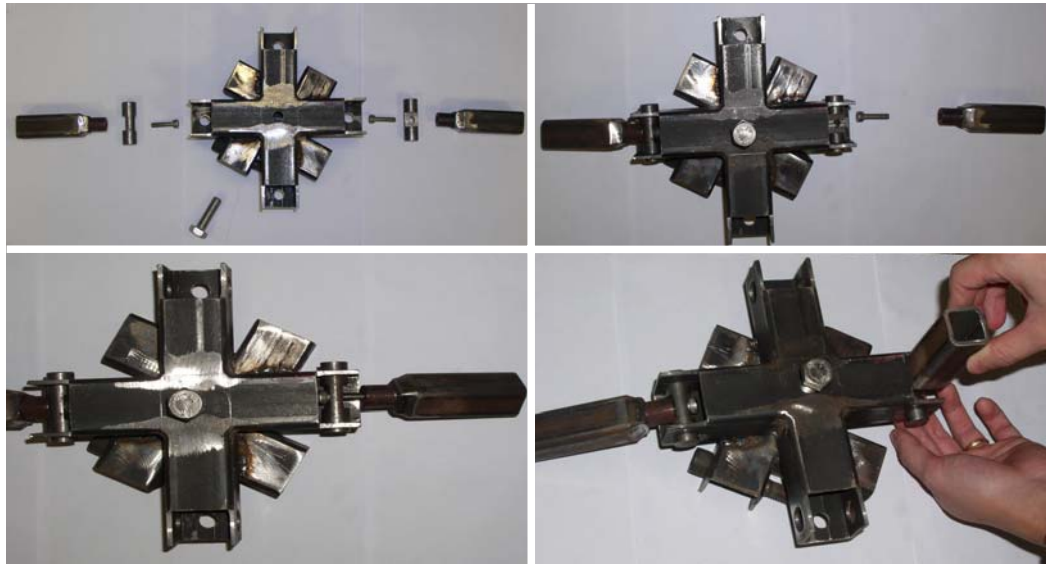

Figure 7.18. Assembly of top strut to upper middle joint.

**Aluminium joint design**

Aluminium is much lighter than steel and thus is considered a competitive material to make industrial joints. The softness of this material makes it suitable for process of cutting, drilling, and cold-forming (e.g. extruding). Aluminium extrusion technology can be used to assure that the cost of joint system is relatively low when a large quantity of joints is produced. Generally, extrusion can be much more economical for high production in comparison with welding or casting technology. In addition, some aluminium has the same structural strength as common structural steel such as Aluminium Grade 6061-T6 (350 MPa strength) but the stiffness of the material is still

about one third of steel. However, strength of aluminium is reduced significantly due to heat and thus welding aluminium needs to be avoided in manufacturing.

In this section, it is proposed that aluminium extrusion can be used to make joints for DTSS. The most commonly extruded aluminium is 6063 (Bralla, 1999) with good extrudability, and moderate strength (160 MPa, about half of strength of common structural steel S350). However, it is recommended that 6061 is used to accommodate high stress at the pin hole due to its high structural strength. A proposal of extruded aluminium joint is shown in Figs. 7.19 and 7.20.



POP structure

Pin hole for through bolt

Top strut

Cable End

Middle joint system

Diagonal strut
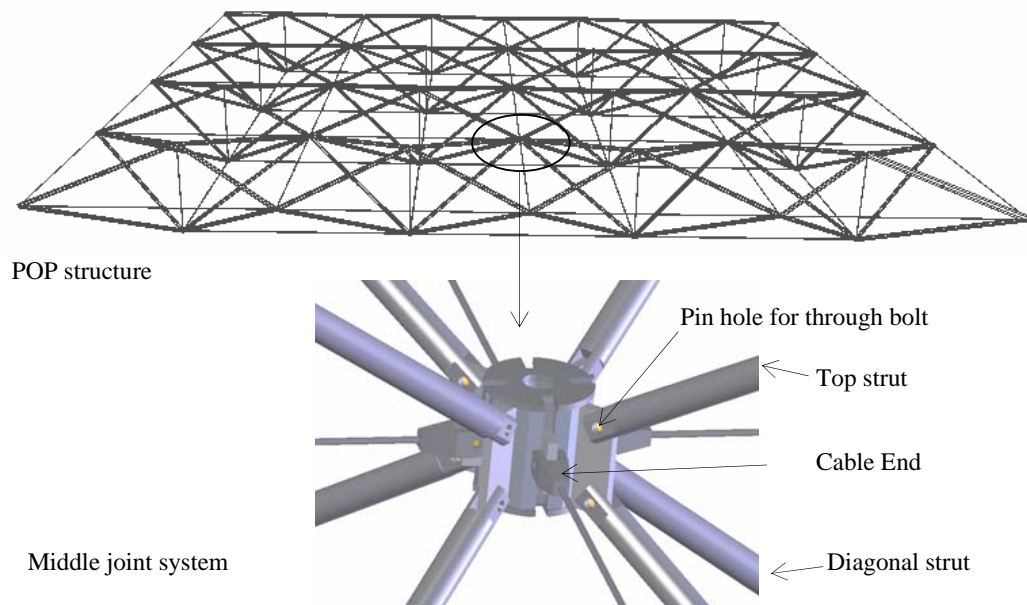
Figure 7.19. Middle joint system of the POP structure.
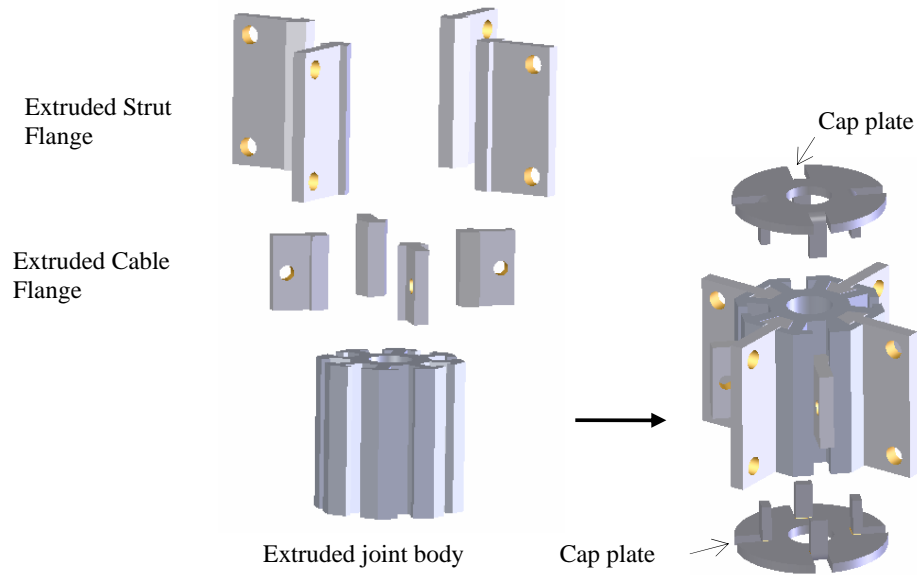
Figure 7.20. Details of the aluminium joint system.

The joint system proposed here includes three parts. One part is the joint body which is a hollow extruded section. Another part is the joint flanges. The others are the two steel cap plates. The joint system of the POP structure is shown in Fig. 7.19. All struts and cables are connected with a bolt through the pin hole (this bolt is hidden in the Figs. 7.19 and 7.20 for clarity). The details of this joint system with three extruded aluminium components are shown in Fig. 7.20. It is noted that threading on aluminium parts of joint is not recommended because of the softness of the material.

## 7.4 An illustrative design with tests on critical components

This section is to design a suitable structure and test on critical components to check the feasibility of the design. A 17.8 m span Pyramid-Pantograph-Pyramid structure (PPP) is proposed to be used as temporary shelter.

166

The structure is required to resist 0.25 kN/m$^2$ Imposed Load (IL), and 0.45 kN/m$^2$ Wind Load (WL), and to be rapidly built and relocatable. The deflection limit is Span/200 = 89 mm.

### 7.4.1 Structural design
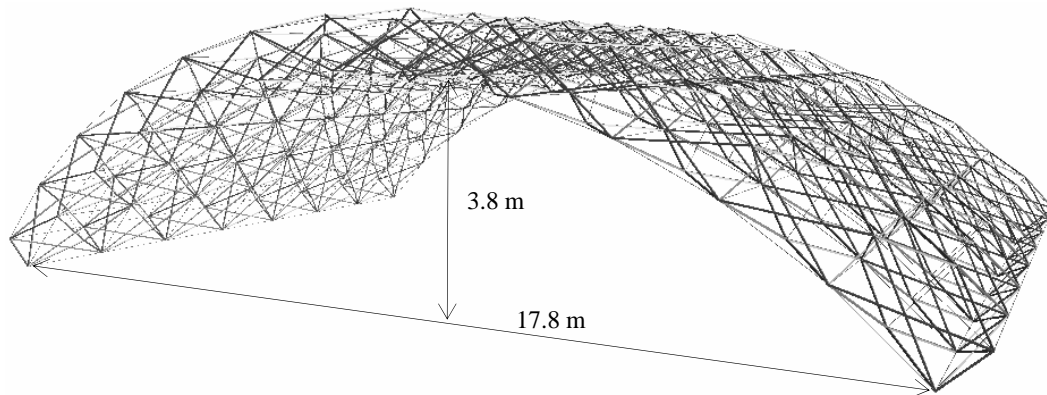


Figure 7.21. Deployable shelter with 17.8 m span.

To optimise manufacturing cost, the welded tube joint design (Figs. 7.17 and 7.18) was chosen. One tube section of 25x25x2.5 mm was chosen for all struts, 40x40x4 mm is chosen for all tube joints, and 6 mm diameter is chosen for cable elements. Steel grade S355 is applied for tubes while minimum breaking strength of cables is 28 kN. Perspective view of the structure is shown in Fig. 7.21.

Advanced non-linear analysis was performed to determine the maximum resistance of the structure. It was found that with this design, the structure can resist the critical load combination 1.4 DL + 1.2 (IL + WL) = 1.4DL + 0.84 kN/m$^2$. The maximum load the structure could carry was 1.4DL+0.875 kN/m$^2$. At this load level, the SLE bar near the support was buckled as shown in Fig. 7.22 while the maximum deflection was

55 mm which is less than the deflection limit of 89 mm. The structure is safe under live load and wind load regarding overall strength and stiffness.
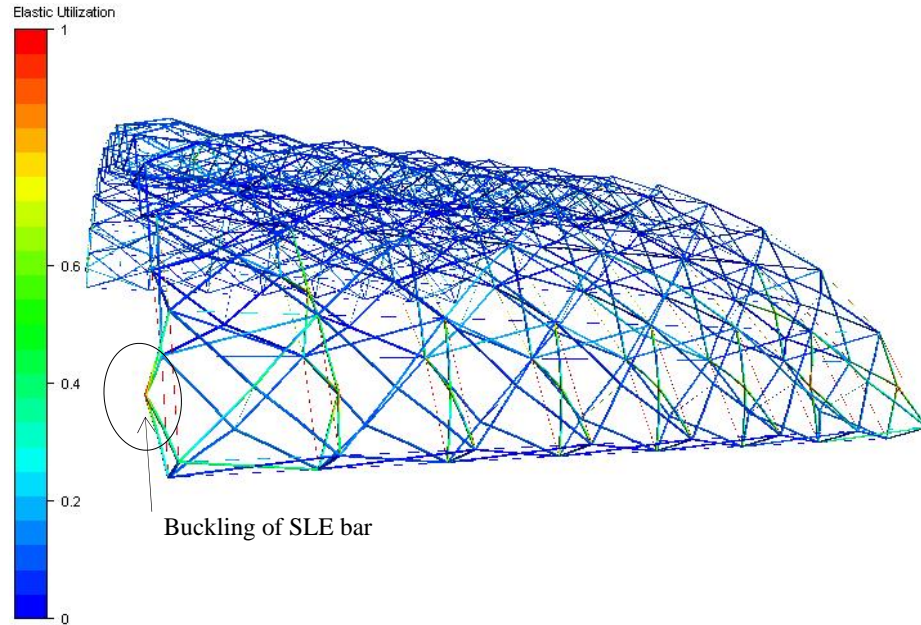


Figure 7.22. Failure of PPP structure.

The maximum force in strut was found to be 26 kN, compression. Tension force appears in cable only. The dominant force in the structure is compression. This means that the joints need to resist a compression force of at least 26 kN. The joints should be tested because they are the structural components that were not analysed.

**7.4.2 Joint tests**

The joint tests are performed to check if the strength of joint is sufficient to resist 26kN compression. The potential failure due to compression test is sectional failure of the tube, the weld, and buckling of the joint flange. It is important that the joint does not fail before the strut fails. If the joint fails before struts, all the struts connected to that joint cannot carry force and will not contribute to load resistance of the structure.

The joint is shown in Fig. 7.23. The components for load tests are eccentric flanges, concentric flanges, and tube ends. The relative position of the joint in the structure is shown in Fig. 7.17.
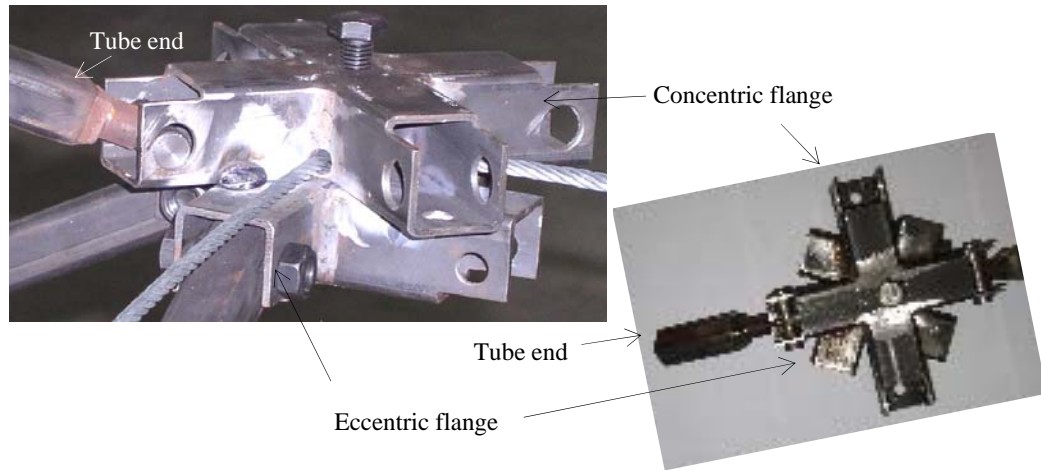


Figure 7.23. Design of steel joint.

### 7.4.2.1 Test on eccentric flanges

The first test was to investigate the strength of the Eccentric Flanges that connect to the SLE as shown in Fig. 7.23. The deformation rate was set at 0.1 mm/minute.



Figure 7.24. Test arrangement for eccentric flanges.
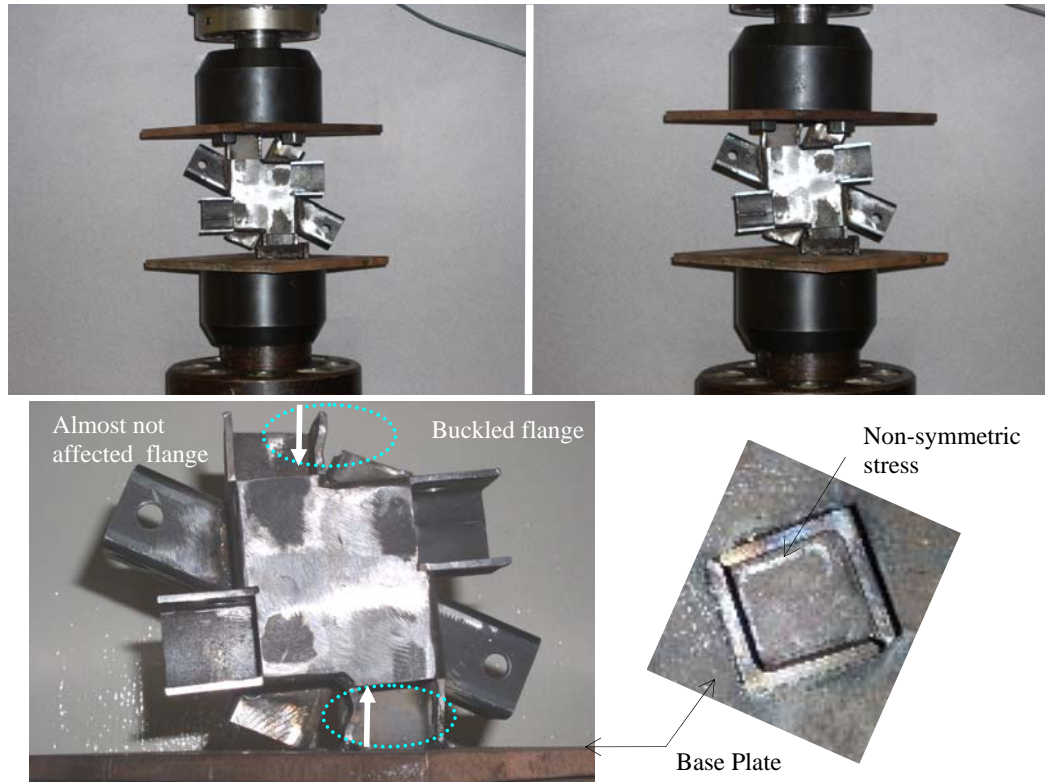
Figure 7.25. Joint rotation and buckling of joint flange.

One end of the joint is welded to a steel plate and the other end is slotted into two welded angles as shown in Fig. 7.24. This will assure the safety of the experiment as the joint may slip off the place due to shear force. The failure of the joint is initiated by the buckling of the joint flange as shown in Fig. 7.25. During the compression, rotation of the joint can be observed by normal eyes due to the eccentricity of loads.

Because the load is not aligned, only one flange of the joint is buckled (Fig. 7.25) at load of 1.5x26 kN while the other flange is almost not affected. The strut will fail (at 26 kN) before the joint starts buckling. The joint finally fails at 2.8x26 kN = 42 kN as shown in Fig. 7.26. Therefore the safety factor for this joint flange is 2.8.
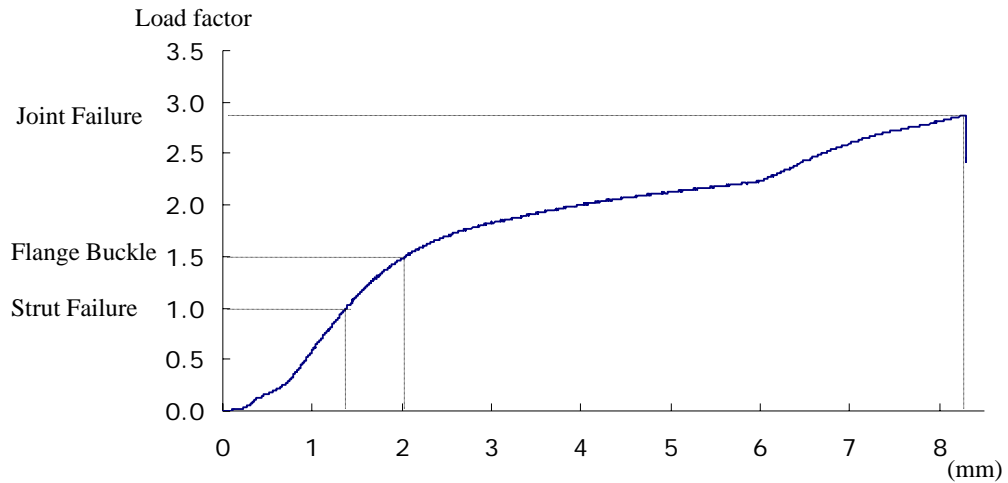
Figure 7.26. Load-displacement curve of test on eccentric flange.

## 7.4.2.2 Test on concentric flanges

The concentric compression test was carried to find out the strength of the concentric flanges which connect to the top/bottom struts. The arrangement also allows test on weld lines as shown in Fig. 7.27.
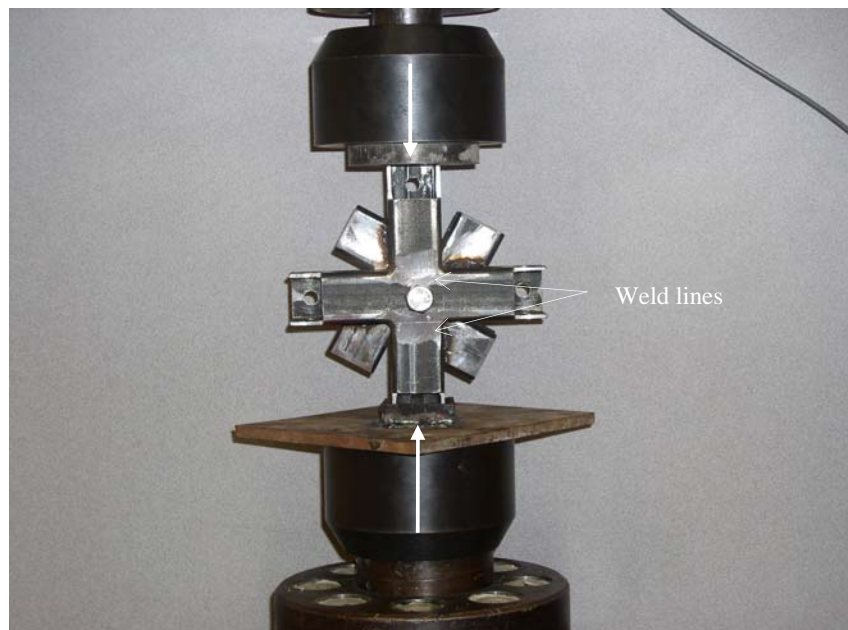


Figure 7.27. Test on concentric flanges.
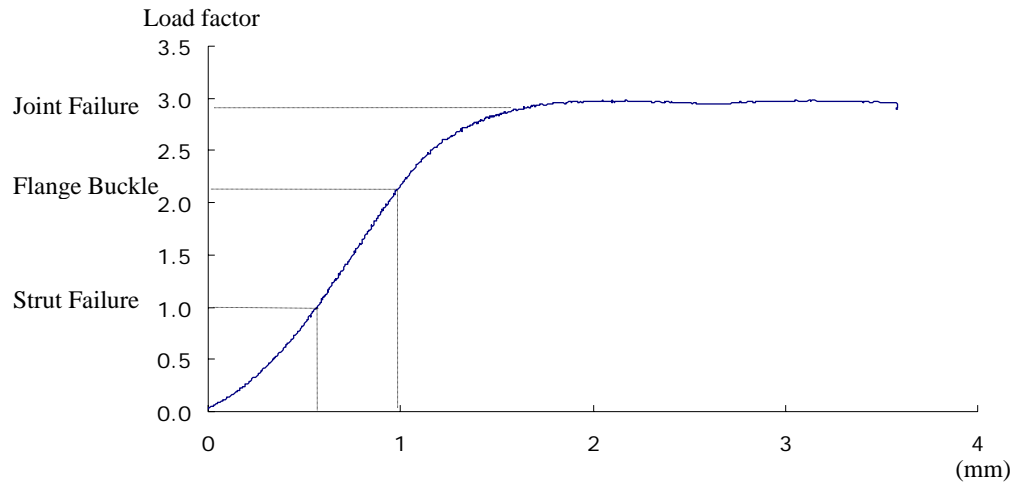
Figure 7.28. Load-displacement curve of test on concentric flanges.
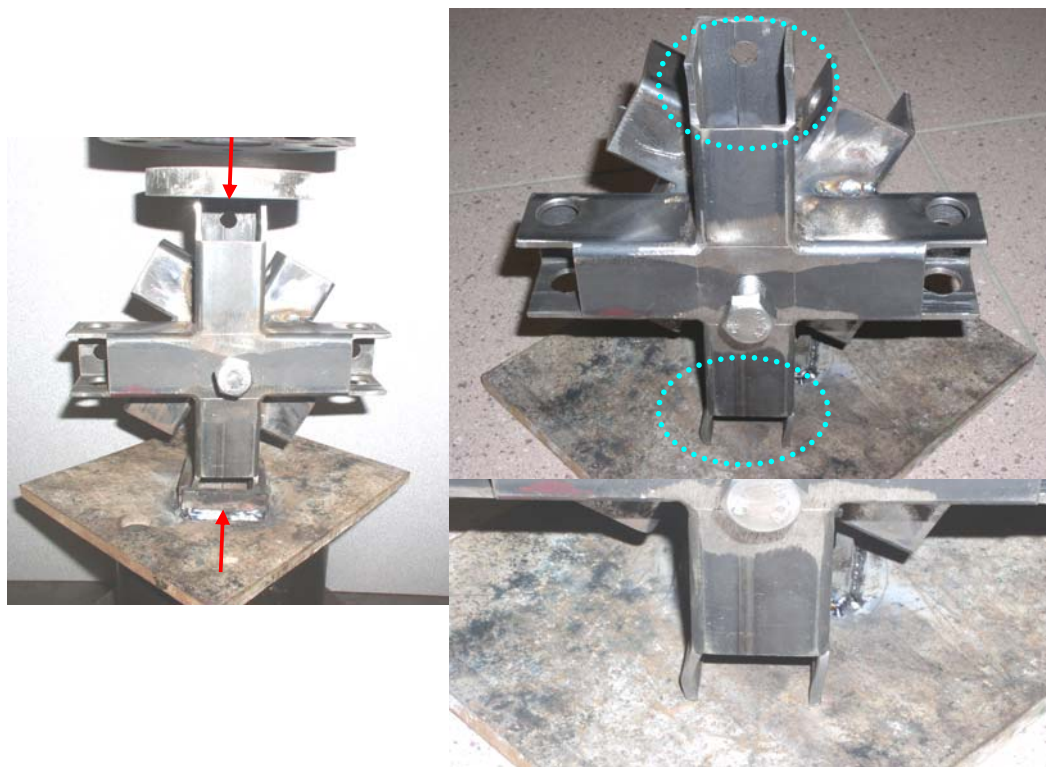


Figure 7.29. Buckle of the concentric flange.

It was found out that the joint fails at 2.9x26 kN but the initial failure was the buckling

of the joint flange, which is found at the load of 2.3x26 kN as shown in Fig. 7.28. The

failure of the flange of the joint can be observed in Fig. 7.29. The safety factor of the concentric flange is therefore estimated to be 2.9.

### 7.4.2.3 Test on tube ends



Figure 7.30. Tube-end test set-up.
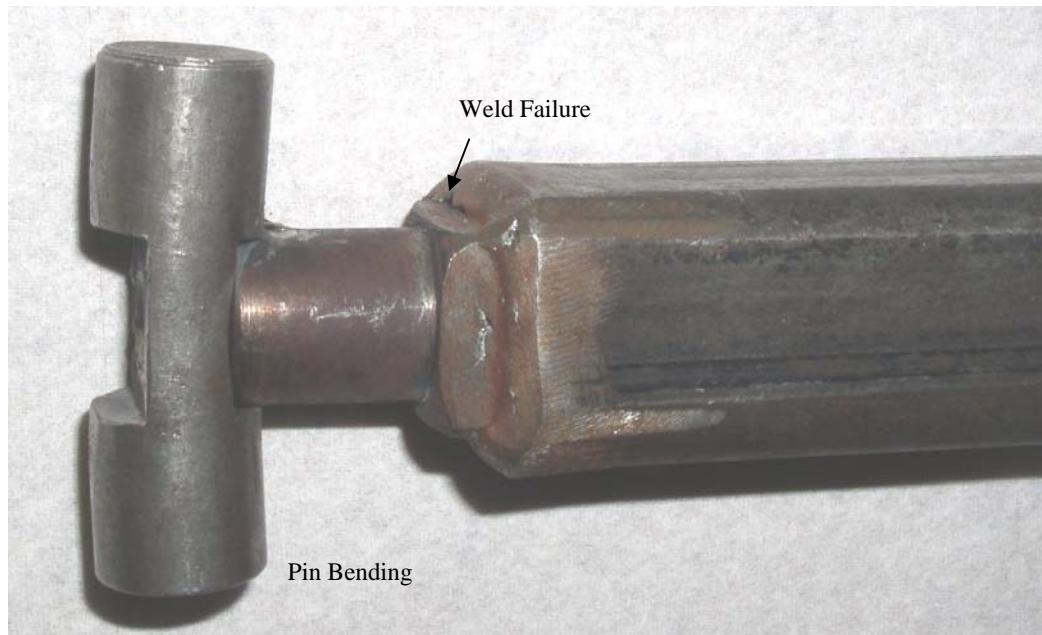


Figure 7.31. Failure mode of the tube end.

The strut end is tested to find out whether the pin and the weld at the end of the tube are strong enough to resist 26 kN. The test set up is shown in Fig. 7.30.

The strength of the tube end is 3.2x26 kN, which is identified by the crack through the weld as shown in Fig. 7.31. The bending of the pin starts at load level of 2x26 kN as can be seen in the Fig. 7.32. However, when the strut fails, the tube end is still in elastic mode and deformation is within manufacturing tolerance. Safety factor of tube end is 3.2
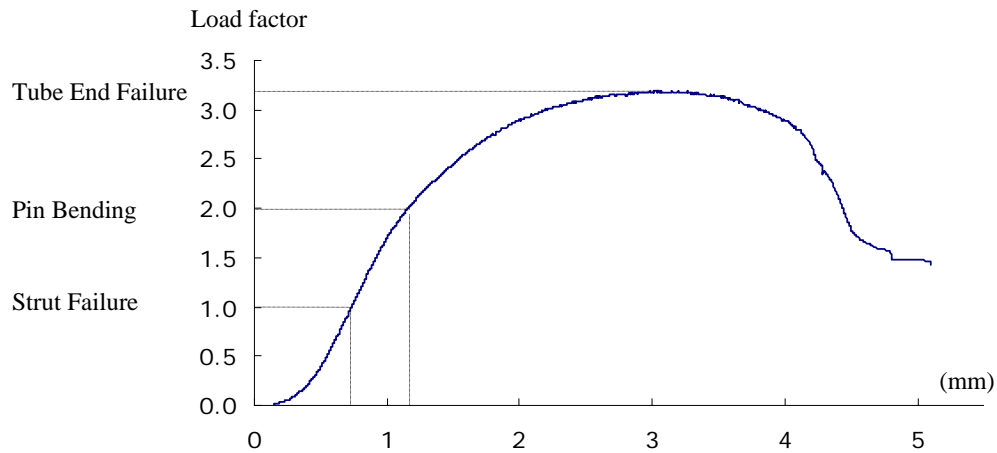


Figure 7.32. Load-displacement curve of test on tube end.

## 7.5 Potential applications

There are two major applications of DTSS, deployable shelter and deployable boom. Although DTSS in deployed and stabilised form is basically a spatial system, the added value of quick deployment and re-foldability make the proposed systems most suitable for framing military shelters (Figs. 7.33, and 7.34), humanitarian shelters (Fig. 7.35), and booms for mounting communication devices (Fig. 7.36).

Deploying Dome

Pyramid-On-Pyramid Dome Structure

Attached Membrane
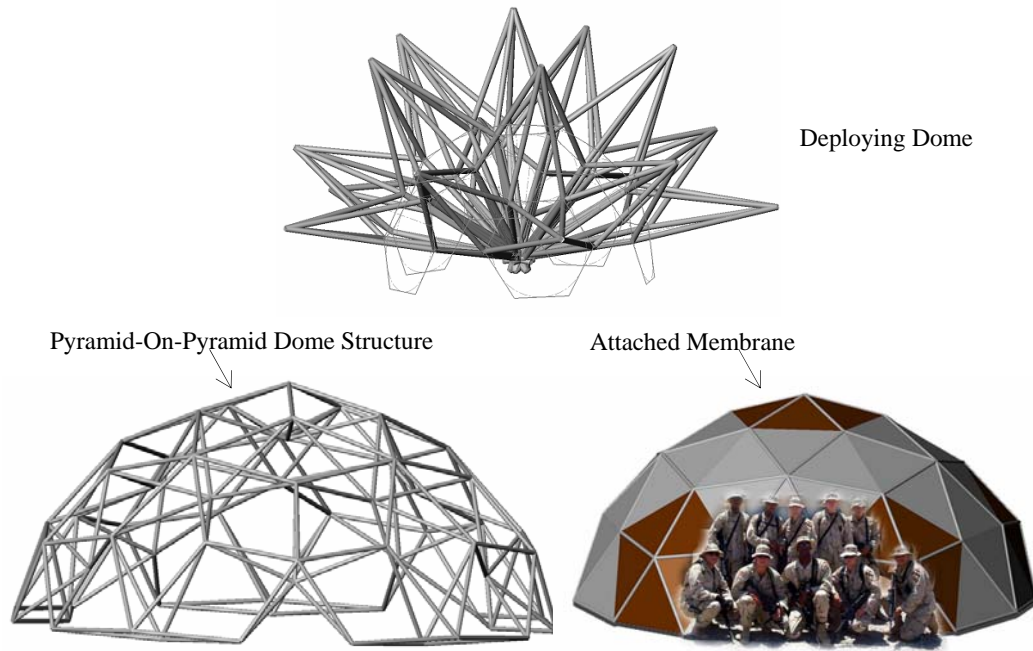
Figure 7.33. Deployable Tension-Strut Dome with membrane covers for military personnel shelter.

Attached Membrane

Pyramid-Pantograph-Pyramid Vault Structure
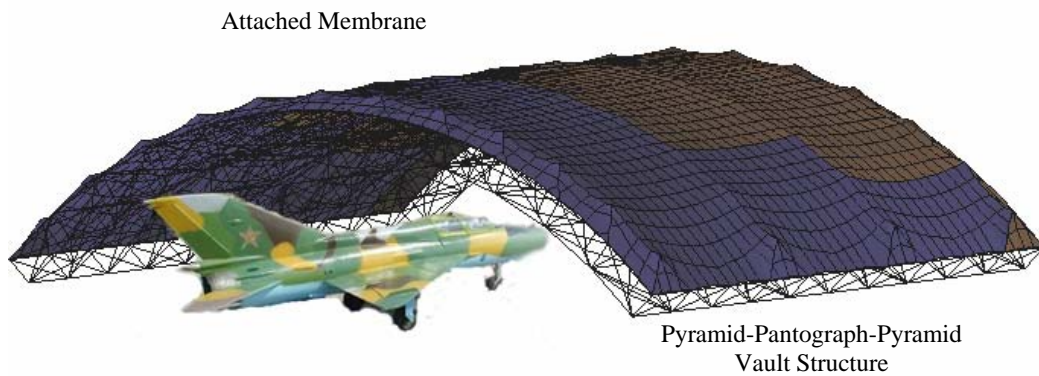
Figure 7.34. Deployable Tension-Strut Vault with membrane covers for military aircraft shelter.
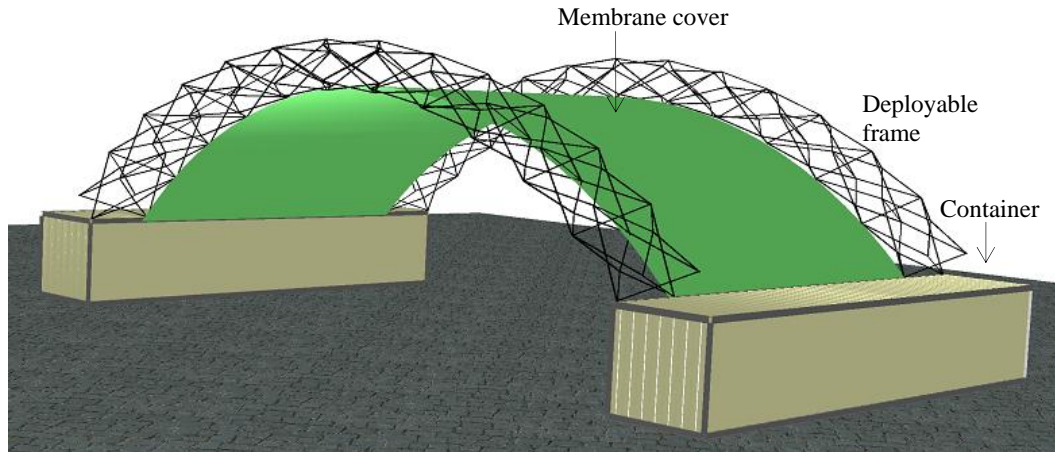
Note: The structures can be folded and packed in containers after the humanitarian mission

Figure 7.35. Humanitarian/emergency relief deployable shelter.

Fig. 7.36 shows XPOP boom in a space station with different functions. In this figure, two XPOP booms are to carry communication devices. The other one is carrying the docking port for shuttle vehicles. One of the booms is still deploying, which illustrates flexibility in the usage of XPOP boom.
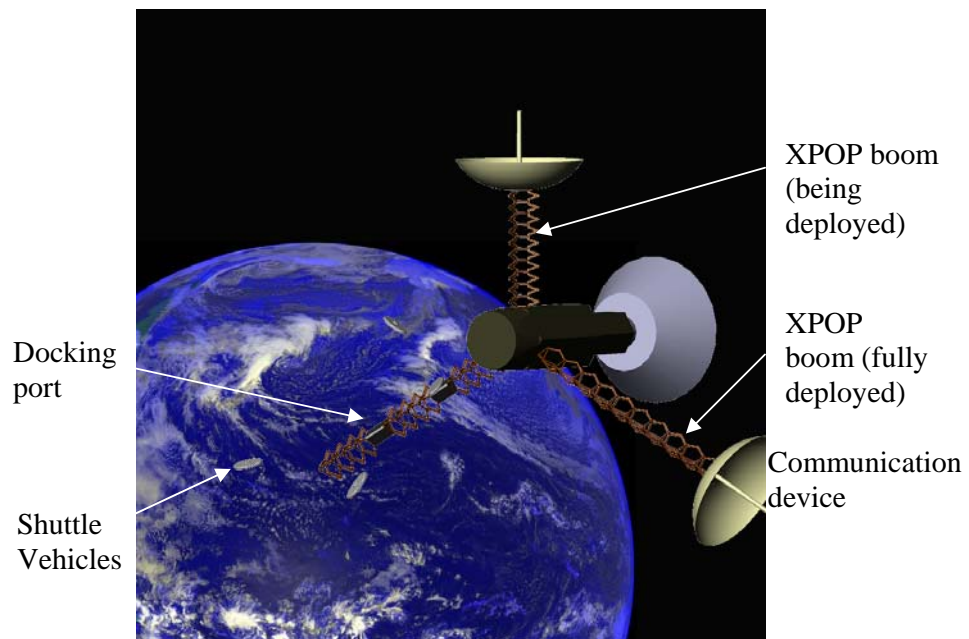


Figure 7.36. Deployable XPOP Boom in space station.

**7.6 Conclusions**

Prototypes were built to verify the deployment concept and manufacturability of Deployable Tension-Strut Structures. It is concluded that all the proposed structures are buildable and can be deployed relatively fast.

Various joint designs for different manufacturing processes are also proposed including designs for extrusion and cutting & welding method. Preliminary assessments are made based on the manufacturing of the joints. For a detailed design for a 17.8 m deployable shelter is proposed. The steel tube joint design was chosen due to economical effectiveness. This assessment is based on the number of steel plates, number of cuts, and number of weld lines. The tests show that the strength of the joints is higher than buckling capacity of the struts. This condition assures that even when the strut failed, the joint will remain elastic to allow redistribution of forces.

To assist the preliminary design of DTSS, several design parameters and strut sections are provided for preliminary design purpose with span length ranging from 24 m to 60 m.

Several application forms of Deployable Tension-Strut Structure (DTSS) have been proposed for commercial, emergency relief, or military purposes.

# CHAPTER 8

# CONCLUSIONS AND RECOMMENDATIONS

Chapter 8 is the ending chapter of the thesis but an opening to potential research directions. The significant achievements of the current project will be summarized and followed by recommendations for the future work. The intellectual property issue will be raised in the last section of this chapter to avoid unnecessary confusion due to large quantity of inventions and creative designs which have been presented in this thesis.

## 8.1 Conclusions

Tsunami, terrorism threats, rapidly deployed military activities, and dynamic commercial activities are the main cause to a global demand for novel structural systems with *rapid deployment capability* and *high structural efficiency*. This thesis is dedicated to *create* and *develop* a series of structural system which can meet these requirements. The new structural system developed in the present research is called *Deployable Tension-Strut Structure* (DTSS).

Deployable Tension-Strut Structures are deployable structural systems which includes strut elements, and collapsible tension elements such as cables or pin-connected rods. These elements are connected by pin-joints with a specific arrangement as described by shape grammar in Chapter 3 so that the structures are deployable. The struts are connected to each other to create a continuous kinematic chain which facilitates deployment of the structure. This is the distinguished geometric feature between DTSS and tensegrity because the later does not allow struts to touch each other.

This thesis introduces the novel DTSS concept and answers the questions of what is the geometric arrangement of struts and cables which suits the proposed concept (shape grammar), how to create such deployable systems, how to design joints to allow deployment, how to analyse DTSS, how to design optimum DTSS, and how effective it is to resist external loadings. All of these questions are answered in Chapters 3, 7, 4, 5, 6 respectively and Chapter 7 presents the indicative design guidelines of DTSS.

Four DTSSs are proposed in this thesis, which are Pyramid-On-Pyramid (POP), Pyramid-In-Pyramid (PIP), Pyramid-Pantograph-Cable (PPC), and Pyramid-Pantograph-Pyramid (PPP). The deployment forms of these structures are investigated and the geometric rules/ shape grammar are derived. It was found out that the relation between geometry and deployment can be summarised as a shape grammar to create more DTSSs. This is analogous to language study where grammar helps to form a sentence. An algorithm to create DTSS has been developed and implemented to automatically generate various forms of DTSS.

A total of 7 prototypes have been built to test the deployability of the tension-strut systems, proposed in Chapter 3. With proper pin-joint design, all the prototypes can be folded into compact forms, deployed to cover a larger area, and can be folded back again into the original compact forms. The DTSSs with scissor-like elements (SLEs) are found to be easier to deploy due to the kinematic chain of SLEs which have only one degree of freedom. It is also found out that the cable jam might cause delay in deployment if it is not carefully controlled during the assembly process.

A series of joint designs is also proposed to allow the deployment of DTSS. The joint designs have accommodated for different manufacturing processes, which are aluminium extrusion, and steel cutting & welding (Chapter 7). Finally, for full scale prototyping, cutting & welding tubular joint design is chosen for manufacturing and testing due to the cost effectiveness of the solution. The tubular joints are tested to prove its strength sufficiency for a 17.8 m DTSS vault.

Besides prototyping and joint designs, the viability of the proposed DTSS concept is studied by comparing its structural efficiency with the equivalent conventional space frames in Chapter 5. The space frame roofs spanning from 36 m to 60 m are studied and the results show that the structural efficiencies of the two systems are comparable. Advanced non-linear analysis methods are introduced in Chapter 4. The optimum design parameters such as Span/Depth ratio and Module height/ Module width ratio are proposed for a range of DTSS spanning from 24 m to 60 m. The mode shapes of DTSS are also investigated and hints on most potential failure modes are deduced. Introduction of pre-tensioning force in the cables is found to affect the shape of the structure like pre-cambering and enhance stability but it does not significantly increase the structural stiffness. Joints and structural component designs as well as methods for manufacturing and assembling are summarised and a set of design guidelines are proposed in Chapter 7.

Chapter 6 investigates deployable boom structures. The content is separated from the other Chapters because boom structures are generally used for space applications only and thus the considerations are different. However, the research topic in Chapter 6 is still within the main spirit of the thesis, which is to develop deployable boom with high

structural efficiency. Two new systems of boom structures are proposed and compared with the existing systems. XPOP boom is found to be the most competitive proposal in this thesis comparing with existing booms because its structural efficiency is among the highest while deployment is effective with low number of deployment motors.

The research works in this thesis has been used to support applications of two patents and one business plan proposal.

## 8.2 Potential future studies

Although sufficient work has been done to develop the design concept of DTSS to technology transfer stage, there are still spaces for further studies.

The use of DTSS for 24 m to 60 m span applications is well supported from this research. However, smaller or larger span applications may be considered and thus further works on this range of span need to be carried out. Optimum design parameters for deep DTSS domes and vaults are different from those derived for flat DTSSs and corresponding values need to be investigated for such applications.

The development of the boom, presented in Chapter 6, is suitable for common civil engineering applications. For more complicated tasks involving automatic and remote control deployment, mechanical design is required.

The use of commutative algebra as the mathematical background for structural analysis is a suggestion. The novelty of the idea is acknowledged and awarded by Hangai Prize

Committee 2005 (in the annual Symposium of International Association of Shell and Spatial Structures). The advantage of using commutative algebra in finite element procedure is the avoidance of re-assembling stiffness matrix, which may lead to significant computational efficiency. However, more proves is needed to show how computationally effective the approach is. The matter of how to implement the approach into commercial software also needs to be verified.

## 8.3 Intellectual property right claims

The current research is a result of multi-discipline works with crossing and sharing ideas and visions among the research group. Therefore, intellectual property right needs to be clearly stated to avoid confusion for later references.

Within the family of DTSSs, three structures of POP, PPP, and PPC are patented by Dr. Krishnapilai Anandasivam and Dr. Richard Liew Jat Yuen, who are the author's PhD supervisors.

PIP and the XPOP boom are invented by the author of this thesis and being patented before the thesis is submitted. The exhaustive design tool to create new DTSSs and the sample output of this tool presented in Chapter 3 is a contribution by the author of this thesis.

All the development works such as analysis, investigation on structural behaviour, detailing designs, and prototypes of DTSSs presented in this thesis are done by the author of this thesis.

# REFERENCES

Adam B, Smith IFC. 2004. "An intelligent spatial tensegrity structures", *Proceedings of IASS 2004 Symposium*, Montpellier, France.

Argyris JH, and Scharpf DW. 1972. "Large deflection analysis of pre-stressed network", *Journal of Structural Division of ASCE*, 633-654.

Atake K. 2000. "ATAKE's structure – new variations of the scissors technique", *Proceedings of MARAS III*, Madrid, Spain, 143-154.

Bangash MYH, Bangash T. 2003. *Elements of spatial structures – Analysis and design*, Thomas Telford Publishing, London, UK.

Bathe JK. 1996. *Finite Element Procedures*, Prentice Hall, London, UK.

Bendsoe MP. 1995. *Optimisation of structural topology, shape, and material*, Springer-Verlag, Berlin, Germany.

Bieniek Z. 2004. "The new geometrical conception of tensegrity extender", *Proceedings of IASS 2004 Symposium*, Montpellier, France.

Bowden ML. 1998. "Deployment devices", In Conley PL. ed. *Space vehicle mechanisms – Elements of successful design*, John Wiley & Sons, USA, 495 - 542

Bulman S, Sienz J, and Hinton E. 2001. "Comparisons between algorithms for structural topology optimization using a series of benchmark studies". *Journal of Computers & Structures*, Vol. 79, 1203-1218.

Bralla JG. 1999. *Design for manufacturability handbook*, Mc Graw-hill, USA.

Brown KN, and Cagan J. 1997. "Optimised process planning by generative simulated annealing", *Journal of Artificial Intelligence for Engineering Design, Analysis and Manufacturing,* Vol. 11, 219-236.

Calladine CR, Pellegrino S. 1991. "First-order infinitesimal mechanisms", *International Journal of Solid Structures*, Vol. 27 (4), 505-515.

Chen, W.F., Goto Y., and Liew, J.Y.R. 1996. *Stability Design of Semi-Rigid Frames*, John Wiley & Sons, Inc, U.S.A.

Coelloa CA, and Christiansen AD. 2000. "Multi-objective optimization of trusses using genetic algorithms", *Journal of Computers and Structures*, Vol. 75, 647-660.

Cox, D., Little, J., and O'Shea, D., 1997. *Ideals, Varieties, and Algorithms: an Introduction to Computational Algebraic Geometry and Commutative Algebra: with 91 Illustrations*, 2nd edition, Springer-Verlag, U.S.A.

Dinca F., and Theodosin C. 1973. "*Non-linear and random vibration*", Academic Press.

Douglas MV. 1993. " *Module For An Articulated Stowable and Deployable Mast*", US patent 5267424.

Eckert C, Kelly I, and Stacey M. 1999. "Interactive generative systems for conceptual design: An empirical perspective", *Journal of Artificial Intelligence for Engineering Design, Analysis and Manufacturing,* Vol. 13, 303-320.

El-Sheikh A. 1998. "Optimum design of space trusses", *Journal of the International Association for Shell and Spatial Structures*, Vol. 39, 159-169.

El-Sheikh A. 1999. "New space truss system—from concept to implementation", *Journal of Engineering Structures*, Vol. 22, 1070-1085.

Escrig F. 1996a. "The adventure of covering a swimming-pool with an X-frame structure", *Proceedings of MARAS II*, Sevilla, Spain, 113-122.

Escrig F. 1996b. "General survey of deployability in architecture", *Proceedings of MARAS II*, Sevilla, Spain, 113-122.

Flemming U. 1986. "More than the sum of parts: The Queen Anne house", *Journal of Environment and Planning B*, Vol. 14, 323-350.

Gantes C. 2001. *Deployable Structures: Application and Design*, WIT Press, USA.

Gasparetto E. 2003. "A new proposal for roll-over protective structures (ROPS) – self-deployable protective structures for agricultural tractors", *Proceedings of the 23rd AGR/CA/T 2003*, Instituto di Ingeneria Agraria, Milan, Italia.

Gomez de Cozar JC, and Garcia Dieguez R. 2000. "System for double-layer deployable structures: processes of formal definition", *Proceedings of MARAS III*, Madrid, Spain, 103 – 112.

Hanaor A. 1988. "Pre-stressed pin-jointed structures – flexibility analysis of pre-stress design", *Journal of Computers & Structures*, Vol. 28, 757-769.

Hangai Y, Wu M. 1999. "Analytical method of structural behaviours of a hybrid structure consisting of cables and rigid structures", *Journal of Engineering Structures*, Vol. 21, 726-736.

Hernandez CH. 1996. "New ideas on deployable structures", *Proceedings of MARAS II*, Sevilla, Spain, 63-72.

Hoberman C. 1990. "Reversibly expandable doubly-curved truss structure", *US Patent*, US4942700.

Hoberman C. 1991. "Radial expansion / retraction truss structures", *US Patent*, US5024031.

Ishii K. 2000. *Structural Design of Retractable Roof Structures*, WIT Press, USA.

Kawaguchi K. 2003. "Pre-stress states of tension-truss and tensegrity", *Proceedings of IASS 2003*, Taipei, Taiwan.

Kawaguchi M. 2004. "Physical models as powerful weapons in structural design", *Proceedings of IASS 2004*, Montpelier, France.

Kawamura H, Osada S, Ohmori H. 2000. "Genetic creation of 3-dimensional truss structures", *Journal of the International Association for Shell and Spatial Structures*, Vol. 41, 163-175.

Kenneth ML, and Uang CM. 2005. *Fundamentals of structural analysis*, Mc-Grawhill, Boston, USA.

Lallemant B. 2002. "Inflatable space-rigidized structures (ISRS) – Inflation subsystem", Aerospace energetic equipment – Avignon.

Langbecker T. 2000. "Foldable positive and negative curvature structures: geometric design and structural response", *Journal of the International Associations for Shell and Spatial Structures*, Vol. 41, 147-161.

Langbecker T. 2001. "Kinematic and non-linear analysis of foldable barrel vaults", *Journal of Engineering Structure*, Vol. 23, 158-171.

Lee BH. 2001. *Analysis, design and implementation of cable-strut structures*, M.Eng dissertation, Department of Civil Engineering, National University of Singapore.

Leite JPB, Topping BHV. 1999. "Parallel simulated annealing for structural optimisation", *Journal of Computers & Structures*, Vol. 73, 545-564.

Liew JYR, Lee BH. 2003. "Experimental study on reciprocal prism (RP) grid for space structures", *Journal of Constructional Steel Research*, Vol. 59, 1363-1384.

Liew JYR, Lee BH, Wang BB. 2003. "Innovative use of star-prism (SP) and di-pyramid (DP) for spatial structures", *Journal of Constructional Steel Research*, Vol. 59, 335-357.

Makowski ZS. 1981. *Analysis, design, and construction of double-layer grids*, Applied Science Publishers, London, UK.

Makowski ZS. 1985. *Analysis, design, and construction of barrel vaults*, Applied Science Publishers, London, UK.

Martinez-Calzon J. 1996. "Two special construction procedures for the erection of the big communication towers of Collserola and Valencia", *Proceedings of MARAS II*, Sevilla, Spain, 337-350.

Miles JC, Sisk JM, and Moore CJ. 2001. "The conceptual design of commercial buildings using a genetic algorithm", *Journal of Computers & Structures*, Vol. 79, 1583-1592.

Mitchell WJ. 1991. "Functional grammars: An introduction", *Proceedings of Computer Aided Design in Architecture 1991*, Los Angeles, USA, 167-176.

Motro R. 2003. *Tensegrity – Structural systems for the future*, Kogan Page Science, London, UK.

Motro R. and Bounderbala M. 1996. "Mobile tensegrity systems", *Proceedings of MARAS II*, Seville, Spain, 103 – 112.

Mukhopadhyay M. 2000. "*Vibrations, dynamics and structural systems*", A.A. Balkema, Rotterdam, Netherlands.

Nooshin H, Disney P. 2000. "Formex Configuration Processing I". *International Journal of Space Structures*, Vol. 15, 1-52.

Nooshin H, Disney P. 2001. "Formex Configuration Processing II". *International Journal of Space Structures*, Vol. 16, 1-56.

Nooshin H, Disney P. 2002. "Formex Configuration Processing III". *International Journal of Space Structures*, Vol. 17, 1-50.

Park HS, and Sung CW. 2002. "Optimization of steel structures using distributed simulated annealing algorithm on a cluster of personal computers", *Journal of Computers & Structures*, Vol. 80, 1305-1316.

Pellegrino S. 1990. "Analysis of pre-stressed mechanisms", *International Journal of Solid Structures*, Vol. 26 (12), 1329-1350.

Pellegrino S, Calladine CR. 1986. "Matrix analysis of statically and kinematically indeterminate frameworks", *International Journal of Solid Structures*, Vol. 22 (4), 409-428.

Ramaswamy GS, Eekhout M, and Suresh GR. 2002. *Analysis, design and construction of steel space frames*, Thomas Telford Publishing, London, UK.

Raskin I, and Roorda J. 1996. "Buckling force for deployable pantographic columns", *Proceedings of MARAS II*, Sevilla, Spain, 305 - 314.

Sastre R. 1996. "Expansible arches", *Proceedings of MARAS II*, Sevilla, Spain, 123-134.

Schlaich M. 2004. "The Messeturm in Rostock-A tensegrity tower", *Journal of the International Association for Shell and Spatial Structures*, Vol. 45, 93-99.

Shea K. 1997. "*Essays of Discrete Structures: Purposeful Design of Grammatical Structures by Directed Stochastic Search*", Ph.D. dissertation, Carnegie Institute of Technology, Carnegie Mellon University.

Shea K, and Cagan J. 1999. "Languages and semantics of grammatical discrete structures", *Journal of Artificial Intelligence for Engineering Design, Analysis and Manufacturing,* Vol. 13, 241-251.

Shea K, and Zhao X. 2004. "A novel noonmark cantilever support: From design generation to realisation", *Proceedings of IASS 2004*, Montpellier, France.

Sim SK, and Duffy AHB. 2004. "Evolving a model of learning in design", *Journal of Research in Engineering Design*, Vol. 15, 40-61.

SINTEF report. 2003. *USFOS 8.0 theory manual*, The Foundation for Scientific and Industrial Research at the Norwegian Institute of Technology, Norway.

Smaili A, Motro R, Raducanu V. 2004. "New concept for deployable tensegrity systems structural mechanism activated by shear forces", *Proceedings of IASS 2004 Symposium*, Montpellier, France.

Snelson K. 1965. "Continuous Tension, Discontinuous Compression Structures", *U.S. patent No. 3169611*.

Song X, Baldwin JD. 1999. "A novel node-based structural shape optimisation algorithm", *Journal of Computers and Structures*, Vol. 70, 569-581.

Stoker J.J. 1950. "*Non-linear Vibration*", Interscience Publishers Inc., New York, USA.

Surrey Space Centre. 2001. "SSTL Weitzman 6 m deployable boom", *Product report in Surrey Satellite Technology LTD*, University of Surrey, UK.

Suzuki H. 2004. "Overview of Mega-float: Concept, Design Criteria and Analysis and Design", *Symposium on Very Large Floating Structures for the Future*, NTNU, Norway.

Stiny G. 1980. "Introduction to shape and shape grammars", *Journal of Environment and Planning B*, Vol. 7, 343-351.

Talvik I. 2001. "Finite element modelling of cable networks with flexible supports", *Journal of Computers & Structures*, Vol. 79, 2443-2450.

Tibert G. 2002. "*Deployable tensegrity structures for space applications*", Ph.D. dissertation, Royal Institute of Technology, Sweden.

Wang BB. 1998. "Cable-strut systems: Part II - cable-strut", *Journal of Constructional Steel Research*, Vol. 45, 291-299.

Wang BB. 2004. *Free-standing tension structures – From tensegrity systems to cable-strut systems*, Spon Press, London, UK.

Westerberg A, Grossmann I, Talukdar S, Prinz F, Fenves S, and Maher ML. 1990. "Applications of artificial intelligence in design research at Carnegie Mellon University's EDRC", *Journal of Artificial Intelligence in Engineering*, Vol. 5.

Wimoth R. 2002. "Aerobraking technology for Earth-Orbit transfer", *Proceedings of 16th Annual/USU conference on small satellites*, NASA Langsley Research Centre.

Yang YB, and Kuo SR. 1994. *Theory and analysis of nonlinear framed structures*, Prentice Hall, Singapore.

Yang Y, and Soh CK. 2002. "Automated optimum design of structures using genetic programming", *Journal of Computers and Structures,* Vol. 8, 1537-1546.

Yau JD, and Yang YB. 2003. "Large deflection analysis of a guided column pulled by a cable", *Proceedings of IASS 2003*, Taipei, Taiwan.

You Z. 1997. "Displacement control of pre-stressed structures", *Journal of Computational Methods in Applied Mechanical Engineering*, Vol. 144, 51-59.

You Z, and Pellegrino S. 1996. "New solutions for foldable roof structures", *Proceedings of MARAS II*, Sevilla, Spain, 35-44.

You Z, and Pellegrino S. 1996b. "Cable-stiffened pantographic deployable structures. Part 1: Triangular mast", *AIAA Journal*, Vol. 34, 813-820.

**Appendix A: Sensitivity of SEI to the change in structural member sizes**

In the paper, structural efficiency of different structural configurations is evaluated and compared to find out the most efficient structures and the optimum design parameters. This means that only the type of structures, the number of modules, and the span/depth ratio is considered in the comparisons. To quantify the structural efficiency of each structural configuration, SEI is proposed.

In this appendix, SEI is shown to be more suitable than self-weight criterion, which is the conventional index, to evaluate structural efficiency of structures. The self-weight of optimum designed structure can be used to evaluate structural efficiency. However, it is not straight forwards to obtain the optimum structural member sizes and thus the suitable self-weight quantity for the evaluation of structural efficiency. SEI is proposed to be less affected by the proportioning of structural member sizes and can be used to evaluate the structural efficiency of a structural configuration. The sensitivity of SEI and self-weight criterion is compared in the following 2 illustrations.

The PPP structure is used for this study with the span of 24 m. The number of modules in a span direction is 10 and 8 while the span/depth ratio is 12 and 10 for illustration 1 and 2, respectively. Different proportions of structural members' sizes are applied to each structural configuration. The result of the study is shown in the table A1 and A2.

In illustration 1, average value of SEI is 2.22 maximum therefore the maximum difference is 0.2 = 9% of average SEI. The average self-weight is 12.94 kg/m² and the maximum difference: 3.2 kg/m² = 25% of average self-weight. Therefore the ratio of difference between SEI and self-weight 9% / 25% = 36%.

Table A1: Illustration 1

| Span (m) | Span/Depth | No. Module | Inclination ratio (%) | Displacement (m) | Self-weight (kg/m²) | L/W | SEI |
|---|---|---|---|---|---|---|---|
| 24 | 12 | 10x10 | 8 | 0.029 | 14.91 | 10 | 2.1 |
| 24 | 12 | 10x10 | 8 | 0.035 | 11.71 | 13 | 2.3 |
| 24 | 12 | 10x10 | 8 | 0.034 | 12.04 | 12 | 2.3 |
| 24 | 12 | 10x10 | 8 | 0.032 | 12.84 | 12 | 2.2 |
| 24 | 12 | 10x10 | 8 | 0.031 | 13.21 | 11 | 2.2 |

Table A2: Illustration 2

| Span (m) | Span/Depth | No. Module | Inclination ratio (%) | Displacement (m) | Self-weight (kg/m²) | L/W | SEI |
|---|---|---|---|---|---|---|---|
| 24 | 10 | 8x8 | 8 | 0.025 | 11.50 | 13 | 2.8 |
| 24 | 10 | 8x8 | 8 | 0.029 | 9.46 | 15 | 3.1 |
| 24 | 10 | 8x8 | 8 | 0.030 | 9.20 | 16 | 3.1 |
| 24 | 10 | 8x8 | 8 | 0.030 | 9.15 | 16 | 3.1 |
| 24 | 10 | 8x8 | 8 | 0.031 | 8.76 | 16 | 3.2 |

In illustration 2, average value of SEI is 3.082 and thus the maximum difference is 0.4 = 12.9% of average SEI. Average self-weight is 9.62 kg/m². Maximum difference is 2.74 kg/m² = 28.5% of average self-weight. The ratio of difference between SEI and self-weight 12.9% / 28.5% ≈ 45%

SEI can be used as the representative index for structural efficiency of a structural

configuration featured by the type of structure, the number of modules, and the

span/depth ratio. It is not as sensitive to the change in structural member sizes as the

self-weight criterion.

## Appendix B: Results of Parametric Study

Table B1: Parametric study of POP structure $(\tan(\alpha) = 0.15)$

| Span (m) | Span/Depth | No. of Module | Displacement (m) | Weight (kg/m²) | L/W | SEI |
|---|---|---|---|---|---|---|
| 60 | 12 | 10 | 0.117 | 22.10 | 4 | 0.7 |
| 60 | 10 | 12 | 0.077 | 24.24 | 4 | 0.8 |
| 60 | 10 | 10 | 0.088 | 19.58 | 5 | 0.9 |
| 60 | 10 | 8 | 0.104 | 14.17 | 6 | 1.1 |
| 60 | 10 | 4 | 0.179 | 15.43 | 6 | 0.8 |
| 60 | 8 | 10 | 0.058 | 22.18 | 4 | 1.0 |
| 60 | 4 | 10 | 0.034 | 31.07 | 3 | 1.0 |
| 48 | 12 | 10 | 0.109 | 13.49 | 7 | 1.0 |
| 48 | 10 | 12 | 0.069 | 17.41 | 5 | 1.0 |
| 48 | 10 | 10 | 0.077 | 16.59 | 6 | 1.0 |
| 48 | 10 | 8 | 0.099 | 10.78 | 8 | 1.2 |
| 48 | 10 | 4 | 0.145 | 9.06 | 9 | 1.2 |
| 48 | 8 | 10 | 0.052 | 19.09 | 5 | 1.1 |
| 48 | 4 | 10 | 0.024 | 34.20 | 3 | 1.0 |
| 36 | 12 | 10 | 0.071 | 14.07 | 6 | 1.0 |
| 36 | 10 | 12 | 0.063 | 16.93 | 5 | 0.9 |
| 36 | 10 | 10 | 0.050 | 15.50 | 6 | 1.1 |
| 36 | 10 | 8 | 0.060 | 9.90 | 9 | 1.5 |
| 36 | 10 | 4 | 0.146 | 9.94 | 9 | 1.0 |
| 36 | 8 | 10 | 0.031 | 13.69 | 6 | 1.6 |
| 36 | 4 | 10 | 0.014 | 23.32 | 4 | 1.5 |
| 24 | 12 | 10 | 0.043 | 11.96 | 7 | 1.2 |
| 24 | 10 | 12 | 0.029 | 16.12 | 6 | 1.1 |
| 24 | 10 | 10 | 0.029 | 11.02 | 8 | 1.6 |
| 24 | 10 | 8 | 0.028 | 11.04 | 8 | 1.6 |
| 24 | 10 | 4 | 0.060 | 7.42 | 11 | 1.6 |
| 24 | 8 | 10 | 0.012 | 16.07 | 6 | 1.8 |
| 24 | 4 | 10 | 0.006 | 27.86 | 4 | 1.7 |
| | | | | Average | | 1.17 |

Table B2: Parametric study of PIP structure (tan $(\alpha) = 0.15$)

| Span (m) | Span/Depth | No. of Module | Displacement (m) | Weight (kg/m$^2$) | L/W | SEI |
|---|---|---|---|---|---|---|
| 60 | 12 | 10 | 0.106 | 19.35 | 5 | 0.8 |
| 60 | 10 | 12 | 0.070 | 24.36 | 4 | 0.8 |
| 60 | 10 | 10 | 0.077 | 20.65 | 5 | 0.9 |
| 60 | 10 | 8 | 0.091 | 15.41 | 6 | 1.1 |
| 60 | 10 | 4 | 0.116 | 16.54 | 6 | 0.9 |
| 60 | 8 | 10 | 0.058 | 24.39 | 4 | 0.9 |
| 60 | 4 | 10 | 0.033 | 38.52 | 3 | 0.9 |
| 48 | 12 | 10 | 0.103 | 14.59 | 6 | 0.9 |
| 48 | 10 | 12 | 0.074 | 17.17 | 5 | 1.0 |
| 48 | 10 | 10 | 0.073 | 16.56 | 6 | 1.0 |
| 48 | 10 | 8 | 0.086 | 11.65 | 7 | 1.2 |
| 48 | 10 | 4 | 0.110 | 10.26 | 8 | 1.2 |
| 48 | 8 | 10 | 0.048 | 19.40 | 5 | 1.1 |
| 48 | 4 | 10 | 0.026 | 32.88 | 3 | 1.0 |
| 36 | 12 | 10 | 0.126 | 9.65 | 9 | 1.0 |
| 36 | 10 | 12 | 0.053 | 14.34 | 6 | 1.2 |
| 36 | 10 | 10 | 0.061 | 11.35 | 8 | 1.3 |
| 36 | 10 | 8 | 0.063 | 8.69 | 10 | 1.6 |
| 36 | 10 | 4 | 0.143 | 5.96 | 14 | 1.5 |
| 36 | 8 | 10 | 0.040 | 14.23 | 6 | 1.3 |
| 36 | 4 | 10 | 0.033 | 23.69 | 4 | 1.0 |
| 24 | 12 | 10 | 0.042 | 10.95 | 8 | 1.3 |
| 24 | 10 | 12 | 0.029 | 12.36 | 7 | 1.4 |
| 24 | 10 | 10 | 0.030 | 11.58 | 7 | 1.5 |
| 24 | 10 | 8 | 0.035 | 8.50 | 10 | 1.8 |
| 24 | 10 | 4 | 0.063 | 6.52 | 13 | 1.7 |
| 24 | 8 | 10 | 0.027 | 11.69 | 7 | 1.6 |
| 24 | 4 | 10 | 0.014 | 23.78 | 4 | 1.2 |

Average   1.19

Table B3: Parametric study of PPC structure ($\tan(\alpha) = 0.15$)

| Span (m) | Span/Depth | No of Module | Displacement (m) | Weight (kg/m$^2$) | L/W | SEI |
|---|---|---|---|---|---|---|
| 60 | 12 | 10 | 0.077 | 25.54 | 4 | 0.8 |
| 60 | 10 | 12 | 0.045 | 30.69 | 3 | 0.9 |
| 60 | 10 | 10 | 0.043 | 23.93 | 4 | 1.1 |
| 60 | 10 | 8 | 0.063 | 22.55 | 4 | 0.9 |
| 60 | 10 | 4 | 0.074 | 31.37 | 3 | 0.7 |
| 60 | 8 | 10 | 0.032 | 28.72 | 4 | 1.1 |
| 60 | 4 | 10 | 0.013 | 52.60 | 2 | 0.2 |
| 48 | 12 | 10 | 0.074 | 18.79 | 5 | 0.9 |
| 48 | 10 | 12 | 0.049 | 19.93 | 5 | 1.0 |
| 48 | 10 | 10 | 0.053 | 18.64 | 5 | 1.1 |
| 48 | 10 | 8 | 0.060 | 15.77 | 6 | 1.1 |
| 48 | 10 | 4 | 0.086 | 16.00 | 6 | 1.0 |
| 48 | 8 | 10 | 0.034 | 20.00 | 5 | 1.3 |
| 48 | 4 | 10 | 0.007 | 57.09 | 2 | 0.2 |
| 36 | 12 | 10 | 0.062 | 12.84 | 7 | 1.2 |
| 36 | 10 | 12 | 0.038 | 17.76 | 5 | 1.1 |
| 36 | 10 | 10 | 0.045 | 13.24 | 7 | 1.3 |
| 36 | 10 | 8 | 0.047 | 12.31 | 7 | 1.4 |
| 36 | 10 | 4 | 0.068 | 15.73 | 6 | 0.9 |
| 36 | 8 | 10 | 0.027 | 15.35 | 6 | 1.5 |
| 36 | 4 | 10 | 0.009 | 28.72 | 4 | 0.4 |
| 24 | 12 | 10 | 0.031 | 11.78 | 7 | 1.4 |
| 24 | 10 | 12 | 0.018 | 15.36 | 6 | 1.5 |
| 24 | 10 | 10 | 0.021 | 12.27 | 7 | 1.7 |
| 24 | 10 | 8 | 0.025 | 9.99 | 9 | 1.8 |
| 24 | 10 | 4 | 0.032 | 10.11 | 8 | 1.6 |
| 24 | 8 | 10 | 0.012 | 14.94 | 6 | 1.9 |
| 24 | 4 | 10 | 0.003 | 30.03 | 3 | 0.3 |
| | | | | | Average | 1.09 |

Table B4: Parametric study of PPP structure (tan($\alpha$) = 0.15)

| Span (m) | Span/Depth | No of Module | Displacement(m) | Weight (kg/m$^2$) | L/W | SEI |
|---|---|---|---|---|---|---|
| 60 | 12 | 10 | 0.088 | 27.52 | 4 | 0.7 |
| 60 | 10 | 12 | 0.062 | 33.01 | 3 | 0.7 |
| 60 | 10 | 10 | 0.060 | 30.87 | 3 | 0.8 |
| 60 | 10 | 8 | 0.070 | 25.39 | 4 | 0.8 |
| 60 | 10 | 4 | 0.104 | 35.20 | 3 | 0.5 |
| 60 | 8 | 10 | 0.044 | 26.50 | 4 | 1.0 |
| 60 | 4 | 10 | 0.011 | 38.12 | 3 | 0.3 |
| 48 | 12 | 10 | 0.067 | 29.09 | 4 | 0.7 |
| 48 | 10 | 12 | 0.056 | 25.27 | 4 | 0.8 |
| 48 | 10 | 10 | 0.062 | 19.41 | 5 | 1.0 |
| 48 | 10 | 8 | 0.098 | 18.25 | 5 | 0.8 |
| 48 | 10 | 4 | 0.045 | 36.57 | 3 | 0.7 |
| 48 | 8 | 10 | 0.044 | 18.70 | 5 | 1.2 |
| 48 | 4 | 10 | 0.015 | 28.24 | 4 | 0.4 |
| 36 | 12 | 10 | 0.057 | 16.72 | 5 | 1.0 |
| 36 | 10 | 12 | 0.038 | 17.33 | 5 | 1.2 |
| 36 | 10 | 10 | 0.046 | 14.32 | 6 | 1.2 |
| 36 | 10 | 8 | 0.052 | 12.95 | 7 | 1.3 |
| 36 | 10 | 4 | 0.030 | 20.20 | 5 | 1.2 |
| 36 | 8 | 10 | 0.030 | 15.07 | 6 | 1.5 |
| 36 | 4 | 10 | 0.008 | 28.17 | 4 | 0.4 |
| 24 | 12 | 10 | 0.026 | 15.94 | 6 | 1.2 |
| 24 | 10 | 12 | 0.017 | 20.02 | 5 | 1.3 |
| 24 | 10 | 10 | 0.019 | 14.50 | 6 | 1.6 |
| 24 | 10 | 8 | 0.022 | 13.32 | 7 | 1.5 |
| 24 | 10 | 4 | 0.039 | 12.78 | 7 | 1.2 |
| 24 | 8 | 10 | 0.014 | 12.30 | 7 | 2.1 |
| 24 | 4 | 10 | 0.003 | 22.26 | 4 | 0.4 |
| | | | | | Average | 0.98 |

Table B5: Parametric study of Space truss structure

| Span (m) | Span/Depth | No of Module | Displacement (m) | Weight (kg/m²) | L/W | SEI |
|---|---|---|---|---|---|---|
| 60 | 12 | 10 | 0.074 | 21.53 | 4 | 0.9 |
| 60 | 10 | 12 | 0.060 | 25.02 | 4 | 0.9 |
| 60 | 10 | 10 | 0.072 | 19.03 | 5 | 1.0 |
| 60 | 10 | 8 | 0.070 | 16.00 | 6 | 1.2 |
| 60 | 8 | 10 | 0.055 | 20.00 | 5 | 1.1 |
| 48 | 12 | 10 | 0.038 | 18.03 | 5 | 1.3 |
| 48 | 10 | 12 | 0.029 | 20.63 | 5 | 1.3 |
| 48 | 10 | 10 | 0.034 | 17.06 | 5 | 1.4 |
| 48 | 10 | 8 | 0.036 | 14.27 | 6 | 1.6 |
| 48 | 8 | 10 | 0.025 | 17.47 | 5 | 1.7 |
| 36 | 12 | 10 | 0.025 | 15.13 | 6 | 1.6 |
| 36 | 10 | 12 | 0.016 | 20.07 | 5 | 1.6 |
| 36 | 10 | 10 | 0.022 | 13.76 | 6 | 1.8 |
| 36 | 10 | 8 | 0.027 | 10.34 | 8 | 2.1 |
| 36 | 8 | 10 | 0.018 | 14.04 | 6 | 2.0 |
| 24 | 12 | 10 | 0.016 | 11.50 | 8 | 2.1 |
| 24 | 10 | 12 | 0.012 | 13.12 | 7 | 2.1 |
| 24 | 10 | 10 | 0.014 | 10.20 | 8 | 2.4 |
| 24 | 10 | 8 | 0.017 | 7.62 | 11 | 2.9 |
| 24 | 8 | 10 | 0.010 | 11.90 | 7 | 2.5 |
| | | | | Average | | 1.90 |

Table B6: Parametric study of PPP structure (tan($\alpha$) = 0.08)

| Span (m) | Span/Depth | No of Module | Displacement (m) | Weight (kg/m$^2$) | L/W | SEI |
|---|---|---|---|---|---|---|
| 60 | 12 | 10 | 0.105 | 21.78 | 4 | 0.8 |
| 60 | 10 | 12 | 0.069 | 22.68 | 4 | 0.9 |
| 60 | 10 | 10 | 0.072 | 22.50 | 4 | 0.9 |
| 60 | 10 | 8 | 0.064 | 23.96 | 4 | 0.9 |
| 60 | 8 | 10 | 0.045 | 21.57 | 4 | 1.2 |
| 48 | 12 | 10 | 0.055 | 18.77 | 5 | 1.0 |
| 48 | 10 | 12 | 0.049 | 21.37 | 5 | 1.0 |
| 48 | 10 | 10 | 0.033 | 18.54 | 5 | 1.4 |
| 48 | 10 | 8 | 0.051 | 17.12 | 5 | 1.2 |
| 48 | 8 | 10 | 0.015 | 18.73 | 5 | 2.0 |
| 36 | 12 | 10 | 0.032 | 16.97 | 5 | 1.3 |
| 36 | 10 | 12 | 0.030 | 18.03 | 5 | 1.3 |
| 36 | 10 | 10 | 0.023 | 14.93 | 6 | 1.7 |
| 36 | 10 | 8 | 0.027 | 12.63 | 7 | 1.8 |
| 36 | 8 | 10 | 0.012 | 12.59 | 7 | 2.6 |
| 24 | 12 | 10 | 0.017 | 12.92 | 7 | 1.8 |
| 24 | 10 | 12 | 0.007 | 14.41 | 6 | 2.6 |
| 24 | 10 | 10 | 0.001 | 13.61 | 7 | 6.5 |
| 24 | 10 | 8 | 0.015 | 8.86 | 9 | 2.7 |
| 24 | 8 | 10 | 0.002 | 11.67 | 7 | 5.8 |
| | | | | | Average | 2.31 |

Table B7: Comparative study

| Span (m) | Span/Depth | No of Module | SEI of PPP tan(α) = 0.15 | SEI of Spatial Truss | SEI of PPP tan(α) = 0.08 |
|---|---|---|---|---|---|
| 60 | 12 | 10 | 0.7 | 0.9 | 0.8 |
| 60 | 10 | 12 | 0.7 | 0.9 | 0.9 |
| 60 | 10 | 10 | 0.8 | 1.0 | 0.9 |
| 60 | 10 | 8 | 0.8 | 1.2 | 0.9 |
| 60 | 8 | 10 | 1.0 | 1.1 | 1.2 |
| 48 | 12 | 10 | 0.7 | 1.3 | 1.0 |
| 48 | 10 | 12 | 0.8 | 1.3 | 1.0 |
| 48 | 10 | 10 | 1.0 | 1.4 | 1.4 |
| 48 | 10 | 8 | 0.8 | 1.6 | 1.2 |
| 48 | 8 | 10 | 1.2 | 1.7 | 2.0 |
| 36 | 12 | 10 | 1.0 | 1.6 | 1.3 |
| 36 | 10 | 12 | 1.2 | 1.6 | 1.3 |
| 36 | 10 | 10 | 1.2 | 1.8 | 1.7 |
| 36 | 10 | 8 | 1.3 | 2.1 | 1.8 |
| 36 | 8 | 10 | 1.5 | 2.0 | 2.6 |
| 24 | 12 | 10 | 1.2 | 2.1 | 1.8 |
| 24 | 10 | 12 | 1.3 | 2.1 | 2.6 |
| 24 | 10 | 10 | 1.6 | 2.4 | 6.5 |
| 24 | 10 | 8 | 1.5 | 2.9 | 2.7 |
| 24 | 8 | 10 | 2.1 | 2.5 | 5.8 |
| Average | | | 1.11 | 1.68 | 1.96 |

**Appendix C: Natural frequencies of Deployable Tension-Strut Structures**

Table C1: Pyramid-In-Pyramid Structures

| Span 60 m | | | | Span 48 m | | | |
|---|---|---|---|---|---|---|---|
| Span/Depth | No. of Module | Mode | f (Hz) | Span/Depth | No. of Module | Mode | f (Hz) |
| 4 | 10 | 1 | 3.51 | 4 | 10 | 1 | 3.74 |
| | | 2 | 4.52 | | | 2 | 4.26 |
| | | 3 | 4.55 | | | 3 | 4.69 |
| 8 | 10 | 1 | 3.75 | 8 | 10 | 1 | 4.87 |
| | | 2 | 7.11 | | | 2 | 9.31 |
| | | 3 | 7.67 | | | 3 | 12.00 |
| 10 | 4 | 1 | 3.03 | 10 | 4 | 1 | 5.29 |
| | | 2 | 8.07 | | | 2 | 11.00 |
| | | 3 | 8.08 | | | 3 | 11.00 |
| 10 | 8 | 1 | 4.68 | 10 | 8 | 1 | 4.95 |
| | | 2 | 9.53 | | | 2 | 9.67 |
| | | 3 | 9.53 | | | 3 | 11.70 |
| 10 | 10 | 1 | 4.51 | 10 | 10 | 1 | 5.33 |
| | | 2 | 9.22 | | | 2 | 11.00 |
| | | 3 | 9.22 | | | 3 | 11.20 |
| 10 | 12 | 1 | 4.46 | 10 | 12 | 1 | 5.14 |
| | | 2 | 8.99 | | | 2 | 10.70 |
| | | 3 | 8.99 | | | 3 | 10.80 |
| 12 | 10 | 1 | 3.98 | 12 | 10 | 1 | 4.46 |
| | | 2 | 8.43 | | | 2 | 9.05 |
| | | 3 | 8.43 | | | 3 | 10.10 |

Table C1: (cont'd)

| Span 36 m | | | | Span 24 m | | | |
|---|---|---|---|---|---|---|---|
| Span/Depth | No. of Module | Mode | f (Hz) | Span/Depth | No. of Module | Mode | f (Hz) |
| 4 | 10 | 1 | 2.51 | 4 | 10 | 1 | 4.64 |
| | | 2 | 3.15 | | | 2 | 7.61 |
| | | 3 | 3.40 | | | 3 | 8.93 |
| 8 | 10 | 1 | 6.48 | 8 | 10 | 1 | 9.10 |
| | | 2 | 12.20 | | | 2 | 17.10 |
| | | 3 | 15.20 | | | 3 | |
| 10 | 4 | 1 | 6.35 | 10 | 4 | 1 | 9.51 |
| | | 2 | 13.30 | | | 2 | 17.00 |
| | | 3 | 13.40 | | | 3 | 17.10 |
| 10 | 8 | 1 | 6.76 | 10 | 8 | 1 | 9.18 |
| | | 2 | 13.10 | | | 2 | 19.30 |
| | | 3 | 15.70 | | | 3 | 22.10 |
| 10 | 10 | 1 | 5.81 | 10 | 10 | 1 | 9.19 |
| | | 2 | 12.00 | | | 2 | 18.80 |
| | | 3 | 14.40 | | | 3 | 21.20 |
| 10 | 12 | 1 | 5.52 | 10 | 12 | 1 | 6.13 |
| | | 2 | 11.60 | | | 2 | 14.30 |
| | | 3 | 13.50 | | | 3 | 18.00 |
| 12 | 10 | 1 | 4.63 | 12 | 10 | 1 | 7.36 |
| | | 2 | 10.50 | | | 2 | 16.20 |
| | | 3 | 10.90 | | | 3 | 19.10 |

Table C2: Pyramid-On-Pyramid Structures

| Span 60 m | | | | Span 48 m | | | |
|---|---|---|---|---|---|---|---|
| Span/Depth | No. of Module | Mode | f (Hz) | Span/Depth | No. of Module | Mode | f (Hz) |
| 4 | 10 | 1 | 5.50 | 4 | 10 | 1 | 3.02 |
| | | 2 | 8.53 | | | 2 | 3.72 |
| | | 3 | 8.53 | | | 3 | 4.96 |
| 8 | 10 | 1 | 3.23 | 8 | 10 | 1 | 5.91 |
| | | 2 | 6.01 | | | 2 | 12.10 |
| | | 3 | 6.09 | | | 3 | 12.10 |
| 10 | 4 | 1 | 3.08 | 10 | 4 | 1 | 4.23 |
| | | 2 | 6.57 | | | 2 | 10.30 |
| | | 3 | 6.89 | | | 3 | 10.50 |
| 10 | 8 | 1 | 3.56 | 10 | 8 | 1 | 5.60 |
| | | 2 | 6.85 | | | 2 | 12.00 |
| | | 3 | 7.13 | | | 3 | 12.00 |
| 10 | 10 | 1 | 3.05 | 10 | 10 | 1 | 3.74 |
| | | 2 | 5.97 | | | 2 | 7.49 |
| | | 3 | 6.11 | | | 3 | 7.50 |
| 10 | 12 | 1 | 4.31 | 10 | 12 | 1 | 3.50 |
| | | 2 | 8.94 | | | 2 | 6.82 |
| | | 3 | 8.94 | | | 3 | 7.38 |
| 12 | 10 | 1 | 3.62 | 12 | 10 | 1 | 3.52 |
| | | 2 | 8.11 | | | 2 | 7.08 |
| | | 3 | 8.11 | | | 3 | 7.35 |

Table C2: (cont'd)

| Span 36 m | | | | Span 24 m | | | |
|---|---|---|---|---|---|---|---|
| Span/Depth | No. of Module | Mode | f (Hz) | Span/Depth | No. of Module | Mode | f (Hz) |
| 4 | 10 | 1 | 5.94 | 4 | 10 | 1 | 15.70 |
| | | 2 | 6.26 | | | 2 | |
| | | 3 | 8.62 | | | 3 | |
| 8 | 10 | 1 | 5.59 | 8 | 10 | 1 | 6.09 |
| | | 2 | 10.20 | | | 2 | 13.10 |
| | | 3 | 10.30 | | | 3 | 14.60 |
| 10 | 4 | 1 | 5.20 | 10 | 4 | 1 | 8.07 |
| | | 2 | 9.95 | | | 2 | 18.80 |
| | | 3 | 10.10 | | | 3 | 19.10 |
| 10 | 8 | 1 | 5.96 | 10 | 8 | 1 | 10.20 |
| | | 2 | 11.90 | | | 2 | 22.90 |
| | | 3 | 12.60 | | | 3 | 22.90 |
| 10 | 10 | 1 | 4.07 | 10 | 10 | 1 | 6.30 |
| | | 2 | 9.71 | | | 2 | 13.30 |
| | | 3 | 10.20 | | | 3 | 15.10 |
| 10 | 12 | 1 | 5.68 | 10 | 12 | 1 | 4.63 |
| | | 2 | 13.00 | | | 2 | 10.80 |
| | | 3 | 13.00 | | | 3 | 11.60 |
| 12 | 10 | 1 | 3.80 | 12 | 10 | 1 | 5.93 |
| | | 2 | 8.85 | | | 2 | 13.40 |
| | | 3 | 9.45 | | | 3 | 13.40 |

Table C3: Pyramid-Pantograph-Cable Structures

| Span 60 m | | | | Span 48 m | | | |
|---|---|---|---|---|---|---|---|
| Span/Depth | No. of Module | Mode | f (Hz) | Span/Depth | No. of Module | Mode | f (Hz) |
| 4 | 10 | 1 | 3.19 | 4 | 10 | 1 | 6.02 |
| | | 2 | | | | 2 | 9.54 |
| | | 3 | | | | 3 | 9.54 |
| 8 | 10 | 1 | 5.53 | 8 | 10 | 1 | 6.39 |
| | | 2 | 6.49 | | | 2 | 6.39 |
| | | 3 | 6.49 | | | 3 | 6.39 |
| 10 | 4 | 1 | 3.40 | 10 | 4 | 1 | 4.37 |
| | | 2 | 4.20 | | | 2 | 4.52 |
| | | 3 | 4.33 | | | 3 | 4.52 |
| 10 | 8 | 1 | 4.78 | 10 | 8 | 1 | 5.73 |
| | | 2 | 7.62 | | | 2 | 8.24 |
| | | 3 | 7.62 | | | 3 | 8.24 |
| 10 | 10 | 1 | 4.76 | 10 | 10 | 1 | 5.67 |
| | | 2 | 7.83 | | | 2 | 9.16 |
| | | 3 | 7.83 | | | 3 | 9.16 |
| 10 | 12 | 1 | 4.54 | 10 | 12 | 1 | 5.66 |
| | | 2 | 7.84 | | | 2 | 7.55 |
| | | 3 | 7.84 | | | 3 | 7.55 |
| 12 | 10 | 1 | 4.04 | 12 | 10 | 1 | 4.99 |
| | | 2 | 7.43 | | | 2 | 9.08 |
| | | 3 | 7.43 | | | 3 | 9.08 |

Table C3: (cont'd)

| Span 36 m | | | | Span 24 m | | | |
|---|---|---|---|---|---|---|---|
| Span/Depth | No. of Module | Mode | f (Hz) | Span/Depth | No. of Module | Mode | f (Hz) |
| 4 | 10 | 1 | 3.46 | 4 | 10 | 1 | 6.17 |
| | | 2 | 3.46 | | | 2 | 6.17 |
| | | 3 | 3.46 | | | 3 | 6.18 |
| 8 | 10 | 1 | 6.69 | 8 | 10 | 1 | 9.06 |
| | | 2 | 6.69 | | | 2 | 9.06 |
| | | 3 | 6.70 | | | 3 | 9.06 |
| 10 | 4 | 1 | 3.52 | 10 | 4 | 1 | 7.36 |
| | | 2 | 5.10 | | | 2 | 8.06 |
| | | 3 | 5.40 | | | 3 | 8.06 |
| 10 | 8 | 1 | 7.32 | 10 | 8 | 1 | 10.70 |
| | | 2 | 9.78 | | | 2 | 12.20 |
| | | 3 | 9.78 | | | 3 | 12.20 |
| 10 | 10 | 1 | 7.34 | 10 | 10 | 1 | 10.70 |
| | | 2 | 9.37 | | | 2 | 13.10 |
| | | 3 | 9.37 | | | 3 | 13.10 |
| 10 | 12 | 1 | 6.94 | 10 | 12 | 1 | 10.20 |
| | | 2 | 10.60 | | | 2 | 14.40 |
| | | 3 | 10.60 | | | 3 | 14.40 |
| 12 | 10 | 1 | 6.02 | 12 | 10 | 1 | 9.34 |
| | | 2 | 9.54 | | | 2 | 15.80 |
| | | 3 | 9.54 | | | 3 | 15.80 |

Table C4: Pyramid-Pantograph-Pyramid Structures

| Span 60 m | | | | Span 48 m | | | |
|---|---|---|---|---|---|---|---|
| Span/Depth | No. of Module | Mode | f (Hz) | Span/Depth | No. of Module | Mode | f (Hz) |
| 4 | 10 | 1 | 2.78 | 4 | 10 | 1 | 2.11 |
| | | 2 | 2.78 | | | 2 | 2.11 |
| | | 3 | 2.78 | | | 3 | 2.11 |
| 8 | 10 | 1 | 4.65 | 8 | 10 | 1 | 5.87 |
| | | 2 | 7.40 | | | 2 | 6.11 |
| | | 3 | | | | 3 | 6.11 |
| 10 | 4 | 1 | 2.57 | 10 | 4 | 1 | 3.31 |
| | | 2 | 4.41 | | | 2 | 5.78 |
| | | 3 | 4.41 | | | 3 | 5.78 |
| 10 | 8 | 1 | 3.75 | 10 | 8 | 1 | 4.80 |
| | | 2 | 6.64 | | | 2 | 6.92 |
| | | 3 | 6.64 | | | 3 | 6.92 |
| 10 | 10 | 1 | 3.94 | 10 | 10 | 1 | 5.01 |
| | | 2 | 7.25 | | | 2 | 8.51 |
| | | 3 | 7.25 | | | 3 | 8.51 |
| 10 | 12 | 1 | 4.47 | 10 | 12 | 1 | 5.58 |
| | | 2 | 8.29 | | | 2 | |
| | | 3 | 8.29 | | | 3 | |
| 12 | 10 | 1 | 3.50 | 12 | 10 | 1 | 4.04 |
| | | 2 | 6.57 | | | 2 | 7.44 |
| | | 3 | 6.57 | | | 3 | 7.44 |

Table C4: (cont'd)

| Span 36 m | | | | Span 24 m | | | |
|---|---|---|---|---|---|---|---|
| Span/Depth | No. of Module | Mode | f (Hz) | Span/Depth | No. of Module | Mode | f (Hz) |
| 4 | 10 | 1 | 2.88 | 4 | 10 | 1 | 2.92 |
| | | 2 | 2.88 | | | 2 | 2.92 |
| | | 3 | 2.88 | | | 3 | 2.92 |
| 8 | 10 | 1 | 7.04 | 8 | 10 | 1 | 8.24 |
| | | 2 | 7.05 | | | 2 | 8.24 |
| | | 3 | 7.05 | | | 3 | 8.24 |
| 10 | 4 | 1 | 5.92 | 10 | 4 | 1 | 6.76 |
| | | 2 | 6.82 | | | 2 | 9.81 |
| | | 3 | 8.54 | | | 3 | 9.99 |
| 10 | 8 | 1 | 6.51 | 10 | 8 | 1 | 9.55 |
| | | 2 | 9.79 | | | 2 | 14.80 |
| | | 3 | 9.79 | | | 3 | 14.80 |
| 10 | 10 | 1 | 6.66 | 10 | 10 | 1 | 10.10 |
| | | 2 | 9.89 | | | 2 | 17.50 |
| | | 3 | 9.89 | | | 3 | 17.50 |
| 10 | 12 | 1 | 6.64 | 10 | 12 | 1 | 11.00 |
| | | 2 | 11.10 | | | 2 | |
| | | 3 | 11.10 | | | 3 | |
| 12 | 10 | 1 | 5.65 | 12 | 10 | 1 | 8.54 |
| | | 2 | 10.80 | | | 2 | 16.60 |
| | | 3 | 10.80 | | | 3 | 16.60 |

# AWARDS

Hangai Prize, IASS 2005 at annual Symposium of International Associations of Shell and Spatial Structures, Bucharest, Romania
(The criteria for the awards was innovation and scientific soundness of the presented technical paper)

# PUBLICATIONS

**International Journal Papers**

Vu KK, Liew JYR, Krishnapillai A, 2005, *Commutative Algebra in Structural Analysis of Deployable Tension-Strut Structures*, Journal of International Associations of Shell and Spatial Structures, Vol. 46

Vu KK, Liew JYR, Krishnapillai A, 2006, *Deployable Tension-Strut Structures: from Concept to Implementation*, Journal of Constructional Steel Research, Vol. 62, pp 195-209.

Vu KK, Liew JYR, Krishnapillai A, 2006, *Deployable Tension-Strut Structures: Structural Morphology Study and Alternative Form Creations*, International Journal of Space Structures, Vol 21, No. 3, pp 149-164

Vu KK, Liew JYR, Krishnapillai A, 2006, *Deployable Tension-Strut Structures*, International Journal of Advanced Steel Construction (submitted)

**International Conference Papers**

Krishnapillai A, Vu KK, Liew JYR, Deploy & Stabilise Spatial Structures, *Proceedings IASS*, September 2004, Montpellier, France

Krishnapillai A, Vu KK, Liew JYR, Fractal Concept of Spatial Structure Design, *Proceedings IASS*, September 2004, Montpellier, France

Vu KK, Liew JYR, Krishnapillai A, Deployable Tension-Strut Structures: The Development and Prospect, *Proceedings KKCNN*, December 2004, Ayuthaya, Thailand

Vu KK, Liew JYR, Krishnapillai A, Pre-stress Effect on Structural Behaviour of Tension-Strut Structures, *Proceedings IASS*, September 2005, Bucharest, Romania

Vu KK, Liew JYR, Krishnapillai A, Commutative Algebra in Structural Analysis of Deployable Tension-Strut Structures, *Proceedings IASS*, September 2005, Bucharest, Romania

Vu KK, Liew JYR, Krishnapillai A, Generative Conceptual Designs of Deployable Tension-Strut Structures, *Proceedings IASS*, September 2005, Bucharest, Romania

Vu KK, Liew JYR, Krishnapillai A, Deployable Tension-Strut Vault: A Design for Deployment, *Proceedings KKCNN*, December 2005, Kaoshung, Taiwan

Vu KK, Liew JYR, Krishnapillai A, Rapidly deployed Tension-Strut Structures, *Proceedings 8th International Conference on Steel Space Composite Structures*, May 2006, Kuala Lumpur, Malaysia

Vu KK, Liew JYR, Tran CT, Krishnapillai A, Deployable Tension-Strut Structures: Design Guidelines, *Proceedings Adaptables*, July 2006, Eindhoven, The Netherlands

Vu KK, Liew JYR, Krishnapillai A, Buildability of Deployable Tension-Strut Structures, *Proceedings IASS*, October 2006, Beijing, China

Vu KK, Liew JYR, Krishnapillai A, Deployable Tension-Strut Structures: Design Concept and Exhaustive Form Variations, *Proceedings 4th International Conference on Steel Structures*, November 2006, Seoul, Korea

Vu KK, Liew JYR, Krishnapillai A, Rapidly Deployable Protective Structures, *Proceedings 2nd International Conference on Design and Analysis of Protective Structures*, November 2006, Singapore


**Public Seminars**


K.K. Vu, 2003, Potential Applications of Deployable Structures, Steel Group Annual Seminar, Department of Civil Engineering, NUS, Singapore

K.K. Vu, 2004, Deployable Tension-Strut Structures, the Novel Concept, Steel Group Annual Seminar, Department of Civil Engineering, NUS, Singapore

K.K. Vu, 2005, Deployable Tension-Strut Structures: Design Issues, Steel Group Annual Seminar, Department of Civil Engineering, NUS, Singapore

K.K. Vu, 2006, Deployable Tension-Strut Structures: Constructability, Steel Group Annual Seminar, Department of Civil Engineering, NUS, Singapore